Volume change behaviour of some geomaterials under combined influence of freeze-thaw and wet-dry cycles: An experimental investigation

Osama Mahdi Al-Hussaini

Geoenvironmental Research Centre
Cardiff School of Engineering
Cardiff University

Thesis submitted in candidature for the degree of Doctor of Philosophy at Cardiff University

December 2017

To...

Al-Hussain ibn Ali ibn Abi Talib

And his sister, Zaynab.

Acknowledgements

In the Name of Allah, the All-Merciful, the All-Compassionate.

Praise be to Allah, the All-Powerful, the All-Knowing, the All-Wise, the All-Generous, the Noble and the Compassionate, for giving me the strength and perseverance to complete this work in pursuit of my dreams.

To my supervisors Dr Snehasis Tripathy, Dr Peter Cleall and Dr Steve Rees, I wish to express my heartfelt gratitude and appreciation for all the support, guidance, patience and time that they have given me this great opportunity in making this thesis a reality.

I am extremely grateful to the technical staff at ENGIN, in particular Harry, Steff, Paul, Richard, Ian, Carl, Jack, Gareth, Garry and Jeff. I am thankful not only for their endless assistance but also for their friendship and encouragement. I would also like to thank the staff of ENGIN Research Office, Chris, Aderyn, Jeanette, Ffion and Sandra for their constant help, support and encouragement.

Special thanks to my dearest friend A. Lecturer Waseem Al-Baghdadi, my mentors and teachers A. Professor Dr Laith Jawad Aziz and A. Professor Dr Muhammed Al-Shakarchi and my role model Professor Dr Asaad Al-Janabi (University of Kufa), for everything they did and do. May the words cannot reveal my deep gratitude to them.

Many thanks to all my friends in GRC; Hassanien, Khabeer, Yahya, Sahar, Suhad, Safaa, Maram, Ahmed, Kai besides Adnan and Ali for providing a very enjoyable and motivating environment.

The completion of my degree would have been impossible without the support of my beloved country “Iraq” by the sponsoring of “Ministry of Higher Education and Scientific research” of my scholarship, Besides the sacrifices of Iraqi national forces and The Public Crowd; i will still owe them for the rest of my life.

My deepest thanks, love and gratitude to all my family, parents, brother; Mustafa, sisters, cousins and for their understanding and support. Extraordinary thanks and love to my best friend and wife; Aalaa and my lovely son, Yosif for being in my life.

Lastly, I thank everyone who has contributed directly or indirectly to this work that is now being presented here.

Abstract

Climate change has led to more extreme weather during the last decades. Seasonally hot weather regions have experienced harsh winters. Similarly, the global warming has contributed to raising the mean summer temperature in the cold regions. Geomaterials in various engineering applications are expected to experience such changes in the weather patterns and may undergo freezing, thawing, wetting and drying processes. This thesis presents an experimental study of the one-dimensional volume change behaviour of some geomaterials under the combined influence of freeze-thaw and wet-dry cycles.

Laboratory tests were carried out on three selected materials (Speswhite kaolin, Pegwell Bay soil and cement kiln dust). A custom-made test set up was used to carry out the laboratory tests that enabled performing the required tests involving freezing, thawing, drying and wetting processes. Initially saturated slurried materials and compacted materials were subjected to freezing and thawing processes to study frost heave and thaw settlement. Compacted materials were taken through several wet-dry cycles and then exposed to freezing and thawing processes to study the impact of intermittent freeze-thaw cycles on the volume change behaviour of the materials. Similarly, compacted materials were subjected to an increasing number of freeze-thaw-wet-dry cycles to study the combined influence of various processes on the volume change behaviour of the materials.

Compacted materials exhibited higher magnitudes of frost heave than initially saturated slurried materials. The swelling and shrinkage strains of compacted materials decreased with an increasing number of wet-dry cycles and attained an equilibrium at which the strains remained very similar. Intermittent freeze-thaw cycles were found to destabilize the equilibrium strain that was achieved during the previous wet-dry cycles; however, a new equilibrium in terms of the vertical strain was attained by the materials with an increasing number of wet-dry cycles. The materials having a history of being exposed to several wet-dry cycles exhibited a higher frost heave, a higher segregation potential and a greater magnitude of thaw settlement as compared to the same materials but without any cyclic wet-dry history. Upon subjected to an increasing number of wet-freeze-thaw-dry cycles, the materials exhibited uprising movement accompanied by strain accumulation prior to attaining an equilibrium at which the vertical strains associated with wetting, freezing, thawing and drying processes were found to be dissimilar; however, the sum of swelling deformation and frost heave was found to be equal to the sum of thaw settlement and shrinkage deformation.

Table of Contents

List of Figures

List of Tables

CHAPTER 1

Introduction

1.1 Background

Scientific studies indicate that extreme weather events (floods, droughts, damaging high winds, extreme heat and cold events) can have negative impacts on society and ecosystems (Meehl et al. 2000). The consensus of atmospheric scientists is that climate change is occurring, both in terms of significant variations in the air temperature and precipitation (O'Neal et al. 2005). More extreme climate events are realized in many parts of the world. In the UK, the winter of 2000/1 was the wettest on record and the period May-July 2007 was the wettest for 250 years (Toll et al. 2008). Globally, 9 of the 10 warmest years since 1860 have occurred since 1990 (World Meteorological Organization, WMO 2001). In permafrost regions, a more pronounced rise in the temperature has been predicted (Matsuoka 2001). This may have the potential to alter the different soil engineering applications (Glendinning 2007). Extreme cold events have also been realized in the hot-seasonal weathering regions of the world (Zhou et al. 2011; Herring et al. 2015).

The seasonal climatic conditions at any location may involve two or more of the processes of wetting, drying, freezing and thawing. These processes directly affect the properties of the soils and hence the stability of the structures found on them. In cold regions of the world freezing and thawing processes are more relevant, whereas soils in the arid and semi-arid regions of the world undergo wetting and drying processes. The effects of freeze-thaw and wet-dry cycles on the volume change behaviour, hydraulic

conductivity, shear strength and soil structure of a variety of soils have been studied extensively in the past by many researchers (Chamberlain and Gow 1979; Camberlain et al. 1990; Benson and Othman 1993; Viklander and Eigenbrod 2000; Konrad 2010; Toll et al. 2012; Zheng et al. 2015; Konrad 1999; Doehne and Stulik 1990; Boardman and Daniel 1996; Thu 2006; Seguel and Horn 2006; Pires et al. 2007; Pires et al. 2008; Nowamooz and Masrouri 2010a, b; Liu et al. 2016; Toll and Ali Rahman 2017).

Volume change in soils cause changes in strength and deformation properties that, in turn, influence stability. Significant variations in climate, such as long droughts and heavy rains, cause cyclic water content changes resulting in edge movement of structures (Fredlund and Rahardjo 1993). Soils and various geomaterials (mixtures of soil and various industrial wastes and admixtures) are usually compacted and used in many civil engineering applications. Similarly, clays are often used as hydraulic barriers. These materials may undergo freeze-thaw cycles in cold climates and wet-dry cycles in the hot or tropical climate. Therefore, it is necessary to understand the effect of freezing, thawing, drying and wetting on the volumetric response of various engineering materials, particularly in the context of climate change impacts on the stability of structures.

Wet-dry effects are more pronounced in expansive soils that exhibit swell-shrink behaviour. Soil scientists and engineers have attempted to study the swell-shrink behaviour of compacted expansive soils (Dif and Bluemel 1991; Day 1994; Al-Homoud et al. 1995; Basma et al. 1996; Rao et al. 2001; Tripathy et al. 2002; Alonso et al. 2005; Rao and Revanasiddappa 2006; Tripathy and Subba Rao 2009). Swelling and shrinkage strain prediction models have been proposed by several researchers (Ranganatham and Satyanarayana 1965; Seed et al. 1962; Crescimanno and Provenzano 1999; Rao et al. 2004).

The cold regions of the world cover large parts of Asia, northern Europe, Alaska, Canada and about a third of the USA. In these regions, pavement and structures are subjected to freezing in the winter and thaw weakening during the spring. Consequently, the mechanical properties of the structures can be greatly affected by seasonal changes in temperature and soil moisture (Simonsen and Isacsson 1999). Structures founded on frost susceptible soils require special considerations for their design (Henry 2000). Several laboratory research works have been aimed at understanding the effects of the freeze-thaw behaviour of soils (Morgenstern and Nixon 1971; Miller 1972; Chamberlain and Gow 1979; Konrad and Morgenstern 1980; Chamberlain 1981a; Penner 1986; Konrad 1988; Viklander 1998) and several frost heave modelling have been established(Konrad and Morgenstern 1981; Thomas et al. 2009). Similarly, various studies have explored the effects of freezing-thawing beside wetting-drying on various properties of soils (Sillanpää and Webber 1961; Pardini et al. 1996; Gullà et al. 2006; Ahmed and Ugai 2011; Diagne et al. 2015).

The volume change behaviour of soils and geomaterials under ether freeze-thaw or wet-dry cycles have been explored in detail by many researchers. However, at the research planning stage, an initial review of the literature revealed that further work was needed to provide an integrated assessment of combined of all these processes and their impact on the volume change behaviour of soils and geomaterials.

Climate change has led to more extreme and unusual weather events in the hot seasonal weathering regions of the world. For example, in countries like Iraq, which has been known by the extremely hot weather with temperature exceeding 50 °C in summer months, experienced snowfall in 2008 for the first time in hundred years (Zhou et al. 2011). Similarly, during the winter of 2013 extreme cold weather was realised in the northern and western territories of Iraq and the Middle East (Herring et al. 2015).

Therefore, although the effects of wet-dry cycles on the behaviour of geomaterials in the temperate regions of the world have been studied by many researchers in the past, it would be necessary to study how freeze-thaw cycles affect the volume change behaviour of soils and geomaterials that have been subjected to several wet-dry cycles.

The literature review suggested that reported works on various particulate geomaterials with different physical and chemical properties and their response to freeze-thaw cycles have been studied in detail. The impact of climate change may cause exposure of geomaterials to processes that the materials had seldom encountered in the past. The materials that currently undergo freeze-thaw cycles may be subjected to wet-dry cycles in the future. Similarly, the materials that currently undergo dry-wet cycles may be subjected to freeze-thaw cycles. Therefore, there is a need to explore the volume change behaviour of various geomaterials by exposing the materials to a combination of a variety of anticipated weathering patterns. This research, therefore, aims to explore the volume change behaviour of geomaterials under predetermined weathering patterns (freezing-thawing, wetting-drying with intermittent freeze-thaw cycles and dry-wet-freeze-thaw cycles).

Three different materials were considered in this research to study the one-dimensional volume change behaviour in response to freeze-thaw and wet-dry cycles. The materials selected for the study were a kaolinite-rich clay (Speswhite kaolin), a frost susceptible natural soil (Pegwell Bay soil) and a cement kiln dust (CKD).

1.2 Study objectives

The main objectives of this study were:

I. To develop an experimental test setup that will permit implementing the freezing, thawing, drying and wetting processes and enable carrying out laboratory tests on a variety of geomaterials.
II. To study the effects of freezing and thawing on the one-dimensional volume change behaviour of the materials with different initial conditions (initially saturated slurried and compacted unsaturated materials).
III. To study the effects wet-dry cycles on the one-dimensional volume change behaviour of materials.
IV. To study the effect of an intermittent freeze-thaw cycles on the one-dimensional volume change behaviour of materials that have been already subjected to a number of wet-dry cycles.
V. To study the effect of wet-freeze-thaw-dry cycles on the volume change behaviour of the materials.

Although the sequence of the climatic processes adopted in this study does not replicate the length of the seasonal climate in a complete manner, the study presents necessary information to understand the volumetric change behaviour under the effects of the four-climatic process that are expected to happen in several regions in the world (e.g. Middle East and the northern hemisphere).

1.3 Thesis overview

A brief description of each chapter is presented below.

CHAPTER 1 presents the background of the research, the main objectives of this research and outline of the thesis.

CHAPTER 2 presents a review of literature pertaining to the studies undertaken. The chapter presents general information about the physics of freezing, thawing, drying and wetting processes and their effects on engineering properties of soils. The experimental studies of both cyclic freeze-thaw and wet-dry on the volume change behaviour soils are discussed. The testing devices used for studying the volume change behaviour of soils under both cyclic freeze-thaw and wet-dry are also presented.

CHAPTER 3 describes the properties of the materials used and the experimental test procedures adopted. The background of the selected materials are first presented followed by various properties of the materials that were determined (initial water content, specific gravity, grain size distribution, Atterberg limits, minerals composition using X-ray diffraction (XRD) and specific surface area). The scanning electron microscope (SEM) pictures at selected conditions of the materials are also presented. The compaction characteristics and consolidation behaviour of the materials used are presented. Further, the details of the testing setup and the response of the measuring system to temperature changes are discussed. Subsequently, the experimental program including testing series and specimen preparation methods are presented in detail.

CHAPTER 4 presents the freezing and thawing results obtained for the three materials used. Initially saturated slurried materials were tested using the test setup described in chapter 3. The vertical strains, temperature profiles, segregation potentials

and the water contents of the materials at the end of freezing and thawing processes are presented.

CHAPTER 5 presents the freezing and thawing results obtained for the three materials used. Compacted specimens at predetermined dry density and water contents were tested by subjecting them to freezing and thawing processes. The test results in terms of vertical strain, segregation potential and water content are compared with the test results obtained for initially saturated slurried materials in chapter 4.

CHAPTER 6 presents the one-dimensional volume change behaviour of the compacted specimens of the materials when subjected to wet-dry cycles. Intermittent freeze-thaw cycles were introduced to study their impact on the volume change behaviour of the materials. The tests results were analysed in terms of vertical strain, temperature profiles, segregation potential and water content changes.

CHAPTER 7 presents the one-dimensional volume change behaviour of the compacted specimen of the materials with increasing number of wet-freeze-thaw-dry cycles. The tests results were analysed in terms of vertical strain, temperature profiles, segregation potential and water content changes.

CHAPTER 8 presents the main conclusions drawn based on the findings of this study.

CHAPTER 2

Literature review

2.1 Introduction

The literature review presented in this chapter provides the background information describing the research that have been carried out previously on the freezing, thawing, wetting and drying behaviour of soils. It aims to present a brief review of the key concepts and focuses on the research works that are relevant to the objectives of the investigation presented in this thesis.

Studies associated with independent and cyclic effects of the freeze, thaw, wet and dry processes on the behaviour of geomaterials (soils, soils modified by admixtures, and various industrial wastes, such as pulverised fly ash, cement kiln dust etc.) are extremely relevant in relation to their applications in a wide range of disciplines, such as ecology, hydrology, agriculture, engineering, and climatology. In the context of geotechnical and geoenvironmental engineering, studies of the effects of various processes on the geomaterials provide crucial information on the long-term stability of a variety of geo-infrastructure.

The topics dealt with in this chapter includes the understanding of the behaviour of soils subjected to freezing, thawing, wetting and drying processes, the physics and processes behind wetting, drying, freezing and thawing as applicable to the behaviour of soils in terms of the volume change, an abstract of some of the important experimental research works that have studied the effects of wet-dry and/or freeze-thaw cycles on soils and the studies that have made an attempt to combine all these processes.

2.2 Physical processes associated with freezing, thawing, wetting and drying

Each of the four processes from freezing, thawing, drying and wetting has an impact on various characteristics of soils in terms of water migration, stress state, volume change and structural changes. The following sections discuss the effects of each process separately.

2.2.1 Freezing process

The freezing process may affect all soil types, but usually has a significant impact on the frost susceptible soils. The main factor associated with the frost susceptibility of soils is the grain-size distribution (Chamberlain 1981a). When soils with significant fine-fractions are subjected to freezing, frost heave (volume increase due to formation of ice within the soil system) occurs as a result of two simultaneous processes, such as pore water in the soil freezes in situ and the water from the unfrozen soil, or possibly from an external source, is sucked to the segregation freezing front where it freezes at subzero temperatures, leading to the development of ice lenses (Konrad 1987).

As the surface temperature of a soil drops below the freezing point, the freezing front penetrates the soil progressively. Unsteady heat flow due to the thermal gradient with depth leads to a decrease of the soil temperature. The phase change of pore water occurs in the so-called ‘frozen fringe’(Miller 1972). When the soil temperature falls below the freezing point, volumetric expansion of water due to phase change (liquid to ice) causes an increment of pore pressure within the unfrozen pores. At the ice/ water interface, a cryogenic suction gradient, which is developed in response to the temperature gradient, draws the pore water in the unfrozen soil towards the freezing front, which in turn raises pore pressure. Moisture accumulation and the volumetric expansion due to

pore water phase change in both the fully frozen soils and ice lens result in frost heave (Thomas et al. 2009). Figure 2.1 shows a schematic representation of a freezing soil.

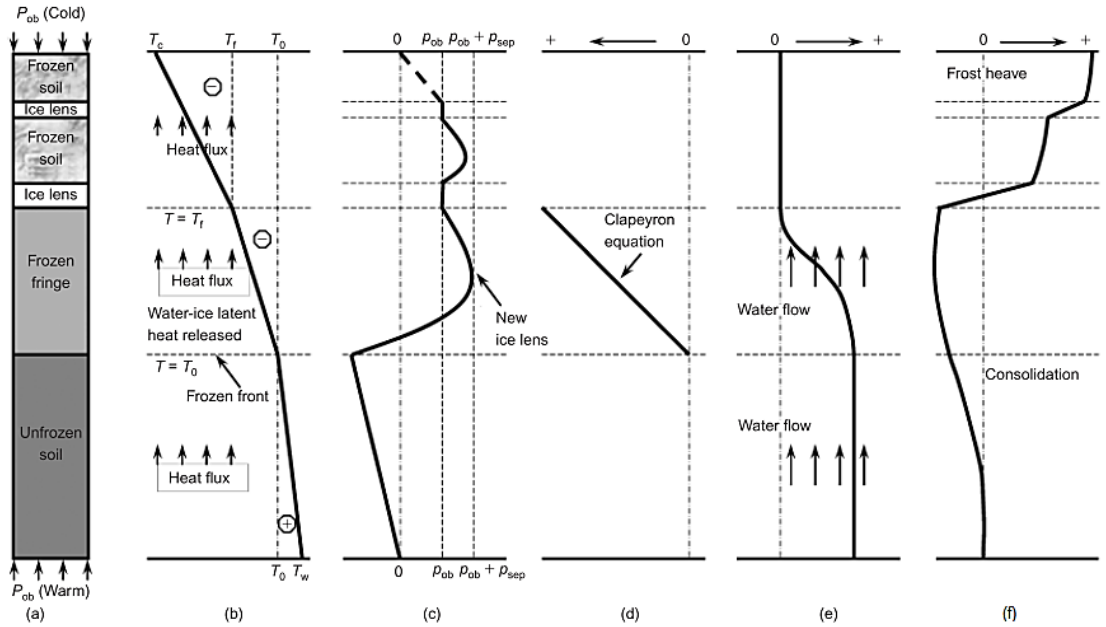

Fig. (2.1): Schematic representation of a freezing soil with ice segregation: (a) layers; (b) temperature; (c) pore pressure; (d) cryogenic suction; (e) water velocity; (f) displacement T_c,T_w, temperature at cold and warm ends, respectively; T_f , temperature at the base of ice lens; T_o, freezing point; pob, surface overburden load; p_{sep}, separation strength) (after Thomas et al. 2009)

Frozen ground properties useful to engineering projects include high strength in compression, excellent bearing capacity, and the impervious nature of frozen ground relative to water seepage. These properties are used by engineers in the design of ground support systems, foundations, earth dams, and other frozen earth structures. (Andersland and Ladanyi 1994).

The harmful side of frozen ground is represented by the complex glacial stratigraphy that leads to potentially difficult and expensive construction problems in some territories (Andersland and Ladanyi 1994), such as in construction of roads and pipelines (Chamberlain et al. 1990). A large increase in the hydraulic conductivity of compacted clay barriers (Zimmie and La Plante 1990; Kraus et al. 1997) and a decrease

in the shear strength are some issues related freeze-thaw cycling of soils (Yong et al. 1982; Wang et al. 2007).

2.2.2 Thawing process

Frozen ground contains ice in several forms, ranging from coatings on soil particles and individual ice inclusions to the ice with soil inclusions. On thawing, the ice melts and changes in the phase occurs to water. For an existing overburden pressure, the soil skeleton must now adapt itself to a new equilibrium void ratio (Andersland and Ladanyi 1994). If the ground has heaved, there will be excess water present which must drain away. The rate at which water is released is controlled by thermal considerations in which case the Terzaghi consolidation theory can be applied to the drainage process (Harris 1995).

Increased moisture content in supporting layers during thawing weakens pavement structures (Janoo and Berg 1996). During spring, thaw of the pavement structure may become saturated from thawing ice, and the bearing capacity can be substantially reduced (Simonsen and Isacsson 1999). In countries with warmer climates (e.g. Scotland) frost thaw weakening is usually related to the weakening of the road after daily freeze-thaw cycles (Aho and Saarenketo 2006).

Ballantyne and Harris (1994) stated that the texture of a thawing soil and the clay content control the geotechnical properties of the soil. Sandy and silty soils have low plastic and liquid limits and low plasticity characteristics. Such soils derive most of their strength from intergranular friction and have little cohesion. Clay soils with higher plastic and liquid limits and much greater plasticity have lower intergranular friction but are highly cohesive. Sandy/silty soils consequently have much lower void ratios and so lower saturation moisture contents than clay soils. Therefore, less water is required for the

sandy/silty soils to reach saturation point. Due to the low plastic and liquid limits, the soils are sensitive to changes in moisture content and will reach a flow condition if the moisture content is greater than the liquid limit. Clay soils, in response to the high pore-water pressures induced by thaw consolidation, often fail along clearly-defined slip surfaces (Ballantyne and Harris 1994).

2.2.3 Drying process

Water is removed from the soil either by evaporation from the ground surface or by evapotranspiration from a vegetative cover (Fredlund and Rahardjo 1993). Fine-grained soils are usually the most affected type of soil by drying. The different phases of shrinkage that result from progressive drying of natural soils: (*i*) structural shrinkage, (*ii*) normal shrinkage, and (*iii*) residual shrinkage (Haines 1923). During structural shrinkage, a few large, stable pores are emptied, and the decrease in volume of the soil is less than the volume of water lost. During the normal shrinkage phase, volume decrease is equal to the volume of water lost (i.e., the slope of the total specimen volume versus water content line is 45°). On further drying, the slope of the shrinkage curve changes and air enters the voids at the shrinkage limit or at the start of residual shrinkage. As the particles come in contact, the decrease in specimen volume is less than the volume of water lost (Tripathy et al. 2002). Stirk (1954) identified the no-shrinkage stage as a fourth phase, when the particles come together closely, and no further shrinkage occurs even with continuous loss of water. Figure 2.2 shows the shrinkage phases and clay aggregates structure with the progress of drying.

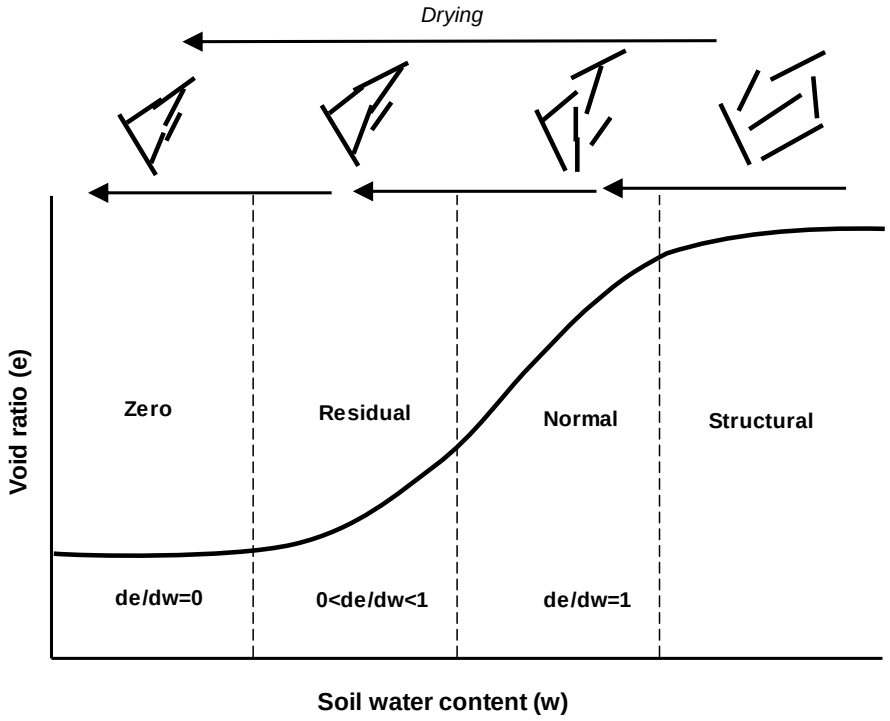

Fig. (2.2): The phases of shrinkage of clay aggregate upon drying process (After Kodikara et al. 1999)

The major mechanisms involved in structure development during drying is the growth and aggregation of soil particles from a stiffer structure, particle aggregation is driven by soil suction that develops as water is removed from soils (Kodikara et al. 1999).

Besides the volumetric change problem associated with swelling-shrinkage behaviour that discussed in the next sections, drying and wetting processes contribute in change in soil properties, such as cone penetration resistance, soil cohesion, adhesion, internal friction and aggregate size (Rajaram and Erbach 1999), shear strength (Guan et al. 2010) and the hydraulic conductivity (Fredlund et al. 1994).

2.2.4 Wetting process

Volume changes due to soil wetting may occur in naturally deposited soils as well as engineered soils (e.g., compacted fills, embankments). Depending on the stress level, some soils exhibit increase in the volume (swell) upon wetting while other soils exhibit a

decrease in volume (collapse) upon wetting. Most compacted clayey soils will experience swelling under low confining stress and collapse under higher confining stresses; the degree of which depends on soil type and stress state. During wetting processes, there are three mechanisms involved in the volume change characteristics of unsaturated soils; (a) swelling of individual aggregates owing to water uptake, (b) aggregate slippage at the inter-aggregate contacts owing to lack of strength to support the externally applied load, leading to collapse compression and (c) distortion of aggregates into the inter-aggregate pore spaces. The relative influence of these controlling factors determines the overall response of the unsaturated clay during wetting.(Alonso et al. 1995; Sivakumar et al. 2006; Sivakumar et al. 2010). In general, all soils are susceptible to wetting-induced collapse when inundated with water under sufficient confining pressure (Cerato et al. 2009). The wetting process effects on other soil properties are always in combined with the drying effects.

Compacted clay fills are affected by the wetting process immediately after construction. They undergo volumetric deformation and loss of shear strength, which can, in turn, lead to a surface settlement or heave, and even collapse or failure at saturation (Sivakumar et al. 2015). Upon wetting, well-compacted fills (i.e. engineered fills) are prone to heave, whereas poorly compacted fills (i.e. un-engineered fills) are prone to settlement. Contrary to popular belief, even engineered fills can pose problems owing to substantive heave at low overburden pressures (Sivakumar et al. 2010).

2.3 Volume change behaviour of soils

Volume changes in soils are accompanied by settlement due to compression, heave due to expansion, and the deformation caused by the shear stresses. Changes in the volume cause changes in the strength and deformation properties that in turn influence the stability of structures (Mitchell and Soga 2005). Volume change in soils is induced

by changes in moisture, environments, and temperature. The effects of seasonal weather changes are important and have been studied by many researchers (Kwiatkowski et al. 2014; Toll et al. 2012; Matsuoka 2001; Day 1994; Toll et al. 2016a; Hui and Ping 2009; Gullà et al. 2006; Qi et al. 2012; Batenipour et al. 2012; Konrad and Lemieux 2005; Smith and Sciences 2004; Aho and Saarenketo 2006; Tang et al. 2018; Nowamooz and Masrouri 2010a; Rosenbalm and Zapata 2017; Liu et al. 2016).

2.3.1 Consolidation settlement

The consolidation settlement is a time-dependent process that occurs in saturated fine-grained soils which have a low coefficient of permeability. The difference between the compression of granular material and the consolidation of cohesive soils is that compression of sands occurs almost instantly, whereas consolidation is a time-dependent process (Holtz and Kovacs 1981).

The consolidation of a saturated soil occurs in three stages, namely initial compression, primary consolidation and secondary compression. While initial compression occurs instantaneously after the application of load, the primary and secondary compressions are time-dependent. The initial compression is due partly to the compression of small pockets of gas within the pore spaces, and partly to the elastic compression of soil grains. Primary consolidation is due to dissipation of excess pore water pressure caused by an increase in effective stress whereas secondary compression takes place under constant effective stress after the completion of dissipation of excess pore water pressure (Budhu 2008).

Terzaghi (1944) derived the classical theory for one-dimensional consolidation for saturated soils based on specific assumptions, Tenaghi's classical derivations incorporated a constitutive equation for saturated soils and a flow law. The constitutive

equation described the deformation of the soil structure with respect to changes in the stress state by using the soil property called the coefficient of volume change (m_v). The flow rate of water during consolidation was calculated in accordance with Darcy's law. Darcy's law relates the flow rate of water to its hydraulic head gradient using the coefficient of permeability (Fredlund and Rahardjo 1993).

The coefficient of permeability (k) can be calculated by using the coefficient of consolidation (C_v). Taylor (1942) proposed the square root-time method. Casagrande and Fadum (1940) proposed the log-time method. The root-time method utilises the early time response, which theoretically should appear as a straight line in a plot of the square root of time versus displacement gage reading. Equation 2.1 can be used to calculate the coefficient of permeability (k):

$$k = C_v . m_v . \gamma_w \quad \text{..... (2.1)}$$

where C_v is the coefficient of consolidation, m_v is coefficient of volume change and γ_w is the unit weight of water. These coefficients can be calculated from Equations (2.2) and (2.3):

$$Cv = \frac{0.196 H_o^2}{t_{50}} \quad \text{..... (2.2)}$$

$$m_v (\mathrm{m}^2/\mathrm{MN}) = \frac{\Delta H}{H_o} \left(\frac{10^3}{\Delta p'}\right) \quad \text{..... (2.3)}$$

where t_{50} is the time correspondent to 50% of the final consolidation settlement, H_o the length of the drainage path and ΔH is the final consolidation settlement, and $\Delta p'$ is the difference in applied effective stress.

In recent decades, a considerable amount of research on the consolidation theory for unsaturated soil has been conducted in the field of geomechanics, with many research

results being accumulated, and with great progress being made (Qin et al. 2008). Several theories on the consolidation of unsaturated soil were made by many researchers, for example, Barden (1965) and Fredlund and Hasan (1979). Besides many studies proposed analytical solutions (Qin et al. 2008; Qin et al. 2010; Ho et al. 2014).

2.3.2 Collapse and Swelling behaviour

Collapsing soils are the soils susceptible to large decrease in bulk volume when they become saturated. Collapse may be triggered by water alone or by saturation and loading acting together. Soils with collapsible structures may be residual, water deposited, or aeolian (Mitchell and Soga 2005). In most cases, the deposits have a loose structure of bulky shaped grains, often in the silt to fine sand range (Mitchell and Soga 2005).

Swelling soils are found throughout the world and have both positive and negative effects associated with their swelling properties. Destructive effects to infrastructure have been reported on the order of billions of dollars per year (Jones and Holtz 1973). On the positive side, the self-healing abilities to swell soils are exploited in the development and design of waste repositories. Compacted swelling clays are often used in these applications. Expansive soil is a worldwide problem that causes extensive damage to civil engineering structures. Certain areas of the United States are more susceptible to damage from expansive soils than other areas, especially those areas that have large surface deposits of clay and climates characterised by alternating periods of rainfall and drought (Day 1994).

Under laterally restrained conditions (i.e. K_o condition) and based on volume–mass relationships between soil solids, water, and air, the volume change of a swollen soil is usually determined in the one-dimensional oedometer swelling test by recording the

change in the height of the specimen. The volume change can be computed using Equation 2.4 (Tripathy et al. 2002).

$$\frac{\Delta V_V}{V_0} = \frac{\Delta H}{H_i} \quad \text{.....(2.4)}$$

where ΔVv is the change in volume, *Vo* is the initial overall volume of the specimen, ΔH is the change in height recorded, and H_i is the initial height of specimens.

2.3.3 Shrinkage behaviour

Shrinkage is the reduction in total volume as the response to the evaporation of water from the soil. Drying a soil sample induces tensile internal stresses (pore water tensions) caused by capillary menisci, which forces particles to reorient and attract to each other, hence leading to shrinkage (Baumgartl and Köck 2004). Shrinkage behaviour is typically caused by evaporation (a change in the temperature), transpiration, and lowering the groundwater table in arid and semi-arid regions. As a particular agricultural problem, shrinkage in soils causes development of cracks which injure the root systems of the crop and depress yields.

Besides the engineering problems related to expansive soils have been reported in many countries of the world but are generally most serious in arid and semiarid regions. As a result, highly reactive soils undergo substantial volume changes associated with the shrinkage and swelling processes. Consequently, many engineered structures suffer severe distress and damage (Tripathy et al. 2002).

2.3.4 Frost heave

Frost heave is the maximum increase in the height of a test specimen during the freezing period (BS 812-124 2009). If the water contained in the voids of a saturated clean

sand or gravel freezes, the structure of the soil remains unchanged. Freezing merely increases the volume of each void by 9% because of the expansion of the water contained in the void. On the other hand, if saturated fine-grained soil freezes, the process involves the formation of lenses of clear ice oriented roughly parallel to the surface exposed to low temperature. The thickness of the individual ice lenses may increase to several centimetres, and the soil subject to freezing assumes the character of a stratified material consisting of alternate lenses of soil and clear ice (Taber 1929, 1930).

The two major components of frost heave are in-situ freezing and segregational frost heave. The in-situ freezing results from in-place expansion of water as it freezes in the pore spaces between soil particles (Konrad 1984). When soil freezes quickly, in-situ freezing causes the majority of the heave. Although water expands approximately 9% in volume when it freezes, this type of frost heave is usually limited to less than about 3% of the depth of the frozen zone in unsaturated soils (McCarthy 1977). The segregational frost heave or ice lensing has the potential to generate very significant frost heave in soils. For ice lensing to occur, three conditions must be met. Firstly, sustained freezing temperatures must exist. Secondly, free water must be available, and thirdly the soil must be frost-susceptible (Mitchell and Soga 2005). Experimental observations suggest that frost heave is caused by ice lensing associated with thermally-induced water migration (Taber 1930). Water migration can take place at temperatures below the freezing point, by flowing via the unfrozen water film adsorbed around soil particles (Sheng et al. 1995).

The frost heave in soils has been investigated both experimentally and theoretically for decades. Soil texture, pore size, overburden pressure, temperature gradient or rate of heat removal and depth to groundwater table are the most important factors that influence frost heave (Taber 1930; Miller 1978; Chamberlain 1981a; Penner 1986; Konrad 1989b; Svec 1989; Nixon 1991; Harris 1995; Rempel 2007; Konrad 2008).

2.3.4.1 Frost heave measurement methods

Terzaghi et al. (1996) stated that, based on the availability of water, two types of frost heave tests had been conducted in the past, namely (*i*) closed system frost heave test and (*ii*) open system frost heave test. The closed system frost heave test is usually carried out with no water source which allows the formation of ice lenses. The growth of the ice lenses probably continues until the water content of the lower part of soil is reduced to the shrinkage limit. The volume increase associated with the freezing of a closed system does not exceed the volume increase of the water contained in the system. In engineering practice, open systems are encountered wherever the vertical distance between the water table and the frost line is smaller than the height of capillary rise of the soil. Because the water that migrates out of the groundwater reservoir is continually replenished, the ice lenses grow continually during the frost periods, and the ground surface located above the zone of freezing rises. This phenomenon is commonly known as frost heave. Figure 2.3 shows the hydraulic boundary conditions of the closed system, open system and the method of transforming open into a closed system by a layer of coarse sand that intercepts capillary flow toward the zone of freezing.

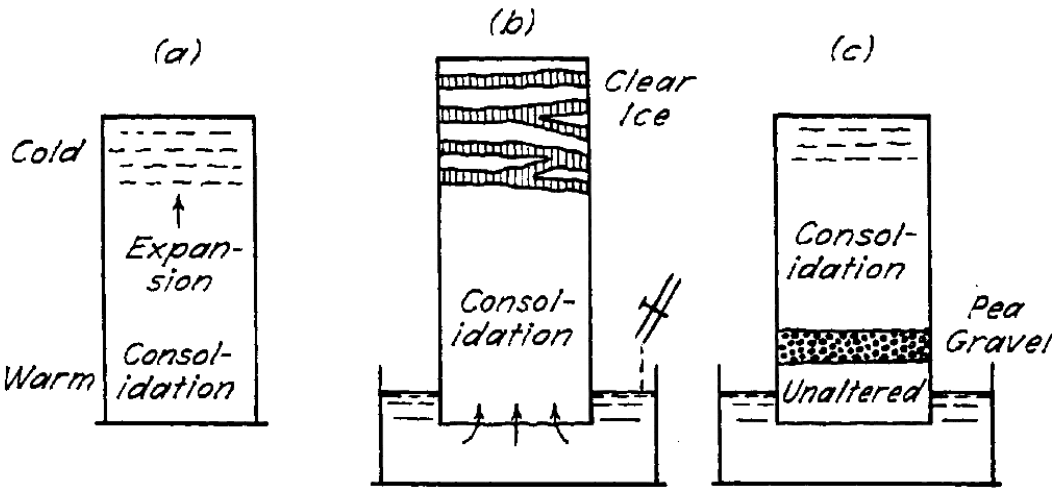

Fig. (2.3): Diagram illustrating frost action in soils (a) Closed system, (b) open system; (c) method of transforming open into a closed system (after Terzaghi et al. 1996).

Several frost heave models are available currently. The models are based on the fundamental principles of thermodynamics and on the experimental observations. The models have been proposed to understand the phenomenon of frost heave and to some extent also in predicting frost heave for engineering purposes, such as the models proposed by Harlan (1973), Gilpin (1980), Konrad and Morgenstern (1981), O'Neill and Miller (1985),Mu and Ladanyi (1987), Padilla and Villeneuve (1992), Nishimura et al. (2009), Thomas et al. (2009), Zheng et al. (2015) and Li et al. (2017).

2.3.5 Thaw settlement

Glendinning (2007) stated that as thawing of a frozen soil takes place, a volume change will occur. This volume change is caused by the phase change of ice to water and from the flow of excess water from the soil. When soil freezes under saturated and closed drainage conditions, in equilibrium with the overburden pressure, the soil will expand as the pore water changes state. The associated volumetric strain can be expressed as the ratio of the densities of liquid water and ice (0.09) multiplied by the porosity of the soil.

Upon thawing under undrained conditions, the soil is expected to return to its initial volume. Additional volume changes can be observed in drained conditions when the soil thaws which results from the mechanical effects, such as consolidation and soil structure changes that take place during previous freezing cycles (Andersland and Ladanyi 2004).

Earliest thaw consolidation tests were done by Tsytovich (1960). A typical result of the thaw-settlement experiment is shown in Figure 2.4. It can be seen that a small decrease in void ratio occurs under frozen conditions for an increase in load (point *A* to *B).* Upon thawing, a large decrease is observed (*B* to *C*) due to phase change and drainage of the excess pore water. The pressure σ_o is usually selected on the basis of the effective

overburden pressure for the field sample. Under an increase in pressure, Δσ, consolidation will take place until a new equilibrium void ratio is reached (point *D*).

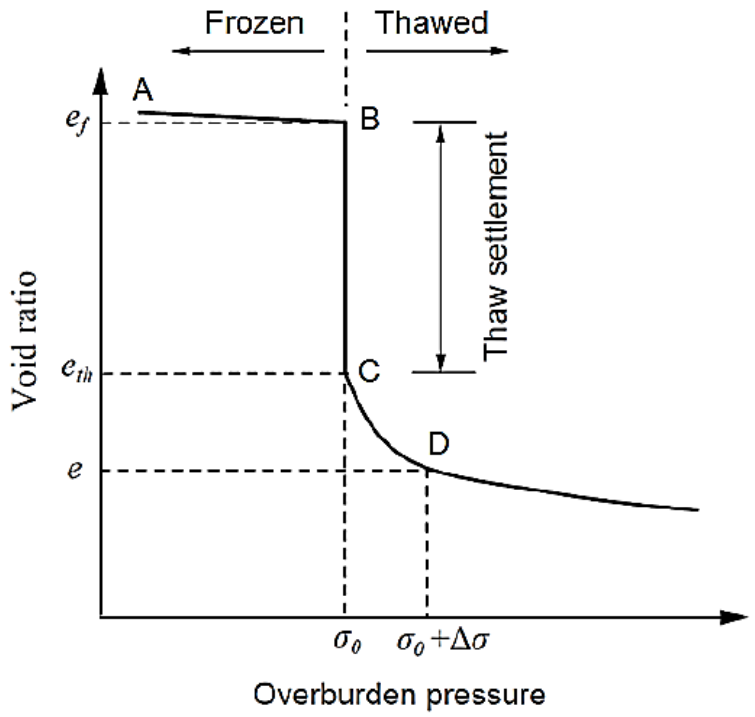

Fig. (2.4): Typical void ratio versus pressure curve for frozen soils subject to thawing (after Andersland and Ladanyi 2004)

Ballantyne and Harris (1994) stated that the generation of pore water pressures during the thawing process depends on the ratio between the rate of thaw and the rate of consolidation. This ratio is known as the thaw-consolidation ratio (*R*). Morgenstern and Nixon (1971) defined the thaw-consolidation ratio, *R*, as a relation between constant relating to depth of thaw (α) to the square root of time as given by the Neumann solution (Carslaw and Jaeger 1959) and is the coefficient of consolidation (C_v).

Morgenstern and Nixon (1971) reported that as a first approximation, a value of *R* greater than unity would predict the danger of pore water pressures being sustained at the thaw line, giving the possibility of instability. In order to validate the theory of one-

dimensional consolidation of thawing, Morgenstern and Smith (1973) and Nixon and Morgenstern (1974) conducted one-dimensional thaw consolidation tests on remoulded clays and undisturbed frozen Arctic soils in a specialised oedometer in which a sudden constant increase in surface temperature could be applied. The test results showed that the soil behaviour could be adequately represented by the theory.

The one-dimensional consolidation of thawing Arctic soils is discussed in further detail in Nixon (1973). Further investigations on thermal properties, the application of residual stress and slope failure of thawing soils was done by Nixon and McRoberts (1973), Nixon and Morgenstern (1973) and McRoberts and Morgenstern (1974).

2.3.6 Segregation potential

Several researchers have attempted to relate frost heave to soil index properties. Furthermore, a lack of uniformity of test equipment, test procedures, and techniques to interpret the results have some of the drawbacks of laboratory frost heave testing (Konrad 1987).

The segregation potential (SP_t) concept introduced by Konrad and Morgenstern (1980, 1981, 1982a, b) has provided the opportunity to develop an engineering approach to address field frost heave problems. Theoretically, the determination of SP_t from laboratory results requires the measurement of the water intake velocity and the temperature gradient in the frozen fringe in a step freezing test in which the soil response is at the "near steady state" condition. The segregation potential theory of frost heave states that the velocity of water arriving, v_φ, at the advancing frost front is related to the temperature gradient in the frozen soil just behind the frost front (Konrad and Morgenstern 1981, 1982b). The SP_t of soil can be determined using Equation 2.5:

$$v_\varphi = SP_t . \Delta T_f \quad \text{..... (2.5)}$$

where v_{φ} is the total water velocity supplied to the active ice lens and ΔT_f is the temperature gradient in the frozen fringe when the soil has reached a steady state condition.

The rate of heave is solely a result of the growth of the final ice lens, and the rate of volume change generated by frost heave is representative of the rate of water migrating to the ice lenses (Konrad and Morgenstern 1981). The total heave rate (*dh*/*dt*) can be calculated from Equation 2.6 (Konrad and Seto 1994):

$$dh/dt = 1.09\, v_{\varphi} \quad \text{.....(2.6)}$$

From Equations 2.4 and 2.5, the SP_t in terms of total heave rate can be found from Equation 2.6 as follow (Konrad and Seto 1994):

$$\mathrm{SP_t} = \frac{v_{\varphi}}{\mathrm{grad\ T_f}} = \frac{(dh/dt)/1.09}{\mathrm{\Delta T_f}} \quad \text{.....(2.7)}$$

The SP_t can be determined experimentally from Equations (2.5) to (2.7) using the corresponding heave rate data and the temperature gradient across the frozen fringe when thermal steady state condition is reached (Konrad and Seto 1994; Konrad 2005; Konrad and Lemieux 2005).

Many researchers have used the SP_t concept to analyse frost heave data from field and laboratory tests. It has been used successfully for predicting the frost heaving effect related to chilled pipelines and artificial ground freezing (Konrad and Morgenstern 1984; Nixon 1982,1992). Konrad (1987) introduced a procedure to calculate the SP_t based on accurate measurements of total heave by taking into account the amount of heave from the in-situ freezing of porewater which yields relevant freezing characteristics of soils.

Konrad (1989) used the concept of SP_t in analysing the laboratory results to show that the temperature of ice lens formation is a function of soil type, gradation, initial water content and void ratio. Konrad (1999) showed that the segregation potential is a good frost-susceptibility indicator, besides providing the possibility to predict frost heave in the field. Konrad (2005) reported that the prediction of segregation potential values, using the reference of frost heave characteristics approach, is more robust and reliable than other empirical approaches that do not specifically distinguish between clay and non-clay fines. Konrad and Lemieux (2005) showed that the segregation potential increases linearly with increasing the kaolinite fraction and that the freeze-thaw cycles had little effect on the value of segregation potential. Batenipour et al. (2012) presented the segregation potential of soils from the data collected from an instrumented full-scale engineered embankment. Recently, Hendry et al. (2016) assessed the frost heave susceptibility of Devon silt and the fines generated from the abrasion based on the rate of segregation heave and the segregation potential under certain freezing conditions.

2.4. Experimental studies of freeze-thaw cycles on soil behaviour

A number of researchers have studied the effects of freezing and thawing on various properties of soils, such as soil structure (Chamberlain and Gow 1979; Eigenbrod et al. 1996; Cui et al. 2014; Aldaood et al. 2014; Zheng et al. 2015), hydraulic conductivity (Chamberlain et al. 1990; Kim and Daniel 1992; Benson and Othman 1993; Bowders and McClelland 1994; Kraus et al. 1997; Viklander and Eigenbrod 2000; Konrad and Samson 2000 a, b; Konrad 2010; Jamshidi and Lake 2014; Fouli et al. 2013; Makusa et al. 2014), shear strength parameters (Simonsen and Isacsson 2001; Cui et al. 2014) and unconfined compressive strength (Solanki et al. 2013; Jamshidi and Lake 2014; Aldaood et al. 2014). Soils with significant fine fractions and exposed to freeze-thaw cycles have been found to show changes in the volume, strength, compressibility,

redistribution of pore water, densification and have exhibited microstructural changes, such as the formation of cracks and particle rearrangement (Konrad 1989c; Kim and Daniel 1992). The Atterberg limits have been shown to get affected. The bearing capacity was found to be reduced due to large pore water pressures when the frozen soil thaws (Viklander and Knutsson 1997).

Cyclic freeze-thaw actions may change the structure of the soils due to the cryogenic suction/pressure generated in the freezing process (Thomas et al. 2009; Wang et al. 2016), besides the change in soil structure particles that cause the formation of ice lenses (Taber 1930; Viklander 1998b). Therefore, the engineering properties of the soil could be changed after experiencing freeze-thaw cycles. The deformation induced by the frost heave and thaw settlement differs depending on the soil type and the stress history of soil (Chamberlain 1981b).

Experimental studies on soils experiencing cyclic freeze-thaw process started during the 1970s. One of the first tries to investigate the cyclic freeze-thaw on normally consolidated fine-grained soil was by Chamberlain and Gow (1979). The soil samples were frozen using a consolidometer apparatus with free access to water. Freeze-thaw cycling was repeated until little or no change in the void ratio, or permeability occurred. The structure and permeability of the tested soils were found to be changed after freeze-thaw cycles. The mechanism was interpreted based on the size of the mineral fraction of the fine soil using two highly idealised arrangements shown in Figure 2.5.

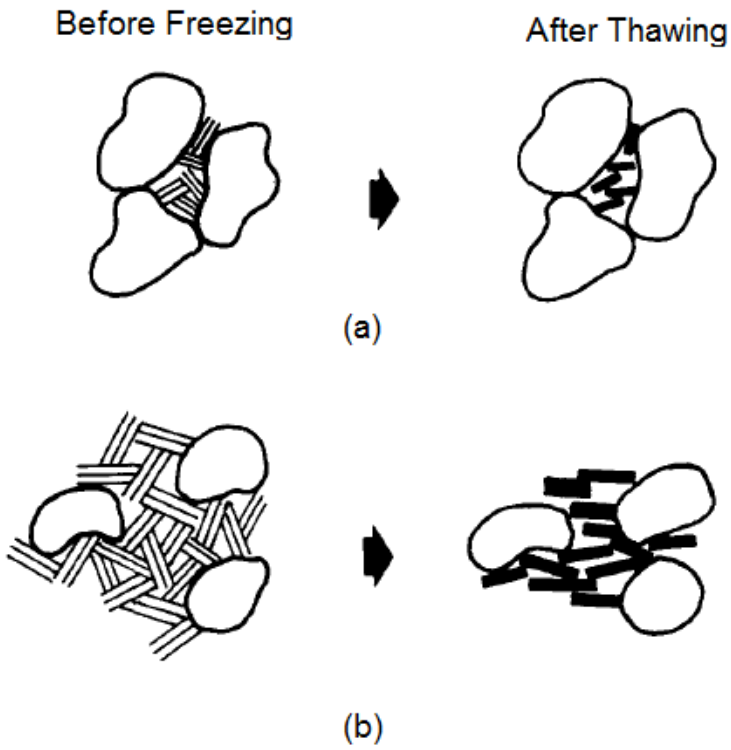

Fig. (2.5): Particle orientations after freeze-thaw cycle: (a) Clayey silts, (b) Silty clay (after Chamberlain and Gow 1979)

With reference to Figure 2.5, for fine soil with fewer clay minerals, such as clayey silts, the large particles (silt) control the packing, while the clay particles are arranged in packets with a flocculated orientation and free to move in the voids (Figure 2.5a). In this case, the coarse-grained particles control the compressibility, whereas the clay particles control the permeability. After freeze-thaw cycles, there is little or no change in the void ratio since the rearrangement of the coarse grains due to freezing is limited. However, the permeability increases because of the freeze-thaw cycles and cause the clay packets to collapse to a denser state, but the packets become more dispersed, leaving wider channels for fluid flow. For fine soil with mostly clay minerals, such as silty clay, the flocculated clay particles form a matrix in which the large grains float without being in contact with each other (Figure 2.5b). In this case, the clay particles control both the compressibility and the permeability. After freeze-thaw cycles, the clay packets are forced to rearrange into a more dispersed and denser state so that a noticeable decrease in void ratio occurs.

However, the densification of the soil does not reduce the permeability, rather the permeability increases because of shrinkage cracks formed after freeze-thaw cycles. Graham and Au (1985) also stated that the freezing caused the development of a clearly defined fissure structure. Softening at low stresses with access to water produced less marked effects.

Chamberlain (1981b) discussed the overconsolidation effect (suction forces) of freezing in soils and developed a method to determine the maximum suction that occurred during the freezing process. The results showed that the thaw settlement appears to be linearly related to the ratio of the initial water content to the plastic limit, and after a freeze-thaw cycle, a decrease in volume is observed as compared to the initial volume of soil before freezing.

Konrad (1989a) conducted repeated freeze-thaw tests on clayey silts with various overconsolidation ratios and found out that the void ratio of thawed soil decreased for lightly overconsolidated soils, but increased for heavily overconsolidated soils. The same research compared the segregation potential after each freeze-thaw cycle. It was observed that the segregation potential reduced after each freeze-thaw cycle, and most of the changes occurred during the first three cycles. Konrad (1989c) presented X-ray photographs of the soil specimens subjected to freeze-thaw cycles. The study indicated that the soil density changes (therefore the structure) and is caused by freezing occurring in the frozen zone at temperatures below that of the warmest ice lens. The tests also showed an increase in hydraulic conductivity of soils after freeze-thaw cycles, which was consistent with the findings of Chamberlain and Gow (1979).

Chamberlain et al. (1990) investigated the effect of freeze-thaw cycles on the permeability and structure of compacted silt-loam-clay soils. The results showed that freeze-thaw cycling caused the void ratio to increase slightly, probably because of the

expansion of water to ice. While the permeability did not follow a regular pattern of increasing or decreasing and the degree of saturation increased significantly after freeze-thaw cycling.

Cyclic one-dimensional open-system freezing and thawing tests were performed by Eigenbrod (1996) on soft, fine-grained soils. Depending upon the initial moisture content and plasticity of the soils, the volume change was found to be as high as 30% after thawing. Eigenbrod et al. (1996) monitored the pore water pressure in one-dimensional freezing and thawing tests on lightly overconsolidated fine-grained soils. The maximum negative pore pressure could be correlated to the compression observed in the soft clay specimen subjected to freezing and thawing, which is often referred to as freeze-thaw consolidation. In the study, stiff clay with water content close to plastic limit did not show freeze-thaw consolidation.

Viklander and Eigenbrod (2000) carried out one-dimensional open system type cyclic freeze-thaw tests on silty and sandy soil specimens with stone inclusions. The effect of compaction water contents on soil heave and stone movements at the end of each freeze-thaw cycle was studied as well. The study showed that both stone heave and soil heave were the highest for soils compacted at optimum water content and the amount of stone heave and soil heave decreased with increasing compaction water contents. There was no heave or stone movement at water content exceeding the optimum water content by 5 to 6 %.

Wang et al. (2007) studied the change in sample height and water content and the mechanical properties of compacted Qinghai–Tibet clay after exposing to a maximum of 21 closed-system freezing and thawing cycles. For the soil investigated, the height of the specimen increased, and the water content decreased with progressing of freeze-thaw

cycles during the first seven cycles. However, after seven freeze-thaw cycles, the movement and the water content of the soil remained constant.

Qi et al. (2008) conducted tests on a silty soil with one freeze-thaw cycle to investigate changes to the engineering properties of the soil. A critical dry unit weight was found beyond which the unit weight of soil, the cohesion and the pre-consolidation pressure decreased. Hui and Ping (2009) performed frost heave and cyclic freeze-thaw tests on red silty clay along the Qinghai-Tibet railway route to investigate the amount of frost heave, the distribution of moisture at the end of the experiment and the final dry density profile. The results showed that the amount of frost heave decreased with the number of freeze-thaw cycles, moisture contents increased in the freezing section and decreased in the unfrozen section, and the dry density of the soil increased in the lower parts and varied in the upper parts where the ice lens development occurred.

Konrad (2010) examined the influence of several freeze-thaw cycles on the hydraulic conductivity changes of a glacial till from Pe´ribonka in Quebec, Canada. Saturated slurried consolidated samples and compacted at dry side of optimum conditions samples were subjected to closed-system freezing, thawing as well as constant-head permeability tests. The results showed that the change in hydraulic conductivity is offset by thaw-induced settlements, which lead to a decrease in the void ratio of the soil. The freeze–thaw-induced decrease in the void ratio is essentially related to the void ratio prior to the freezing process.

Aldaood et al. (2014) investigated the impact of freeze-thaw cycles on the mechanical and mineralogical behaviour of gypseous soils stabilised with lime following the ASTM procedure. The water content and volume changes were evaluated for the tested specimen. The water content increased greatly in the first cycle and then slightly during

the following cycles in all the soil samples, whereas the volume change increased continuously with the number of cycles.

Wang et al. (2016) conducted tests that included frost heave-thaw shrinkage and microstructure changes during freeze-thaw cycles to evaluate the volume change rate of loess stabilised with cement, lime, and fly ash. The stabilised samples exhibited approximately 20% of volume change than the pure loess.

2.4.1 Influence of initial conditions on freeze-thaw behaviour

The initial void ratio and the degree of compaction have significant impacts on the microstructural changes taking place in the soil when exposed to freeze-thaw cycles. This process is schematically illustrated in Figure 2.6 for initially loose and dense soils. Viklander (1998a) stated that for the loose soil, the volume increase during freezing is caused by ice-lensing, and the volume decrease during thawing is due to the consolidation of the soil matrix. Therefore, the density tends to increase, and the larger soil particles come closer. On the other hand, in the initially dense soil, the volume tends to increase during freezing, and during thawing, most of the volume increase will disappear as the soil matrix consolidates. In the final condition, the volume remains the same as prior to freezing owing to the absence of microstructural changes. The soil particles, therefore, have essentially the same position after freeze/thaw as before freezing causing a net volume increase of the soil while making the soil structure slightly looser than prior to freezing. The findings reported by Chamberlain and Gow (1979) and Eigenbrod (1996) supported the earlier works.

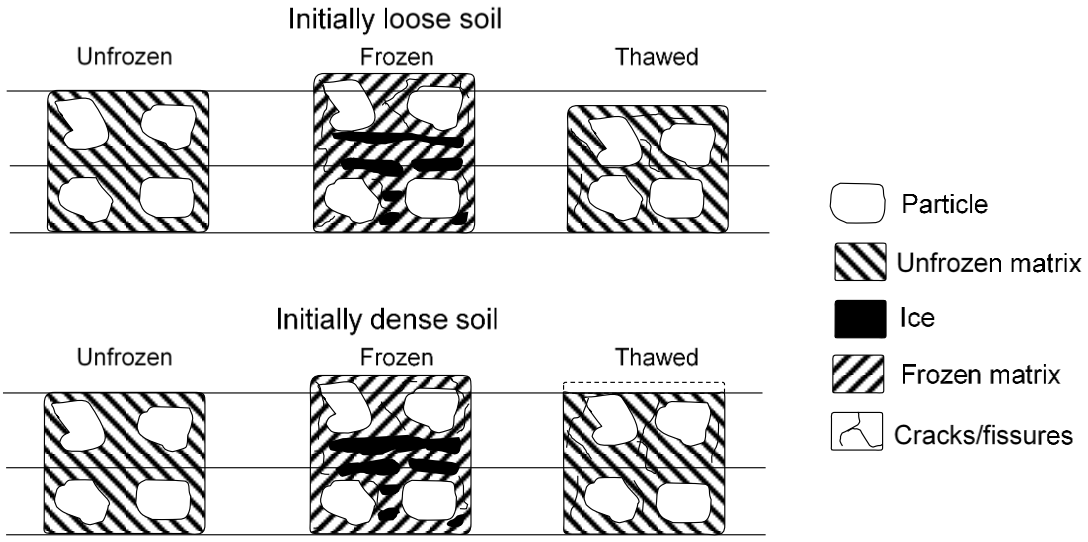

Fig. (2.6): Microstructural effects due to freezing and thawing (after Viklander 1998a)

Viklander (1998a) conducted a set of freezing and thawing tests on fine-grained non-plastic till, with each experienced eighteen freeze-thaw cycles. The void ratios decreased for samples with the initially high void ratio (e = 0.56) and increased for samples with the initially low void ratio (e = 0.25). The residual void ratio ranged from 0.31 to 0.40 for both initially dense and loose soils after 1 to 3 freezing cycles. Viklander (1998b) measured the movements of an embedded stone in compacted till using the X-ray technique after exposing the soil to 10 cycles of freeze-thaw. The finding supports the idea that a residual void ratio (e^{res}) exists in a till after a certain number of freezing and thawing (N_{res}). Soils with low initial void ratio will become looser, and the void ratio will approach the residual value, whereas the initially loose soils will become denser and the void ratio will also approach the ultimate residual value as shown in Figure 2.7.

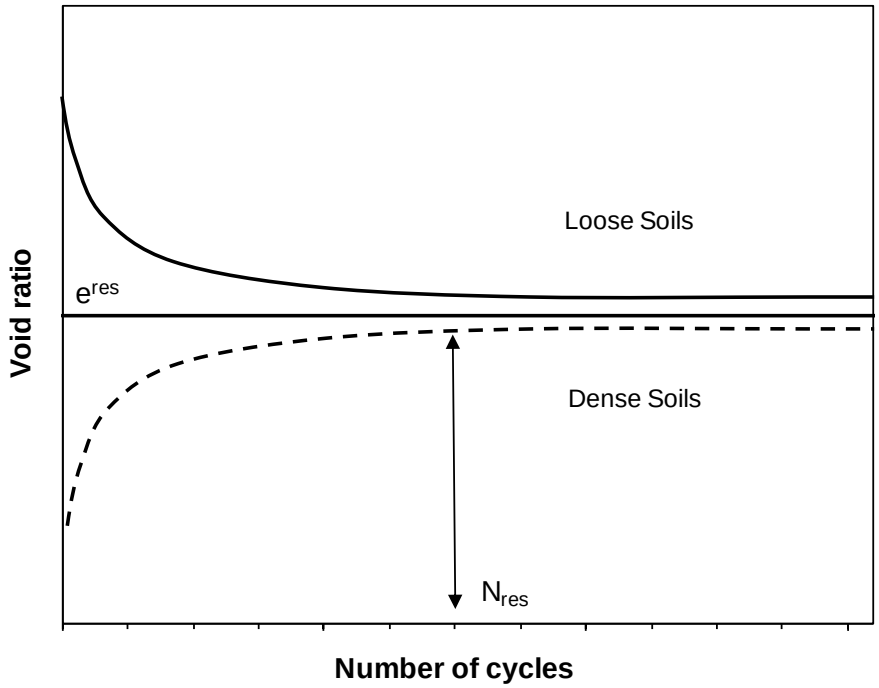

Fig. (2.7): Residual void ratio in terms due to number of freeze-thaw cycles (after Viklander, 1998a)

Qi et al. (2008) tested compacted samples of a silty soil (Lanzhou loess), with the dry unit weight ranging from 15.3 to 17.3 kN/m^3 and under different freezing conditions to explore freeze–thaw-induced changes on the engineering properties of the soil. They stated that under the same freezing condition, there is a critical dry unit weight which will influence the dry unit weight after freeze-thaw cycles. When the dry unit weight is smaller than the critical value, the soil is densified by freeze-thaw; when the dry unit weight is larger than the critical value, the dry unit weight of the soil decreases. Soils compacted at critical dry unit weight; the dry unit weight remains unchanged after freeze-thaw cycles. These findings are quite compatible with the conclusions reported by Wang et al. (2015).

2.4.2 Factors affecting the volume change behaviour of soils due to freezing-thawing

Besides the effects of soils types and its classification on the frost heave and thaw settlement that reported in sections 2.3.4 and 2.3.5, one of the most important factors that influence the volume change behaviour soils during freezing-thawing cycles is the freezing rate or the cooling rate (Penner 1986; Konrad 1987; Konrad 1988; Benson and Othman 1993). Svec (1989) stated that a thinner freezing fringe accompanied by a lower segregation temperature would result in a higher rate of heave. In the high range of frost-penetration rates, the freezing process becomes so fast that there is not enough time to establish significant water flow between successive locations of ice segregation sites. As a result, the heave rate must decrease.

The ice segregation takes place if the pore pressure reaches a threshold value and a new ice lens forms in the direction of heat removal (Miller 1978; Gilpin 1980; O'Neill and Miller 1985; Nixon 1991). Moisture accumulation and the volumetric expansion due to pore water phase change in both the fully frozen soils and ice lens result in the frost heave (Thomas et al. 2009). Therefore, researchers have used different types of insulation to ensure one-dimensional heat removal (Chamberlain et al. 1990; Eigenbrod 1996; Viklander 1998a, b).

2.5 Cyclic wet-dry behaviour of soils

Wetting-drying processes are considered to be linked to the seasonal weathering processes. These processes tend to modify the mechanical properties of soils. Weathering causes both physical and chemical phenomena in which air and water play a major role (Gullà et al. 2006). Many researchers have studied the effects of wetting-drying cycles on the engineering and physical properties of soils, such as the change in fabrics (Kodikara et al. 1999; Seguel and Horn 2006; Nowamooz and Masrouri 2010a, b), the unsaturated

haydraulic condictivity (Fredlund et al. 1994; Boardman and Daniel 1996; Huang 1998; Lin and Benson 2000; Malusis et al. 2011) and the unsaturated shear strength parameters (Allam and Sridharan 1981; Gan and Fredlund 1996; Vanapalli et al. 1996; Gallage and Uchimura 2006; Guan et al. 2010; Goh et al. 2014; W. Liu et al. 2016a), besides the therotical models to simulate the wer-dry behaviour (Gallipoli et al. 2003a, b; Gallipoli 2012).

Numerous investigations have been conducted that have focused on the change of volumetric and mechanical properties of soils due to wetting-drying cycles (Osipov et al. 1987; Dif and Bluemel 1991; Al-Homoud et al. 1995; Pardini et al. 1996; Sivakumar et al. 2006). Fine-grained soils undergo volume increase (swell) when the water content is increased as a consequence of suction reduction. On the other hand, an increase in suction results in a reduction in the volume of collapsible soil and induces shrinkage due to a reduction in the water content (Fredlund and Rahardjo 1993).

The effects of cyclic wet-dry processes on the volume change behaviour of soil are related to swelling and shrinkage behaviour of expansive soils. Expansive soil is a term generally applied to any soil or rock material that has the potential for shrinking or swelling under changing water content. An increase in water content causes the soil to swell. The shrinkage of soil is caused by evaporation and evapotranspiration. Problems associated with expansive soils are widespread throughout the five continents (Chen 2012).

A number of research studies are available on laboratory cyclic swell-shrink tests on compacted expansive soils. Day (1994) studied the cyclic swell-shrinkage behaviour of a compacted silty clay soil by inundating soil samples in distilled water and dried the samples under the sunshine. The soil exhibited near constant swelling and shrinkage strain after several wet-dry cycles. The results showed that the first cycle of wet-dry

produced low values of both swell and shrinkage, but the amount of swell or shrinkage dramatically increased with the increasing of cycles and as a result increased in the volume of the compacted silty clay soil. Al-Homoud et al. (1995) investigated the swell-shrinkage behaviour of six collected soils from different locations of Irbid, Jordan. The results showed that equilibrium in terms of deformation occurred after 4 to 5 swell-shrink cycles accompanied by rearrangement of particles during cyclic wetting and drying processes.

Swell-shrink tests involving full and partial shrinkage cycles on four selected expansive soils are reported by Basma et al. (1996). The result pointed out that an equilibrium can be attained after several cycles. Destruction of large aggregates and fabric changes were found to take place with increasing number of cycles. Tripathy et al. (2002) used a modified odometer setup to conduct cyclic swell-shrink tests. The results showed that the equilibrium swell-shrink path in terms of water content and void ratio depends upon the surcharge pressure and swell-shrink pattern. Subba Rao and Tripathy (2003) studied the effect of ageing on the swell-shrink behaviour under various surcharges. The results showed that the ageing effect remains (a decrease in swelling strain) for soils subjected to lower shrinkage magnitudes. The effect of a change in swell-shrinkage pattern was also studied by Tripathy and Subba Rao (2009). The results showed that the equilibrium state was accompanied by fatigue of swelling and a decrease in the volumetric strain for the specimens subjected a greater shrinkage magnitude.

Rosenbalm and Zapata (2017) conducted tests involving wetting-drying cycles to study the volume change behaviour of soils collected from Anthem, Arizona, and Denver, Colorado. The samples were tested at different initial compacted conditions and at different net normal stresses. The results showed that the swelling and shrinkage strains and the swell pressure reached equilibrium after four cycles of wetting and drying.

2.6 Testing devices for studying freeze-thaw and wet-dry behaviour of soils

Several devices have been used to study the effect of freeze-thaw and wet-dry cycles on the volume change behaviour of soils. Some of the devices are based on conventional devices, particularly for performing the cyclic wet-dry tests. Most of the devices used so far for conducting freeze-thaw tests are uniquely designed. The following sections review the main features of some of the devices.

2.6.1 Freeze-thaw test devices

U.S. Army Cold Regions Research and Engineering Laboratory (CRREL) consolidometer (Figure 2.8) was one of the first apparatus that used to study the effect of freezing and thawing on the volume change and permeability fine-grained soils. It consists of a Teflon-lined Plexiglas cylinder with a 63.5-mm inside diameter and 152.4-mm outside diameter and contains thermoelectric cooling devices for controlling unidirectional freezing (Chamberlain et al. 1990)

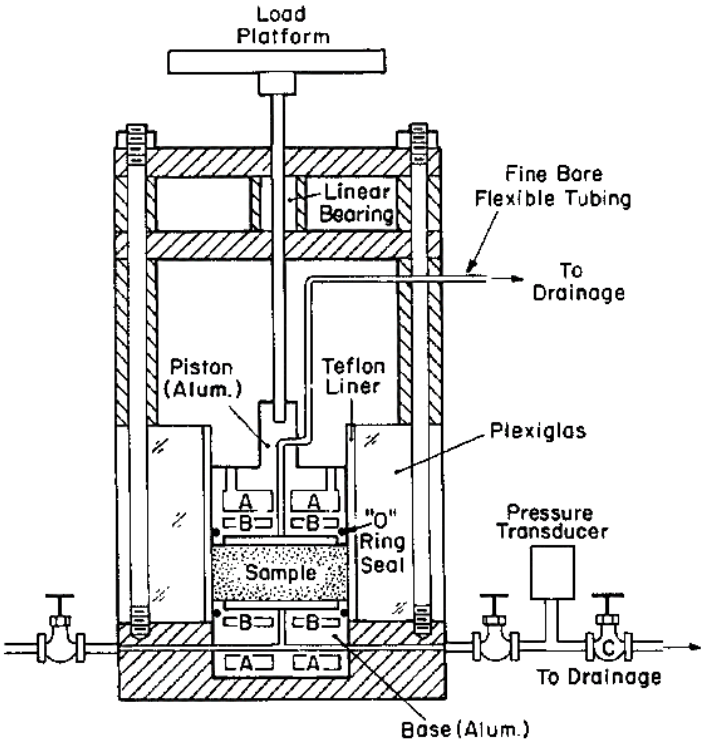

Fig. (2.8): Consolidometer for freezing-thawing on soils permeability test (after Chamberlain and Gow, 1979).

Eigenbrod (1996) used an open system device for conducting cyclic freeze-thaw tests on soft normally consolidated clays at low-stress levels (Figure 2.9). The test setup consisted of a PVC cylinder with an inside diameter of 95 mm and a height of 210 mm. Lithium grease was applied to the walls of the cylinder to mitigate adfreezing effect (i.e. frictional resistance developed between soil specimen and the cylinder wall during the freezing process). A continuous supply of water was made to the specimen placed inside insulated boxes to ensure one-dimensional freezing. The vertical deformation was recorded during the test by using a dial gauge.

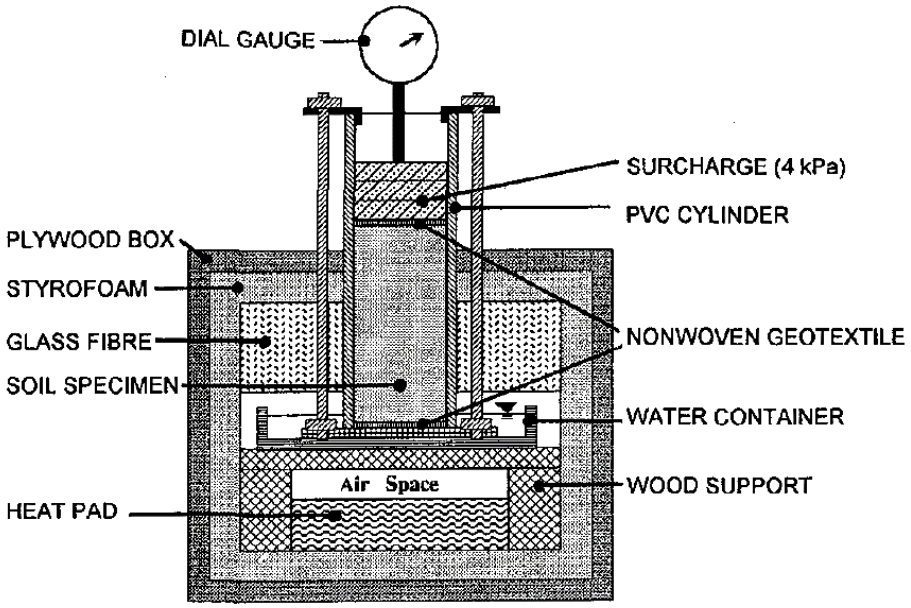

Fig. (2.9): Setup for one-dimensional, open system cyclic freezing-thawing tests (after Eigenbrod, 1996)

Viklander (1998) tested the permeability of small and large samples of a fine-grained till by using three different types of rigid-walled permeameters (52, 77, 297 mm in diameter, and 180, 450, 380 mm in height) (Figure 2.10). For freezing, two different methods were used. In the first method, the perimeter of the largest cylinder was covered by 70 mm of insulation (Styrofoam). Thus, the sample was frozen and thawed one-dimensionally in a closed system, in each stage at a constant temperature. The smaller cylinders were covered with 50 mm Styrofoam insulation to ensure one-dimensional freezing in a closed system by storing in a cold-room. The perimeter of the cylinders and the base were insulated. Therefore, the freezing propagated in one dimension from the upper surface.

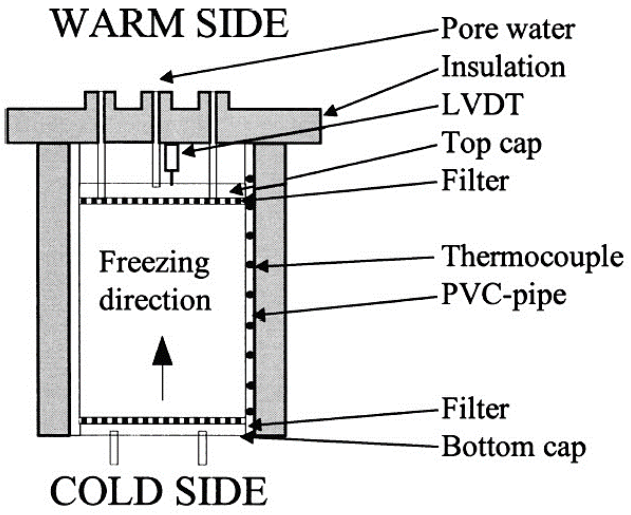

Fig. (2.10): A view of large rigid wall PVC parameter type "F" (after Viklander, 1998a)

A plexiglass cylinder (Figure 2.11) was used by Viklander and Eigenbrod (2000) for testing a silty sandy soil in order to study movements of embedded stones and to measure how the overall permeability was influenced by freeze-thaw cycles in an open-system cylinder. The bottom of the soil was connected to an external water supply in order facilitate unrestricted ice lens formation during freezing and drainage during thawing. The cylinders were 250 mm in high with a diameter of 100 mm. The vertical movements were measured along a rod, which was attached to the stone and extended above the soil surface.

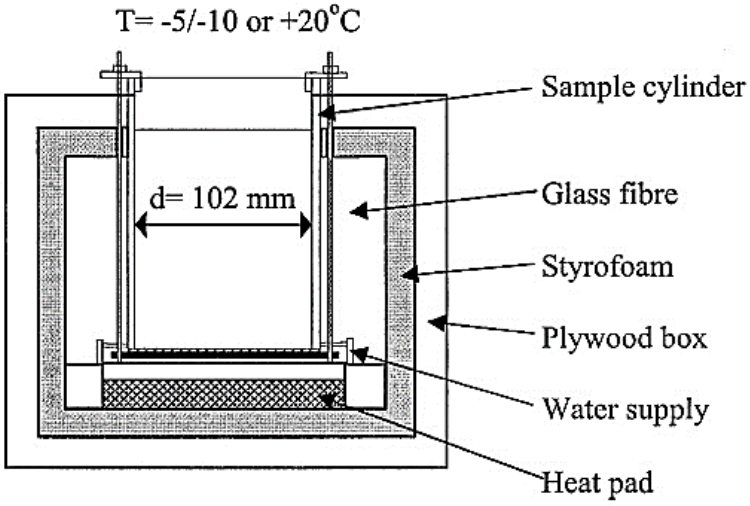

Fig. (2.11): Laboratory equipment used in test (after Viklander and Eigenbrod 2000)

Qi et al. (2008) carried out freeze-thaw tests on a compacted silty soil samples. All soil samples had a diameter of 101 mm and height of 150 mm (Figure 2.12). The prepared samples were placed in a cell and then placed in an environmental box for freeze-thaw processes in a closed-system (i.e. no water supply was made during the tests). Some vaseline was applied on the wall of the cell to reduce the frictional effect on frost heave and thaw settlement. The samples were frozen unidirectionally from the top under a constant temperature. The freezing process was stopped when frost heave ceased. The samples were then allowed to thaw until thaw settlement stabilised.

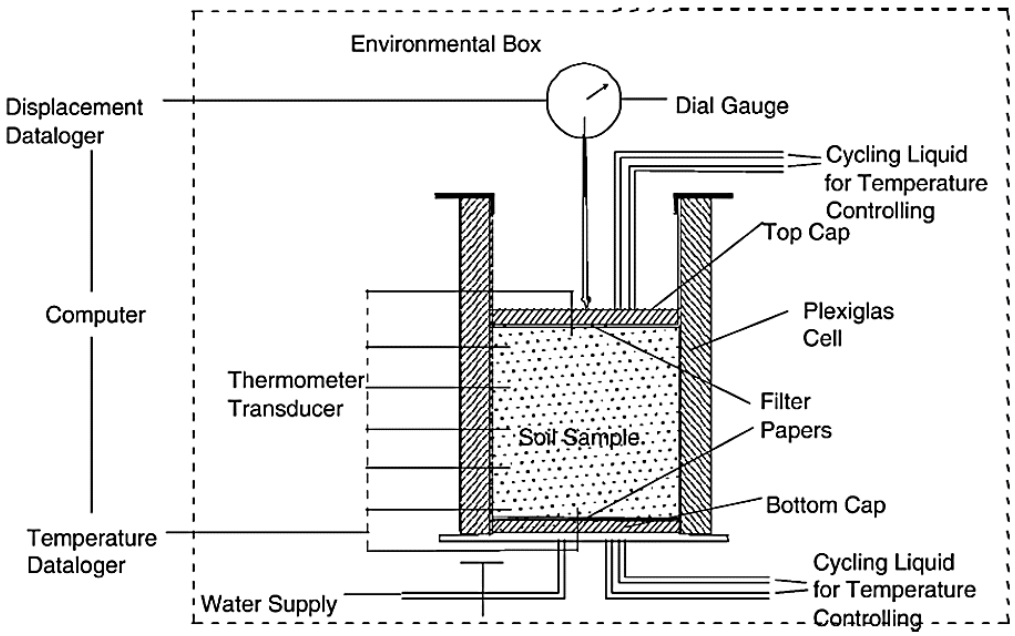

Fig. (2.12): A schematic diagram of the freeze-thaw apparatus (after Qi et al. 2008)

Wang et al. (2015) used a testing system to determine frost heave and thaw subsidence of subgrade fill materials from the Nagqu Logistics Center Yard (NLCY) along the Qinghai–Tibet railway. The test set up consisted of a sample cell, top and bottom cold plates, commercial constant-temperature cold baths, a Markov bottle, insulation cotton, temperature and displacement sensors and a data acquisition system, as shown in Figure 2.13.

.

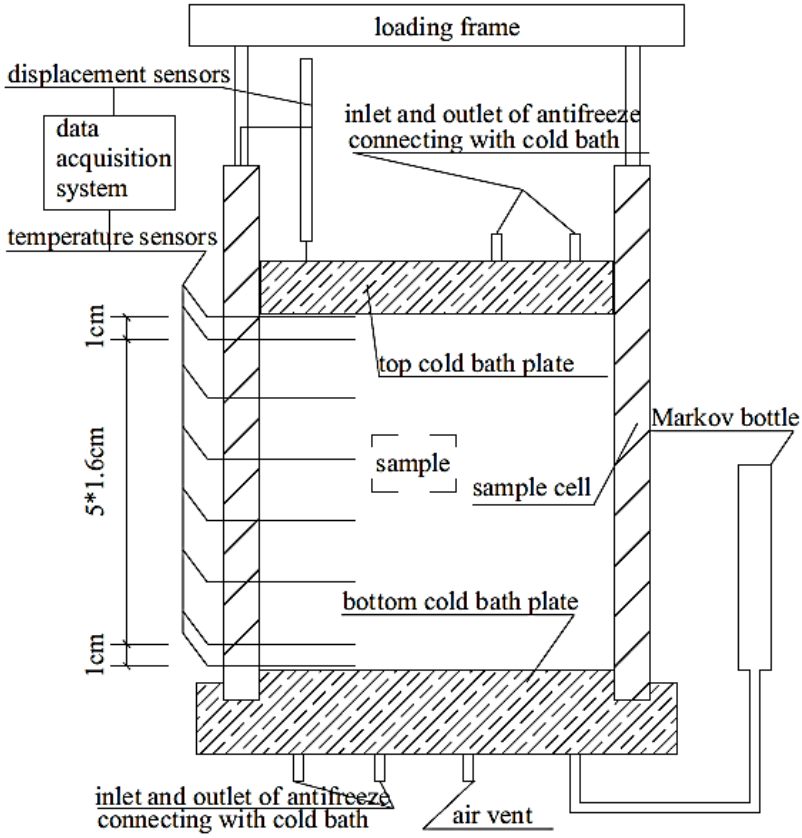

Fig. (2.13): Test devise for frost heave and thaw subsidence tests (after Wang et al. 2015)

Based on the reviewed devices the following are considered to be the main features of the freeze-thaw test set ups: (*i*) the specimen size allowed exposure to freeze and thaw processes, (*ii*) the side insulation exists to ensure the unidirectional freezing, (*iii*) the temperature change measured at several locations along the length of the tested specimens, (*iv*) appropriate arrangements were made to mitigate the friction and adfreezing effects during heaving of the specimens, and (*v*) the source of water satisfied an open-system of testing.

2.6.2 Wet-dry test devices

Tripathy et al. (2002) conducted cyclic swell-shrink tests on compacted specimens of expansive soils using a modified fixed ring oedometer cell (Figure 2.14). Soil samples were compacted to a height of 13 ± 0.5 mm directly in a stainless steel oedometer ring,

76.2 mm in diameter and 38 mm in height. The apparatus facilitated swelling, as well as shrinkage of the soil specimens under predetermined surcharge pressures. The setup consists of a fixed-ring oedometer cell placed inside a stainless-steel container (outer jacket). The outer face of the outer jacket holds a 1 kW capacity coil tightly sandwiched between two flexible asbestos sheets. The flexible asbestos sheets serve as an insulator. The two ends of the coil were connected to porcelain connectors to which power was provided through a temperature controller. A known surcharge pressure was applied to each specimen using the lever arm of action of the oedometer frame. The same device was used by Tripathy and Subba Rao (2009) to study in detail the effect of changes in shrinkage pattern on the swell-shrink behaviour of compacted expansive soils.

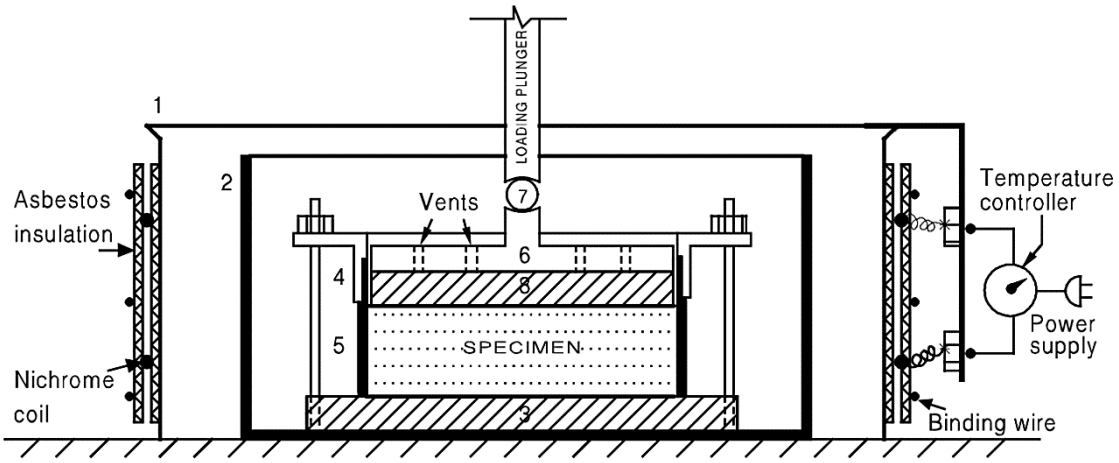

Fig. (2.14): Schematic diagram of the experimental setup. 1, outer stainless steel jacket; 2, water jacket; 3, bottom porous stone; 4, outer ring; 5, specimen ring; 6, pressure pad; 7, pressure ball; 8, top porous stone(after Tripathy et al. 2002).

Dif and Bluemel (1991) studied the effect of cyclic drying and wetting on the volume change behaviour of undisturbed specimens of expansive soils using a modified oedometer cell (Figure 2.15). The cell was made of Perspex to minimise the weight of the apparatus so that weighing accuracy was ensured. The modified cell was calibrated according to ASTM D 2435. The deflections from the calibration test were subtracted

from the deflection of the test of samples for each load increment. All specimens were 70 mm in diameter and 20 to 25 mm in thickness to minimise the side friction effect.

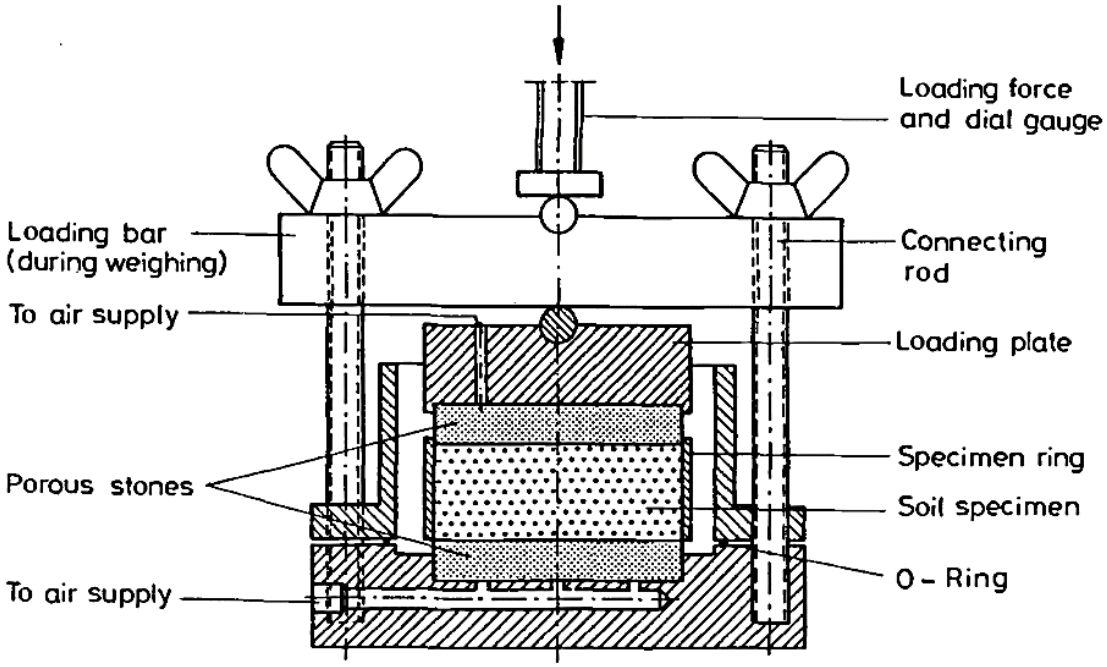

Fig. (2.15): The modified oedometer cell (after Dif and Bluemel 1991)

Al-Homoud et al. (1995) and Basma et al. (1996) used a conventional odometer to carry out swell-shrink tests of expansive soils. The soil samples were air-dried to initial water content within the laboratory environment. Several other researchers have studied the volume change response of soil samples subjected to wetting and drying cycles with the controlled suction technique (Alonso et al. 2005; Liu et al. 2012; Nowamooz et al. 2013).

It can be recognised that the technique used for assessing the volume change behaviour under wet-dry cycles is less complex than the freeze-thaw tests. In the cyclic wet-dry tests the temperature along the specimens was measured. The source of heating is not essential to conduct drying cycles. The specimens used were smaller than the dimensions of the specimen needed for freeze-thaw tests.

2.7 Combined freezing, thawing, wetting and drying effects on soils

One of the earliest research on the combined effects of the four processes (wetting, drying, freezing and thawing) is reported by Sillanpää and Webber (1961). These researchers studied the change in the mean weight diameter (MWD) of aggregates, which is the sum of the mass fraction remaining on each sieve after sieving multiplied by the mean aperture of the adjacent sieves (Legout et al. 2005). The tests conducted on three fractions (natural aggregates of size 2 to 3 mm, aggregates prepared by crushing the natural aggregates and aggregates obtained from sieving dry soils). The materials were exposed to many cycles of wetting-drying before implementing freezing-thawing cycles in predetermined sequences. They found that the wet-dry cycles increased the MWD of larger particles, but it has a limited effect on the smaller aggregates, whereas the cyclic freeze-thaw significantly decreased the MWD of the large aggregates and increased in the case of crushed aggregates.

Several researcheres have studied the effects of freezing-thawing separately from wetting-drying effects on soils. Pardini et al. (1996) investigated the freezing-thawing or wetting-drying cycles on erosion effects on the structure and porosity of a clay-silt soil from Spain. They stated that changes in the water content and structural modification of soils may occur due to the weathering processes. Priemé and Christensen (2001) investigated the effects of drying-wetting and freezing-thawing on the emission of nitrous oxide, carbon dioxide and methane from soil cores from sites in three different countries. Similarly, Daou et al. (2016) determined the impact of climatic processes on soil microbial functions of four different soils under various series of freezing-thawing or drying-rewetting cycles. Additionally, some researchers have investigated the impacts of weathering processes on various properties of rocks (Kim 2013; Özbek 2014). A study of the effect of heating and freezing temperatures on the pore size distribution of saturated

kalinite clays is reported by Darbari et al. (2017) using scanning electron microscope/focused ion beam (SEM/FIB) techniques. They stated that the increase in the size of the larger pores was found to be more than the increase in the size of the small pores upon freezing because of the larger water volume in the former, whereas the smaller pores increase in size upon heating, while the size of the larger pores decreases as a result of the anisotropic thermal expansion coefficient of clay particles.

Testing the durability regarding compressive strength and a loss of weight of soil of stabilised soils against both the effects of freezing-thawing and wetting-drying cycles have been studied according to ASTM D560/D560M (2015) by Ahmed and Ugai (2011). They investigated the effect of environmental factors in terms of freeze-thaw and wet-dry cycles, on the durability of soil stabilised with recycled gypsum ranging from 0 to 20%. They stated that freeze-thaw cycles have a significant effect on the durability reduction of stabilised soil as compared to the effect of wet-dry cycles. Similarly, Diagne et al. (2015) tested the durability of recycled clay bricks (RCB) mixed with recycled concrete aggregates (RCA) as an unbound base course in road construction with different mixtures under a number of freeze-thaw and wet-dry cycles and its effects on the soil-water characteristic curve (SWCC). The results showed that the durability of pavement could be influenced by repeated freeze-thaw cycles, wet-dry cycles, or a combination of both.

Gullà et al. (2006) investigated the effects of wetting-drying-freezing-thawing cycles on the compressibility and shear strength of overconsolidated natural clay from south Calabria, Italy. The standard equipment (oedometer and direct shear box) were used in the study. The results showed that cycles of different processes caused a change in the initial microstructure, a decrease in the compression index, an increase in the swelling index and a decrease in the peak shear strength of the soil. Recently, Kong et al. (2017) conducted dry-wet-freeze-thaw cycles on a yellow-brown swelling mudstone from the

Jilin-Hunchun high-speed railway line in Yanji, China. The changes in shear strength characteristics were studied using consolidated drained (CD) triaxial test and microstructure investigation were carried out on the samples as well. The results showed the shear strength decreases as the number of dry-wet-freeze-thaw cycles increases.

From different perspectives, the comparison between the soil-freezing characteristic curve (SFCC) and soil-water characteristic curve (SWCC) was made by many researchers as an attempt to link the frozen-unsaturated properties of soils. Koopmans and Miller (1966) measured both the SFCC and SWCC for three different soils and stated the similarity between both curves due to the similarity in the physical processes that the soil experienced. Therefore, the SFCC can be used as a tool to estimate or predict the SWCC (Black and Tice 1989; Spaans and Baker 1996; Liu et al. 2013; Ma et al. 2017). Additionally, Ren and Vanapalli (2017) stated that the SFCC exhibits hysteretic behaviour similar to the SWCC.

From a detailed review of the literature presented in this chapter, it can be concluded that research works on the combined effects of the weathering processes (freezing, thawing, wetting and drying) on the volume change behaviour of geomaterials are very limited. Reported works on various particulate geomaterials with different physical and chemical properties and their response to cycles of dry-wet-freeze-thaw cycles are scarce. The impact of climate change may cause exposure of geomaterials to processes that the materials had never encountered before. Some of the examples are the soils from the Middle East, and similar examples can be drawn from a number of other places which are currently being exposed to excessive drying and flooding conditions. Additionally, the materials that currently undergo freeze-thaw cycles may be subjected to wet-dry cycles in the future. Similarly, the materials that currently undergo dry-wet cycles may be subjected to freeze-thaw cycles. Therefore, there is a need to explore the volume

change behaviour of various geomaterials by exposing the materials to a combination of a variety of anticipated weathering patterns. This research, therefore, aims to explore the volume change behaviour of geomaterials under predetermined weathering patterns (freezing-thawing, wetting-drying with intermittent freeze-thaw cycles and dry-wet-freeze-thaw cycles).

2.8 Concluding remarks

In this chapter, a brief review of the concepts of freezing, thawing, wetting and drying as well as the volumetric response of soils to these processes are presented. A review of the experimental research of both cyclic freeze-thaw and cyclic wet-dry on various properties of soils were included. The testing devices used for studying the effects of both cyclic wet-dry and freeze-thaw processes on the volume change behaviour of soils are presented. Additionally, studies involving various weathering processes and their effects on various properties of soil are discussed to highlight the scientific research gap.

A review of literature highlighted some specific aspects related to freezing, thawing, wetting and drying of soils. These include:

(1) The volume change response depends upon the properties of soils.

(2) The initial conditions and freezing mode have significant effects on the frost heave of frost-susceptible soils

(3) In general, the size of tested specimens for studying the freeze-thaw effects is larger than the specimens for studying the wet-dry effects.

(4) Different techniques and procedures have been used by various researchers to conduct either cyclic freeze-thaw or cyclic wet-dry tests.

(5) The temperature changes along the depth of samples during freeze-thaw tests are required for analysing and interpreting the test results.

(6) The combined effects of freezing, thawing, drying and wetting on geomaterials have not been fully investigated yet.

CHAPTER 3

Materials and methods

3.1 Introduction

The engineering properties of soils (viz., volume change, shear strength, permeability) depend upon the physical properties of the soil solids and chemical properties of the pore fluid (Mitchell and Soga 2005). This chapter presents the properties of materials used in this research. The compaction characteristics and consolidation behaviour of the materials used are presented along with the fabric and structure of the materials under selected conditions. The device used along with the main features, description of the components and the working principles are presented. The experimental program, the experimental methods and the procedures adopted for preparing specimens for various laboratory tests are described. The works presented in this chapter are summarised at the end of this chapter.

3.2 Materials used

The investigation has been carried out on three different materials, namely a kaolinite-rich clay, Speswhite kaolin, a frost susceptible natural soil collected from Pegwell Bay, known as Pegwell Bay soil, and a cement kiln dust collected from a local cement industry. The next sections discuss each of these materials.

3.2.1 Speswhite kaolin

Speswhite kaolin is highly refined kaolin with ultra-fine particle sizes. Speswhite kaolin was procured from IMERYS Minerals Ltd., Par, Cornwall, U.K. Speswhite kaolin has been extensively used by several researchers to study the behaviour of unsaturated soils (Cao et al. 2002; Sivakumar et al. 2007; Thom et al. 2007; Sivakumar et al. 2010; Boyd and Sivakumar 2011; Tripathy et al. 2014; Sivakumar et al. 2015). The frost heave response of Speswhite kaolin have been reported (Hendry et al. 2016).

3.2.2 Pegwell Bay soil

The geological formation seen in various parts of eastern Kent in South East England suggests that the area was underlain by continuous permafrost during the Dimlington Stadial (26-13 14C ka BP) (Ballantyne and Harris 1994). The Pleistocene periglaciation has resulted in the formation of high frost susceptible chalk, periglacial and aeolian sediments in Pegwell Bay (Figure 3.1). An aeolian deposit (wind-deposited soil) usually contains sand and silt as the main constituents. Disturbed samples of Pegwell Bay soil were collected from Pegwell Bay, Kent, U.K, during a periglacial and glacial engineering field trip organised by University of Sussex (site location shown in Figure 3.2). The loess was chosen as one of the test materials in this study because it has been extensively used in research dealing with frozen soil and many published data are

available on the characteristics of such soils (Fookes and Best 1969; Weir et al. 1971; Le Riche 1973; Derbyshire and Mellors 1988; Murton et al. 2003).

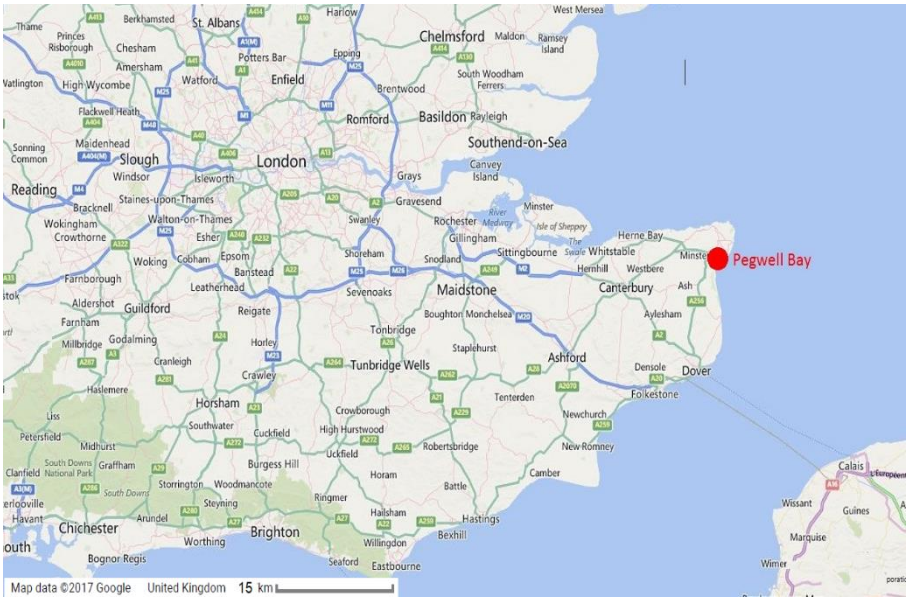

Fig. (3.1): Map showing Pegwell Bay (Google Inc. 2017)

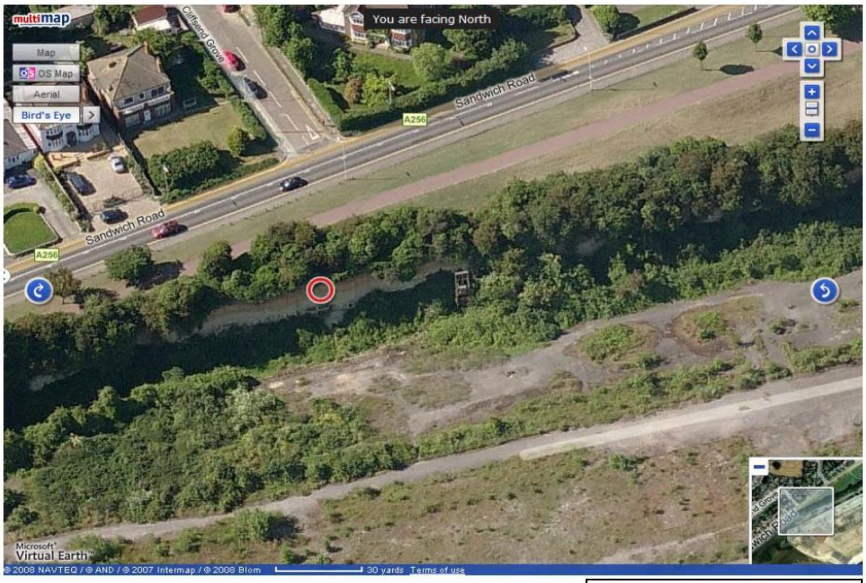

Fig. (3.2): Sampling site at Pegwell Bay (the photograph is extracted from the field trip information brochure)

3.2.3 Cement kiln dust

The cement kiln dust (CKD) is a fine powdery material that is formed during the cement manufacturing process. The accumulated amount of CKD is a source of concern due to the disposal problems associated with the material. More than 3,500,000 metric tons of CKD that are unsuitable for recycling during the cement manufacturing process are disposed of in the United States (Todres et al. 1992). Studies in the past have explored the suitability of the material in various civil engineering applications (Baghdadi et al. 1995; Moon et al. 2008; Albusoda and Salem 2012). CKD samples are usually collected from electrostatic precipitators during the production of cement clinker (Siddique 2006). The cementitious properties of CKD make this by-product an effective stabiliser for stabilising weak soils (Siddique 2006; Sariosseiri and Muhunthan 2008; Solanki et al. 2013). A number of studies have reported the permeability, compressibility and shear strength behaviour of CKD-soil mixtures (Baghdadi et al. 1995; Miller and Azad 2000; Albusoda and Salem 2012; Nasr 2015). Studies concerning the volume change behaviour of CKD due to freezing, thawing, drying and wetting processes have not been explored in the past. The CKD used in this investigation was supplied by a local cement company.

3.3 Properties of materials used

The properties of the materials studied are presented in the following sections.

3.3.1 Initial water content

The initial water contents of the materials were determined by oven drying method. The materials were dried in an oven at 105 °C (BS 1377-2 1990). The initial water content of Speswhite kaolin was found to be 1.1%. Similar values of the initial water content have been reported by other researchers (Singh 2007; Tadza 2011). The

initial water content of Pegwell Bay soil samples were found to vary between 5.3 to 8%. These values of initial water contents of the soil were anticipated since the samples were collected after a rain fall event. The soil samples were pulverised, mixed and stored in airtight containers prior to using for various laboratory tests. The initial water content of the CKD was found to be about 0.2%. The initial water contents of the materials were considered during preparation of specimens for various tests.

3.3.2 Specific gravity

The specific gravity of the materials was determined by pycnometer method (BS 1377-2 1990). Deionized water was used for determining the specific gravity of the Speswhite kaolin and Pegwell Bay soil, whereas kerosene was used for determining the specific gravity of the CKD. The specific gravity of Speswhite kaolin was found to be 2.61. The values of the specific gravity of Speswhite kaolin reported by several researchers (Cao et al. 2002; Singh 2007; Tripathy et al. 2014; Chung et al. 2016) were found to be similar to that found in this study. The specific gravity of Pegwell Bay soil was found to be 2.69. Derbyshire and Mellors (1988) have reported a similar value of specific gravity for the soil. The specific gravity of the CKD was found to be 2.72.

3.3.3 Particle size distribution

The grain size distribution curves of the materials were established by using a laser diffractometer. A Malvern Mastersizer X3000 laser diffractometer (Malvern Instruments Ltd., Malvern, U.K) was used for this purpose. The diffractometer employs two forms of optical configuration, such as a conventional Fourier optics and a reverse Fourier optics that allow measuring scattering at much higher angles. Thus, using the diffractometer, a particle size up to 0.1 mm can be detected. The diffractometer consists of a helium-neon red laser source, a flow cell, an optical lens and a detector. The helium-

neon laser source forms a collimated and monochromatic beam of light known as the analyser beam. The flow cell accommodates a soil suspension. The suspension comprises of soil sample mixed with deionized water. For minimizing the flocculation, a dispersion unit is used to mix the dry soil sample and water by a mechanical stirrer that disperses the particles by the ultrasound system. The dispersion unit is a sample feeder that pumps the soil suspension into the flow cell where the analyser laser beam falls on the individual particle and gets diffracted. The optical lens collects the diffracted light and focus it onto the detector. The detector remains stationary and coaxial with the laser axis regardless of particle movement in the flow cell and analyses the diffracted light and sends the information to a computer for processing.

For any material considered (Speswhite kaolin, Pegwell Bay soil and CKD), one gram of dry powder was first mixed in 50 ml of deionized water and then introduced into the dispersion unit that was already filled with deionized water. The sample was mixed thoroughly in the dispersion unit and fed into the flow cell of the Mastersizer. The optical lens used had a focal length of 45 mm. Since the CKD is a cementitious material, the Sodium hexametaphosphate solution as a disperse regent was used to get more accurate results.

Figure 3.3 shows the particle size distribution curves of the materials obtained from the laser diffractometer tests. The grain size distribution curves of the materials indicated that Speswhite kaolin had 93.6% particle size finer than 2 μm and 6.4% of fine silt-size particles. Pegwell Bay soil contained about 7.3% of sand, 84.3% of silt, and 8.4% of clay-size fractions. The cement kiln dust contained about 70% silt-size fraction and 30% clay-size fraction. As can be seen, the materials studied had more than 35% of particles finer than 0.06 mm and can be classified under fine-grained soils.

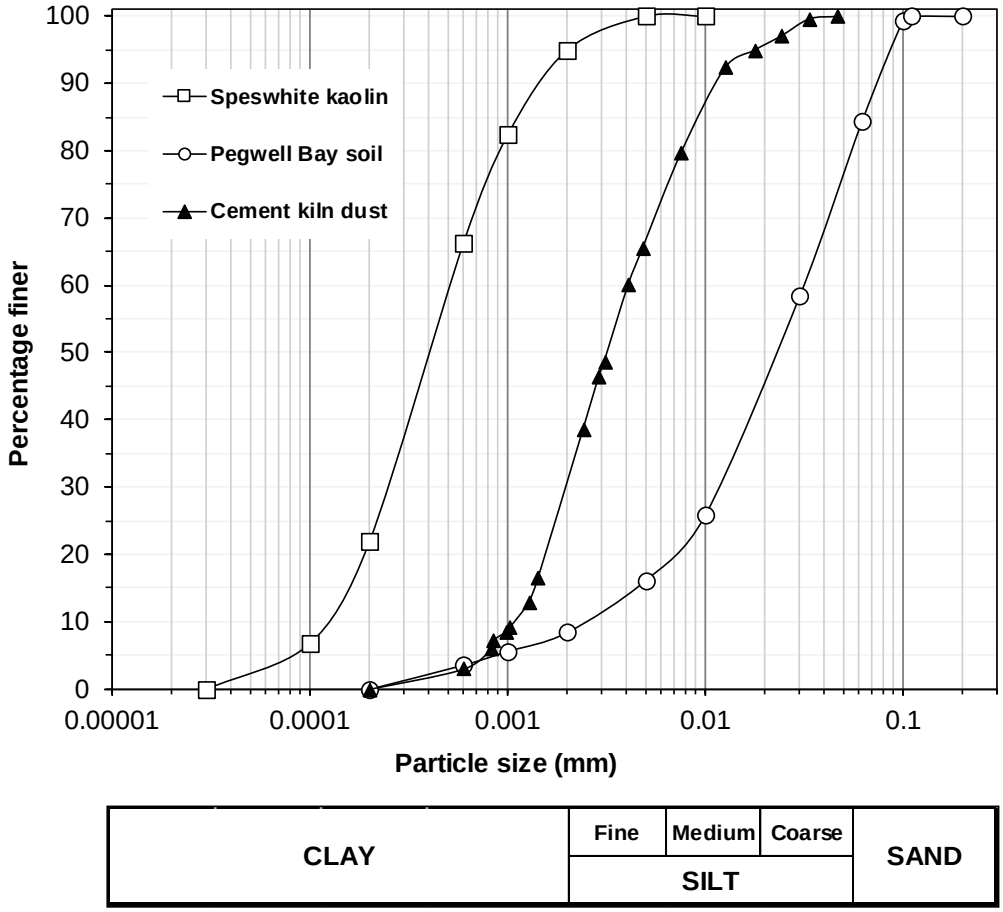

Fig. (3.3): Particle size distribution curves of the materials used

3.3.4 Atterberg Limits

The Atterberg limits (i.e. liquid limit, plastic limit and shrinkage limit) were determined following methods described in BS 1377-2 (1990) and ASTM D4943−08. The liquid limits were determined by cone penetrometer method. The liquid limits of Speswhite kaolin, Pegwell Bay soil and cement kiln dust were found to be 68.5%, 29.5% and 41%, respectively. The plastic limits of the materials were determined by the standard thread rolling method. The plastic limits of Speswhite kaolin, Pegwell Bay soil and cement kiln dust were found to be 42%, 19.2% and 27% respectively. Similar values of Atterberg limits have been reported by Cao et al. (2002), Singh (2007) and Chung et al. (2016) for Speswhite kaolin and Pegwell Bay soil by Derbyshire and Mellors (1988).

According to Unified soil classification system, Speswhite kaolin, Pegwell Bay soil and CKD can be classified as CH, CL and ML respectively.

The shrinkage limits of the materials were determined following the molten wax method described in ASTM D4943−08. For the shrinkage limit tests, specimens were prepared at 1.2 times their respective liquid limit values. The mixtures were placed within shrinkage dishes. The mass of the specimens was monitored at predetermined times until no further reductions in the mass were noted. The specimens were then removed for water content determination, and further volume measurements were carried out using the molten wax method. The shrinkage limits of Speswhite kaolin, Pegwell Bay soil and cement kiln dust were found to be 32.7%, 16% and 21% of water content respectively.

3.3.5 Mineral compositions

The mineral composition of the materials used were determined by X-ray diffraction (XRD) method (Grim 1953; Mitchell and Soga 2005). According to Bragg's law, the XRD identifies the minerals based on the relationship between the angle of incidence of the X-rays (θ) to the c-axis spacing (d). A Philips automated powder diffractometer PW 1710 (PANalytical, Cambridge, U.K.) was used for the XRD analyses. The diffractometer consists of a goniometer (specimen holder), a copper X-ray generator and a controller. The materials were grounded to powder to minimise the orientation preference and to maximise the sample representativeness. The materials in powder form and with the initial water contents were tested.

The X-ray diffraction test results of the materials are shown in Figure 3.4. Semi-quantitative analyses were conducted to determine the percentage of various minerals. The XRD test results indicated that the dominant mineral in Speswhite kaolin was kaolinite (95%). A trace of illite (4%) was also found. Pegwell Bay soil was found to be

composed of quartz (78%) and other minerals, such as calcite (16%) and dolomite (6%). Similarly, the cement kiln dust was predominantly contained calcite (85%) and silica (14%).

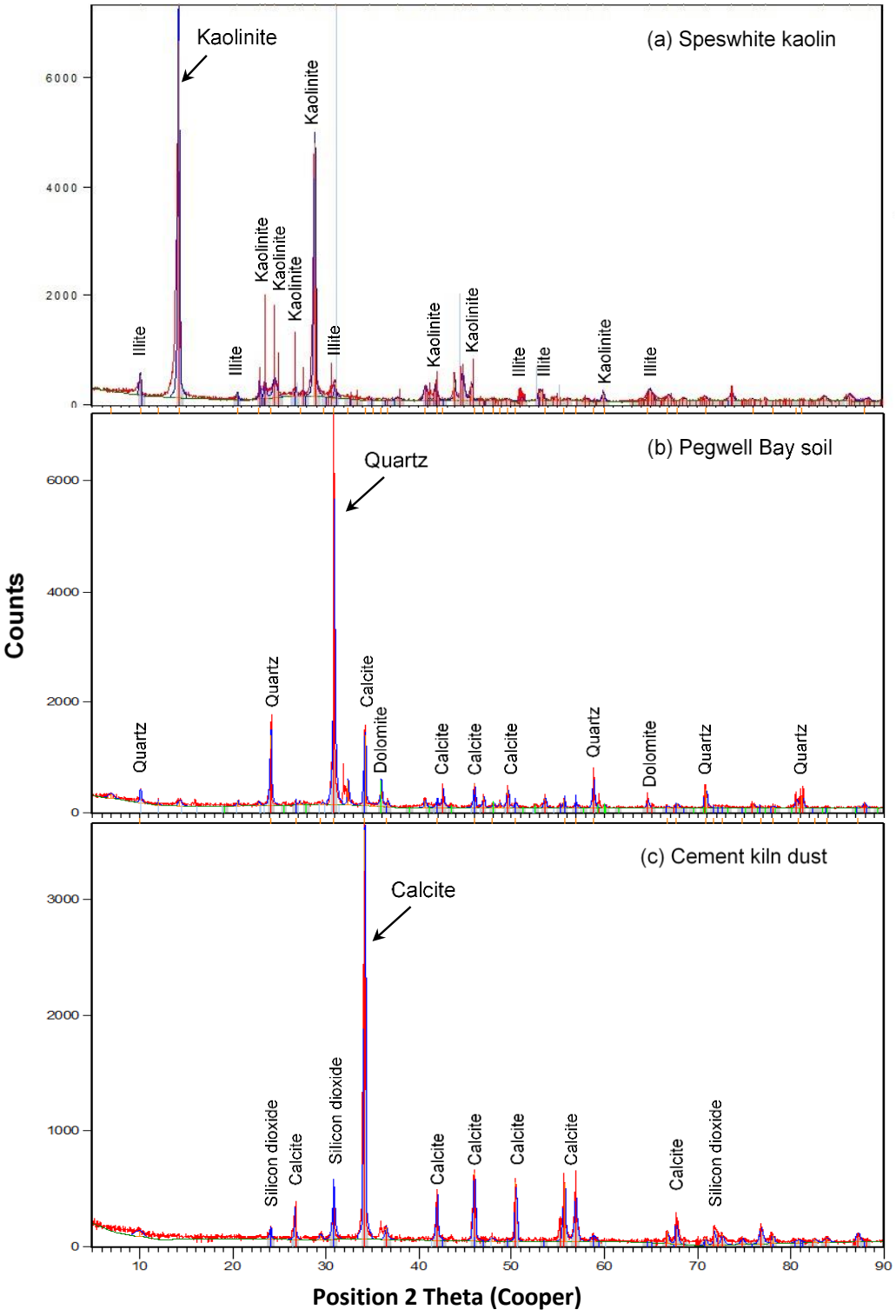

Fig. (3.4): X-ray diffraction patterns of (a) Speswhite kaolin, (b) Pegwell Bay soil and (c) cement kiln dust

3.3.6 Specific surface area

The total specific surface areas of the materials were determined based the Malvern Mastersizer X 3000 laser diffractometer analysis. Nonexpanding clay mineral, such as kaolinite typically possesses a specific surface area ranging from 10 to 40 m^2/g (Grim 1953; Mitchell and Soga 2005). The total specific surface area of Speswhite kaolin was found to be 7.63 m^2/g. A similar value of the specific surface area has been reported by Tadza (2011). The values of the specific surface area for Pegwell Bay soil and the cement kiln dust were found to be 0.41 m^2/g and 0.58 m^2/g respectively.

3.3.7 Microstructural analysis (SEM study)

Microstructural studies are usually made to improve understanding of the macroscopic behaviour and physical properties of compacted and natural soils (Romero and Simms 2008). The mechanical behaviour of soils (e.g. volume change and shear strength) is widely recognised as being associated with the microstructural arrangement (fabric and structure) (Burton et al. 2015).

Microstructural investigations were carried out by using a scanning electron microscope (SEM) on samples of the materials that were prepared at water contents greater than the corresponding liquid limits and further air-dried prior to the SEM studies. Figures 3.5, 3.6 and 3.7 show the scanning electron photomicrographs of Speswhite kaolin, Pegwell Bay soil and cement kiln dust respectively at two different magnifications.

Similar to results of particle size analysis test and specific surface area, the SEM results of Speswhite kaolin shows that the predominant particle size is less than 2 μm as shown in Figure 3.5a and b. Some silt-size particles were also detected. The SEM results of Pegwell Bay soil results show that silt size (<63 μm) is the predominant size as shown

in Figure 3.6a and b. On the other hand, the SEM results of cement kiln dust show fine silt size fractions as the predominant size, as shown in Figure 3.7a and b.

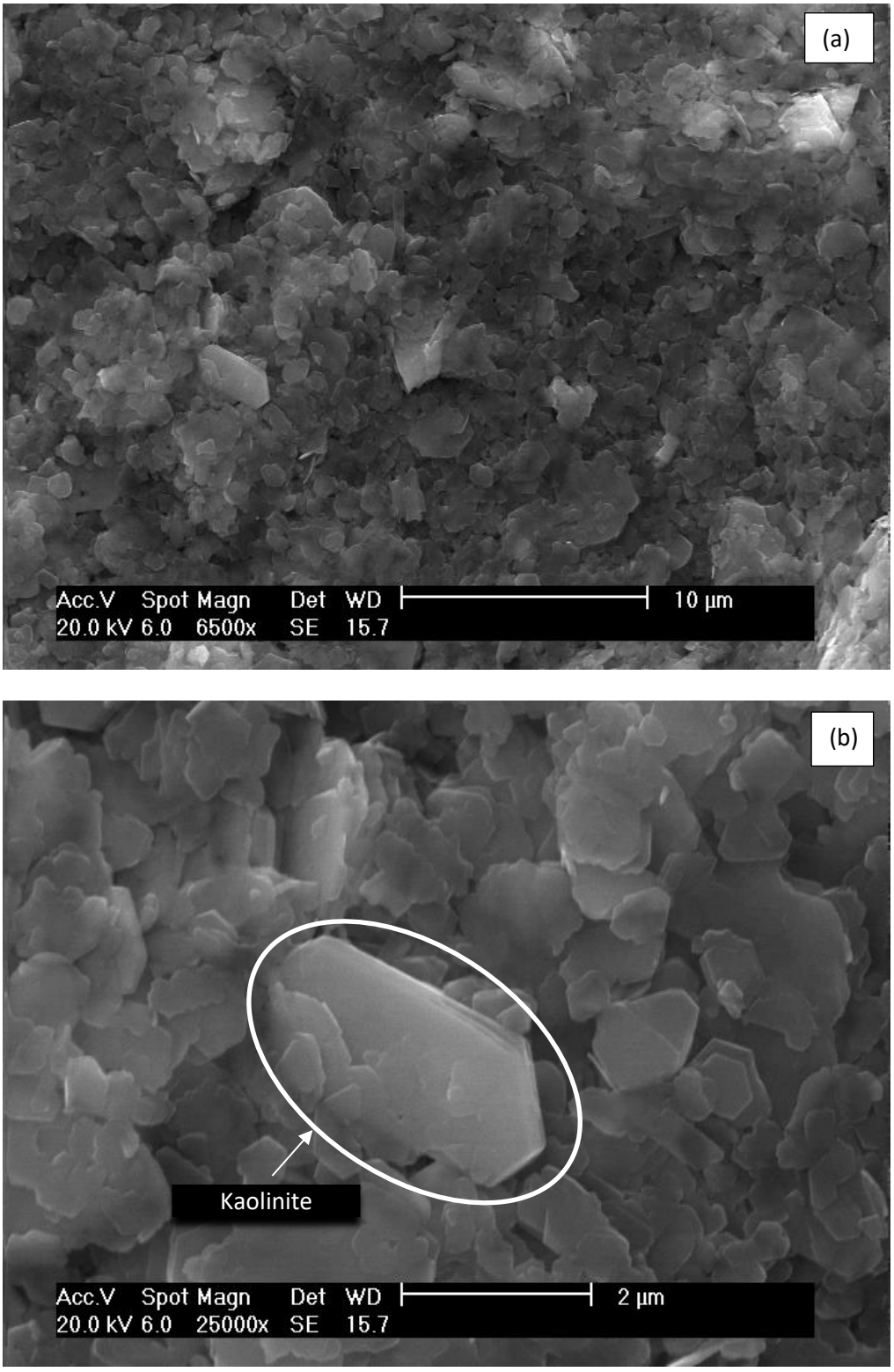

Fig. (3.5): SEM photomicrographs of Speswhite kaolin (a) 10 µm scale, and (b) 2 µm scale

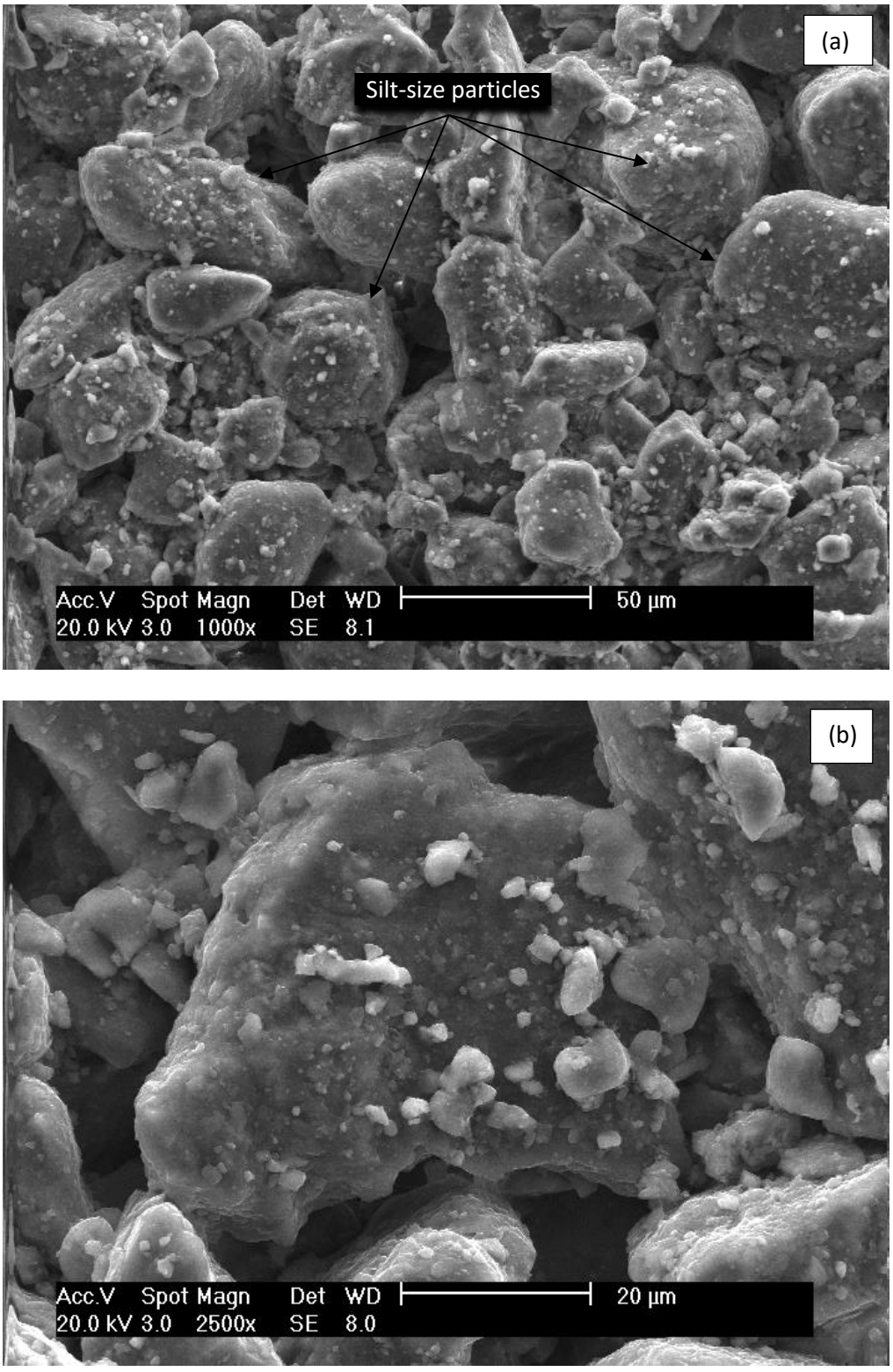

Fig. (3.6): SEM photomicrographs of Pegwell bay soil (a) 50 µm scale, and (b) 20 µm scale

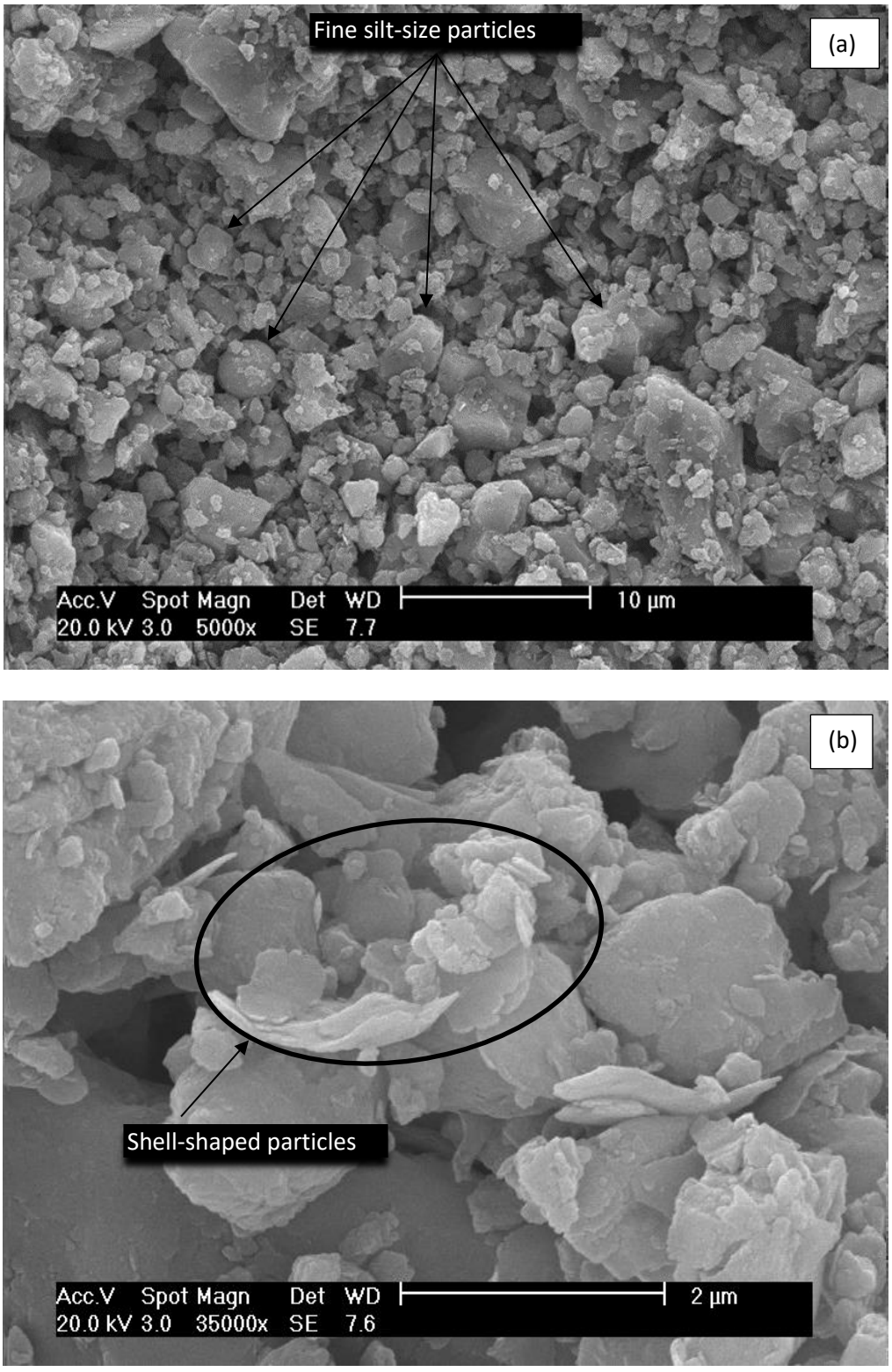

Fig. (3.7): SEM photomicrographs of cement kiln dust (a) 10 µm scale, and (b) 2 µm scale

3.4 Frost susceptibility

Frost heave susceptibility of soil is defined as the propensity for the soil to accumulate ice during freezing and to heave. The frost-susceptible soil is the soil in which ice accumulation causes frost heave during freezing or thaw weakening during thawing, or both (ASTM D5918). Classification methods based on particle size are by far the most extensively used tests for determining the frost susceptibility of soils. The simplest of these tests include only grain size as the determining factor (Chamberlain 1981a). Since there were three different fine-grained materials used in this study, finding the level of frost susceptibility was essential to understand the behaviour of the materials during freezing process.

Chamberlain (1981a) presented one of the earliest frost susceptibility criteria based on soil classification system. Based on the criteria, Speswhite kaolin, Pegwell Bay soil and cement kiln dust were classified as medium, medium to high and medium to very high frost susceptible materials respectively. In addition, based on the second level of the Swiss frost susceptibility criteria, the three materials considered as high frost susceptible soil since they were classified as CH, CL and ML respectively. On the other hand, the U.S. Army Corps of Engineers frost design soil classification system (1965) gave a wide range of "very low to very high" susceptibility for all materials. As a result, a significant susceptibility to frost should be expected for all materials based on their grain size distribution and Atterberg limits.

3.5 Compaction characteristics

The standard Proctor compaction tests (British Standard light compaction tests) were carried out by following the procedure laid out in BS 1377-4 (1990). The materials were compacted in three layers in a compaction mould having a volume of 0.001 m^3 (1000 cm^3) using 27 blows per layer and with a 2.5 kg hammer falling through a height of 300 mm.

The compaction curves of Speswhite kaolin, Pegwell Bay soil and cement kiln dust are shown in Figures 3.8, 3.9 and 3.10 respectively. The optimum water content (OWC) for Speswhite kaolin remained close to the degree of saturation of 90% (OWC = 26.7%). For Pegwell Bay soil, the optimum water content remained close to the degree of saturation of 85% (OWC = 16.2%). For the cement kiln dust, the optimum water content was found to be slightly above the degree of saturation of 90% (OWC = 27.6%). The values of maximum dry unit weight for Speswhite kaolin, Pegwell Bay soil and cement kiln dust were found to be 14.56, 17.27 and 14.86 kN/m^3 respectively.

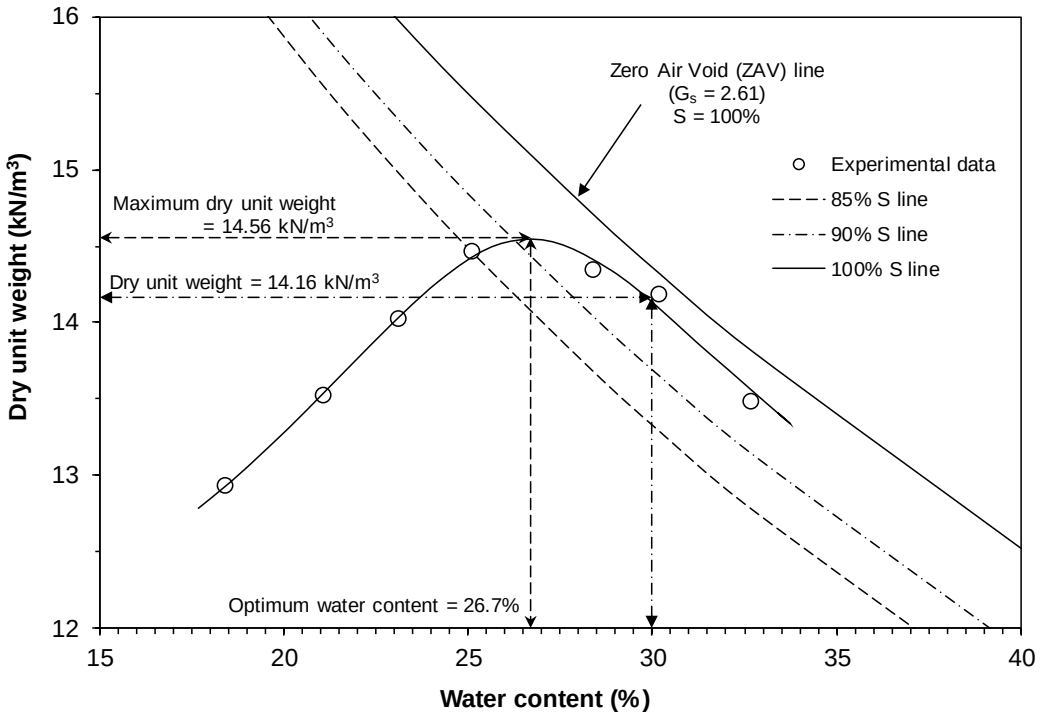

Fig. (3.8): Standard Proctor compaction curve of Speswhite kaolin

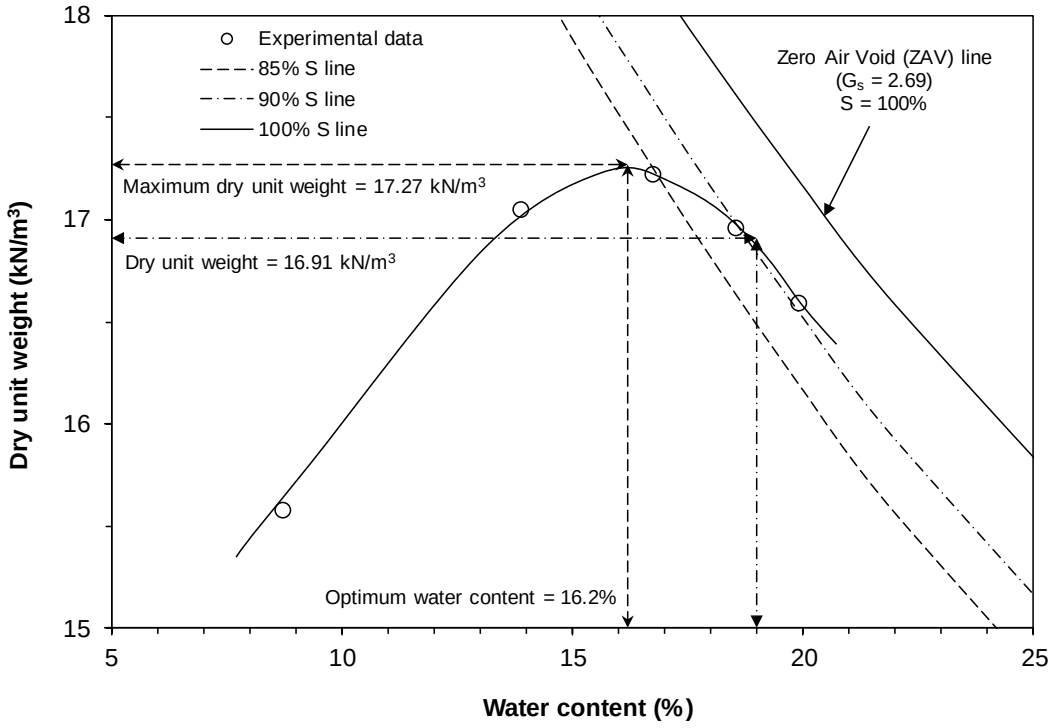

Fig. (3.9): Standard Proctor compaction curve of Pegwell Bay soil

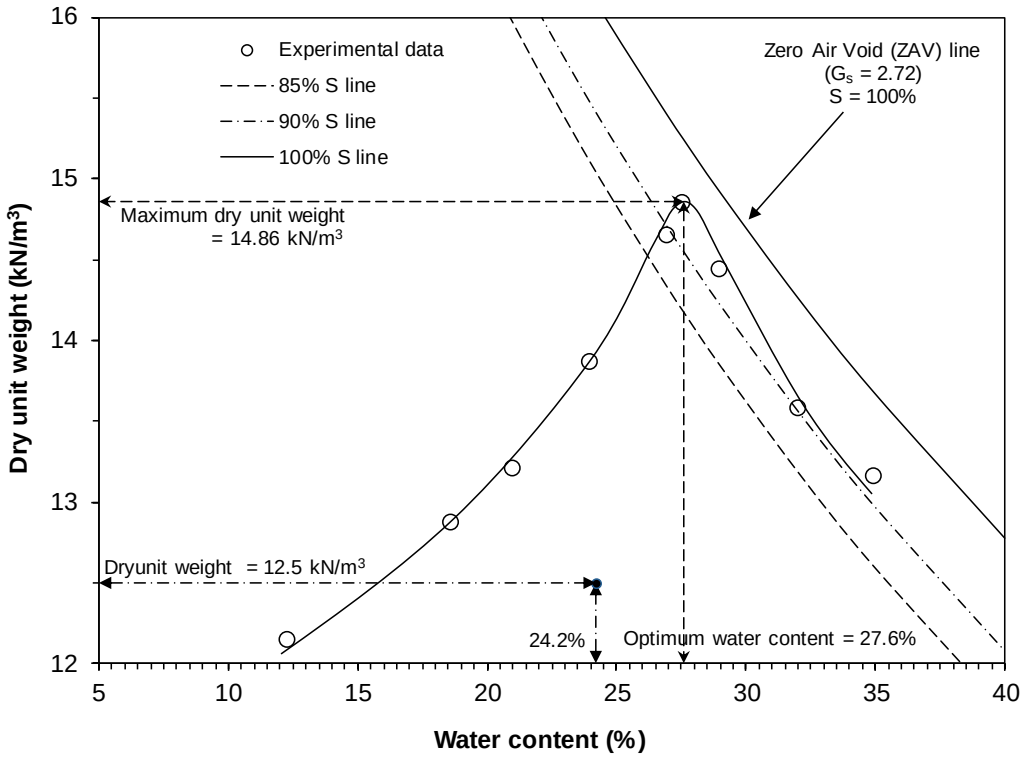

Fig. (3.10): Standard Proctor compaction curve of the cement kiln dust used

3.6 Compressibility behaviour

One-dimensional consolidation tests were carried out on initially saturated slurried specimens of the materials following the procedure laid out in BS 1377-5 (1990). The initial water contents of the specimens correspond to 1.2 times the liquid limits of the materials. The vertical pressure was applied in a step-wise manner from 5 kPa to 400 kPa during the loading process. The diameter and height of the specimens were 100 and 19 mm respectively.

Figure 3.11 shows the consolidation test results in terms of the applied vertical pressure and void ratio. At smaller applied vertical pressures, the void ratios of the materials remained in the order of the liquid limit. A higher liquid limit of the material produced a greater void ratio (Speswhite kaolin > Cement kiln dust > Pegwell Bay soil).

At an applied vertical pressure greater than about 80 kPa, the pressure-void ratio plot of cement kiln dust remains above that of Speswhite kaolin.

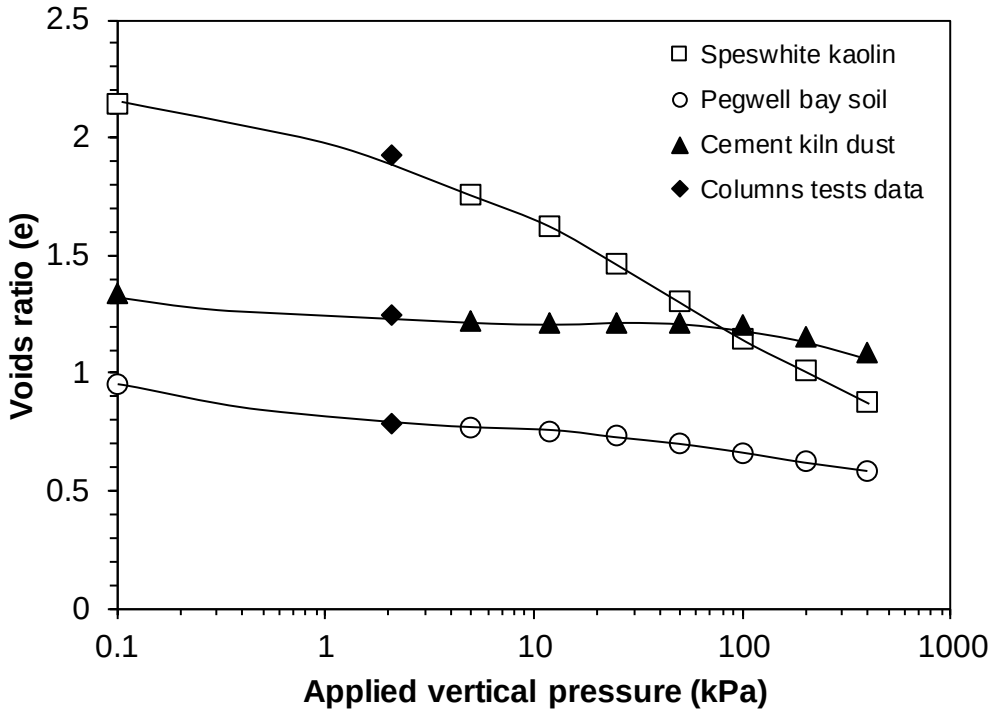

Fig. (3.11): One-dimensional consolidation test results of the materials used

3.7 Experimental methods

The main objective of this investigation was to explore the volume change behaviour of various geomaterials when subjected to either independent or a combination of various seasonal climatic processes, such as freezing, thawing, wetting and drying. Laboratory tests were carried out by considering some selected sequences of the seasonal climatic processes and with predetermined fluid and temperature boundary conditions. A custom-made test set up was used to carry out the laboratory tests that enabled performing the required tests involving all the processes. The following sections present the details of the test up, responses of the testing system to sub-zero and enhanced temperatures, and the procedures adopted for preparing specimens for the tests.

3.7.1 Details of the test setup

The test setup (Figures 3.12 and 3.13) used in this study was comprised of a column cell assembly, a Vortex Tube, a top cooling/heating chamber, four linear variable displacement transformers (LVDTs), thermocouples, a porous stone, a water reservoir, a thermal insulation jacket (a 30 mm thick rock-wool layer covered with a 3.7 mm thick reflective foil), an air supply system, and a data acquisition system (a datalogger and a personal computer).

The column cell assembly and some of the accessories have been available at the School of Engineering laboratories, Cardiff University. The test setup was initially developed to carry out freeze-thaw tests on frost-susceptible soils. In this study, the test setup was modified to carry out laboratory tests involving freezing, thawing, drying and wetting processes.

The components of the column cell assembly are a single-flanged exterior mould (120.8 mm internal diameter, 247 mm high and 6 mm wall thickness) and a step-flanged interior mould, also known as the specimen mould (103.3 mm internal diameter, 259 mm high and 6 mm wall thickness) (see Figures 3.12 and 3.13). Both moulds are made from polyvinyl chloride (PVC). The bottom of the exterior mould is fixed to a solid PVC base that in turn is mounted on a stable platform. The exterior mould accommodates a hollow acrylic cylinder (117.4 mm external diameter and 62.5 mm high) at the bottom. A 6.2 mm-thick and 117.4 mm diameter acrylic disc with holes is attached to the top of the hollow acrylic cylinder. A porous stone (102.5 mm diameter and 86.5 mm high) rests on top of the acrylic disc. The specimen mould is positioned to rest on the acrylic disc. A difference in the outer diameter of the specimen mould (115.3 mm) and the internal diameter of the exterior mould (120.8 mm) enables accommodating the cables of the thermocouples, and the specimen mould can move vertically in an upward direction.

A specimen to be tested can be prepared in the specimen mould. The diameter and height of the specimen are 103.3 mm and 65 mm respectively. The dimension of the space above the specimen (107.5 mm) was such that upon placing the top cooling/heating chamber (112 mm), the top part of the chamber protruded out above the specimen mould by about 4.5 mm. Saturated slurried specimen with very high water contents can be prepared after the column cell is assembled, whereas a compacted specimen can be prepared separately in the specimen mould. In the latter case, the specimen mould along with the specimen can then be positioned in the exterior mould in such way that the base of the cylindrical specimen remains in contact with porous stone and the bottom of the specimen mould rests on the acrylic disc. During the saturation process, water can be supplied from a water reservoir through the inlet located on the PVC base. Water flow to the specimen takes place in an upward direction from the water reservoir and the bottom water reservoir (acrylic cylinder) and through the porous stone.

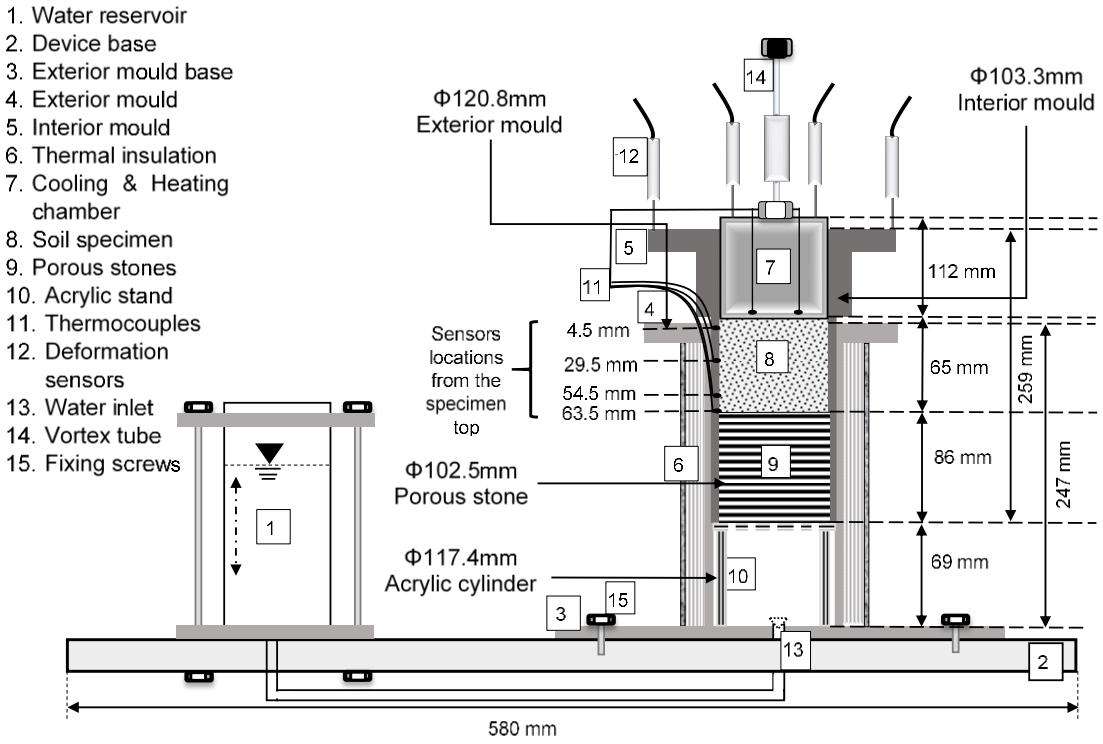

Fig. (3.12): A schematic of the test setup

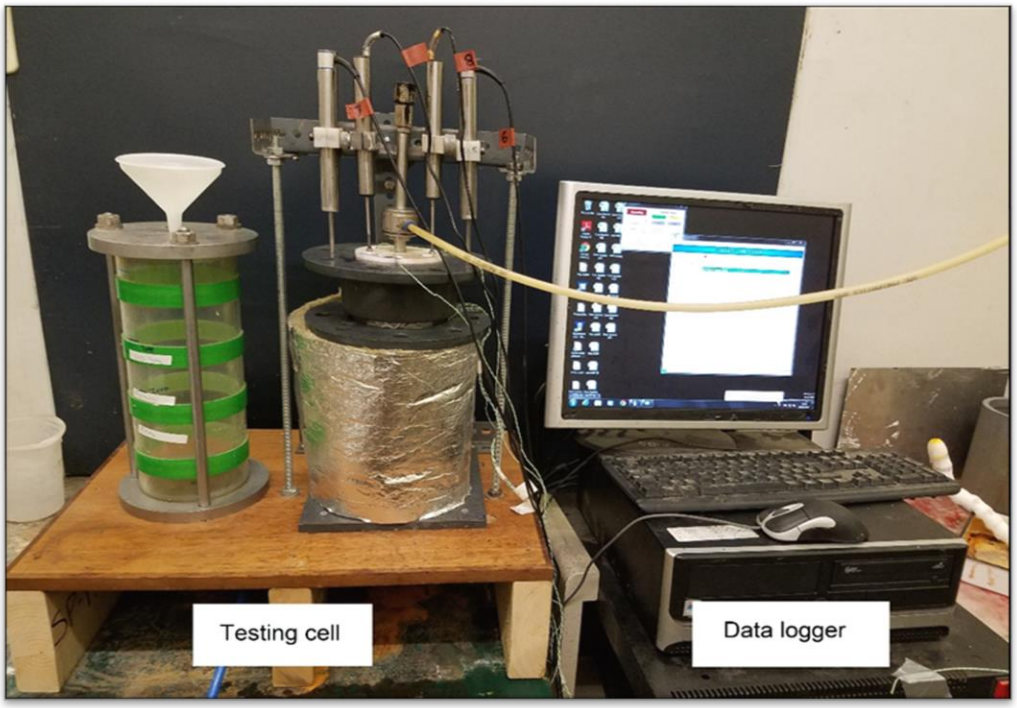

Fig. (3.13): A photograph of the test setup

3.7.1.1 Thermocouples

The inner wall of the specimen mould carries four thermocouples at predetermined heights. The positions of the thermocouples are such that once a specimen is prepared, they remain at distances of 4.5, 29.5, 54.5 and 63.5 mm from the top of the specimen. The thermocouples provide information concerning the surface temperatures at predetermined depths of the specimen. The temperatures measured by these sensors are denoted as TC1 - 4.5 mm, TC2 – 29.5 mm, TC3 - 54.5 mm and TC4 – 63.5 mm.

The thermocouples used in this study were comprised of RS Pro K Type thermocouple (1.0 m long and 0.6 mm diameter), and RS Pro IEC Miniature Plugs that were used to connect the probes to the data logger (www.uk.rs-online.com) (Figure 3.14). The probes had chromel (90% nickel and 10% chromium), and alumel (95% nickel, 2% manganese, 2% aluminium and 1% silicon) alloys welded at the measuring junction. The chromel and alumel wires are considered as +ve and –ve polarities respectively. The temperature measurement range of the probes used was from – 50 to + 250 °C with a response time of 0.7 seconds. As per the specifications provided by the supplier, the accuracy of the thermocouples meets the tolerance requirement of class-1 K Type thermocouples (±1.5 °C).

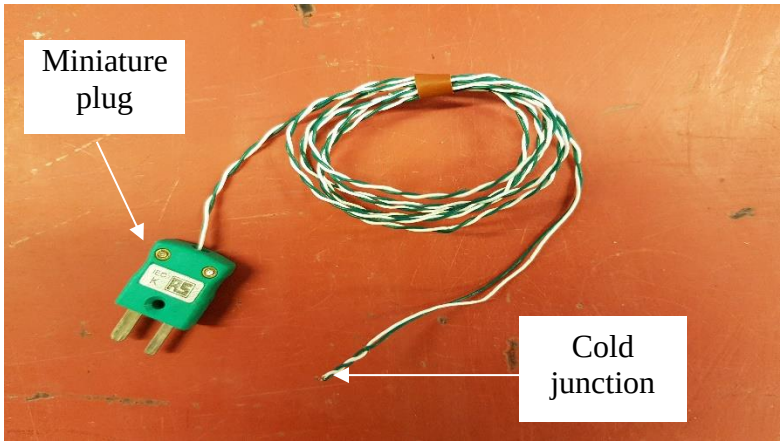

Fig. (3.14): A photograph of the K type thermocouple used

3.7.1.2 Vortex Tube

A Vortex Tube allows cooling and heating of the air at the same time. Vortex Tubes have a number of industrial applications, such as ultrasonic cold welding, spot cooling, product cooling, chamber cooling, machine cooling and electronic cooling (Wang et al. 2009).

In this investigation, the temperature at the top of the specimen was lowered to sub-zero temperatures during the freezing process, whereas it was increased above the ambient temperature during the drying process. In both cases, Vortex Tubes were used. During the freezing process, a Vortex Tube was directly connected to the top cooling/heating chamber to supply cold air (see Figures 3.12 and 3.13), whereas during the drying process an auxiliary Vortex Tube was used to supply hot air into the top chamber.

Figures 3.15a, b and c show the various components and the air flow mechanism in a Vortex Tube. An increase in the temperature of the air takes place when the gas molecules move faster, whereas a decrease in the temperature of the air takes place when the velocity of gas molecules decreases. Compressed air is fed transversely into the generation chamber of the Vortex Tube (also called as vortex chamber or spin chamber) and made to spin by a generator. The air moves down the long tube in which hot air separates outwards and towards the wall of the tube due to the inertia of motion, whereas the cold air is pushed to the centre of the tube. The cold air flows in the middle of the tube in the opposite direction to the hot air. A percentage of the hot air is made to exit, whereas the remaining air flows towards opposite end (cold end).

The cold fraction is defined as the percentage of input compressed air released through the cold end of the Vortex Tube. The cold fraction of the air can be adjusted by

two ways, such as via the control relief valve located at the hot end and by using an appropriate generator inside the vortex chamber (located nearer to the cold end).

The Vortex Tube used in this investigation was from Meech International, Witney, Oxfordshire, UK (www.meech.com). The commercially available medium Vortex Tube used in this study had a total length of about 212.3 mm and the diameter of the spin chamber was about 44.5 mm (see Figures 3.15 a, b). The generators supplied with the Vortex Tube can be used to achieve the desired cold fraction temperatures. According to the manufacturer specifications, the control relief valve can be kept at a position of two and half rotation from close to achieve a cold fraction value of 70%. From this point, the control valve can be adjusted to allow more or less air to exit the cold end. The Vortex Tubes can produce temperatures as low as 50 °C below the inlet air temperature. A similar rise in the temperature can be achieved in the positive temperature range. For example, at a compressed air pressure of 700 kPa and with the air temperature of 19 °C, a temperature drop of 40 °C and a temperature rise of 80 °C is achievable when an appropriate generator is used (www.meech.com).

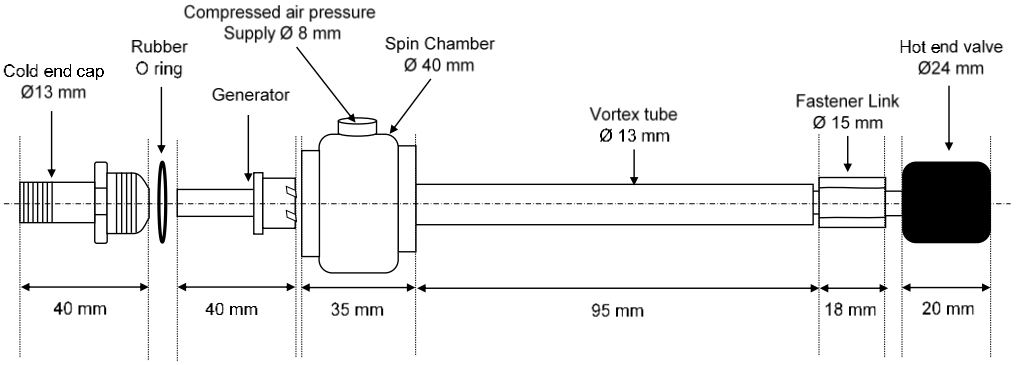

(a)

(b)

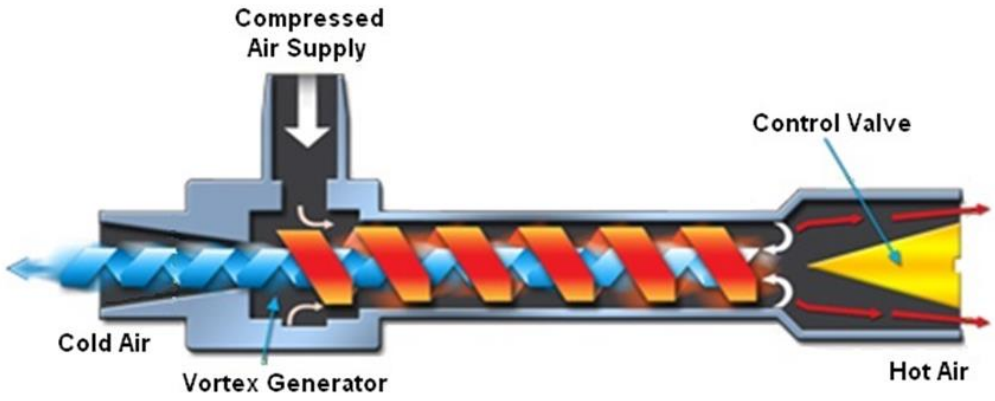

(c)

Fig. (3.15): (a) A schematic showing various components of a Vortex Tube, (b) a photograph of various components and (c) cold and hot air separation within a Vortex Tube (modified Fig. 3 from Carrascal and Sala Lizarraga 2013)

The generators used in the Vortex Tube are designed to produce either low or high cold fraction. The low cold fraction generators allow less than 50% of the air flow through the cold end, whereas the high cold fraction generators allow more than 50% of the air flow through the cold end. The low cold fraction generators are suitable to generate lowest air temperatures, but may not be very efficient, whereas the high cold fraction generators can be used at the desired coldest temperatures and are considered to be more efficient. Similarly, a production of the hot air depends on the type of generator used. Table 3.1 presents the generator types (usually indicated by their colour and catalogue number), cold fraction designation and the cold end air temperatures that can be generated for a compressed air temperature of 19°C (www.meech.com).

Table 3.1: Achievable temperature by using various spin generators (compressed air pressure = 540 kPa, air temperature = +19 °)

Colour of Generator	Green	White	Grey	Brown	Red	Yellow	Blue	Beige
Cold fraction	Low	Low	Low	Low	High	High	High	High
Temperature (°C)	- 36	- 34	- 24	- 19	- 33	- 35	- 23	- 17

During a test involving the freezing process, the cold end of the Vortex Tube was connected to the central part of the top cooling/heating chamber (as shown in Figures 3.12 3.13 and 3.16a). The top cooling/heating chamber (101 mm diameter and 112 mm high) was a composite cylinder with a stainless steel side. A copper base (1.8 mm thick) and a polytetrafluoroethylene (PTFE) disc (12.5 mm thick) attached firmly to the top open end of the stainless cylinder (Figure 3.16a). The PTFE disc had six air vents each 10 mm in diameter and located at an equal angle on a concentric circle of diameter 80 mm. Two K Type thermocouples were attached to the inner surface of the copper base for monitoring

the temperature within the cooling/heating chamber (Figure 3.16b). The average temperature measured by these two thermocouples are denoted as TC0 - 0 mm.

(a)

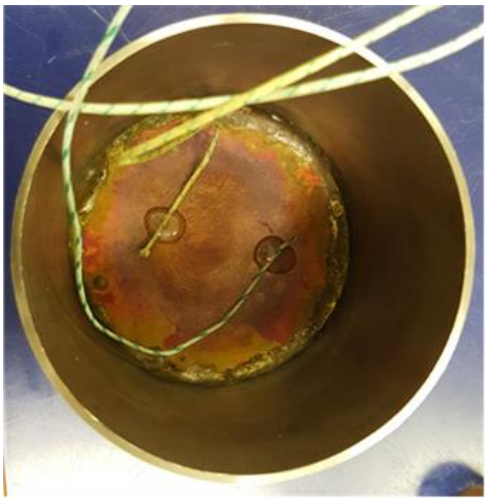

(b)

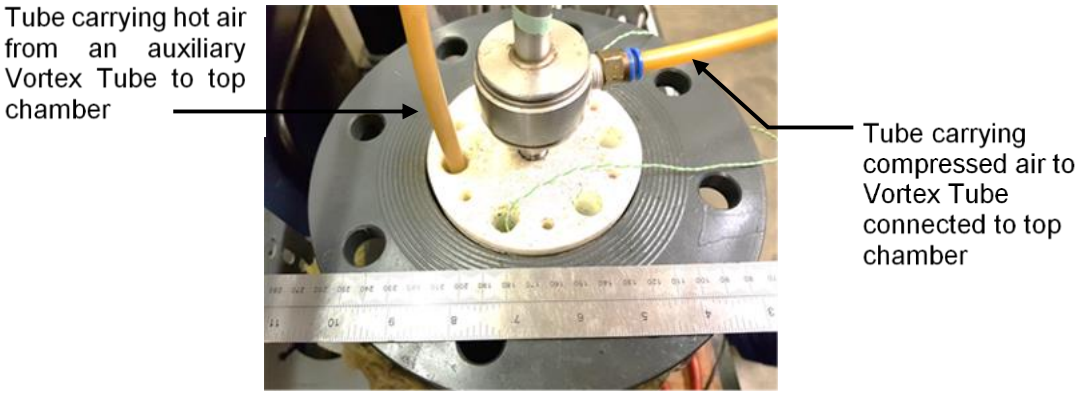

(c)

Fig. (3.16): (a) Vortex Tube connection to the top cooling/heating chamber, (b) Inside of the top chamber showing the attached thermocouples and (c) Arrangement showing hot air and compressed air supply to the top chamber

During a test involving the drying process, the air supply to the Vortex Tube connected to the top chamber was shut off to terminate the production of cold air. A spare Vortex Tube was used to supply the hot air to the top chamber. The hot air produced by the spare Vortex Tube was taken through a temperature resistance tube connected to the hot end control valve and an air vent located at the top of the chamber (see Figure 3.16c). A noise muffler (cold end silencer) was attached to the cold air exhaust on the left to reduce the noise level (Figure 3.17). The cold air released from the cold end of the Vortex Tube was not utilised.

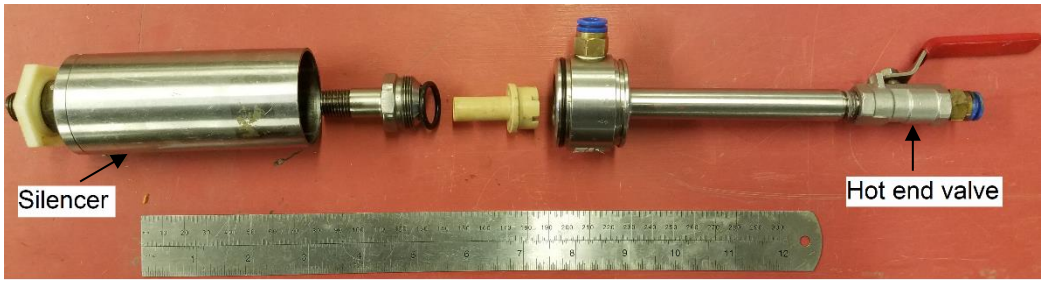

Fig. (3.17): Arrangement of components of Vortex Tube during production of hot air

The air supply to the Vortex Tube during a test was continuous from a 7 bar (700 kPa) line available in the laboratory. The pressurised air exited the top chamber via the vents located on the top of the chamber. The copper base of the chamber acted as the interface between the applied air temperature within the chamber and the outside medium. The outer thermal insulation used (see Figures 2.12 and 3.13) comprised of a 30 mm thick rock-wool layer covered with a 3.7 mm thick reflective foil.

The temperature of the copper base depends upon (*i*) the temperature of the air entering the chamber or exiting the Vortex Tube, (*ii*) the temperature of the air within and outside the chamber and (*iii*) the specific heat capacity of the materials which will influence the time required to obtain an equilibrium temperature. Trial tests were carried out to study the influence of generator type used on the temperature of the air (cold or

hot) generated within the top chamber. The design of the system did not allow a direct measuring of the temperature of the copper base. Since the thermocouples were located very close to the copper base (see Figure 3.16b), it was assumed that the measured temperature by thermocouples (TC0 – 0 mm) represents the surface temperature of the copper base. Based on the trial tests for generating both cold and hot air within the top cooling/heating chamber, it was noted that using a green generator the temperature recorded by the thermocouples was – 19 °C ± 0.5 °C, whereas using a beige generator the temperature measured by the thermocouples was 52 ± 1.5 °C. These generators were used while performing the freezing and drying tests.

3.7.1.3 Vertical deformation measurement

High precision linear variable displacement transformers (LVDTs) were used to measure the vertical deformations of the specimens and the specimen mould (Figures 3.12 and 3.13). The S series LVDT used in this study (Figure 3.16) is produced by Solarton Metrology (www.solartonmetrology.com). The measurement range, linearity, resolution and operating temperature range of the LVDTs were 50 mm, 0.2% (for the entire range), 0.3μm and - 40 to +120 °C respectively.

Two LVDTs were used on the top cooling/heating chamber that provided the deformation of the specimens during freezing, thawing, wetting and drying stages of the tests, whereas two more LVDTs were used to measure the deformation of the specimen mould during all stages of the tests. The average values of the measured deformations by the LVDTs located on top of the cooling/heating chamber is presented as deformation of the specimen, whereas the average values of the deformations measured by the LVDTs on top of the specimen mould are presented as the deformation of the specimen mould.

Fig. (3.18): A photograph of the LVDT used in this study

3.7.1.4 Data acquisition system

As many of the tests carried out in this investigation were long-term tests, a data acquisition system was used to monitor various data. A System 8000 data acquisition system from Micro-Measurements (www.vishaypg.com/micro-measurements) in conjunction with a personal computer were used for this purpose. The system includes a scanner with eight channels. Each channel can be configured via the Micro-Measurements StrainSmart® software to accept signals from the thermocouples and the voltage sensors (LVDTs). The model 8000-8-SM scanner communicates with a host personal computer via an ethernet connection. The software was utilised to configure, control and acquire data from the System 8000 data acquisition system. During the tests, the deformation and temperature data were collected every minute.

3.7.2 Response of the measuring system to temperature changes

Four identical test setups were used to carry out the laboratory tests. The components of the column cell assembly, such as the specimen and the exterior moulds, the top cooling/heating chamber, and the porous stone were expected to be subjected to thermal loadings due to the applications of subzero temperature of – 19 ±0.5 °C during the freezing process and an enhanced temperature of 52 ±1.5 °C during the drying phase of the tests. Therefore, it was necessary to understand the response of the test set up, particularly concerning the vertical deformation associated with expansion and contraction due to thermal loadings.

A dummy specimen (100 mm diameter and 50 mm high) made of aluminium alloy 6082-T6 (coefficient of thermal expansion, $\alpha = 24 \times 10^{-6}$ mm/mm/°C) was chosen to study the behaviour of the system when subjected to thermal loading. During the tests, the dummy specimen was placed on the porous stone. Both the exterior and the specimen moulds were assembled. The Vortex Tube with the appropriate generator was used to supply either cold or hot air into the top chamber. Measurements of the temperature were carried out within the top cooling/heating chamber, and at distances of 0, 25 and 50 mm from top of the dummy specimen. The vertical deformations of the top cooling/heating chamber and the specimen mould were measured until the values remained constant. The outer thermal insulation used comprised of a 30 mm thick rock-wool layer covered with a 3.7 mm thick reflective foil.

Figures 3.19 and 3.20 show the temperature and deformation results for the freezing and heating tests on the dummy aluminium alloy specimen respectively. As can be seen in Figure 3.19, within the top cooling/heating chamber, a drop in the temperature from the room temperature (21.9 °C) to about -19 °C occurred within about 50 minutes. The temperature decreased to about - 6.5 °C at 0 mm and – 2.5 °C at 25 and 50 mm at the end of the test. A vertical deformation of – 0.65 mm (contraction) was measured at the top of the chamber. This deformation included the deformation of the dummy specimen and the deformation of the top chamber. The specimen mould underwent a contraction of 0.39 mm.

Figure 3.20 shows that within the cooling/heating chamber an increase in the temperature from the room temperature to about 53 °C occurred in about 300 minutes. The temperatures at other levels remained within about 43 to 45 °C. An increase in the temperature caused an expansion of the dummy specimen, the top chamber and the

specimen mould. The vertical deformations measured on top of the cooling/heating chamber and the specimen mould were 0.72 and 0.33 mm respectively.

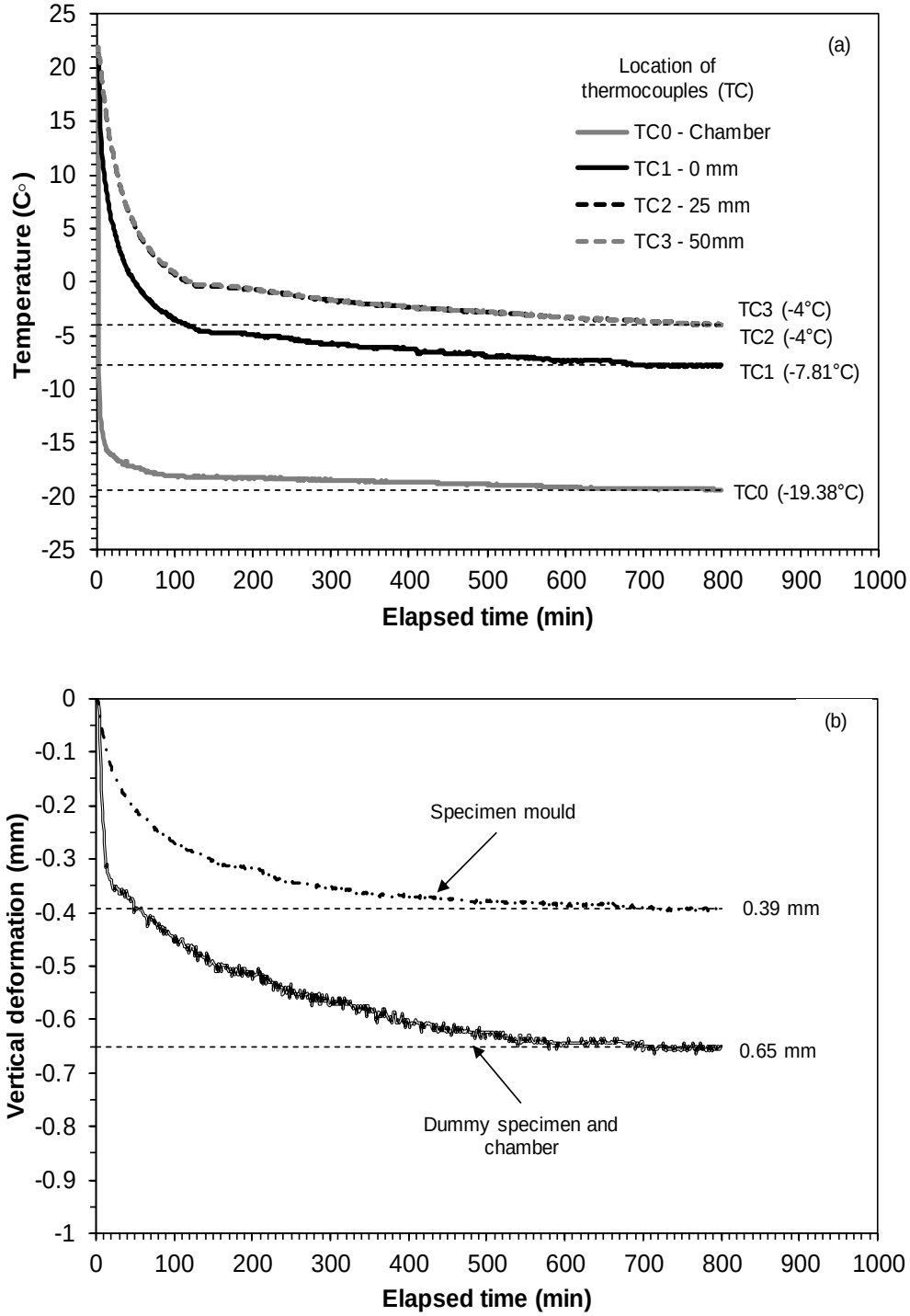

Fig. (3.19): Effect of lowering the top chamber temperature in the presence of a dummy specimen (a) Elapsed time versus temperature and (b) elapsed time versus vertical deformation

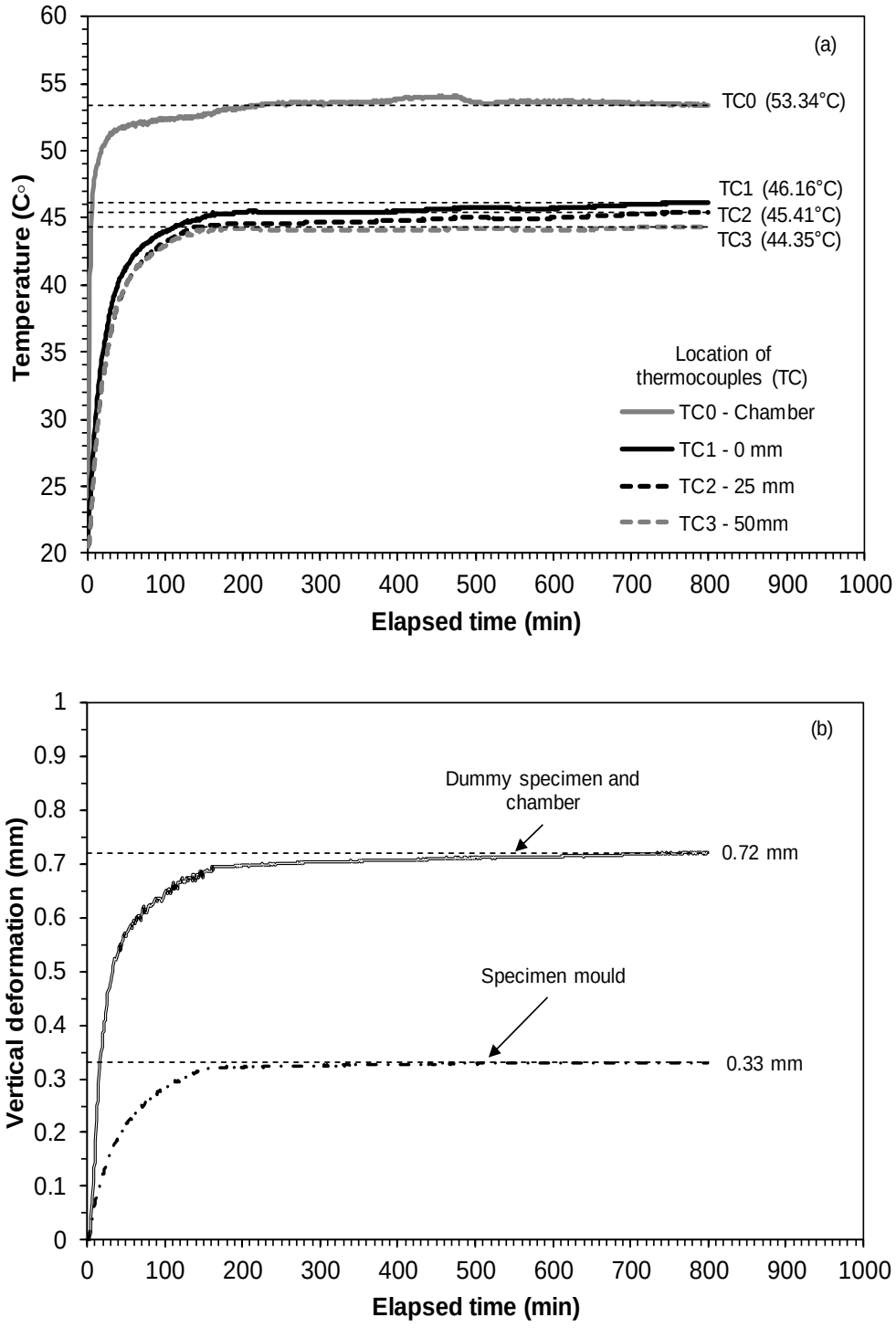

Fig. (3.20): Effect of increasing the top chamber temperature in the presence of a dummy specimen (a) Elapsed time versus temperature and (b) elapsed time versus vertical deformation

The magnitudes of thermal contraction and expansion of any material can be calculated by considering the coefficient of linear thermal movement of the material, the temperature change and the length of the specimen. The deformations of the dummy specimen for both applied freezing and heating temperature conditions were calculated. Based on the actual measured deformations, the calculated deformations and the temperature changes within the top chamber, the measuring system corrections were calculated and are shown in Table 3.2. These corrections were applied to the measured vertical deformations of the materials in actual tests.

The correction factors towards the deformation of the specimen mould were calculated for both freezing and heating tests. The measured vertical deformations of the specimen mould due to a decrease and an increase in the top chamber temperature were considered to calculate the correction factors. For a drop in the temperature of 40.9 °C, the calculated correction factor was + 0.01 mm/°C (0.39/40.9), whereas, for an increase in the temperature of 32.6 °C, the calculated correction factor was – 0.01 mm/°C (0.33/32.6). The lateral expansion and contraction was not considered since the interior mould was free supported at the edges (i.e., free to move vertically) during the thermal loading, according to Plastic Pipe Institute (PPI) report (2001).

Table 3.2: Determination of measuring system correction factors

Parameters	Lowering top chamber temperature to – 19 °C	Increasing top chamber temperature to +53 °C
Change in top chamber temperature (°C)[1]	40.9	32.6
Average temperature change of aluminium alloy specimen (°C)[2]	26.4	24.8
Calculated deformation (mm)[3]	0.032	0.039
Actual deformation measured on the top cooling/heating chamber	0.65	0.72
Correction factor (mm/°C)[4]	+ 0.015	- 0.021

Note: [1] difference between initial ambient temperature and final temperature

[2] difference between initial ambient temperature and average final temperature

[3] based on specimen length of 50 mm

[4] (Actual deformation – calculated deformation)/ calculated deformation

3.8 Experimental program

In total four series of tests were conducted on the three selected materials (see Figure 3.21). In test series I, initial saturated slurried specimens of the materials were subjected to a freezing and a thawing process. In test series II, compacted-saturated specimens of the materials were subjected to a freezing and a thawing process. In test series III, compacted specimens were subjected to cycles of wetting and drying. At several predetermined stages, freezing and thawing processes were introduced (intermittent freeze-thaw). In test series IV, compacted specimens of the materials were subjected to wet-freeze-thaw-dry cycles.

The water table (the level of water in the water reservoir) position (see Figures 3.12 and 3.13) was different for various stages of the tests. For the wetting, saturation and consolidation stages, the water table remained at the top of the specimen. During the freezing and thawing processes, the water table remained at the top of the porous stone, whereas during the drying process no water was supplied to the specimens.

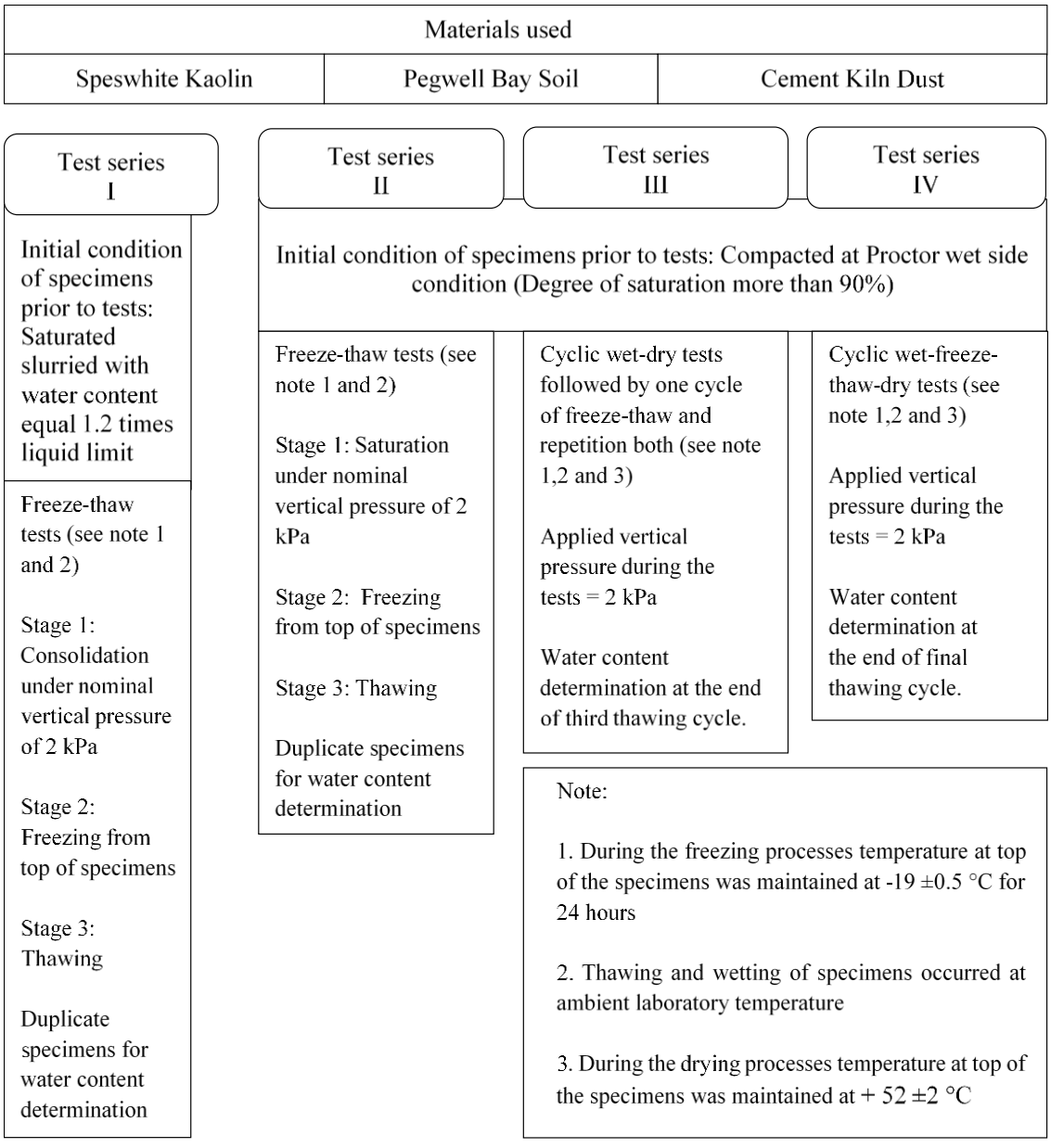

Fig. (3.21): Experimental program

3.8.1 Details of specimen preparation and test procedures

3.8.1.1 Freeze-thaw tests on saturated slurried specimens (Test series I)

Initially saturated slurried specimens of the materials were prepared by thoroughly mixing the chosen materials with water. The targeted water content in all cases was equal to 1.2 times the corresponding liquid limit of the materials. The mixtures were stored in sealed plastic bags and kept in airtight containers to allow for water equilibration to take place for at least 48 hours. The specimens (103.3 mm diameter and 65 mm high) were prepared in the specimen mould of the column cell. Sufficient care was taken to avoid the formation of air bubbles in the specimens. The mass of the mixture considered for preparing the specimens was monitored that allowed determining the dry unit weights and the void ratios of the specimens. Table 3.3 shows the initial water content, initial dry unit weights and void ratio of the specimens.

Table 3.3: Initial conditions of the specimens in Test series I (Freeze-thaw tests on initially saturated slurried specimens)

Specimen	Initial conditions of specimen		
	Water content (%)	Dry unit weight (kN/m^3)	Void ratio (e)
Speswhite kaolin	82.3	8.11	2.148
Pegwell Bay soil	35.4	13.51	0.951
Cement kiln dust	49.2	11.40	1.337

The top cooling/heating chamber was positioned on top of the specimen. The equivalent vertical pressure corresponding to the mass of the top chamber was equal to 2 kPa. This was considered as the nominal applied vertical pressure (seating pressure). The specimens were allowed to consolidate under the vertical pressure of 2 kPa. Following the consolation phase, a freezing stage commenced by lowering the temperature at the top of the specimen. The Vortex Tube was used for this purpose. The freezing process was terminated at the end of 24 hours. A thawing stage followed the freezing stage. During the thawing stage, the supplied air pressure to the Vortex Tube was shut off, and the specimen underwent the thawing process at ambient laboratory temperature. The vertical deformation of the specimen and the specimen mould and the temperature at predetermined depths during the freezing and thawing stages were monitored. The water contents of the specimens at the end of freezing and thawing stages were determined by the oven-drying method. Duplicate specimens were used for determining the water contents at the end of each stage. The results of the laboratory tests on initially saturated slurried specimens are presented in Chapter 4.

3.8.1.2 Freeze-thaw tests on compacted specimens (Test series II)

In Test series II, compacted specimens were used. The initial compaction conditions of the specimens are shown in Table 3.4 and on the compaction curves in Figures 3.8, 3.9 and 3.10. As can be seen in Figures 3.8 to 3.10 the chosen specimen conditions falls on the wet-side of the optimum conditions of the materials. Material-water mixtures were prepared by thoroughly mixing the materials with the required quantities of water. The mixtures were stored in sealed plastic bags and kept in airtight containers to allow for water equilibration to take place for at least 48 hours.

Table 3.4: Initial compaction conditions of the specimens in Test series II, III and IV

Material	Initial compaction conditions			
	Water content (%)	Dry unit weight (kN/m^3)	Void ratio (*e*)	Compaction Pressure (kPa)
Speswhite kaolin	30	14.16	0.808	740
Pegwell Bay soil	19	16.91	0.561	652
Cement kiln dust	24.2	12.50	1.330	644

Compacted specimens were prepared by statically compacting the mixtures in the specimen mould by using a static compaction machine (Figure 3.22). Two stainless steel pistons (spacers) were used while preparing the compacted specimens. The bottom piston (102.5 mm diameter and 86.5 mm high) had the same dimensions as the porous stone, whereas the top piston (101 mm diameter and 107 mm high) created the required space for the top cooling/heating chamber. The displacement rate adopted during the static compaction 1.25 mm/min (Venkatarama-Reddy and Jagadish 1993). The differences between the applied static compaction pressures for preparing the specimens remained less than 100 kPa. The specimens were tested immediately after the compaction process.

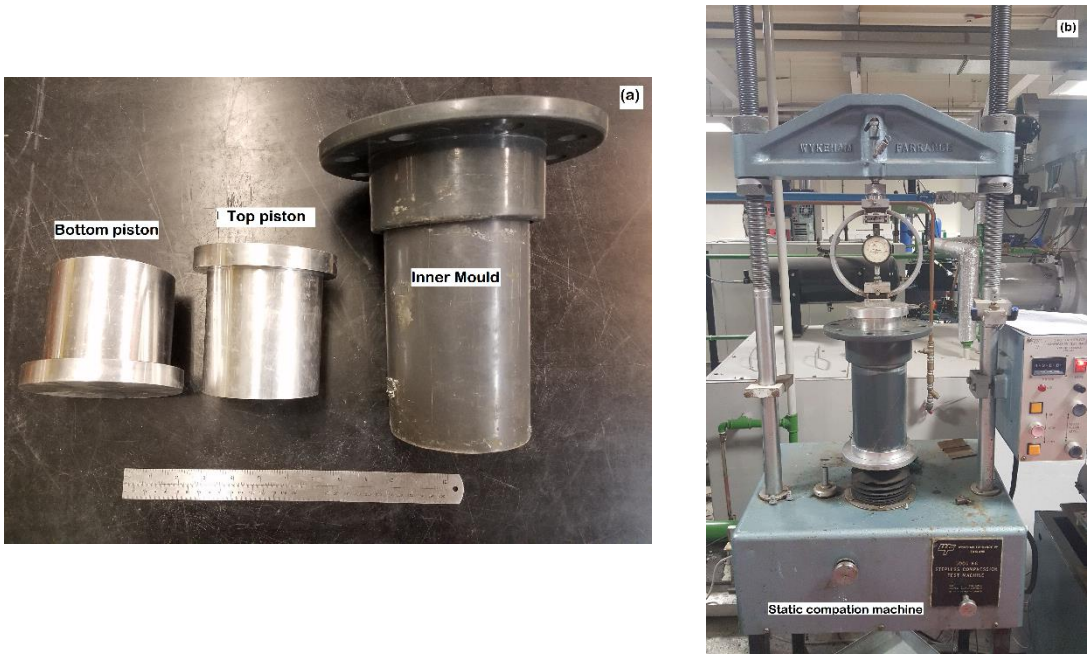

Fig. (3.22): (a) Specimen mould and pistons used during preparation of compacted specimens and (b) Static compaction setup

The top cooling/heating chamber was positioned on top of the specimen which applied a vertical pressure of 2 kPa. Compacted specimens were allowed to saturate for 24 hours by maintaining the water table at the top of the specimen (wetting stage). Following the saturation phase, a freezing stage commenced by lowering the temperature at the top of the specimen by using the Vortex Tube. The water table during the freezing process was maintained at the bottom of the specimen. The freezing process was terminated at the end of 24 hours. A thawing stage followed the freezing stage. During the thawing stage, the supplied air pressure to the Vortex Tube was shut off, and the specimen underwent the thawing process at ambient laboratory temperature. The water table remained at the top level of the porous stone during the thawing process. The vertical deformation of the specimen and the specimen mould and the temperature at predetermined depths during the freezing and thawing stages were monitored. The water contents of the specimens at the end of freezing and thawing stages were determined by the oven-drying method. Duplicate specimens were used for determining the water

contents at the end of each stage. The results of the laboratory tests on compacted specimens subjected to freezing and thawing processes are presented in Chapter 5.

3.8.1.3 Cyclic wet-dry tests followed by freezing and thawing processes on compacted specimens (Test series III)

In Test series III compacted specimens were used. The initial compaction conditions of the specimens are shown in Table 3.4. The procedure adopted for preparing compacted specimens are presented in section 3.8.1.2.

Compacted specimens were allowed to saturate for 24 hours by maintaining the water table at the top of the specimen (wetting stage). Following the saturation stage, hot air was supplied to the top chamber from an auxiliary Vortex Tube. No water was supplied to the specimens during the drying stage. The drying stage was terminated when the vertical deformation measured at the top chamber attained a constant value. The specimens were subjected to several wetting and drying cycles until the vertical deformations during wetting and drying remained constant. At this stage, freezing and a thawing stage were introduced. Further, the cyclic wetting and drying stages were reinstated to explore what are the impacts of intermittent freezing and thawing processes on the vertical deformation of the materials. The wet-dry process until attaining an equilibrium in terms of the vertical deformation and an introduction of the freeze-thaw process was repeated. The tests were terminated after the third thawing stage. The vertical deformation of the specimen and the specimen mould and the temperature at predetermined depths during all stages of the tests were monitored. The water contents of the specimens at the end of the last thawing stage were determined by the oven-drying method. The results of the laboratory tests on compacted specimens subjected to wet-dry cycles followed by intermittent freeze-thaw processes are presented in Chapter 6.

3.8.1.4 Cyclic wet-freeze-thaw-dry tests on compacted specimens (Test series IV)

Compacted specimens of the materials were used in Test series IV. The initial compaction conditions of the specimens are shown in Table 3.4. The procedure adopted for preparing compacted specimens are presented in Section 3.8.1.2.

In Test series IV, compacted specimens were allowed to saturate for 24 hours by maintaining the water table at the top of the specimen (wetting stage). Following the saturation phase, the temperature at the top of the specimen was lowered for applying the freezing front temperature for 24 hours. The Vortex Tube connected to the top chamber was used for this purpose. The water table was maintained at the top of the porous stone. A thawing stage followed the freezing stage, whereas a drying stage followed the thawing stage. During the thawing stages, the water table was located at the top of the porous stone, whereas no water supplied during the drying stages and the temperature within the top chamber was increased by supplying dry air from an auxiliary Vortex Tube. The specimens were subjected to several cycles of wetting, freezing, thawing and drying. The vertical deformation of the specimen and the specimen mould and the temperature at predetermined depths during the freezing and thawing stages were monitored. The water contents of the specimens at the end of a predetermined thawing stage were determined by the oven-drying method. The results of the laboratory tests on compacted specimens subjected to wet-freeze-thaw-dry cycles are presented in Chapter 7.

3.9 Summary

In this chapter the background of the materials used and the properties of the materials were presented. A summary of various properties of the materials is presented in Table 3.5. The details of the laboratory test set up and the components, the responses of the test set up to thermal loadings, the experimental program including specimen preparation methods and experimental procedures adopted to carry out various tests were presented.

As can be seen in Table 3.5, the properties of the materials used in this investigation differ quite significantly. The environmental loading in the forms of wetting, drying, freezing and thawing are expected to influence the magnitude of vertical deformation of the materials. The combinations of the climatic processes considered in this study are unique that will enhance the fundamental understanding of the volume change behaviour of the materials when subjected to various climatic processes. Additionally, the suitability of the materials for various engineering applications can be explored.

Table 3.5: Properties of materials used

Properties	Speswhite kaolin	Pegwell Bay soil	Cement kiln dust
Specific gravity	2.61	2.69	2.72
Atterberg limits			
Liquid limit, *LL* (%)	68.5	29.5	42
Plastic limit, *PL* (%)	42	19.2	27
Plasticity index, *PI*	26.5	10.3	15
Shrinkage limit, *SL* (%)	32.7	16	21
Specific surface area, *S* (m^2/g)	7.63	0.41	0.58
Particle size distribution			
Sand (%)	0	7.3	0
Silt (%)	6.4	84.3	70
Clay (%)	93.6	8.4	30
BS light compaction characteristics			
Optimum water content (%)	26.7	16.2	27.6
Maximum dry unit weight (kN/m^3)	14.56	17.27	14.86
Mineralogy			
Calcite (%)	--	16	85
Dolomite (%)	--	6	--
Kaolinite (%)	95	--	--
Illite (%)	4	--	--
Quartz (%)	--	78	--
Silicon oxide (%)	--	--	14

CHAPTER 4

Freeze-thaw tests on initially saturated slurried specimens

4.1 Introduction

The freeze-thaw action is considered to be one of the most destructive actions that can induce significant damages to many engineered structures located in seasonally frozen soil areas (Wang et al. 2016). The freezing temperature has been of some concern to the temperate regions of the World. For example, in 2013, a winter storm in various parts of the Middle East caused significant distress to the mankind. This suggests that studies of the engineering behaviour of soils by involving freezing and thawing processes are extremely relevant to various regions of the World, particularly under the changing climatic conditions.

The influences of frost heave and thaw settlement have been known to affect various engineering structures, such as pavements and foundations of buildings. The magnitudes of frost heave and thaw settlement are primarily related to the soil types and freeze-thaw conditions (Chamberlain and Gow 1979; Chamberlain 1981a; Simonsen and Isacsson 1999). For example, after freezing and thawing processes, loose saturated soils may tend to densify, whereas dense soils may become looser (Konrad 1989d). During the period of freezing, the state of water in the pores of soils changes from the liquid (water) to solid (ice). Additionally, under appropriate stress and hydraulic boundary conditions ice lens formation prevails. Similarly, the temperature increase following the freezing

process causes a change in the state of water from solid (ice) to liquid (water) accompanied by the settlement of soils (Zhang and Kushwaha 1998; Thomas et al. 2009).

A number of studies in the past have reported the frost heave and thaw settlement in case of a variety of soils (Jackson et al. 1966; Morgenstern and Nixon 1971; Morgenstern and Smith 1973; Nixon and Morgenstern 1974; Chamberlain and Gow 1979; Konrad and Morgenstern 1980; Chamberlain 1981b; Konrad 1987; Chamberlain et al. 1990; Konrad and Seto 1994; Eigenbrod 1996; Viklander 1998a, b; Konrad and Lemieux 2005; Thomas et al. 2009; Zhou and Zhou 2012; Hendry et al. 2016). Fine-grained soils (clays and silts) possess greater water holding capacities than coarse-grained soils. Therefore, it may be anticipated that the freezing action of ice will greatly disrupt the engineered structures constructed on such soils (Cui et al. 2014). Soils are usually compacted in many civil engineering constructions. Additionally, various industrial wastes are currently being considered as admixtures to stabilise problematic soils. These geomaterials may undergo freeze-thaw cycles in cold climates. Therefore, it is necessary to understand the effect of freezing and thawing on the volumetric response of various engineering materials.

The engineering behaviour of materials in various geotechnical and geoenvironmental engineering applications are usually studied by considering initially saturated slurried conditions (i.e., water content greater than the liquid limit) of the materials (Eigenbrod 1996; Konrad 2005; Hendry et al. 2016). The outcomes of such studies encompass a wide range of compaction conditions. Additionally, the results from such studies are usually compared with the results for compacted materials.

The objective of this chapter was to study the volume change behaviour of the chosen materials (Speswhite kaolin, Pegwell Bay soil and cement kiln dust) as affected

by one cycle of freezing and thawing. Initially saturated slurried specimens of the materials were considered in this chapter (Test series I; section 3.8). The experimental program presented in section 3.8 is recalled in section 4.2. Section 4.3 presents the test results and discussion. The main findings from this chapter are summarised in section 4.4.

4.2 Experimental program

Specimens were prepared at water contents corresponding to 1.2 times the liquid limits of the chosen materials. The specimens were prepared within the specimen mould (see Figure 3.12). The tests were carried out using the test set up shown in Figures 3.12 and 3.13. Table 3.3 shows the initial conditions of the specimens. The diameter and height of the specimens were 103.5 and 65 mm respectively. The tests were carried out at an applied vertical pressure of 2.0 kPa (Test series I; section 3.8).

The vertical deformation of the specimens during consolidation, freezing and thawing processes were measured at the top of the cooling/heating chamber. Additionally, the vertical deformations of the specimen mould during the freezing and thawing stages were measured. During the freezing process, the temperature at the top of the specimens was lowered to -19.5 ± 0.5 C° and maintained for 24 hours, whereas the thawing process occurred at the ambient laboratory temperature. The temperature at predetermined levels was also monitored. During the consolidation process, the water table was at the top the specimens, whereas during freezing and thawing stages the water table was at the bottom of the specimens. The supplied water to the specimens was at ambient laboratory temperature (21 ± 2 °C). Two specimens were tested for each material. This allowed determining the water content of the specimens at the end of freezing and thawing stages.

4.3 Test results and discussion

4.3.1 Consolidation behaviour at nominal vertical pressure

Figure 4.1 shows the consolidation behaviour of the materials under a nominal pressure of 2.0 kPa. The test results are presented in terms of vertical deformation and change in the height of specimens on a semi-log scale in Figure 4.1. The magnitudes of consolidation settlement, heights after consolidation, the coefficient of consolidation (C_v), the coefficient of volume change (m_v) and coefficient of permeability (k) of the materials are presented in Table 4.1. The C_v values were calculated based on log-time method (Terzaghi et al. 1996). The m_v and k values were calculated based on the Terzaghi's consolidation theory. The void ratios of the materials at an applied vertical pressure of 2.0 kPa are shown in Figure 3.11.

It can be seen from Figures 3.11 and 4.1 that the consolidation settlement of cement kiln dust specimen was significantly lesser than the other materials considered. A smaller deformation of cement kiln dust is attributed due to the effect of the cement phase reaction which formed bonding between particles (Buchwald and Schulz 2005). The order of the void ratio of the materials at the nominal applied pressure of 2.0 kPa remained consistent with the results obtained at other applied vertical pressures.

The coefficient of consolidation (C_v) decreases with an increase in the plasticity index. The plasticity index of Pegwell Bay soil, cement kiln dust and Speswhite kaolin were 10.3, 15, 24% respectively (see chapter 3). The values of C_v of Pegwell Bay soil and cement kiln dust specimens (see Table 4.1) were found to be of the similar order of magnitude. The C_v of Speswhite kaolin was found to be lesser by order of magnitude than the other two materials. The m_v was found to be affected by the vertical strain. The coefficient of permeability of Pegwell Bay soil and cement kiln dust is found to be similar

(10^{-8} m/s). The *k* of Speswhite kaolin was found to be 10^{-9} m/s. The values of *k* for Pegwell Bay soil and cement kiln dust specimens were found to be in the range of poor permeable silty materials, whereas it was found to be similar to impervious homogenous clays in case of the specimen of Speswhite kaolin (Casagrande and Fadum 1940; Terzaghi et al. 1996). The differences in the coefficient of permeability may influence the freeze and thaw behaviour of these materials since both the ice lens formation during the freezing process and the consolidation settlement during the thawing process are affected by the permeability of the material (Morgenstern and Nixon 1971; Morgenstern and Smith 1973; Konrad and Morgenstern 1980).

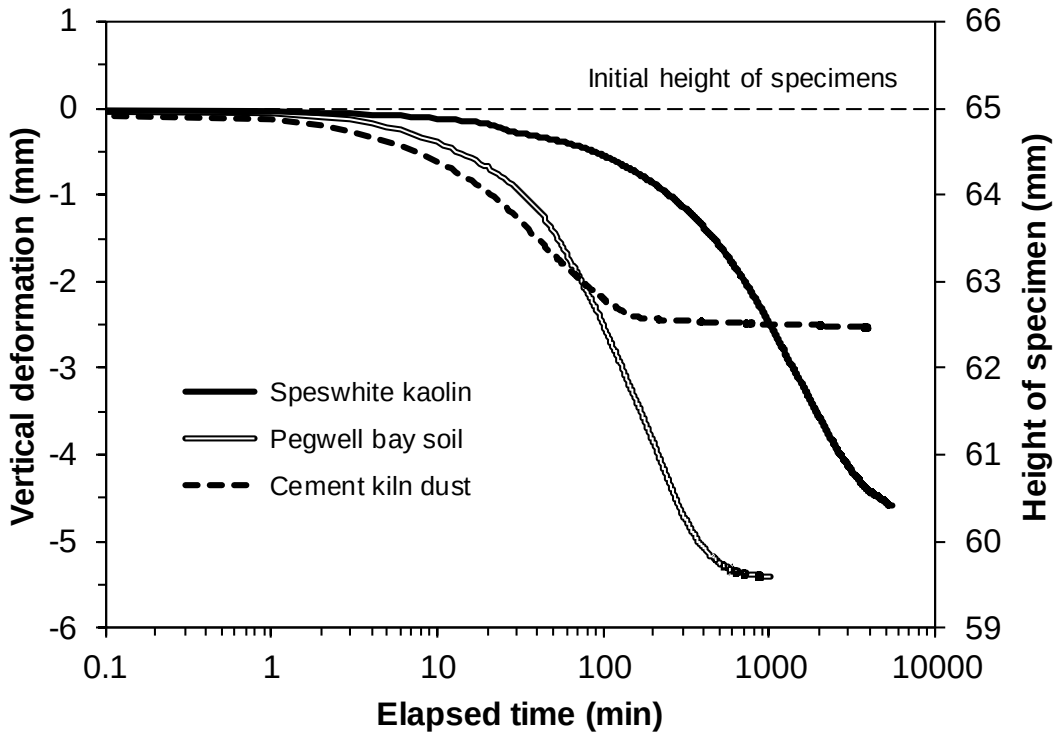

Fig. (4.1): Consolidation behaviour of the materials studied under a nominal vertical pressure of 2.0 kPa

Table 4.1: Vertical deformation, height of specimen, coefficient of consolidation (C_v), coefficient of volume change (m_v) and coefficient of permeability (k) of the materials for applied vertical pressure of 2.0 kPa

Specimen	Vertical deformation (mm)	Height of specimen after consolidation (mm)[a]	C_v (m^2/year)	m_v (m^2/MN)	k (m/sec)
Speswhite kaolin	4.60	60.40	0.497	35.38	5.28×10^{-9}
Pegwell Bay soil	5.41	59.59	3.921	83.23	4.89×10^{-8}
Cement kiln dust	2.53	62.47	14.04	19.46	8.25×10^{-8}

[a] Initial height of specimens = 65 mm

4.3.2 Development of frost heave during the freezing process

4.3.2.1 Thermocouple positions after consolidation

The positions of the thermocouples from top of the specimens prior to the consolidation process were at 0 (TC0), 4.5 (TC1), 29.5 (TC2), 54.5 (TC3) and 63.5 mm (TC4). The thermocouple TC0 measured the air temperature within the top cooling/heating chamber, whereas the other thermocouples (TCs1 to 4) were in contact with the specimen and located on the wall of the specimen mould at the predetermined heights. The cooling junction of the thermocouples in contact with the specimen had coverage of about 1.0 mm.

The decrease in the height of the initially saturated slurried specimens under an applied vertical pressure of 2.0 kPa affected the positions of the thermocouples with reference to the top of the specimens. Table 4.2 shows the original and modified positions of the TCs with reference to the top of the specimens by considering the height changes of the specimens due to consolidation under an applied pressure of 2.0 kPa (see Table 4.1 for the settlement values).

Table 4.2: The original and modified positions of the thermocouples with reference to the top of the specimens

Thermocouple number	Original position of thermocouples with reference to the top of specimen (mm)	New positions of the thermocouple with reference to the top of specimen (mm)		
		Speswhite kaolin	Pegwell Bay soil	Cement kiln dust
TC0	0	0	0	0
TC1	4.5	-0.1	-0.91	1.97
TC2	29.5	24.9	24.09	26.97
TC3	54.5	49.9	49.09	51.97
TC4	63.5	58.9	58.09	60.97

It can be noted in Table 4.2 that the positions of TC1 for Speswhite kaolin and Pegwell Bay soil specimens remained above the top of the specimens by 0.1 and 0.91 mm as shown by the negative values. By considering a 1.0 mm coverage of the cooling junction of the thermocouples, it can be stated that for these cases the measured temperatures by TC1 represent the temperatures corresponding to the top levels of the specimens. At all other levels, the measured temperatures correspond to the temperatures at modified depths of the specimens.

4.3.2.2 Frost heave development

The elapsed time versus temperature and vertical deformation (vertical strain) during the freezing process for Speswhite kaolin, Pegwell Bay soil and cement kiln dust specimens are shown in Figures 4.2, 4.3 and 4.4 respectively. The revised thermocouple positions are shown in the legends. The vertical deformation of the specimen mould during the tests are also shown in Figures 4.2 to 4.4. The temperature profiles within the specimens at time intervals of 1, 2, 3, 10 and 24 hrs are shown in Figure 4.5.

The test results presented in Figures 4.2a, 4.3a and 4.4a showed that the temperature at the top of the specimens decreased from the ambient laboratory temperature to subzero temperatures within less than about twenty minutes for all cases, as indicated by the temperatures measured by TC0. The temperature within the cooling/heating chamber remained constant at about -19 to -20 °C after more than about 60 minutes and until the end of the freezing stage. With increasing depth of the specimens, the temperature decreased at the relatively slower rate. At smaller depths, the temperature decreased and remained constant after about seven hours (see the measured temperatures by TCs 1 and 2), whereas at larger depths changes in the temperature became lesser after about 15 hours as indicated by the temperature readings of TCs 3 and 4.

The temperatures measured by TC0 and TC1 in case of Speswhite kaolin and Pegwell Bay soil specimens were different although both measured the temperatures closer to the top of the specimens. The differences between the temperatures measured by TC0 and TC1 are attributed to the the thermal conductivity of the mediums (air in case of TC0 and soil specimens in case of TC1) and an exposure of the measurement locations to ambient conditions in the annular space between the two PVC moulds which in turn increased the temperature surrounding TC1.

A comparison of the thermal profiles of the specimens (Figure 4.5) indicated that except some initial differences in the temperature at various salient levels, the thermal profiles of the specimens at the end of 24 hours period were very similar for all the materials studied. Towards the bottom of the specimens, small positive values (+ 1.5 to 3 °C) of the temperature was noted (see the data of TC4s), whereas the temperatures at the top were negative (-12 to -14 °C; see the data of TC1) indicating that a part of the specimens remained at frozen state and a part remained at unfrozen state.

A drop in the temperature at the top of the specimens within less than about 20 minutes caused ice formation at and near the top end of the specimens. The top end of the specimens remained adhered to the wall of the specimen mould (adfreezing effect) by the ice formed between them which in turn did not allow the expansion of the specimens to occur in an upward direction due to the development of side friction. The expansion of the specimens occurred towards the bottom end (in the direction of least resistance). In order to explain this phenomenon, Figure 4.6 shows the schematics of the test set up after consolidation and at the end of the freezing stage.

The similarities and differences in the specific features of the schematics presented in Figures 4.6a and b are: (*i*) the top and bottom levels of the porous stone remained unchanged (levels A-A and B-B repsectively), (*ii*) the bottom level of the specimen remained unchanged (level B-B); this indicates that the position of the water table was maintained at the base of the specimens during the tests and (*iii*) the volume change of speicmens due to the freezing process was accompanied by lifting of the specimen mould from level A-A to C-C which in turn caused the top of the specimen to shift upward from level D-D to E-E. The vertical deformation measured at the top of the cooling/heating chamber represents the deformation of the specimen (Δh), whereas the deformation of the specimen mould was measured by the two outer LVDTs. The total height of the specimen

after the freezing stage became ($h_0 + \Delta h$), where h_0 is the height of specimen prior to the commencement of the freezing process.

Various methods have been adopted to mitigate the side friction during the freezing tests, such as the use of multi-ring specimen container and by applying various lubricants to the inner surface of specimen rings (lubricated Teflon film, lithium grease, petroleum jelly, vaseline etc.) (Chamberlain 1981b; Eigenbrod et al. 1996; Penner 1986; Eigenbrod 1996; Konrad and Seto 1994; Qi et al. 2008). The main features of the tests conducted in this study were that the specimen mould was a single PVC cell and the frost front moved in a downward direction from the surface of the specimens that caused the expansion of the specimens towards the higher temperature end.

The average values of the LVDT readings at the top of cooling/heating chamber and at top of specimen mould are presented as the deformation of the specimens and deformation of the specimen mould in Figures 4.2b, 4.3b, and 4.4b. A decrease in the temperature caused the development of frost heave in all the materials (Figures 4.2b, 4.3b and 4.4b). The frost heave in the materials was on account of a change in the density of liquid water to the density of ice and formation of the ice lenses. Note that a change in the state of water from liquid to solid may cause a volume expansion of only 9% (with reference to the volume of water). The primary heave (O'Neill and Miller 1985) was noticed for the specimen of Speswhite kaolin during the first three hours, whereas no frost heave was exhibited by the specimens of Pegwell Bay soil and cement kiln dust for up to an hour of the tests. Eigenbrod (1996) stated that no heave takes place during the freezing process for certain materials because an increase in the volume is balanced by the volume decrease due to the compression process.

The vertical deformation of the specimens and the specimen mould were found to be similar in case of Speswhite kaolin specimen, whereas a minor difference of less than about 1.0 mm was noted between the two in case of Pegwell Bay soil and cement kiln dust specimens. The vertical deformation associated with frost heave for Speswhite kaolin, Pegwell soil and cement kiln dust specimens were found to be 21.1, 16.3 and 16.4 mm respectively. The vertical deformation did not attain an equilibrium at the time of termination of the freezing process. A similar trend of a non-equilibrium in the frost heave can be noted from the reported works of various researchers (Chamberlain 1981a; Konrad and Lemieux 2005; Hendry et al. 2016).

The vertical strain values were calculated based on the change in height and the height of the specimens prior to the freezing process. The vertical strain of Speswhite kaolin, Pegwell soil and cement kiln dust specimens were found to be 35, 27.3 and 26.2% respectively.

Based on the temperatures measured by TC1 and TC4 at an elapsed time of 60 minutes and the corresponding heights of the specimens, the calculated thermal gradients for Speswhite kaolin, Pegwell Bay soil and cement kiln dust specimens were found to be 0.39, 0.38 and 0.33 °C/mm respectively. The thermal gradient further decreased with an elapsed time for all cases and attained about 0.2 °C/mm at the end of 24 hours. This indicates that thermal gradient did not remain constant throughout the tests.

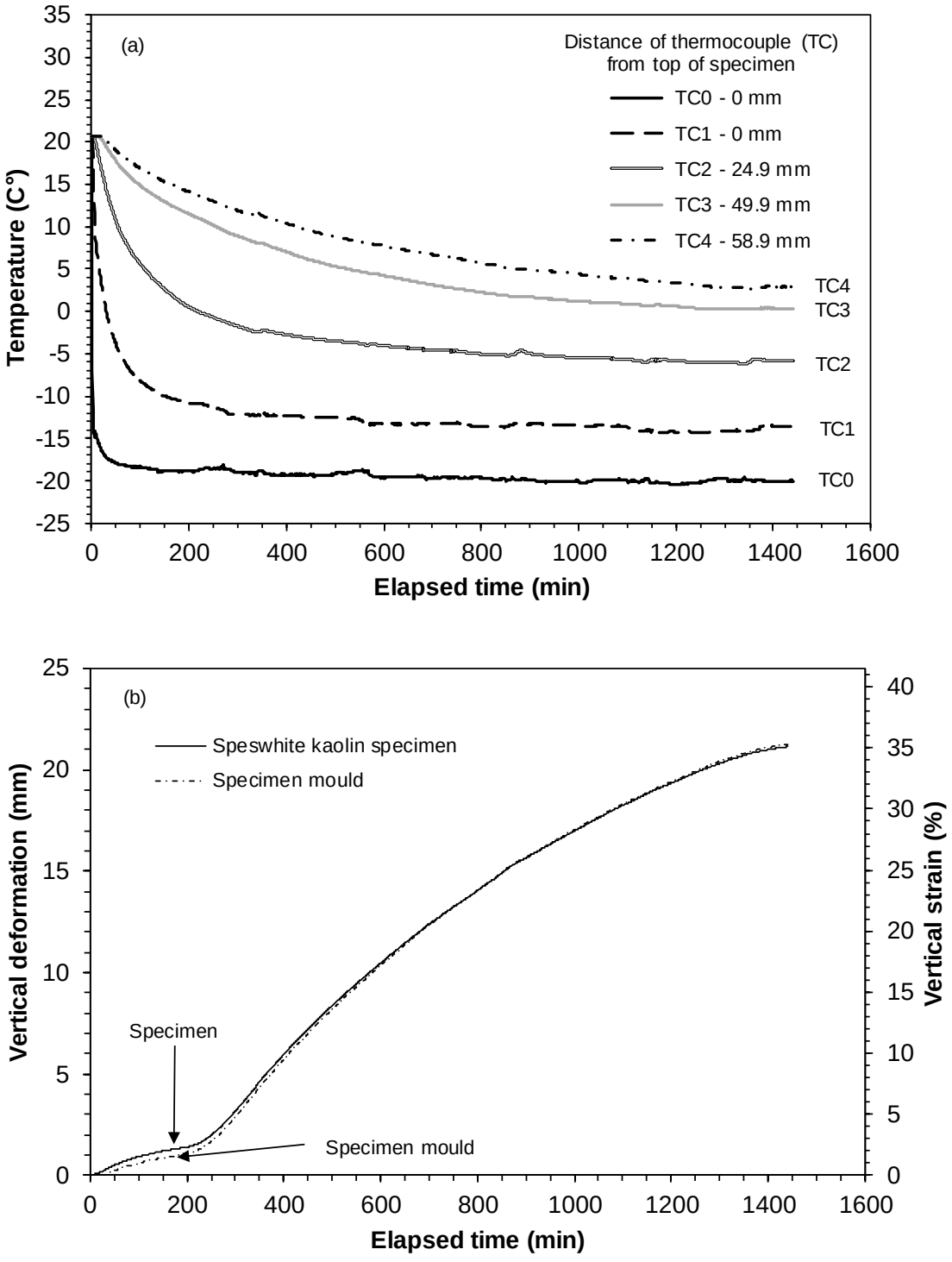

Fig. (4.2): (a) Elapsed time versus temperature and (b) Elapsed time versus vertical deformation and vertical strain for Speswhite kaolin specimen during the freezing process

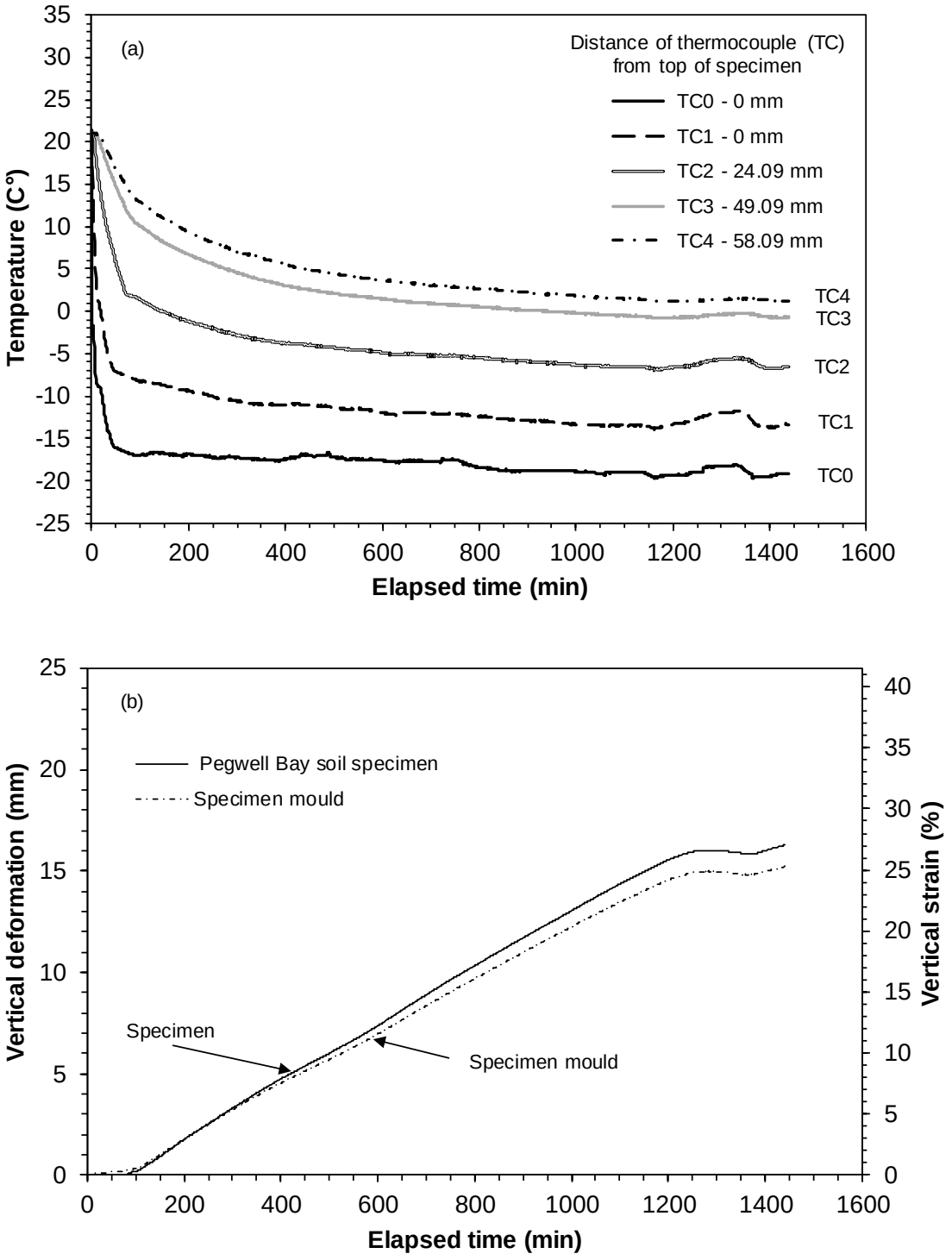

Fig. (4.3): (a) Elapsed time versus temperature and (b) Elapsed time versus vertical deformation and vertical strain for Pegwell Bay soil specimen during the freezing process

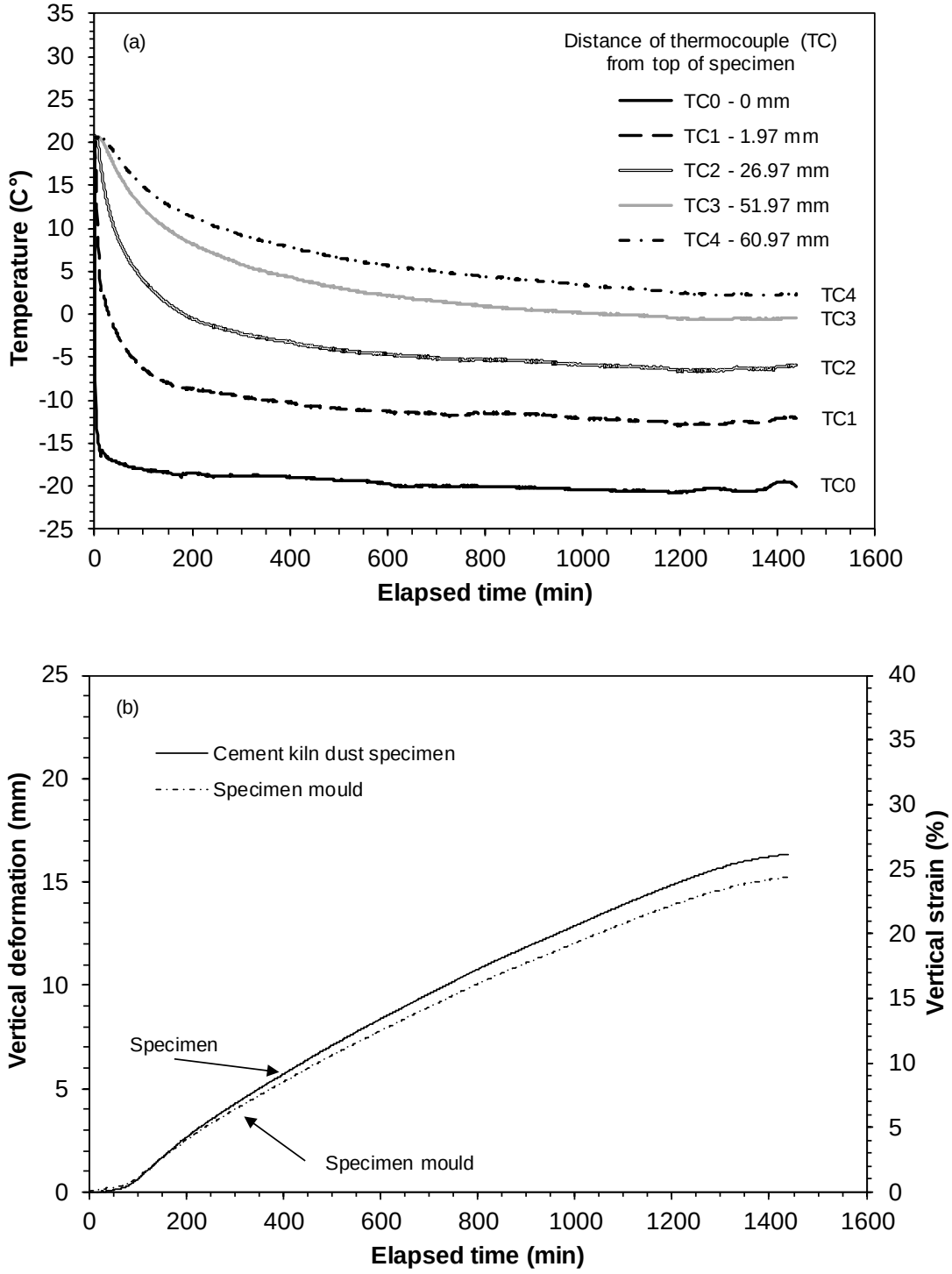

Fig. (4.4): (a) Elapsed time versus temperature and (b) Elapsed time versus vertical deformation and vertical strain for cement kiln dust specimen during the freezing process

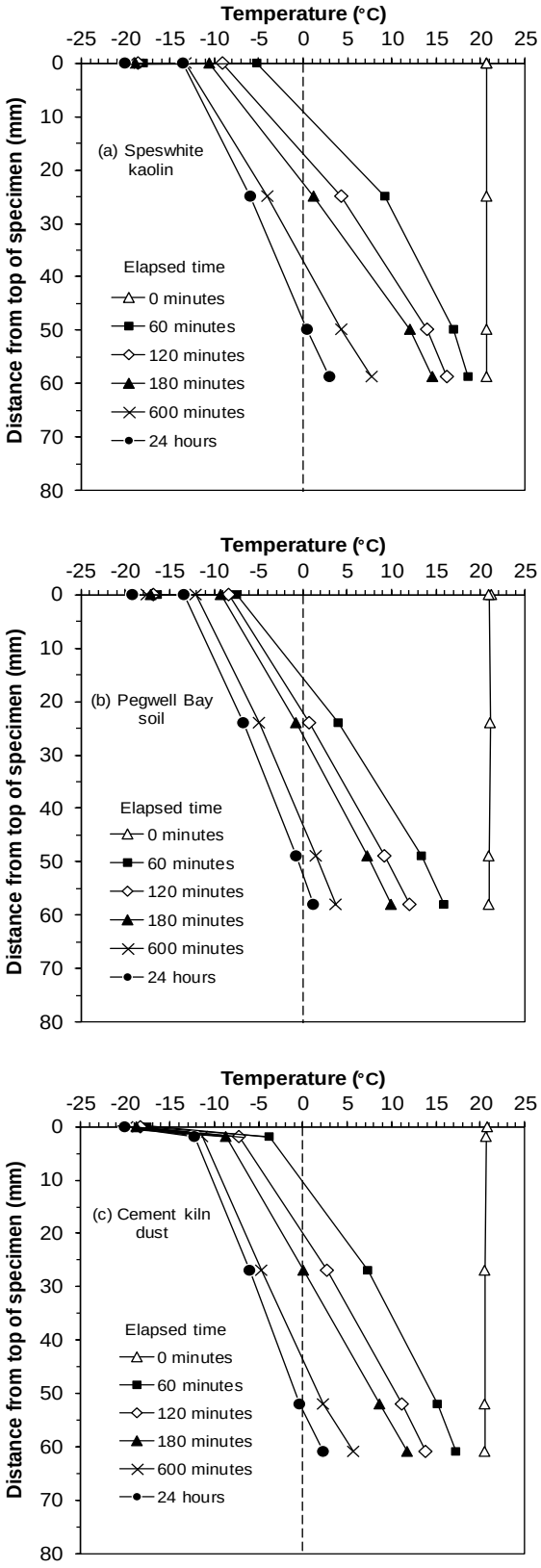

Fig. (4.5): Temperature profiles during freezing of specimens from the top at times 0, 1, 2, 3, 10 and 24 hours

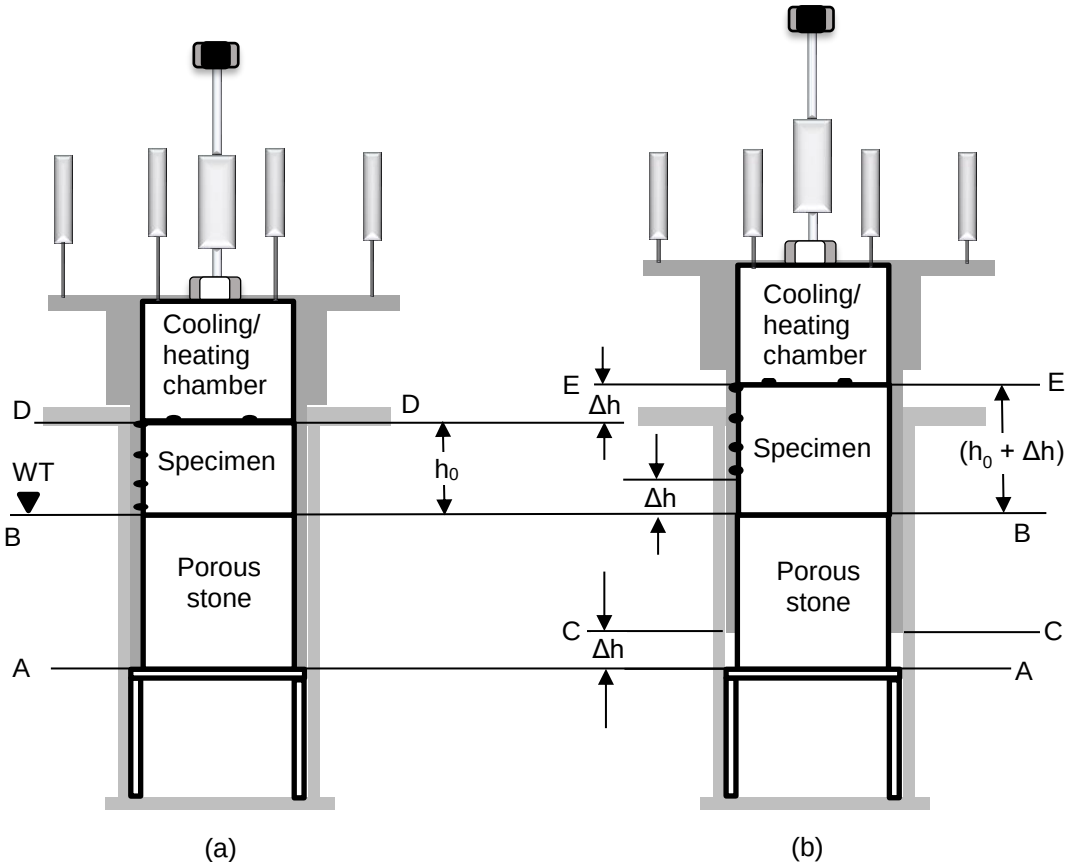

Fig. (4.6): Schematics of the test set up showing various salient features (a) after consolidation and (b) after the freezing process

4.3.2.3 Segregation potential

Konrad and Morgenstern (1980) stated that the permeability of the frozen fringe (i.e. a zone of soil between the ice lens and the unfrozen soil (Miller 1972)) controls the movement of moisture into the ice-water interface. The velocity of water arriving at an advancing frost front is related to the temperature gradient in the frozen soil just behind the frost front (Konrad and Morgenstern 1980, 1981, 1982)**.** As a frost front advances into the soil, moisture is drawn to it, and it is the coupling of the heat and mass flow that constitutes the complex element in the theory of frost heave(Konrad and Morgenstern 1980). The segregation potential is often used to calculate the frost heave in soils.

The measured frost heave of the specimens is presented in Figure 4.7. As can be seen in Figure 4.7, a thermal steady state was reached after an elapsed time of 450 min in all cases. Table 4.3 presents the parameters that were derived from the frost heave results and the segregation potentials (SP_t) of the materials used in this study. The frost heave rate (dh/dt) were calculated based on the frost heave (dh) and the elapsed time (dt) after the steady state. The unit of (dh/dt) in Figure 4.7 is mm/minute, whereas that presented in Table 4.3 is mm/hr. The values of velocity of arriving pore water (v_φ) were calculated based on the heave rates and using Equation 2.6. The temperatures T1 and T2 corresponding an elapsed time of 600 minutes were considered for calculating the temperature gradients (ΔT_f) in the frozen fringe when the materials had reached a steady state condition. The values of T1 and T2 were obtained from the TC1 and TC4 data. The segregation potential (SP_t) for the materials were calculated based on Equation 2.7 (Konrad and Morgenstern 1980, 1981, 1982).

It can be seen in Table 4.3 that between Speswhite kaolin and Pegwell Bay soil, the frost heave rate (dh/dt) and the velocity of water flow (v_φ) decreased with a decrease in the liquid limit. This trend was found to be not applicable for cement kiln dust which had a higher liquid limit than Pegwell Bay soil but showed a lesser heave rate. The ΔT_f values were found to be not significantly different but followed the trend noted for dh/dt and v_φ. The segregation potential depends upon the freezing rate (Konrad and Morgenstern 1981). The segregation potentials of the materials for the freezing rate adopted in this study (it decreased from 10 to 15 mm/hr during the first hour to about 2 mm/hr at 24 hrs) were found to be slightly different for the materials as shown in Table 4.3. The segregation potentials of Speswhite kaolin, Pegwell Bay soil and cement kiln dust were calculated for an elapsed time of 24 hrs and were found to be 4.0, 3.10 and 2.62 respectively. An increase in the segregation potential with elapsed time is attributed due

to a change in the freezing rate which increased from 10 to 15 mm/hr to about 2 mm/hr at the time of termination of the tests.

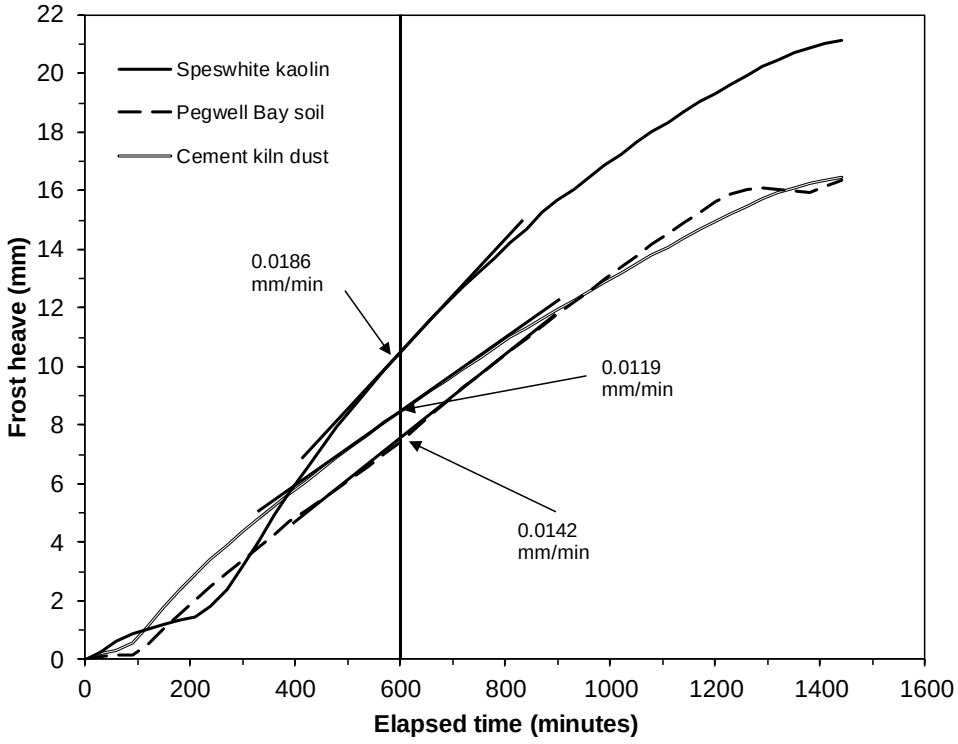

Fig. (4.7): Identification of steady-state frost heave for the materials studied

Table 4.3: Heave rate (*dh/dt*), velocity of water flow (v_φ), thermal gradient (ΔT_f) and segregation potential (SP_t) of the initially saturated slurried materials.

Specimen	*dh* (mm)	*dt* (min)	*dh/dt* (mm/hr)	v_φ = (*dh/dt*)/1.09 (mm/hr)	T1[1] (°C)	T2[1] (°C)	t (mm)	ΔT_f = [(T1-T2)/t] (°C/mm)	SP_t = (v_φ/ ΔT_f) (mm^2/°C.hr)
Speswhite kaolin	8.0	430	1.12	1.03	-13.3	+7.7	58.90	0.36	2.85
Pegwell Bay soil	7.1	500	0.85	0.78	-12.0	+3.7	58.09	0.27	2.88
Cement kiln dust	6.9	580	0.71	0.65	-11.2	+5.8	59.00	0.29	2.25

[1]T1 and T2 are the temperatures corresponding to an elapsed time of 600 minutes that were measured by thermocouples TCs 1 and 4 respectively (see Figure 4.5). The thickness of specimen (t) is the distance between the TC1 and TC4 (see Table 4.2; note that for Speswhite kaolin and Pegwell Bay soil specimens, the positions of TC1 was at the top of the specimens).

4.3.3 Thaw settlement

The specimens after the freezing stage were subjected to a thawing stage in order to complete one cycle of freezing and thawing. The commencement of thawing stage took place by terminating the cold air supply to the top cooling/heating chamber. The drainage was free during this stage. Figures 4.8, 4.9 and 4.10 show the elapsed time versus temperature and vertical deformation (vertical strain) of Speswhite kaolin, The temperature profiles corresponding to various time intervals are shown in Figure 4.11.

It can be seen from Figures 4.8a, 4.9a and 4.10a that the temperature at all depths increased with an elapsed time. For all figures, it can be recognised that the temperature stayed steady for a while and rose after that, this might be attributed to the redistribution of melted water from the frozen part of specimens. After about 600 min, the temperatures at all salient depths were nearly equal for each specimen (Figure 4.11) and further increased to attain the ambient laboratory temperature after more than about 1000 min.

The thawing process was accompanied by melting of ice within the specimens. The LVDTs positioned on the top cooling/heating chamber and on the specimen mould showed downward movements of both. Referring back to Figure 4.6, the level C-C of the specimen mould shown in Figure 4.6b reverted to level A-A, as shown in Figure 4.6a. Additionally, the top level of the specimen (i.e. level C-C in Figure 4.6b) shifted downwards indicating that settlement of the specimens had occurred.

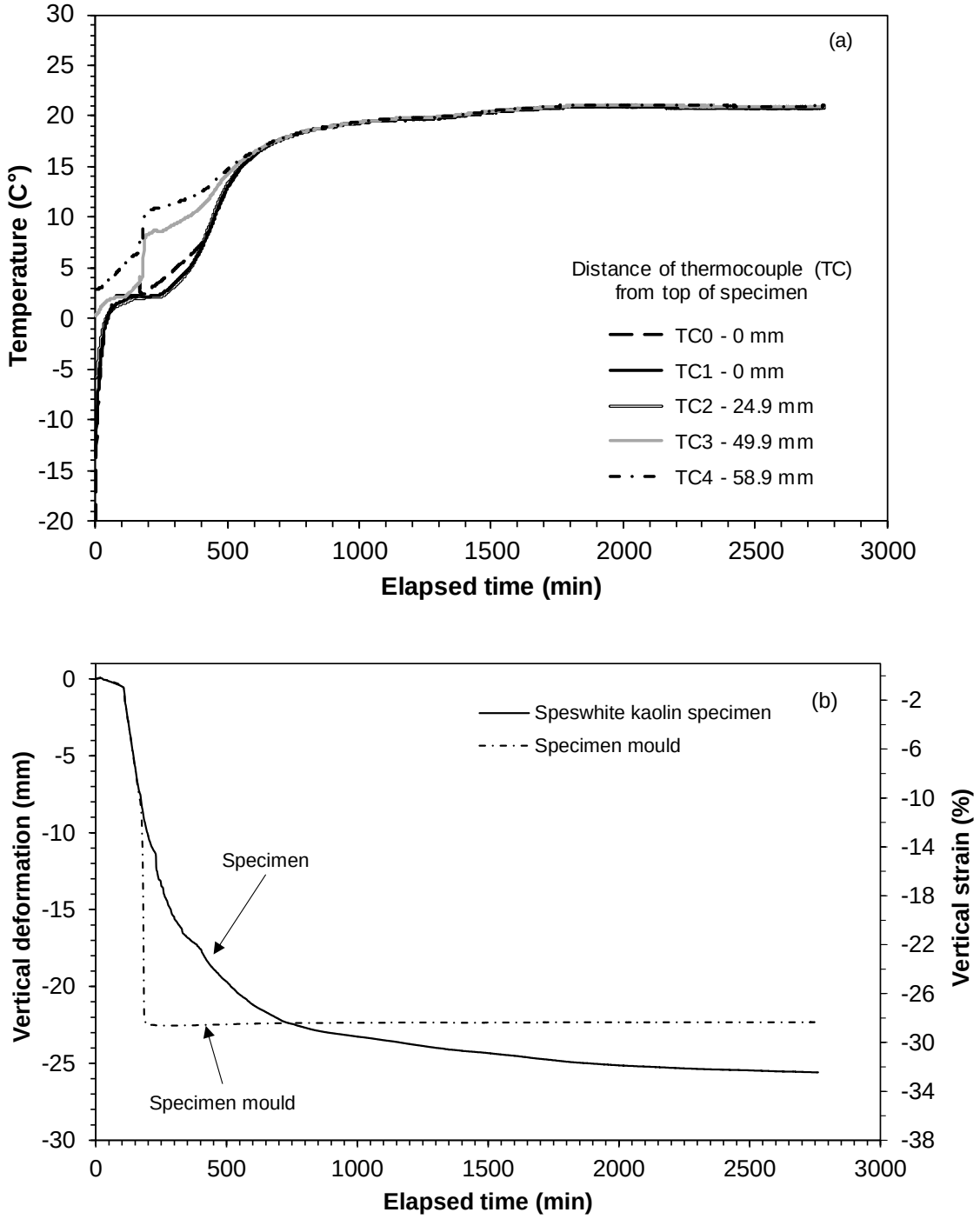

Fig. (4.8): (a) Elapsed time versus temperature and (b) Elapsed time versus vertical deformation and vertical strain for Speswhite kaolin specimen during the thawing process

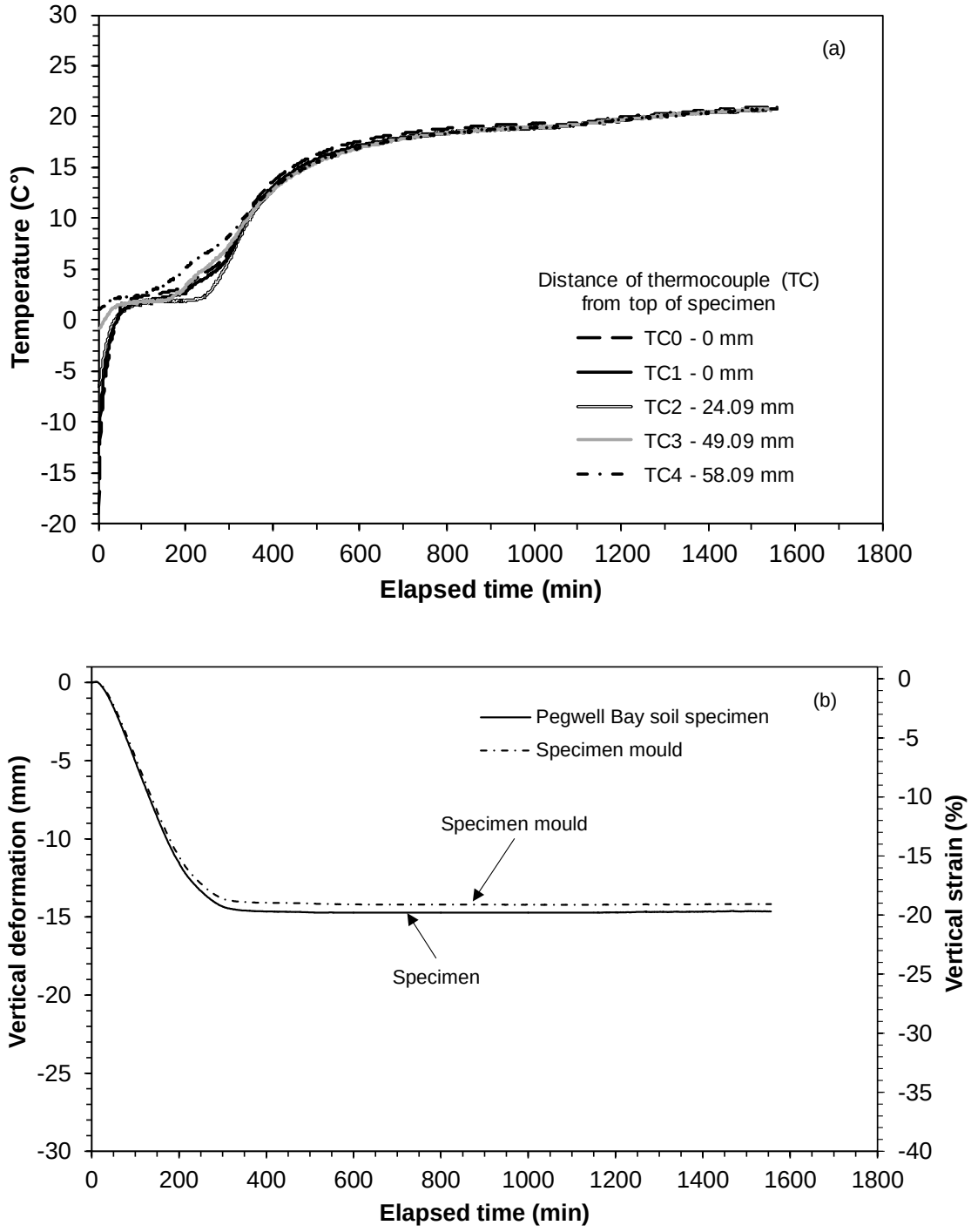

Fig. (4.9): (a) Elapsed time versus temperature and (b) Elapsed time versus vertical deformation and vertical strain for Pegwell Bay soil specimen during the thawing process

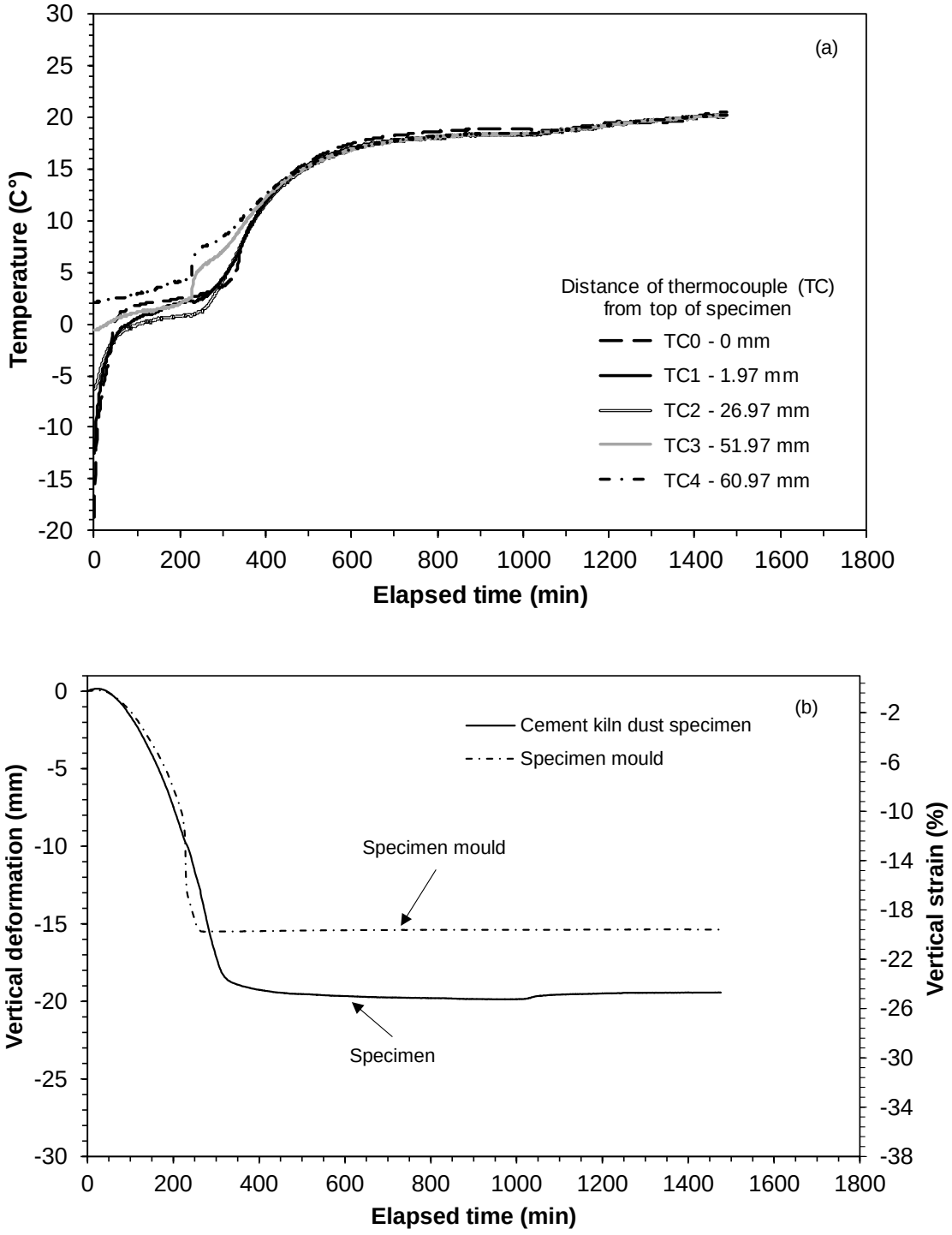

Fig. (4.10): (a) Elapsed time versus temperature and (b) Elapsed time versus vertical deformation and vertical strain for cement kiln dust specimen during the thawing process

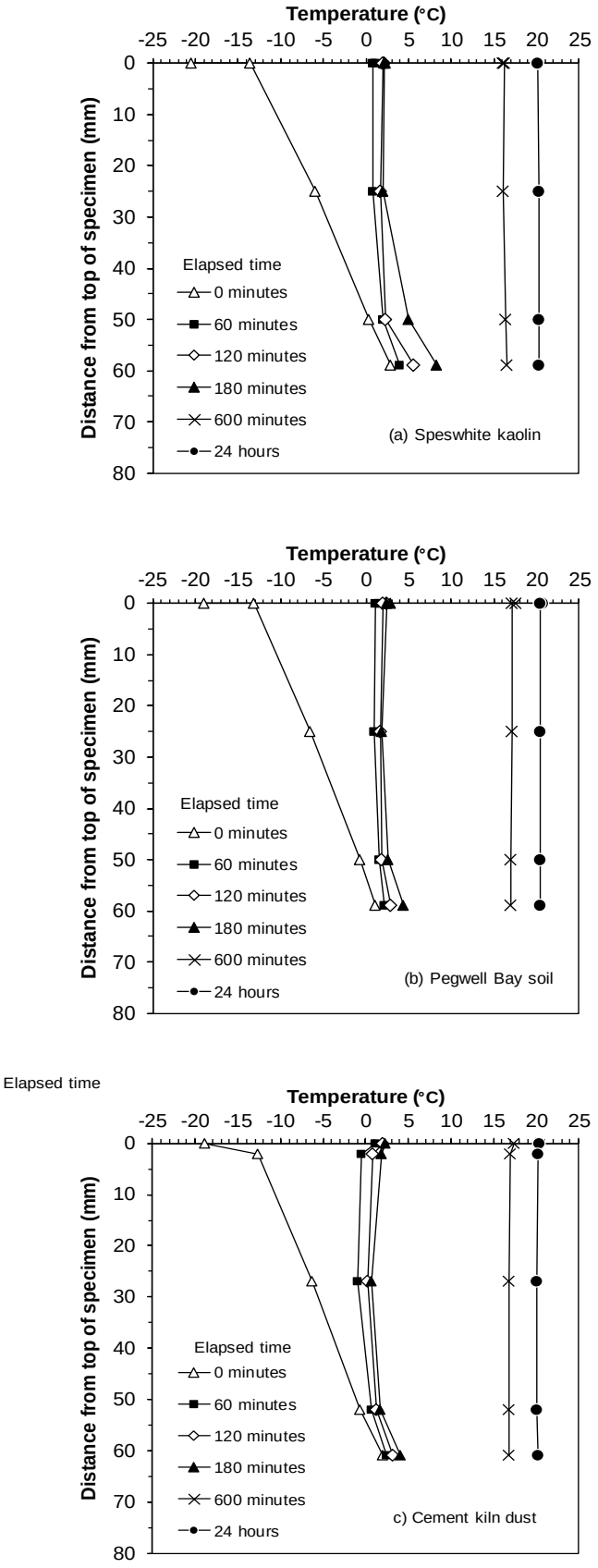

Fig. (4.11): Temperature profiles during thawing of specimens at times 0, 1, 2, 3, 10 and 24 hours

Two very distinct behaviours were noted for during the thawing stage (see Figures 4.8 to 4.10), such as (*i*) the rate at which both the specimen and the specimen mould settled were different; for Speshwite kaolin, the specimen mould settled at a much faster rate than the specimen, whereas in others, both occurred at an equal rate and (*ii*) the settlement of Speswhite kaolin and cement kiln dust were greater than that of the vertical deformation of the specimen mould, whereas the specimen and the specimen mould showed near equal deformations for the Pegwell Bay soil specimen. The test results showed that frictional resistance developed at the top end of the specimens due to the adfreezing depends upon the material type. The effect persisted during the thawing process for Pegwell soil and cement kiln dust specimens.

4.3.3.1 Vertical strain during thawing

Figure 4.12 compares the thaw settlements of the specimens. Table 4.4 shows the heights of the specimens prior to the thawing stage, the magnitudes of thaw settlement, the heights of the specimens at the end of thawing stage and the vertical strain values of the materials. The vertical strains were calculated based on the heights of the specimens at the end of the freezing stage (i.e. heights prior to the thawing stage).

Figure 4.12 shows that an additional heave occurred for all specimens immediately after the thawing process commenced (see inset of Figure 4.12). Cheng and Chamberlain (1988) noted small magnitudes of heave that occurred during thawing of some soils. The occurrence of heave during the thawing process was believed to be governed by a regulation mechanism in which case, as the water migrates from the thawed zone into the frozen zone, the ice and the unfrozen water in the frozen soil are no longer in equilibrium in terms of the energy state. Thus, ice formation occurred in the frozen portion of the thawing soil. Eigenbrod et al. (1996) and Eigenbrod (1996) stated that an increase in soil

volume was partly associated with the decrease in effective stress resulting from the increase in pore-water pressure.

The test results presented in Figure 4.12 and Table 4.4 clearly showed that the magnitude of settlement and vertical strain remained as per the order: Speswhite kaolin, cement kiln dust and Pegwell Bay soil. The vertical strain during thawing was smaller than their counterparts during the freezing process (i.e. 35, 27.3 and 26.2%).

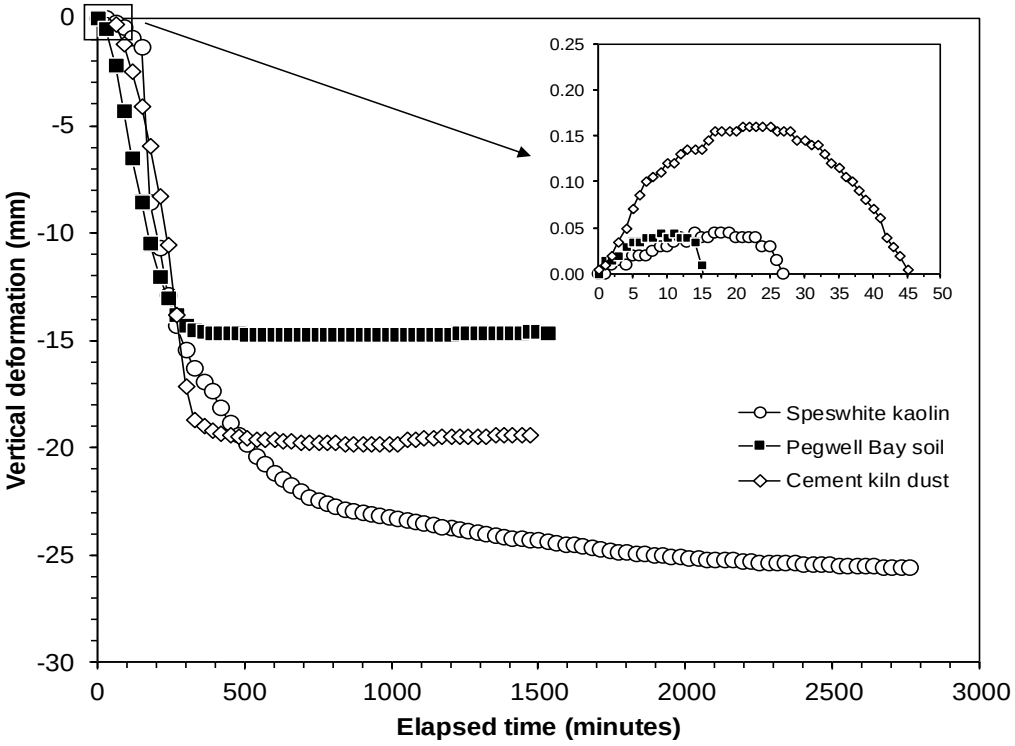

Fig. (4.12): Thaw settlements of the materials

Table 4.4: Thaw settlement and vertical strain of the materials studied

Material	Height of specimen before thawing stage (mm)	Thaw settlement (mm)	Height of specimen at the end of thawing stage (mm)	Vertical strain (%)
Speswhite kaolin	81.5	25.6	55.9	31.4
Pegwell Bay soil	75.9	14.2	61.7	18.7
Cement kiln dust	78.9	19.4	59.5	24.6

The magnitude of settlement during the thawing process depends upon the amount of water present in the material. The thawing of soils causes an increase in the pore water pressure. The pore water pressure dissipates with time which depends upon the permeability of the material. Graham and Au (1985) stated that as thawing progresses downwards from the ground surface, the water escapes easily through the spaces formerly occupied by ice, leaving a fissured clay with reduced moisture content. Chamberlain (1981b) stated that when the ice melts, the aggregates of soil particles usually cannot reabsorb all the water immediately after thawing. Consequently, soils are frequently weaker after thawing than before freezing. With time and proper drainage, the initial strength usually returns.

Figures 4.13 and 4.14 show the height and dry density of the specimens at the end of consolidation under the nominal vertical pressure, freezing and thawing processes. The dry densities of the specimens at the end of each stage were calculated based on the dry mass of the materials and the total volumes at the end of each stage.

It can be seen in Figures 4.13 and 4.14 that as compared to the height of the specimen at the end of consolidation, the height of the specimen due to one cycle of

freezing and thawing decreased and the dry density increased at the end of thawing stage for Speswhite kaolin and cement kiln dust. The height and dry density at the end of thawing remained similar to that prior to the freezing process for Pegwell Bay soil. Therefore, a permanent vertical deformation was noted due to one cycle of freezing and thawing in case of Speswhite kaolin and cement kiln dust. An increase in the dry density for these cases suggested that a denser packing of particles was attained after one cycle of freezing and thawing, similar to that was noted by Konrad (1989) for initially saturated loose soils. Further increase in dry density (decreasing in voids) would be expected with the increasing of freeze-thaw cycles until reaching to the residual void ratio (e^{res}) according to Viklander (1998a).

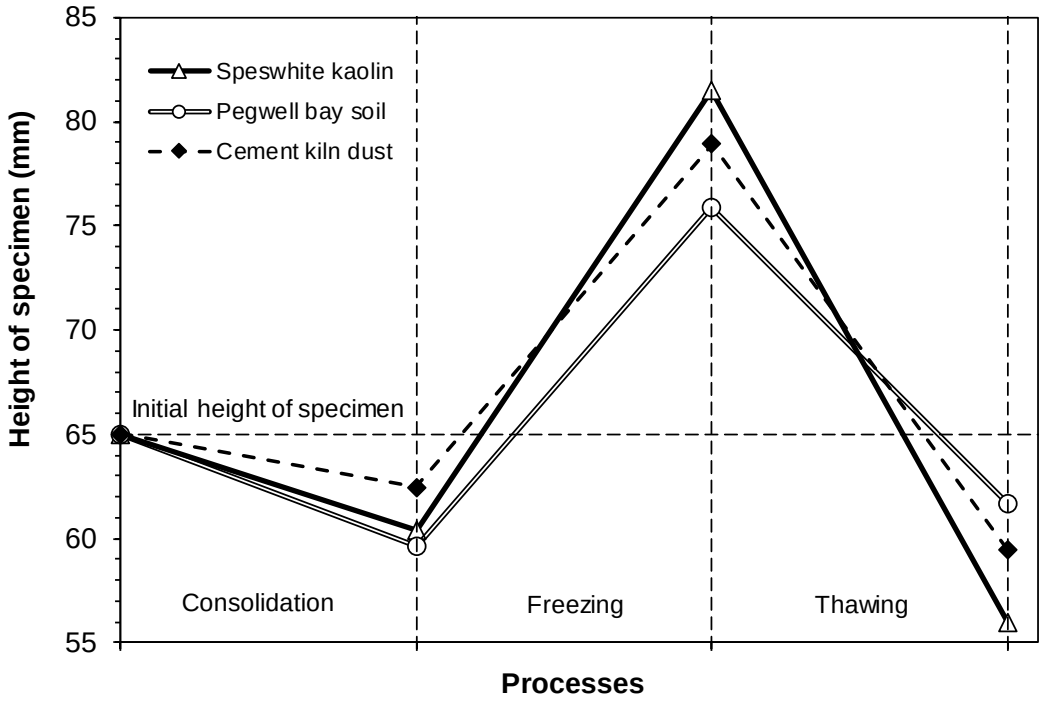

Fig. (4.13): Changes in the height of specimens at the end of various stages of the tests

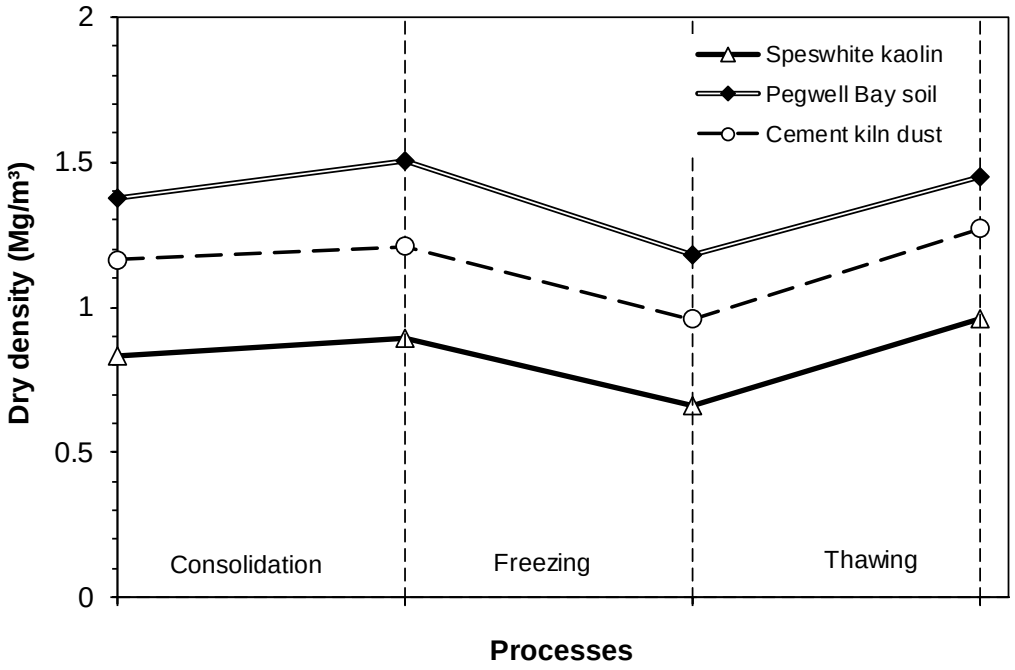

Fig. (4.14): Changes in the dry density of specimens at the end of various stages of the tests

4.3.3.2 Water content at the end of freezing and thawing processes

Figure 4.15 shows the water content of the specimens at the end of freezing and thawing stages. The initial water contents of the specimens (i.e. the water contents after the consolidation stage) are shown in Figure 4.15.

It can be seen in Figure 4.15 that due to the freezing process an increase in the water content of the specimens occurred towards the three-quarter depth of the specimens, whereas the water content generally decreased after the thawing stage. An increase in the water content during freezing is attributed to the formation of ice lenses on account of the movement of water from the base of the specimens in an upward direction. The water content increases at three quarter depth for Speswhite kaolin specimen was about three and half times that of the initial water content, whereas for the specimens of Pegwell Bay soil and cement kiln dust an increase in the water content at and near the same depth was more than about two and half times than the initial water contents. The water content was

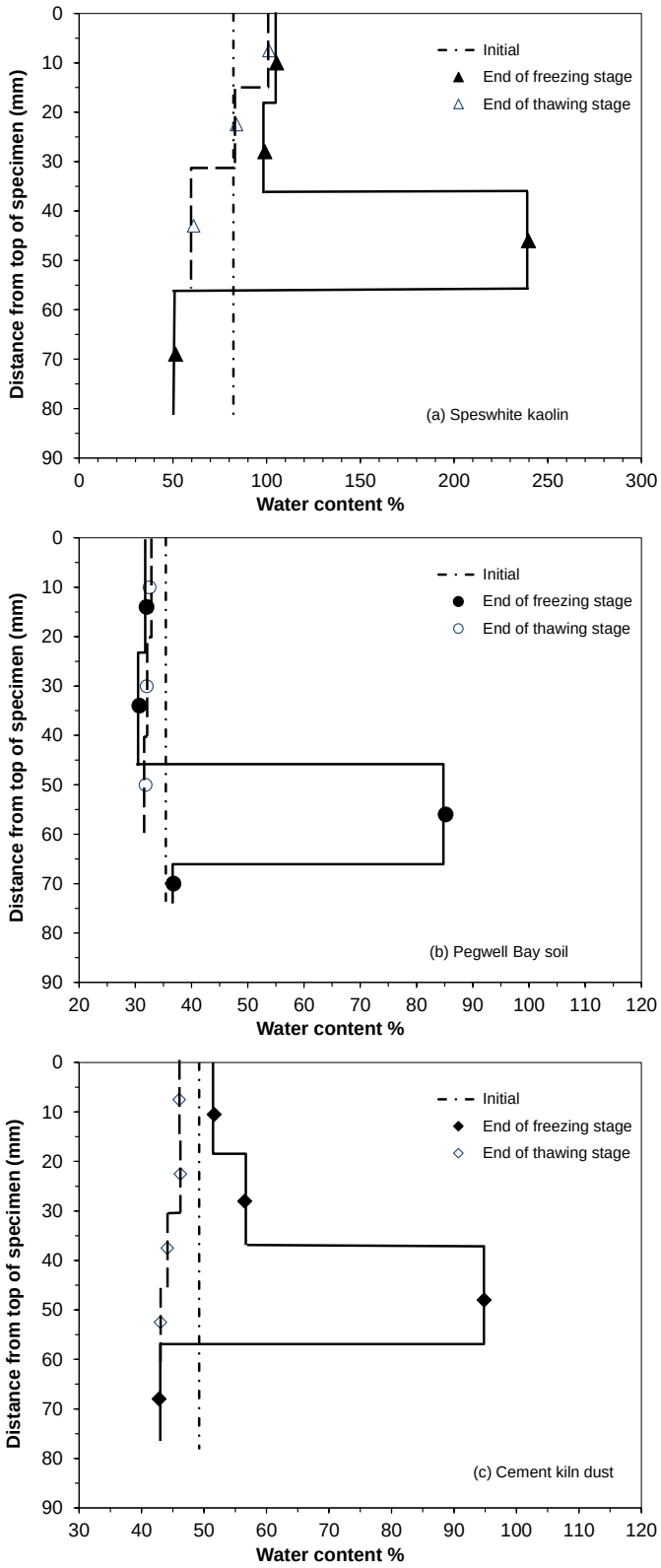

Fig. (4.15): Water content profiles after freezing and thawing stages for (a) Speswhite kaolin, (b) Pegwell Bay soil and (c) Cement kiln dust

less increase towards the top of the specimens. A decrease in the water content due to thawing is primarily due to the thaw-consolidation. A very similar water content all depths for Pegwell Bay and cement kiln dust specimens can be attributed due to a higher permeability of the materials as compared to that of Speswhite kaolin.

4.4 Concluding remarks

This chapter presented the freezing and thawing test results of initially saturated slurried materials. The materials selected for the study (Speswhite kaolin, Pegwell Bay soil and cement kiln dust) had very high fine fractions (100% for Speswhite kaolin and cement kiln dust and about 93% for Pegwell Bay soil). The vertical deformations during freezing and thawing were measured. The temperature at various salient depths was monitored during the tests. The water content of the specimens at the end of freezing and thawing stages were also measured. The following points emerged from the test results.

1. At a nominal applied vertical pressure of 2 kPa, the consolidation settlement of Pegwell Bay soil was found to be greater than that of Speswhite kaolin and cement kiln dust. The values of coefficient of permeability of Pegwell Bay soil and cement kiln dust were found to be similar (10^{-8} m/s), whereas the permeability of Speswhite kaolin was found to be an order of magnitude lesser (10^{-9} m/s) than the other two materials.
2. The vertical strain associated with the frost heave was found to be the greater for Speswhite kaolin (35%) than the other two materials. The vertical strain due to the frost heave of Pegwell Bay soil (27.3%) was found to be greater than that of cement kiln dust (26.2%).
3. The segregation potential is an important parameter which is often used to assess frost heave of particulate systems. The segregation potentials of Speswhite kaolin

and Pegwell Bay soil were found to be similar (2.85 and 2.88 $mm^2/°C.hr$, respectively), whereas it was found to be lesser for cement kiln dust (2.25 $mm^2/°C.hr$).

4. The vertical strain associated with thaw settlement was found to be the greater for Speswhite kaolin (31.4%) than the other two materials. The vertical strain due to thaw settlement of Pegwell Bay soil (18.7%) was found to be lesser than that of cement kiln dust (24.6%).
5. The water content of the materials increased at the end of the freezing process, whereas it decreased at the end of thawing process. The increase in the water content is primarily attributed due to volume expansion associated with the change in state of water and formation of ice lenses.

CHAPTER 5

Freeze-thaw tests on compacted specimens

5.1 Introduction

Soils and various geomaterials (mixtures of soil and various industrial wastes and admixtures) are usually compacted and used in many civil engineering applications. The use of natural soils and mixtures of soils and admixtures are in the areas of pavements, railway formations and backfill etc. Similarly, clays are often used as hydraulic barriers. Examples of the use of clays include liners and covers for landfills, liners for ponds and waste lagoons, and caps for remediation of contaminated sites. In cold regions, compacted geomaterials may be subjected to freezing and thawing processes during the winter months (Othman et al. 1994). Chamberlain et al. (1990) and Benson and Othman (1993) have shown that freezing and thawing affects the structure of compacted soils. The effects of freezing and thawing processes on the volumetric deformation of compacted geomaterials are of significant interest (Konrad 1989c). The objective of this chapter was to study the volume change behaviour of the compacted specimens of Speswhite kaolin, Pegwell Bay soil and cement kiln dust as affected by one cycle of freezing and thawing under a nominal applied pressure of 2.0 kPa.

This chapter is presented in several sections. The experimental program is recalled in section 5.2 (Test series II; section 3.8). Section 5.3 presents the test results and discussion. In section 5.3, the vertical strain due to the frost heave during the freezing process, the heave rate, the segregation potential, the vertical strain due to settlement during the thawing process, and the water contents at the end of freezing and thawing stages are presented and compared with the test results obtained for initially saturated

slurried materials in chapter 4. The main findings from this chapter are summarised in section 5.4.

5.2 Experimental program

Compacted specimens were prepared within the specimen mould by statically compacting the chosen materials to the targeted dry densities at predetermined water contents. For each material, one compaction conditions (dry density and water content) was chosen. Compaction of the specimens was carried out using a static compaction machine (Figure 3.22). The tests were carried out using the test set up shown in Figures 3.12 and 3.13. Table 3.4 shows the initial compaction conditions of the specimens tested. The diameter and height of the specimens were 103.5 and 65 mm respectively. The freeze-thaw tests were carried out at an applied vertical pressure of 2.0 kPa (Test series II; section 3.8).

The vertical deformation of the specimens during saturation, freezing and thawing processes were measured at the top of the cooling/heating chamber. Additionally, the vertical deformations of the specimen mould were measured during all stages of the tests. The temperature at the predetermined levels was also monitored. The saturation of the specimens was carried out at the room temperature. The supplied water to the specimens was at ambient laboratory temperature of 21 ± 2 °C. During the saturation process, the water table was kept at the top the specimens, whereas during freezing and thawing stages the water table was kept at the bottom of the specimens. During the freezing process, the temperature at the top of the specimens was lowered to -19.5 ± 0.5 °C and maintained for 24 hours, whereas the thawing process occurred at the ambient laboratory temperature. Two specimens were tested for each material. This allowed determining the water contents of the specimens at the end of freezing and thawing stages.

5.3 Test results and discussion

5.3.1 Volume change during the saturation process

Prior to subjecting the compacted specimens to one cycle of freezing and thawing, the specimens were saturated (see section 3.8.1.2). Figure 5.1 shows the vertical deformation and change in the height of the specimens during the saturation process. Table 5.1 presents the magnitudes of vertical deformation, the heights of specimens at the end of satration process, the vertical strains, the displacements of the specimen mould during the saturation process and the net increase in the distance of the thermocouple positions as compared to the top of the specimens at the end of the saturation process.

It can be seen in Figure 5.1 that all specimens invariably exhibited swelling accompanied by an increase in the height. A lifting of the specimen mould occurred in all cases as the specimens exhibited swelling (Table 5.1). The vertical deformation and vertical strain of Speswhite kaolin were found to be far greater than of the other materials that exhibited very minor swelling deformations. This is attributed to a higher specific surface area of the clay as compared to the two other materials (Table 3.5) and a low intensity of applied stress (2.0 kPa) during the saturation process.

The displacement of the specimen mould during the swelling of the specimens occurred against the frictional resistance developed at the interface between the specimen and the inner surfaces of the specimen moulds. The test results showed that the frictional resistance in case of Speswhite kaolin specimen was greater.

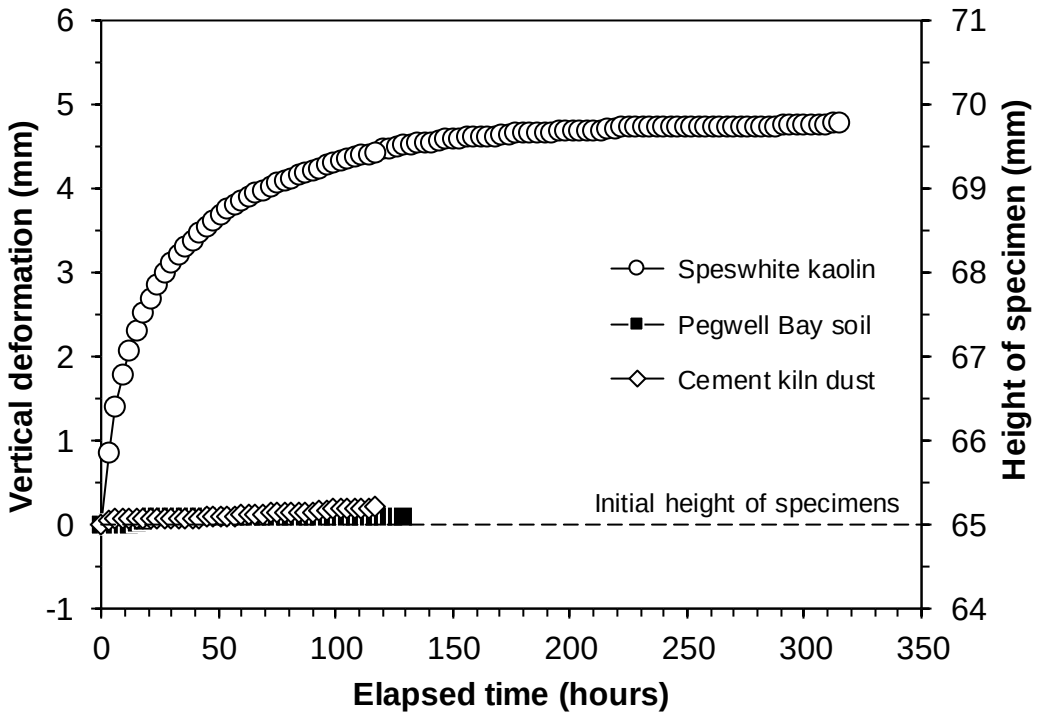

Fig. (5.1): Vertical deformation of the compacted materials during the saturation process (applied stress during saturation = 2.0 kPa)

Table 5.1: Vertical deformation, height of specimen after saturation, specimen mould displacement and net increase in distance of thermocouples from specimen top

Specimen	Vertical deformation of specimen (mm)	Height of specimen after saturation process (mm)[a]	Vertical strain (%)	Specimen mould displacement (mm)	Net increase in distance of thermocouples from specimen top (mm)
Speswhite kaolin	4.79	69.79	7.4	2.26	2.53
Pegwell Bay soil	0.10	65.10	0.15	0.01	0.09
Cement kiln dust	0.22	65.22	0.34	0.02	0.20

[a] Initial height of specimens = 65 mm

5.3.2 Development of frost heave during the freezing process

5.3.2.1 Thermocouple positions after saturation

The positions of the thermocouples from top of the specimens prior to the saturation process were at 0 (TC0), 4.5 (TC1), 29.5 (TC2), 54.5 (TC3) and 63.5 mm (TC4) (section 3.7.1.1). The increase in the height of the compacted specimens during the saturation process and lifting of the specimen mould affected the positions of the thermocouples with reference to the top of the specimens. Table 5.2 shows the initial and modified positions of the TCs with reference to the top of the specimens. The new position of the TCs were calculated based on the initial distances and the net increase in the distances of thermocouples from the top of the specimens as shown in Table 5.1.

Table 5.2: The original and modified positions of the thermocouples with reference to the top of the specimens

Thermocouple number	Original position of thermocouples with reference to the top of specimen (mm)	New positions of the thermocouple with reference to the top of specimen (mm)		
		Speswhite kaolin	Pegwell Bay soil	Cement kiln dust
TC0	0	0	0	0
TC1	4.5	7.03	4.59	4.7
TC2	29.5	32.03	29.59	29.7
TC3	54.5	57.03	54.59	54.7
TC4	63.5	66.03	63.59	63.7

5.3.2.2 Frost heave development

The elapsed time versus temperature, vertical deformation and vertical strain during the freezing process for Speswhite kaolin, Pegwell Bay soil and cement kiln dust specimens are shown in Figures 5.2, 5.3 and 5.4 respectively. The revised thermocouple positions are shown in the legends of Figures 5.2 to 5.4. The vertical deformation of the specimen mould during the tests are also shown in Figures 5.2 to 5.4. The temperature profiles within the specimens at time intervals of 0, 1, 2, 3, 10 and 24 hrs are shown in Figure 5.5. The temperature prior to the commencement of the freezing process for Pegwell Bay soil specimen was about 24 °C, whereas for the other materials it was about 18.5 °C.

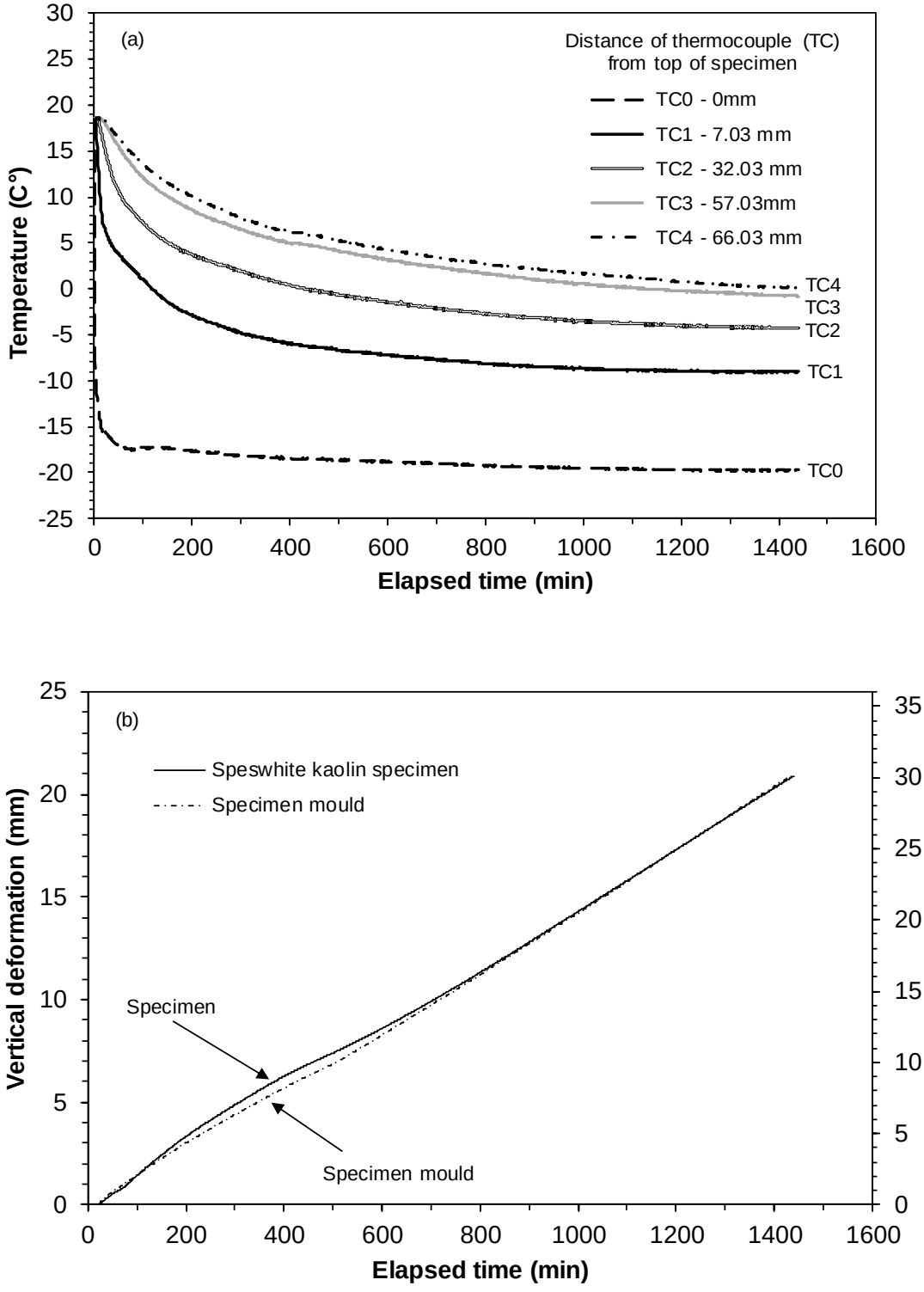

Fig. (5.2): (a) Elapsed time versus temperature and (b) Elapsed time versus vertical deformation and vertical strain for Speswhite kaolin specimen during the freezing process.

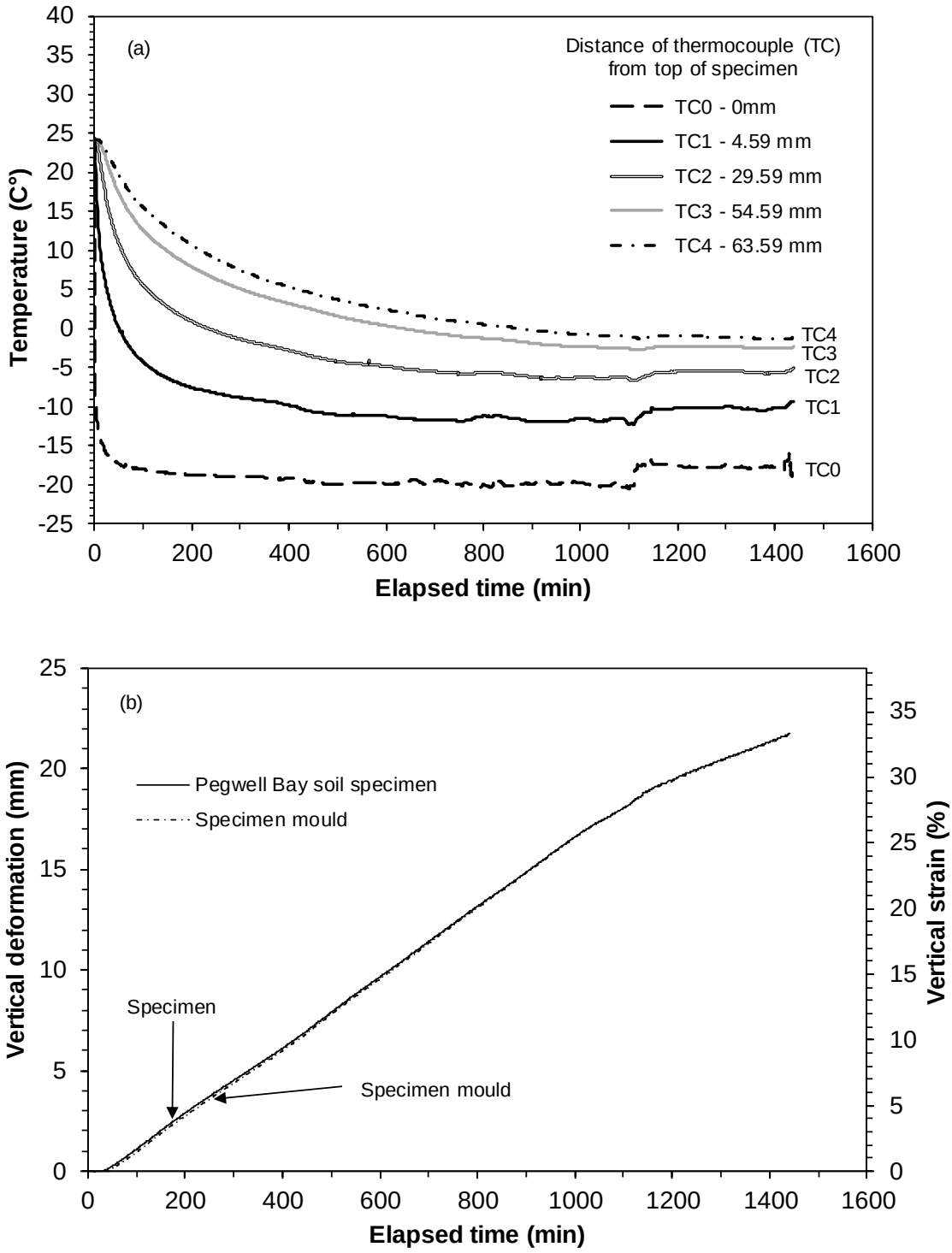

Fig. (5.3): (a) Elapsed time versus temperature and (b) Elapsed time versus vertical deformation and vertical strain for Pegwell Bay soil specimen during the freezing process.

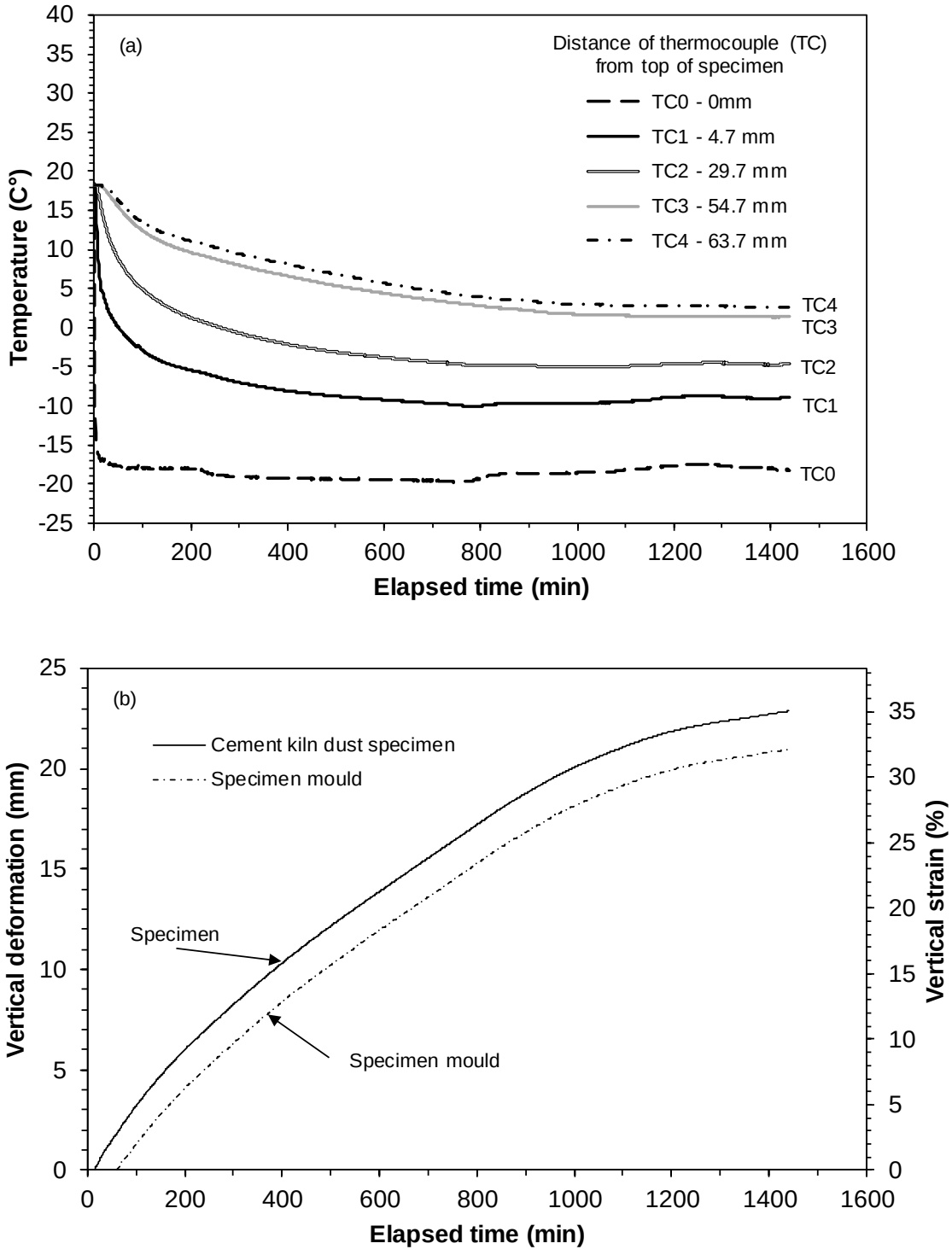

Fig. (5.4): (a) Elapsed time versus temperature and (b) Elapsed time versus vertical deformation and vertical strain for cement kiln dust specimen during the freezing process.

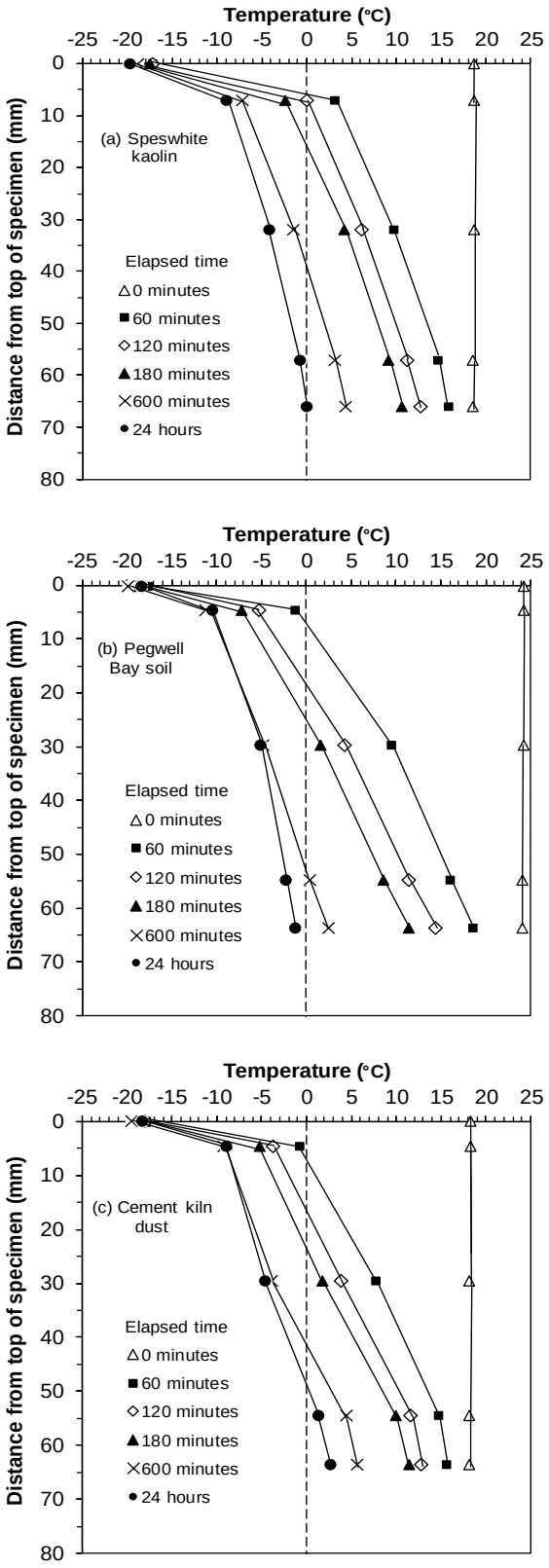

Fig. (5.5): Temperature profiles during freezing of specimens from the top at times 0, 1, 2, 3, 10 and 24 hours.

The test results presented in Figures 5.2a, 5.3a and 5.4a showed that the temperature at the top of the specimens decreased from the initial temperatures to subzero temperatures within less than about twenty minutes for all cases, as indicated by the temperatures measured by TC0. The temperature within the cooling/heating chamber remained constant at about -19 to -20 °C after more than about 60 minutes. A slight increase in the temperature was noted for Pegwell Bay soil and cement kiln dust specimens towards the end of the freezing stage; however, the temperature yet remained negative at the top of the specimens. With increasing depth of the specimens, the temperature decreased at the relatively slower rate. With an elapsed time, a variation of the temperature at all predetermined depths was less (see the measured temperatures by TCs 1, 2, 3 and 4).

The test results in Figure 5.5 showed that for any specimen a difference between the temperature was noted at large specimen depths at longer elapsed times, whereas towards the top of the specimen the temperatures remained very similar. For cement kiln dust, towards the bottom of the specimen small positive values (+ 2 to 3 °C) of the temperature was noted (see the data of TCs 3 and 4), whereas the temperatures towards the top were negative (- 5 to - 9 °C; see the data of TCs 1 and 2) indicating that a part of the cement kiln dust specimen remained at frozen state and a part remained at unfrozen state. The temperature at all depths for the specimens of Speswhite kaolin and Pegwell Bay soil remained negative indicating that for these cases the specimens were nearly frozen. Konard (1989a) stated that subzero temperatures do not always indicate the samples are completely frozen. A part of water within soil system can be considered to be frozen, whereas the amount of unfrozen water increases with an increase in the amount of clay fractions.

A comparison of the thermal profiles of the specimens (Figure 5.5) indicated that there were differences in the temperature profiles of the specimens of Speswhite kaolin and other materials at all elapsed times considered, including at the end of the freezing stage. This was not evident in case of initially saturated slurried specimens which exhibited near similar temperature profiles towards the end of the freezing stage (Figure 4.5). The impact of the differences in the temperature measurement locations (i.e. positions of thermocouples) was found to have a minor influence on the temperature profiles. The test results suggested that for compacted specimens, the type of material (mineralogy and composition), initial compaction conditions, particle rearrangement and the swollen volumes of the materials influenced the temperature profiles.

The adfreezing effect was also found to persist in case of the compacted specimens as that occurred in case of initially saturated slurried specimens. A drop in the temperature at the top of the specimens within less than about twenty minutes caused ice formation at and near the top end of the specimens. The expansion of the specimens occurred towards the bottom end (in the direction of least resistance) as also noted in case of initially saturated slurried specimens in chapter 4. The changes in the salient features during the frost heave of the specimens are shown in Figure 4.6. The position of the water table during the freezing stage did not change. The volume change of specimens due to the freezing process was accompanied by the lifting of the specimen mould. The vertical deformation measured at the top of the cooling/heating chamber represents the deformation of the specimen (Δh), whereas the deformation of the specimen mould was measured by the two outer LVDTs (Figure 4.6). The total height of the specimen after the freezing stage became ($h_0 + \Delta h$), where h_0 is the height of specimen prior to the commencement of the freezing process (see Figure 4.6).

The average values of the LVDT readings at the top of cooling/heating chamber and at top of specimen mould are presented as the deformation of the specimens and deformation of the specimen mould in Figures 5.2b, 5.3b, and 5.4b. A decrease in the temperature caused the development of frost heave in the compacted materials (Figures 5.2b, 5.3b and 5.4b). The frost heave in all cases commenced after about twenty minutes with no indication of any primary heave. The vertical deformation did not attain equilibrium at the time of termination of the freezing process. A similar trend of a non-equilibrium in the frost heave can be noted from the reported works of various researchers (Chamberlain 1981b; Konrad and Lemieux 2005; Hendry et al. 2016) and also in chapter 4 for initially saturated slurries materials.

The vertical deformation of the specimens and the specimen mould were found to be similar in case of Speswhite kaolin and Pegwell Bay soil, whereas a difference of less than about 1.5 mm was noted between the two in case of cement kiln dust specimen. Table 5.3 presents the vertical deformations due to frost heave, heights of the specimens at the end of the freezing stage and the vertical strains associated with frost heave for the three materials tested. The vertical strain values were calculated based on the change in height and the height of the specimens prior to the freezing process.

Table 5.3: Frost heave and vertical strain associated with frost heave for the compacted materials

Material	Frost heave (mm)	Height of specimen at the end of freezing stage (mm)	Vertical strain due to frost heave (%)[a]
Speswhite kaolin	20.9 (21.1)	90.7	30.0 (35)
Pegwell Bay soil	21.7 (16.3)	86.8	33.3 (27.3)
Cement kiln dust	22.9 (16.4)	88.1	35.1 (26.2)

[a] Values within brackets are for initially saturated slurried specimens

It can be seen in Table 5.3 that the magnitude of vertical deformation associated with frost heave for compacted specimens of Speswhite kaolin, Pegwell Bay soil and cement kiln dust were found to remain within about ± 1.0 mm. For Speswhite kaolin, the vertical deformations of compacted specimen (i.e. 20.9 mm) and initially saturated slurried specimen (21.1 mm, chapter 4) were similar, whereas the vertical deformations of compacted Pegwell Bay soil and cement kiln dust specimens were found to be significantly greater than their initially saturated slurried counterparts which exhibited vertical deformation of 16.3 and 16.4 mm respectively (see the values within brackets in Table 5.3 and section 4.3.2.2 in chapter 4). The vertical strains of compacted specimens of Pegwell Bay soil and cement kiln dust were greater than that of compacted Speswhite kaolin. In case of slurried materials, the reverse was the trend; in which case, the specimen of Spweswhite kaolin exhibited a greater vertical strain due to frost heave. The results indicated that compacted-saturated materials may exhibit significantly higher volume change during the freezing process as compared to initially saturated slurried materials.

Based on the temperatures measured by TC1 and TC4 at an elapsed time of 60 minutes and the corresponding heights of the specimens, the calculated thermal gradients

for Speswhite kaolin, Pegwell Bay soil and cement kiln dust specimens were found to be 0.21, 0.33 and 0.28 °C/mm respectively, as against their initially saturated slurried counterparts as 0.39, 0.38 and 0.33 °C/mm respectively. The thermal gradient further decreased with an elapsed time for all cases and attained about 0.15, 0.20 and 0.20 °C/mm for Speswhite kaolin, Pegwell Bay soil and cement kiln dust respectively at the end of 24 hours. This indicates that thermal gradient did not remain constant throughout the tests as that occurred in case of the initially saturated slurried specimens in which case a temperature gradient at the end of the freezing stage was very similar (of 0.20 °C/mm) (section 4.3.2.2).

5.3.2.3 Segregation potential

Figure 5.6 shows the measured frost heave of the specimens. As can be seen in Figure 5.6, a thermal steady state was reached after an elapsed time of 400 min in all cases. Table 5.4 presents the parameters that were derived from the frost heave results and the segregation potentials (SP_t) of the compacted materials used in this study.

The frost heave rate (*dh/dt*) were calculated based on the frost heave (*dh*) and the elapsed time (*dt*) after the steady state. The unit of (*dh/dt*) in Figure 5.6 is mm/minute, whereas that presented in Table 5.4 is mm/hr. The values of velocity of arriving pore water (v_φ) were calculated based on the heave rates and using Equation 2.6. The temperatures T1 and T2 corresponding an elapsed time of 600 minutes were considered for calculating the temperature gradients (ΔT_f) in the frozen fringe when the materials had reached a steady state condition. The values of T1 and T2 were obtained from the TC1 and TC4 data. The segregation potential (SP_t) for the materials were calculated based on Equation 2.7 (Konrad and Morgenstern 1980; 1981; 1982). The relevant parameters in Table 5.4 for initially saturated slurried materials are shown within brackets for comparing with the compacted materials.

It can be seen in Table 5.4 that between Speswhite kaolin and Pegwell Bay soil, the frost heave rate (*dh/dt*), the velocity of water flow (v_φ) and the segregation potential (SP_t) increased with a decrease in the liquid limit. The same trend was also noted between Speswhite kaolin and cement kiln dust. Although the origins of Pegwell Bay soil and cement kiln dust were entirely different; however, very similar values of (*dh/dt*), v_φ, ΔT_f and SP_t were noted.

As compared to the initially saturated slurried specimen, the heave rate and the velocity of water flow decreased for the compacted specimen of Speswhite kaolin, whereas the parameters increased for the compacted specimens of Pegwell Bay soil and cement kiln dust. The temperature gradient decreased, whereas the segregation potential increased in all cases. The vertical pressure at which the specimens were tested (2 kPa) was far lesser than the applied compaction pressures during the preparation of the specimens (650 to 750 kPa, Table 3.4). Therefore, the tests in this study can be considered to be on the overconsolidated specimens of the materials.

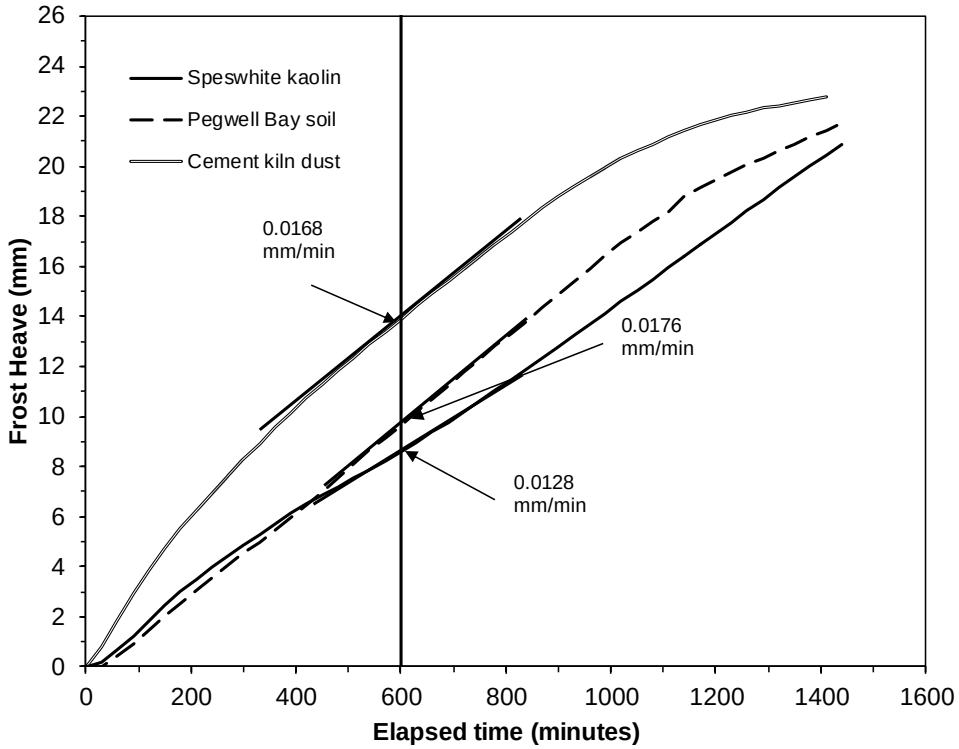

Fig. (5.6): Identification of steady-state frost heave for the materials studied

Table 5.4: Heave rate (*dh/dt*), velocity of water flow (v_φ), thermal gradient (ΔT_f) and segregation potential (SP_t) of compacted saturated materials.

Specimen	*dh* (mm)	*dt* (min)	*dh/dt* (mm/hr)	v_φ = (*dh/dt*)/1.09 (mm/hr)	T1[1] (°C)	T2[1] (°C)	t (mm)	ΔT_f = [(T1-T2)/t] (°C/mm)	SP_t = ($v_\varphi/\Delta T_f$) (mm^2/°C.hr)
Speswhite kaolin	5.1	400	0.77 (1.12)	0.71 (1.03)	-7.2	+4.2	59.0	0.19 (0.36)	3.74 (2.85)
Pegwell Bay soil	6.7	380	1.06 (0.85)	0.97 (0.78)	-11.2	+2.4	59.0	0.23 (0.27)	4.22 (2.88)
Cement kiln dust	8.4	500	1.01 (0.71)	0.92 (0.65)	-9.2	+5.6	59.0	0.25 (0.29)	4.04 (2.25)

[1]T1 and T2 are the temperatures corresponding to an elapsed time of 600 minutes that were measured by thermocouples TCs 1 and 4 respectively (see Figure 5.5). The thickness of specimen (t) is the distance between the TC1 and TC4 (see Table 5.2; note that for Speswhite kaolin and Pegwell Bay soil specimens, the positions of TC1 was at the top of the specimens). Values within brackets are for initially saturated specimens.

Konrad (1989a) stated that increasing the density of soil, by compaction or overconsolidation, decreases the void ratio but also decreases the hydraulic conductivity, thereby controlling the rate of growth of ice lenses. Rutledge (1940) stated that below the critical density, frost action is directly proportional to density; above the critical density, frost action is inversely proportional to density.

Konrad (1989b)'s investigation showed that there may be two cases of a change in the segregation potential, such as (*i*) specimens with lower void ratio (higher OCR) may exhibit lower segregation potential than normally consolidated specimens and (*ii*) the combined effects of decreasing void ratio and increasing suction at the frost line may result in decreasing the segregation potential. An increase in the segregation potential for

compacted materials as compared to the initially saturated slurried specimens in this study is attributed due to the structure and fabric of compacted materials which are favourable to the formation of ice lenses causing an overall increase in the segregation potential.

5.3.3 Thaw settlement

The specimens after the freezing stage were subjected to a thawing stage in order to complete one cycle of freezing and thawing. The commencement of thawing stage took place by terminating the cold air supply to the top cooling/heating chamber. The drainage was free during this stage.

Figures 5.7, 5.8 and 5.9 show the elapsed time versus temperature and vertical deformation (vertical strain) of Speswhite kaolin, Pegwell Bay soil and cement kiln dust respectively. The temperature profiles corresponding to various time intervals are shown in Figure 5.10.

It can be seen from Figures 5.7a, 5.8a and 5.9a that the temperature at all depths increased with an elapsed time. After about 600 min, the temperatures at all salient depths were nearly equal for each specimen (Figure 5.10) that further increased to attain the ambient laboratory temperature.

The thawing process was accompanied by melting of ice within the specimens. The LVDTs positioned on the top cooling/heating chamber and on the specimen mould showed downward movements of both. Therefore, the thaw settlement was accompanied by a downward movement of the specimen mould due to a loss of friction at the boundaries and settlements of the specimens. The magnitudes of deformation of the specimens and the specimen mould were found to be very similar (Figures 5.7 to 5.9).

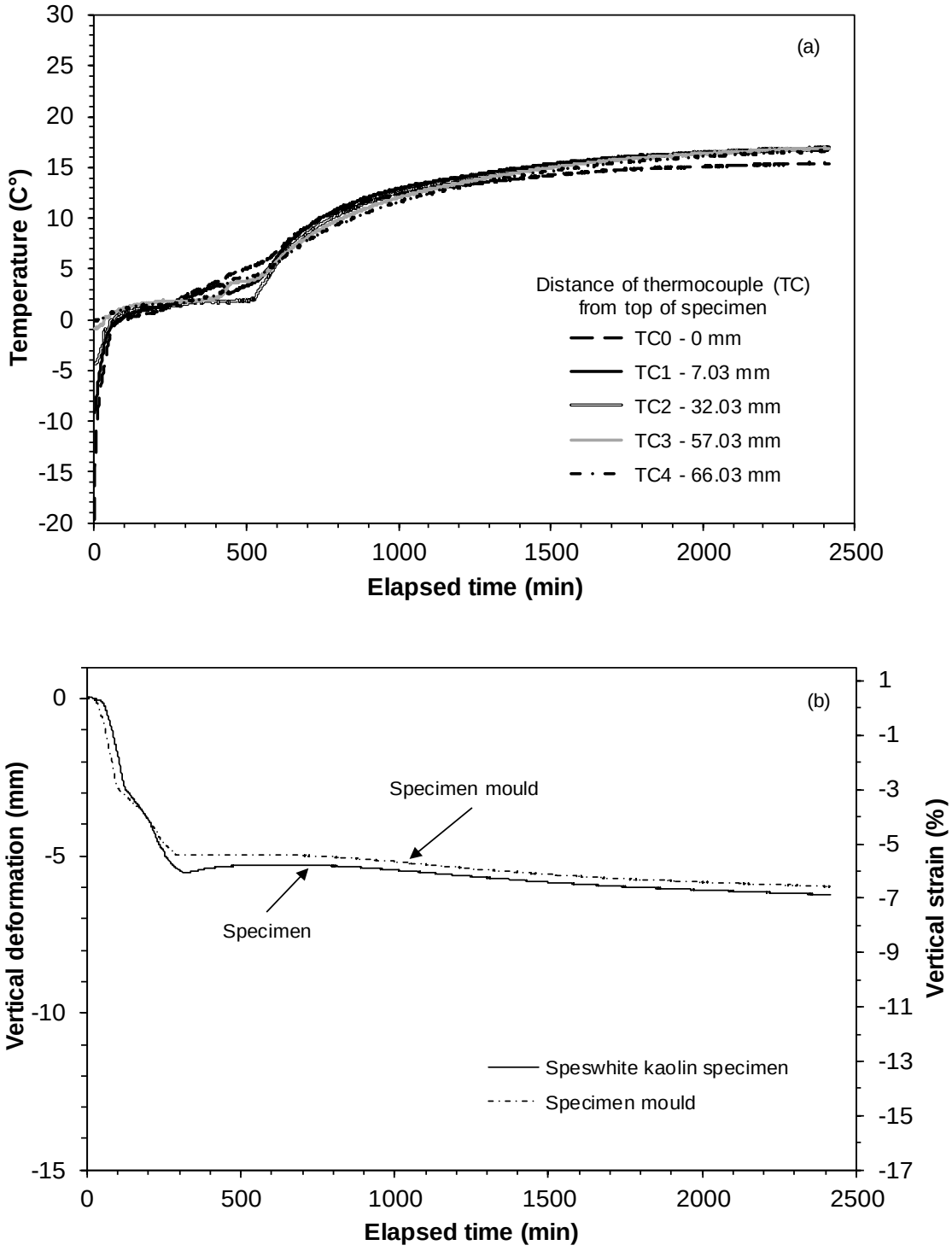

Fig. (5.7): (a) Elapsed time versus temperature and (b) Elapsed time versus vertical deformation and vertical strain for Speswhite kaolin specimen during the thawing process.

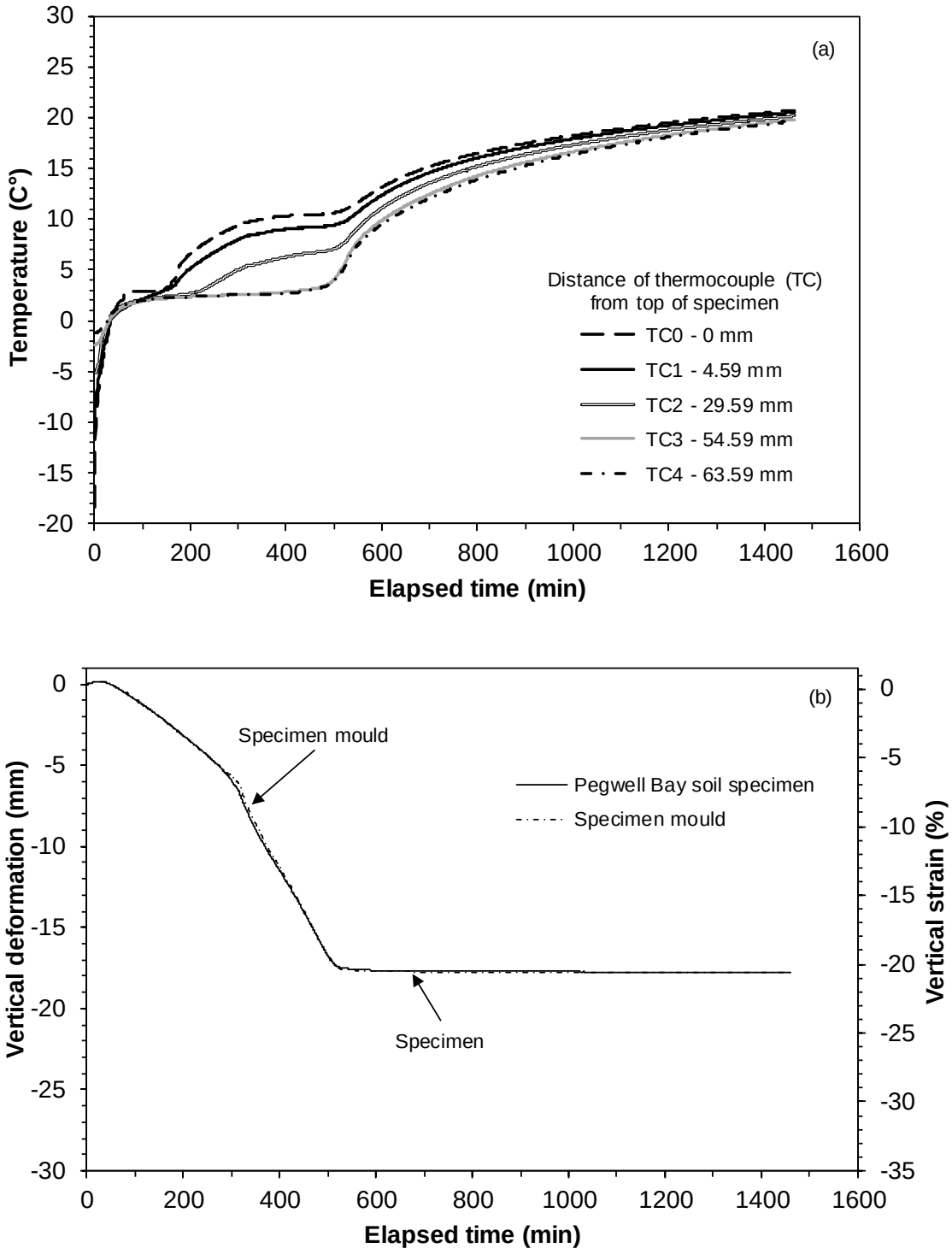

Fig. (5.8): (a) Elapsed time versus temperature and (b) Elapsed time versus vertical deformation and vertical strain for Pegwell Bay soil specimen during the thawing process.

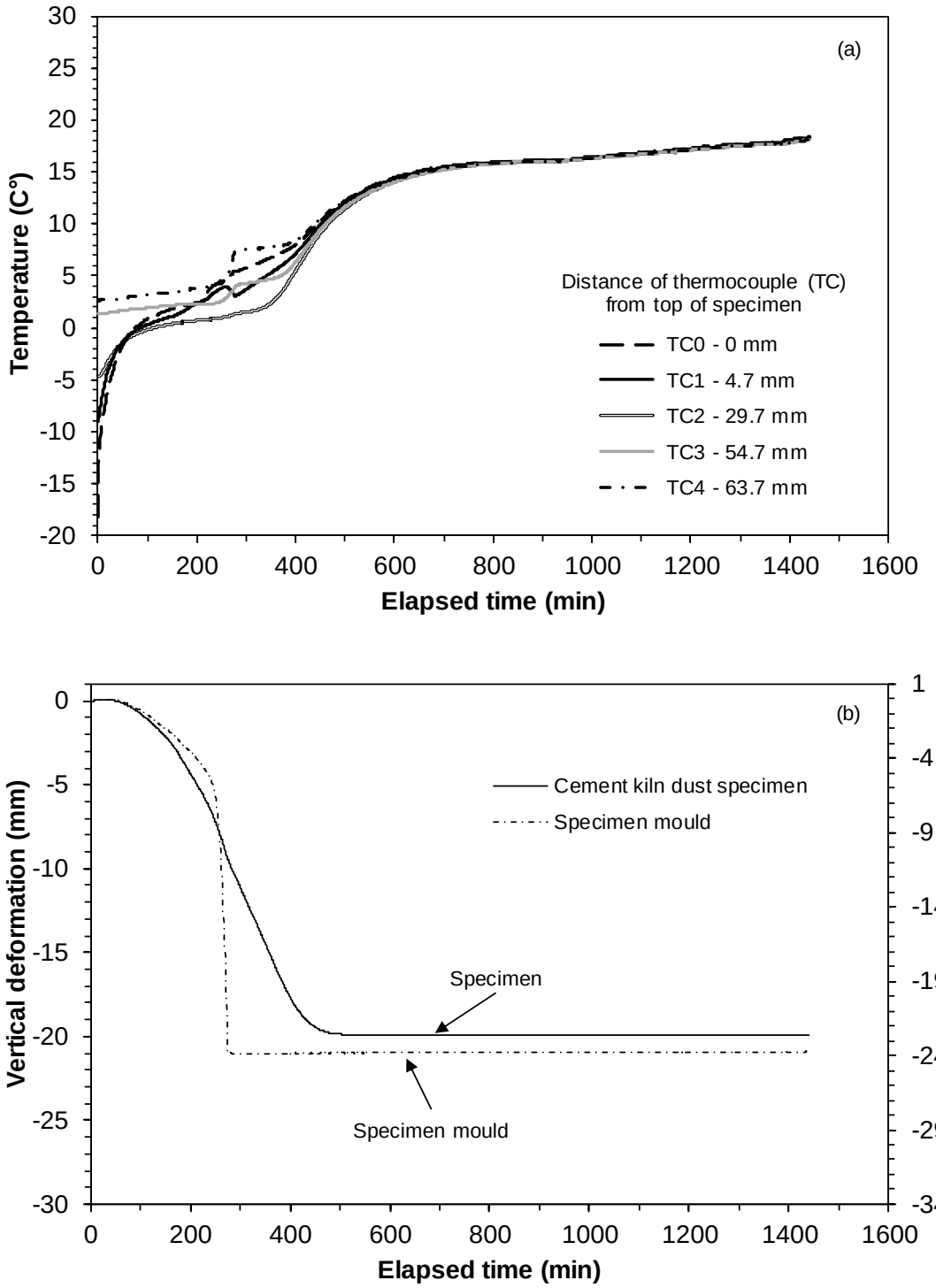

Fig. (5.9): (a) Elapsed time versus temperature and (b) Elapsed time versus vertical deformation and vertical strain for cement kiln dust specimen during the thawing process.

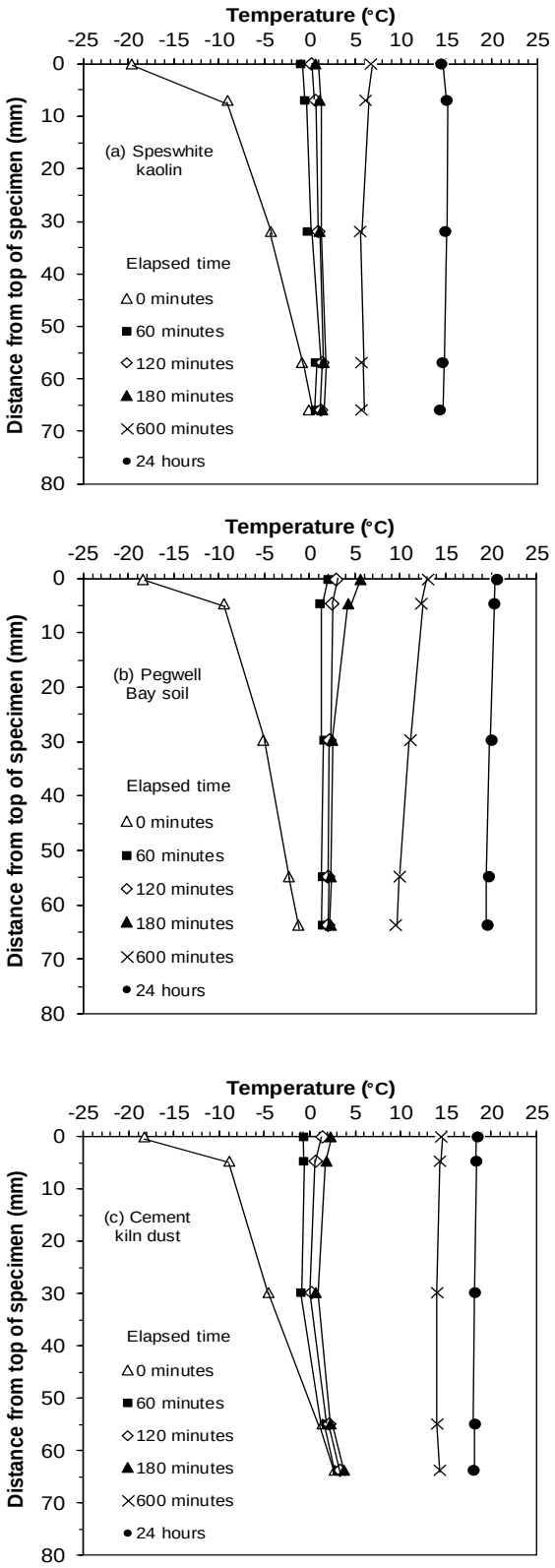

Fig. (5.10): Temperature profiles during thawing of specimens at times 0, 1, 2, 3, 10 and 24 hours.

Figures 5.7b, 5.8b and 5.9b showed that the rates at which both the specimens and the specimen moulds settled were different. For the specimens of Speshwite kaolin and Pegwell Bay soil, the rates of settlement of the specimen moulds and the specimens were similar, whereas the specimen mould settled and attained an equilibrium much earlier than that occurred for the specimen in case of cement kiln dust. The test results showed that frictional resistance developed at the top end of the specimens due to the adfreezing depends upon the material type and which is recoverable in the cases of all the materials. Additionally, no additional thaw consolidation took place as that occurred in case of initially saturated slurried specimens (Figures 4.8 to 4.10). The test results showed that the specimen mould positions remained unaltered as that of the positions noted at the end of saturation stage for all the materials.

5.3.3.1 Vertical strain during thawing

Figure 5.11 compares the thaw settlements of the specimens tested. Table 5.5 shows the heights of the specimens prior to the thawing stage, the magnitudes of thaw settlement, the heights of the specimens at the end of thawing stage and the vertical strain values of the materials. The vertical strains were calculated based on the heights of the specimens at the end of the freezing stage (i.e. heights prior to the thawing stage). For the sake of comparison, the relevant parameters for the initially saturated slurried materials are shown within brackets in Table 5.5.

Figure 5.11 shows that an additional heave occurred for all specimens immediately after the thawing process commenced (see inset of Figure 5.11). Similar observations have been made by Cheng and Chamberlain (1988), Eigenbrod et al. (1996) and Eigenbrod (1996). An increase in the volume of the materials is attributed due to a decrease in effective stress resulting from the increase in pore-water pressure (Eigenbrod et al. 1996; Eigenbrod 1996).

The test results presented in Figure 5.11 and Table 5.5 clearly showed that the magnitude of settlement and vertical strain remained as per the order: cement kiln dust, Pegwell Bay soil and Spewhite kaolin. The vertical strain during thawing were smaller than their counterparts during the freezing process (i.e. 30.0, 33.3 and 35.1%, Table 5.3). Additionally, the thaw settlement and vertical strain for compacted of Speswhite kaolin were found to be smaller than that occurred for the initially saturated slurried specimen (see values within brackets in Table 5.5), whereas for others the thaw settlement and vertical strain were found to be greater for compacted specimens as compared to the initially saturated slurried specimens. The magnitude of settlement during the thawing process depends upon the amount of water present, the development of pore water pressure and permeability of the material (Chamberlain 1981b; Graham and Au 1985).

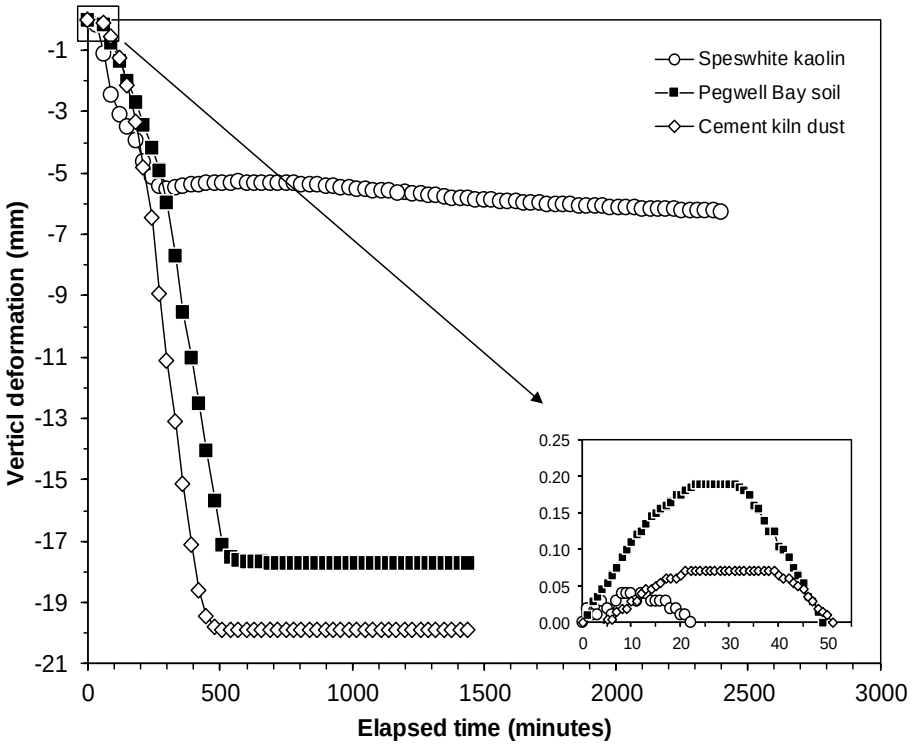

Fig. (5.11): Thaw settlement of the materials

Table 5.5: Thaw settlement and vertical strain of the materials studied

Material	Height of specimen before thawing stage (mm)[1]	Thaw settlement (mm)	Height of specimen at the end of thawing stage (mm)	Vertical strain (%)[1]
Speswhite kaolin	90.7	6.2 (25.6)	84.5	6.8 (31.4)
Pegwell Bay soil	86.8	17.7 (14.2)	69.1	20.4 (18.7)
Cement kiln dust	88.1	19.9 (19.4)	68.2	22.6 (24.6)

[1] Values within brackets are for initially saturated slurried specimens

Figures 5.12 and 5.13 show the height and dry density of the specimens at the end of saturation process under the nominal vertical pressure, freezing and thawing processes. The dry densities of the specimens at the end of each stage were calculated based on the dry mass of the materials and the total volumes at the end of each stage.

It can be seen in Figures 5.12 and 5.13 that as compared to the heights of the specimens at the end of saturation, the heights of the specimens due to one cycle of freezing and thawing increased and the dry density decreased at the end of thawing stage. Therefore, a permanent positive vertical deformation was noted due to one cycle of freezing and thawing as against a permanent negative vertical deformation in case of initially saturated slurried materials (Figures 4.13 and 4.14). Viklander (1998a) stated that a decrease in the dry density due to freeze/thaw effects is associated with the difference in the particle rearrangement between freezing and thawing process which may not be identical leading to a net volume increase of soils and making the soil structure slightly looser than prior to freezing.

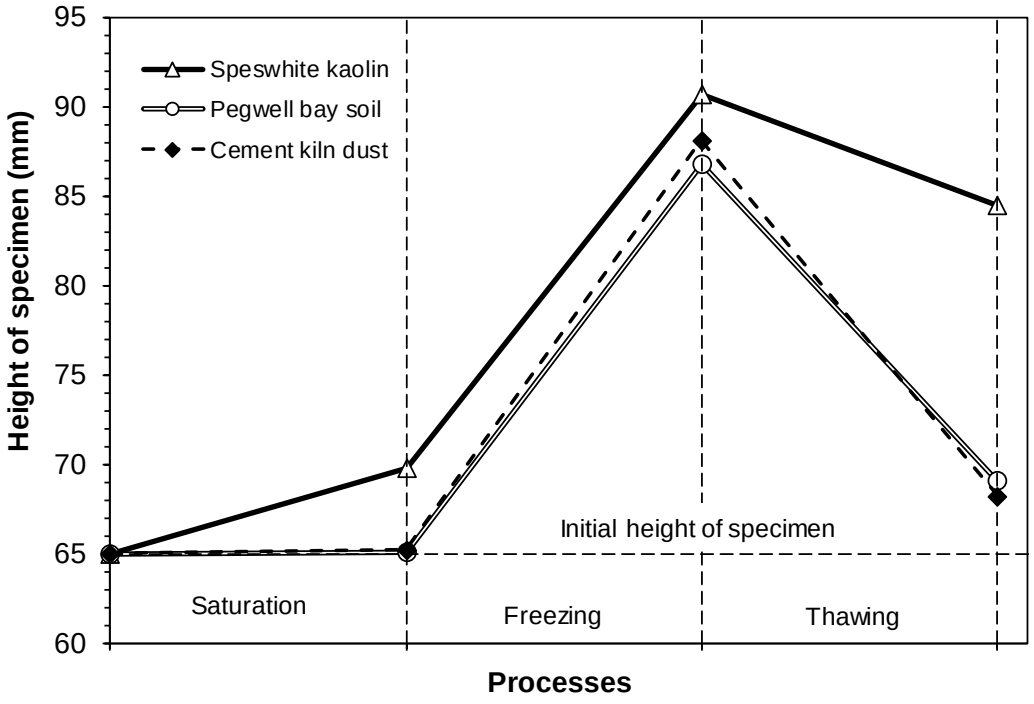

Fig. (5.12): Changes in the height of specimens at the end of various stages of the tests

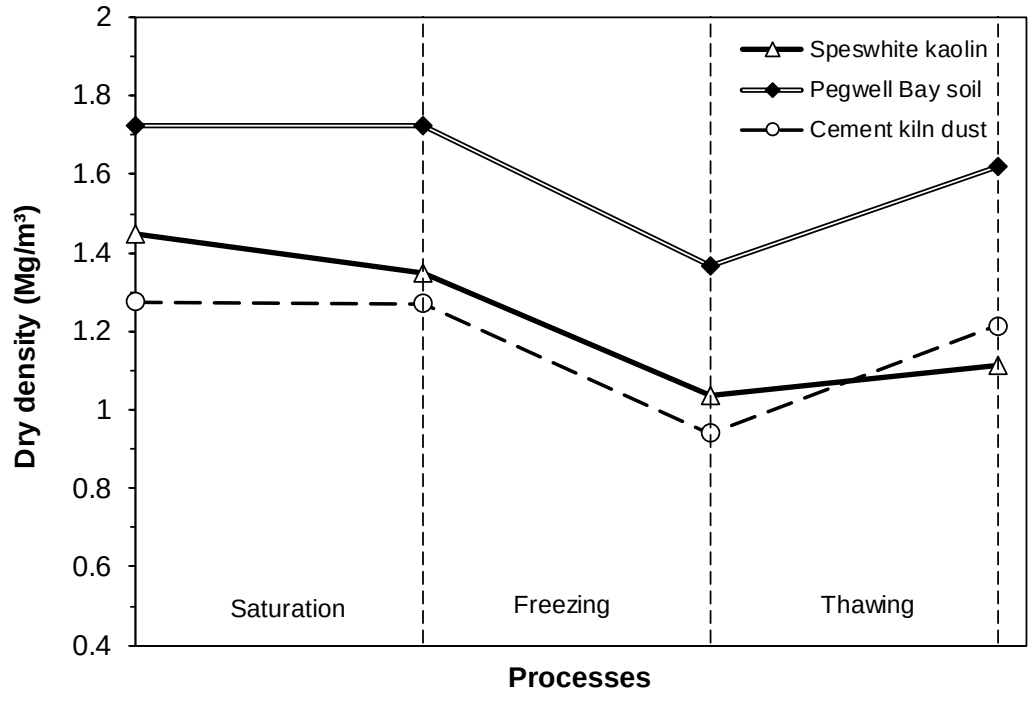

Fig. (5.13): Changes in the dry density of specimens at the end of various stages of the tests

5.3.3.2 Water content at the end of freezing and thawing processes

Figure 5.14 shows the water content of the specimens at the end of freezing and thawing stages. For the sake of comparisons, the initial compaction water contents of the specimens are shown in Figure 5.14.

It can be seen in Figure 5.14 that due to the freezing process there was an increase in the water content of the specimens at all depths. The increase in the water content of the specimens was more intense towards the three-quarter depth of the specimens. The water content remained higher than the initial compaction water contents at the end of thawing stage in all cases. An increase in the water content during freezing is be attributed due to the formation of ice lenses on account of the movement of water from the base of the specimens in an upward direction. The water content increases at three-quarter depth for Speswhite kaolin specimen was about two and half times that of the initial water content, whereas it was about three and five times higher in cases of the specimens of Pegwell Bay soil and cement kiln dust respectively. The water content increase towards the top of the specimens of Speswhite kaolin and cement kiln dust was quite significant.

A decrease in the water content due to thawing is primarily due to the thaw-consolidation process. The water content of Speswhite kaolin specimen was found to increase at the end of the thawing as compared to the end of the freezing stage, particularly above the mid-height of the specimen indicating that water flow took place in an upward direction during the thawing process. An increased water content during the thawing process was not evident in other materials in which case the water content at the end of thawing stage was very similar throughout the specimens.

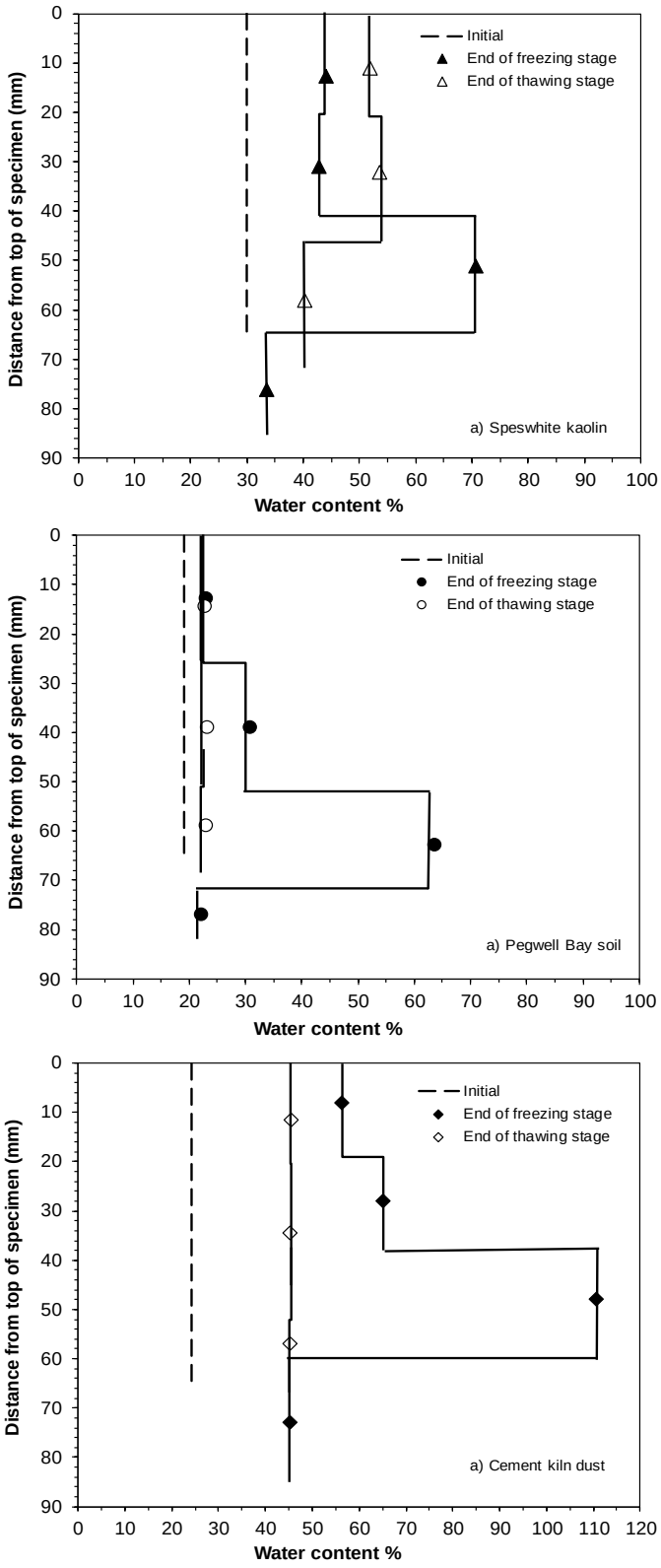

Fig. (5.14): Water content profiles after freezing and thawing stages for (a) Speswhite kaolin, (b) Pegwell Bay soil and (c) Cement kiln dust

5.4 Concluding remarks

This chapter presented the freezing and thawing test results of compacted specimens of the chosen materials (Speswhite kaolin, Pegwell Bay soil and cement kiln dust). The vertical deformations during freezing and thawing were measured. The temperature at various salient depths were monitored during the tests. The water content of the specimens at the end of freezing and thawing stages were also measured. The following points emerged from the test results.

1. Compacted specimens of the materials exhibited swelling strain of different magnitudes during the saturation process under an applied vertical pressure of 2.0 kPa. The swelling strain of Speswhite kaolinite (about 7.5%) was higher than that of the other materials which exhibited very minor swelling (<0.50%). A higher swelling of Speswhite kaolin is attributed due to a greater specific surface area of the clay as compared to the other materials studied.
2. The vertical strain associated with the frost heave was found to be the higher for compacted cement kiln dust specimen (35.1%) than compacted specimens of Pegwell Bay soil (33.3%) and Speswhite kaolin (30.0%). As compared to the frost heave of initially saturated slurried specimens, the frost heave vertical strain of compacted Speswhite kaolin was found to be lower, whereas it was higher for compacted Pegwell Bay soil and cement kiln dust specimens.
3. The frost heave rate (dh/dt), the velocity of water flow (v_φ) and the temperature gradient at steady state (ΔT_f) decreased, whereas the segregation potential (SP_t) increased for a compacted specimen of Speswhite kaolin as compared to the initially saturated slurried specimen of the material. For compacted Pegwell Bay soil and cement kiln dust, all the stated parameters were found to increase as

compared to the initially saturated slurried specimens. The test results indicated that compacted materials may exhibit higher frost heave under certain stress and hydraulic boundary conditions.

4. The vertical strain associated with thaw settlement was found to be the lesser for Speswhite kaolin (6.8%) than the other two materials (20.4% and 22.6% for Pegwell Bay soil and cement kiln dust respectively). The vertical strain associated with thaw settlement of compacted Speswhite kaolin was found to be lower than the initially saturated slurried specimen of the same material, whereas it was found be higher for compacted specimens of Pegwell Bay soil and cement kiln dust as compared to the initially saturated slurried specimens.
5. Except the compacted Speswhite kaolin specimen, the water content of the materials increased at the end of the freezing process, whereas it decreased at the end of thawing process. For the former, a redistribution of the water content took place during the thawing process with an increase in the water content towards the top of the specimen.

CHAPTER 6

Effects of wet-dry and intermittent freeze-thaw cycles on volume change behaviour

6.1 Introduction

In nature, geomaterials are usually exposed to various climatic processes which cause the materials to undergo wetting, drying, freezing and thawing. The cycles of wetting and drying have been related to the formation of soil aggregates in non-aggregated soils (Utomo and Dexter 1982). Cyclic wetting and drying processes affect the physical and chemical properties, volume change, water retention and mechanical behaviour of soils (Rajaram and Erbach 1999; Allam and Sridharan 1981; Kodikara et al. 1999; Lin and Benson 2000; Albrecht and Benson 2001; Liu et al. 2016; Day 1994; Tripathy et al. 2002; Subba Rao and Tripathy 2003; Alonso et al. 2005; Tripathy and Subba Rao 2009; Rosenbalm and Zapata 2017; Toll et al. 2016a, b; Lawton et al. 1992; Fleureau et al. 2002).

Climate changes have led to more extreme and unusual weather events in the hot-seasonal weathering regions of the world. For example, in countries like Iraq, which has been known by the extremely hot weather with temperature exceeding 50 °C in summer months, experienced snowfall in 2008 for the first time in hundred years (Zhou et al. 2011). Similarly, during the winter of 2013 extreme cold weather was realised in the northern and western territories of Iraq and the Middle East (Herring et al. 2015). Therefore, although the effects of wet-dry cycles on the behaviour of geomaterials in the temperate regions of the world have been studied by many researchers in the past, it would

be necessary to study how an intermittent freeze-thaw cycle affects the behaviour of geomaterials.

The objectives of this chapter were; (*i*) to study the one-dimensional volume change behaviour of the compacted specimens of Speswhite kaolin, Pegwell Bay soil and cement kiln dust with increasing number of wet-dry (WD) cycles and (*ii*) to study the impact of intermittent freeze-thaw (FT) cycle on the volume change behaviour of the materials that were previously exposed to a number of WD cycles .

This chapter is presented in several sections. The experimental program (Test series III; section 3.8) is recalled in section 6.2. Under test results and discussion (section 6.3), the experimental results involving the WD cycles with intermittent FT cycles of compacted materials are presented. The temperature profiles, the volume change of the materials upon exposure to cycles of wetting and drying, the frost heave and settlement during the thawing processes and the water content of the materials at the end of various stages are presented in Section 6.3. The concluding remarks are presented in section 6.4.

6.2 Experimental program

The experimental program and the experimental methods for testing the compacted specimens by subjecting them to cyclic wet-dry processes followed by freezing and thawing processes are presented in detail in chapter 3 (Test series III; section 3.8). Compacted specimens were prepared within the specimen mould (Figure 3.22) by statically compacting the chosen materials to the targeted dry densities at predetermined water contents. For each material, one compaction condition (dry density and water content) was chosen. Compaction of the specimens was carried out using a static compaction machine (Figure 3.22). Table 3.4 shows the initial compaction conditions of the specimens tested. The diameter and height of the specimens were 103.5 and 65 mm respectively.

The sequence of the climatic processes adopted in this study was inspired by the recent climatic conditions in the Middle East territories which are usually warm to extreme hot throughout the year with rainfall and dry winter periods accompanied by some extreme frozen periods. The duration of the seasons can have a significant impact on various geomaterials. The experimental program adopted in this study does not replicate the length of the seasons and are only laboratory-scale testing of materials with assumed temperature and hydraulic boundary conditions for predetermined periods of testing.

The sequence of the climatic processes adopted in this study was by subjecting compacted specimens of the materials to cycles of wetting and drying until the equilibrium was attained in terms of the vertical deformation of the specimens. Then, one cycle of an intermittent freeze-thaw process was introduced. Once the freeze-thaw cycles were completed, the specimen was further subjected wet-dry cycles followed by another

cycle of freeze-thaw and so on. The cyclic tests were carried out at an applied vertical pressure of 2.0 kPa using the test set up shown in Figures 3.12 and 3.13. The details of the test set up are presented in section 3.7.1. The vertical deformation of the specimens during wetting, drying, freezing, and thawing processes were measured at the top of the cooling/ heating chamber. Additionally, the vertical displacements of the specimen mould were measured during all stages of the tests. The temperature at the predetermined levels along the depth of the specimens was monitored during the tests.

The wetting of the specimens was carried out at the room temperature until the deformation of the specimens was found to be stabilised. The supplied water to the specimens was at ambient laboratory temperature of 21 ± 2 °C. The temperature at the top of the specimen was maintained at 52 ± 1.5 °C during the drying process (section 3.7.1.2). The drying stage was terminated when the vertical deformation of the specimen attained a constant value. After termination of the drying stage and before starting the next wetting stage, a duration of 24 hours was allowed for the temperature in the specimen to attain the room temperature. The vertical deformation at that stage was recorded prior to the commencement of the next wetting stage. During the freezing process, the temperature at the top of the specimens was lowered to -19 ± 0.5 °C and maintained for 24 hours, whereas the thawing process occurred at the ambient laboratory temperature. No water was supplied to the specimens during the drying process. During the wetting process, the water table was kept at the top the specimens, whereas during freezing and thawing stages the water table was kept at the bottom of the specimens.

6.3 Test results and discussion

The results of the cyclic WD tests with intermittent FT cycles for compacted specimens of Speswhite kaolin, Pegwell Bay soil and cement kiln dust are presented in Figures 6.1 to 6.9. The vertical deformation of the specimens at the end of each cycle and the vertical deformation of the specimen mould are shown in Figures 6.1a, 6.4a and 6.7a. As can be seen, for each material, a number of WD cycles were implemented along with three FT cycles for each case. A FT cycle was introduced at the end of a wetting cycle. At the end of a FT cycle, the specimens were subjected to a drying cycle prior to implementing the subsequent wetting cycle. The displacements of the specimen mould for each stage are shown in Figures 6.1a, 6.4a and 6.7a. Figures 6.1b, 6.4b and 6.7b show the equilibrium temperatures for each stage of the tests. The ambient laboratory temperatures during the tests are also shown in Figures 6.1b, 6.4b and 6.6b. Figures 6.2, 6.5 and 6.8 show the temperature profiles in the specimens at the end of various cycles of drying, freezing and thawing. Figures 6.3, 6.6 and 6.9 show the elapsed time versus vertical deformation of the specimens for various wetting, drying, freezing and thawing cycles.

Tables 6.1, 6.2 and 6.3 show the magnitudes of vertical deformation and vertical strain of the materials studied corresponding to various cycles of wetting, drying, freezing and thawing for Speswhite kaolin, Pegwell Bay soil and cement kiln dust respectively. The vertical strain of the specimens was calculated based on the change in the height of the specimen in any stage and the initial height of the compacted specimen (65 mm) and expressed as a percentage. This allowed interpreting the magnitude and location of movement bands of the specimens with an increasing number of WD and intermittent FT cycles.

A complete WD cycle in this test series is comprised of one wetting (W) and one drying (D) cycles. The intermittent freeze-thaw cycles are indicated as FT1, FT2 etc. The type of a movement band (uprising, descending) with increasing number of cycles depends upon the positions of the highest and the lowest deformations or strains with reference to the zero deformation or zero strain. The magnitude of a movement band is the difference in the magnitudes of the highest and lowest deformations or strains in that cycle. Figure 6.10 shows the vertical strain of the specimens with increasing number of WD and intermittent FT cycles.

The response of the specimens to temperature and hydraulic boundary conditions was reflected on the changes in the height of the specimens in each stage of the tests. The positions of the thermocouples with respect to the top of the specimen changed during the tests. Therefore, for the sake of consistency in the presentation of the test results, the initial positions of the thermocouples (Section 3.7.1.1) were considered for presenting the temperature data.

6.3.1 Temperature profiles

It can be seen in Figures 6.1, 6.4 and 6.7 that the temperature at the top of the specimens and at the boundaries remained at room temperature during the wetting cycles. The temperature at the top of the specimens was increased to about + 52 °C during the drying cycles. In some drying cycles, the temperature at the top of the specimens was about 54 °C. During the freezing process, the temperature at the top of the specimens was lowered down to -19 °C, whereas the temperature of the specimens attained the ambient laboratory temperature during the thawing stages. The rise and fall of the temperature during the appropriate cycles were consistent indicating that the test set up and the accessories (the Vortex Tube assemblies) functioned efficiently during the tests.

Referring to Figures 6.1, 6.2, 6.4, 6.5, 6.7, and 6.8, the temperatures along the depth of the specimens at the end of the drying cycles were found to be lower than that of the applied temperature at the top of the specimens, as indicated by the readings of the thermocouples (TC1 to TC4). Similarly, the temperatures measured at various depths of the specimens for the freezing cycles remained higher (less negative) than that of the applied temperature at the top of the specimens. The differences in the temperatures along the depth of the specimens are attributed to the thermal conductivity of the materials which depends upon the volume-mass properties (water content and dry density).

Differences in the temperature profiles of the specimens between various drying cycles can be noted in Figures 6.2a, 6.5a and 6.8a. In this case, the temperature at all salient depths generally decreased with an increase in the wet-dry cycle. For the same material, a decrease in the temperature for a given applied thermal gradient is associated with an increase in the porosity of the materials.

The differences in the temperature profiles were also noted in case of the intermittent freezing cycles, particularly for the specimen of Speswhite kaolin (Figure 6.2b). In this case, the temperature at all salient depths decreased (became more negative) as the number of intermittent freezing cycle increased. For the specimens of Pegwell Bay soil and cement kiln dust (Figures 6.5b and 6.8b), the temperature profiles for the intermittent freezing cycles did not exhibit any significant changes. The temperature at the end of thawing stages remained similar to that of the ambient laboratory temperature in all cases (Figures 6.2c, 6.5c and 6.8c). The test results showed that wet-dry cycles could result in an enhanced heat flow. Additionally, in a clay-rich soil (Speswhite kaolin) this can affect the temperature profile during the freezing process.

6.3.2 Vertical deformation and vertical strain

For the specimen of Spewhite kaolinite, the upward and downward displacements of the specimen mould were noted during the wetting and drying cycles respectively (Figure 6.1a). The displacement of the specimen mould during the wetting and drying cycles for the tests on the specimens of Pegwell Bay soil and cement kiln dust was insignificant (Figures 6.4a and 6.7a). The upward and downward movements of the specimen mould occurred during the intermittent FT cycles for all tests (see Figures 6.1, 6.4 and 6.7). The displacement of the specimen mould was anticipated as shown in the test results presented in chapters 3, 4, and 5. These movements did not leave any residual strain which indicated that there was not any loss of materials during the tests.

The shapes of the elapsed time versus vertical deformation plots for the specimens during wetting, drying, freezing and thawing were found to be dissimilar (Figures 6.3, 6.6 and 6.9). This primarily due to the different mechanisms associated with swelling, shrinkage, freezing and thawing processes. For any given process, the magnitude of deformation and the time required to attain equilibrium in terms of the vertical deformation were found to vary. In general, the magnitude of deformation decreased and the time to attain equilibrium was found to reduce with an increase in WD and intermittent FT cycles.

6.3.2.1 Speswhite kaolin (Table 6.1 and Figures 6.1, 6.2, 6.3)

For the specimen of Speswhite kaolin, with an increase in WD cycles, the vertical deformations slightly increased and then remained nearly constant. At equilibrium, the vertical deformation and the associated vertical strain due to wetting as well as due to drying were found to be about 5.4 mm and 8.3% respectively. The magnitude of frost heave (= 23.5 mm) due to the introduction of a freezing stage in cycle FT1 and the

associated vertical strain (= 36.1%) were found to be greater than the values noted for the same specimen when it was subjected to a freezing process from compacted condition (see chapter 5, Table 5.3). Similarly, as compared to the magnitude of thaw settlement of the specimen in freeze-thaw test (chapter 5, Table 5.5), the thaw settlement of the specimen in the FT1 cycle was also found to be higher (13.8 mm and 21.2%). Following the FT1 cycle, the deformations during the wetting and drying cycles and the associated strains in cycles 4, 5, 6 and 7 were found to be destabilised; the deformations during the drying cycles were greater than that occurred during the wetting cycles. The FT2 cycle was implemented when the difference between the strains in wetting and drying cycles reduced to about less than 0.5%. The introduction of FT2 cycle did not influence the frost heave significantly (as compared to that occurred in cycle FT1), but the thaw settlement was found to increase significantly. The deformations and the associated vertical strains in further WD cycles after the FT2 cycle were found to be decreased to about 3.0 mm and 4.5% respectively. The magnitude of frost heave and the vertical strain in cycle FT3 were found to be similar to that occurred in cycle FT2.

The test results clearly showed that WD cycles caused a decrease in the vertical strains associated with wetting and drying processes and an increase in the frost heave and thaw settlement of Speswhite kaolin. Intermittent FT cycles tend to destabilise the equilibrium strain that was achieved during the previous WD cycles; however, a new equilibrium in terms of vertical strain was attained by the material with an increasing number of WD cycles, but with a reduced equilibrium strain.

6.3.2.2 Pegwell Bay soil (Table 6.2 and Figures 6.4, 6.5, 6.6)

The vertical deformations of the specimen of Pegwell Bay soil during the wetting and drying cycles were found to be insignificant. The frost heave (= 15.4 mm) and the thaw settlement (= 13.3 mm) and the associated vertical strains due to the implementation

of cycle FT1 were found to be smaller than the values noted for the same specimen when it was subjected to a freeze-thaw cycle from compacted condition (see chapter 5, Tables 5.3 and 5.5). Following the FT1 cycle, the deformations during the wetting and drying cycles and the associated strain in cycles 3, 4, and 5 were found to be destabilised; the deformations during the drying and wetting cycles were found to be dissimilar but remained less than 0.5%. The implementation of the FT2 cycle influenced both the frost heave and the thaw settlement significantly. Both frost heave and thaw settlement increased by about 1.5 fold (as compared to that occurred in cycle FT1). The deformations and the associated vertical strains in further WD cycles following the FT2 cycle were found to be similar to that occurred in earlier WD cycles. The magnitudes of frost heave and thaw settlement and the associated vertical strains in cycle FT3 were found to be increased as compared to that occurred in cycles FT1 and FT2.

The test results clearly showed that WD cycles did not cause any appreciable volume change of Pegwell Bay soil, whereas the intermittent FT cycles caused an increase in the frost heave and thaw settlement of this material, similar to that occurred in case of Speswhite kaolin.

6.3.2.3 Cement kiln dust (Table 6.3 and Figures 6.7, 6.8, 6.9)

The vertical deformations of the specimen of cement kiln dust during the wetting and drying cycles were found to be insignificant. The frost heave (= 28 mm) and thaw settlement (= 27.5 mm) due to the implementation of cycle FT1 were found to be greater than the values noted for the same specimen when it was subjected to a freeze-thaw cycle from compacted condition (see chapter 5, Tables 5.3 and 5.5). Following the FT1 cycle, the deformations during the wetting and drying cycles and the associated strains in cycles 4, 5, and 6 were found to be destabilised; the deformations during the drying and wetting cycles were found to be dissimilar but remained less than 0.5%. The FT2 cycle influenced

both the frost heave and the thaw settlement. Both frost heave and thaw settlement were found to be increased (as compared to that occurred in cycle FT1). The deformations and the associated vertical strains in further WD cycles after the FT2 cycle were found to be similar to that occurred in earlier WD cycles and remained less than 0.5%. The magnitude of frost heave and the vertical strain in cycle FT3 were found to be similar to that occurred in cycles FT1 and FT2.

The test results clearly showed that WD cycles did not cause any appreciable volume change of cement kiln dust, whereas the intermittent FT cycles caused an increase in the frost heave and thaw settlement of this material, similar to that occurred in case of Speswhite kaolin and Pegwell Bay soil.

Lin and Benson (2000) and Albrecht and Benson (2001) have shown that the hydraulic conductivity of compacted soils tends to increase after undergoing several WD cycles. Therefore, an increase in the frost heave and thaw settlement following WD cycles for the materials in this study is attributed to an increase in the hydraulic conductivity that caused the inflow of water and formation of ice lenses and a expulsion of water during the thawing process the amount of which were greater than that occurred in case of compacted specimens that were subjected to one cycle of freezing and thawing.

During the commencements of thawing stages, additional heaves were noted for both the Speswhite kaolin and the cement kiln dust specimens, whereas no additional heave occurred in the Pegwell bay soil specimen (Figures 6.3d, 6.6d and 6.9d). The additional heave is associated with a decrease in effective stress resulting from the increase in pore-water pressure (Eigenbrod et al. 1996; Eigenbrod 1996).

6.3.3 Movement band

The swell-shrink movement type associated with cyclic wet-dry processes in soils depends upon several factors, such as the applied pressure, shrinkage magnitude, compaction conditions and the type of material (Tripathy et al. 2002; Tripathy and Subba Rao 2009). A shifting of the vertical movement band in an upward direction with an increasing number of swell-shrink cycles (uprising movement) with or without any accumulation of plastic strain generally occurs under smaller applied pressures and partial shrinkage of soil specimens. A complete downward shift of the movement band (descending movement) occurs in case of higher applied pressures and full shrinkage conditions. The movement type in the case of geomaterials due to alternate freezing and thawing depends upon the initial density. Viklander (1998a) stated that a net increase in the void ratio of compacted soils occurs upon freeze-thaw processes due to changes in the particle rearrangements.

Figure 6.10a shows that the WD and intermittent FT cycles caused uprising movement in case of all the three materials studied; however, the accumulation of plastic strain occurred in the cases of Pegwell Bay soil and cement kiln dust. For these cases, with an increase in WD cycles, the volumes of the specimens at the end of the drying cycles were found to greater than the initial volume. The equilibrium band movement (i.e. the difference in the magnitudes of strain corresponding to the end of wetting and drying cycles decreased from 8.5 to 4.8% in case of Speswhite kaolin, whereas in the other two materials the changes in the equilibrium WD band movement were insignificant. The band movement due to FT cycles was found to increase with an increase in the number of cycles for all three cases.

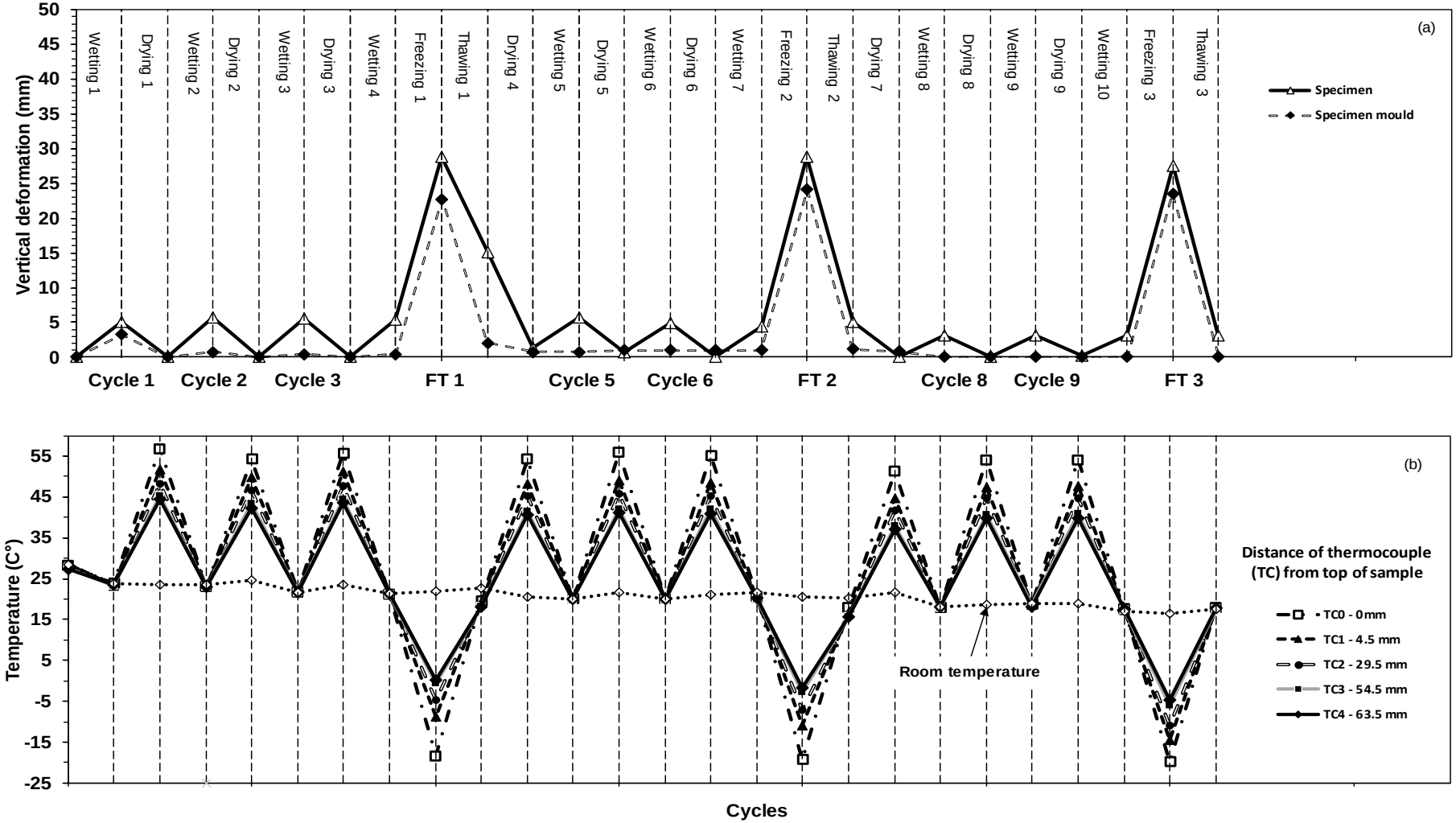

Fig. (6.1): (a) Vertical deformation and (b) temperature changes of Speswhite kaolin specimen with increasing WD and intermittent FT cycles

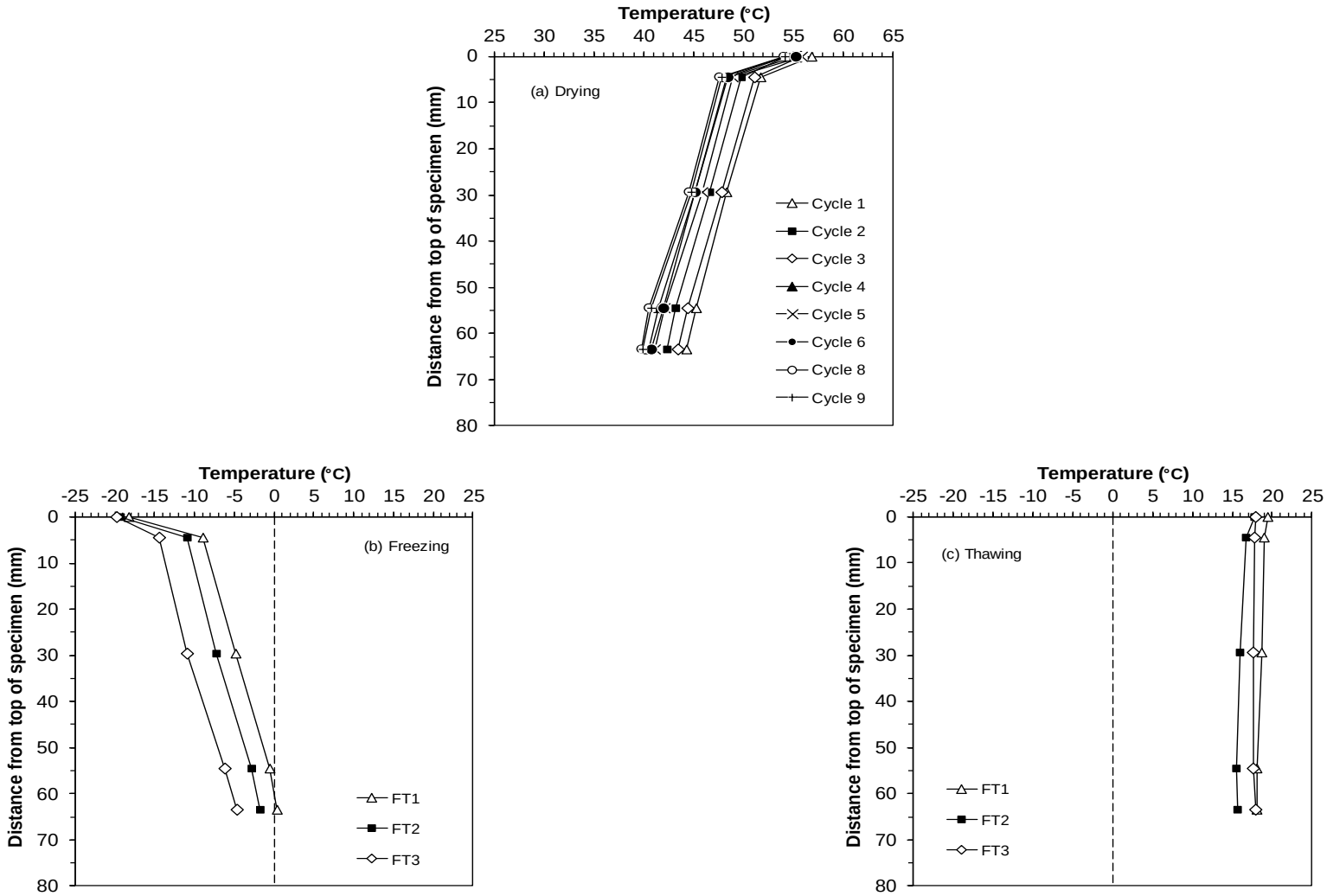

Fig. (6.2): Temperature profiles at the end of (a) drying, (b) freezing and (c) thawing stages with increasing WD and intermittent FT cycles for Speswhite kaolin

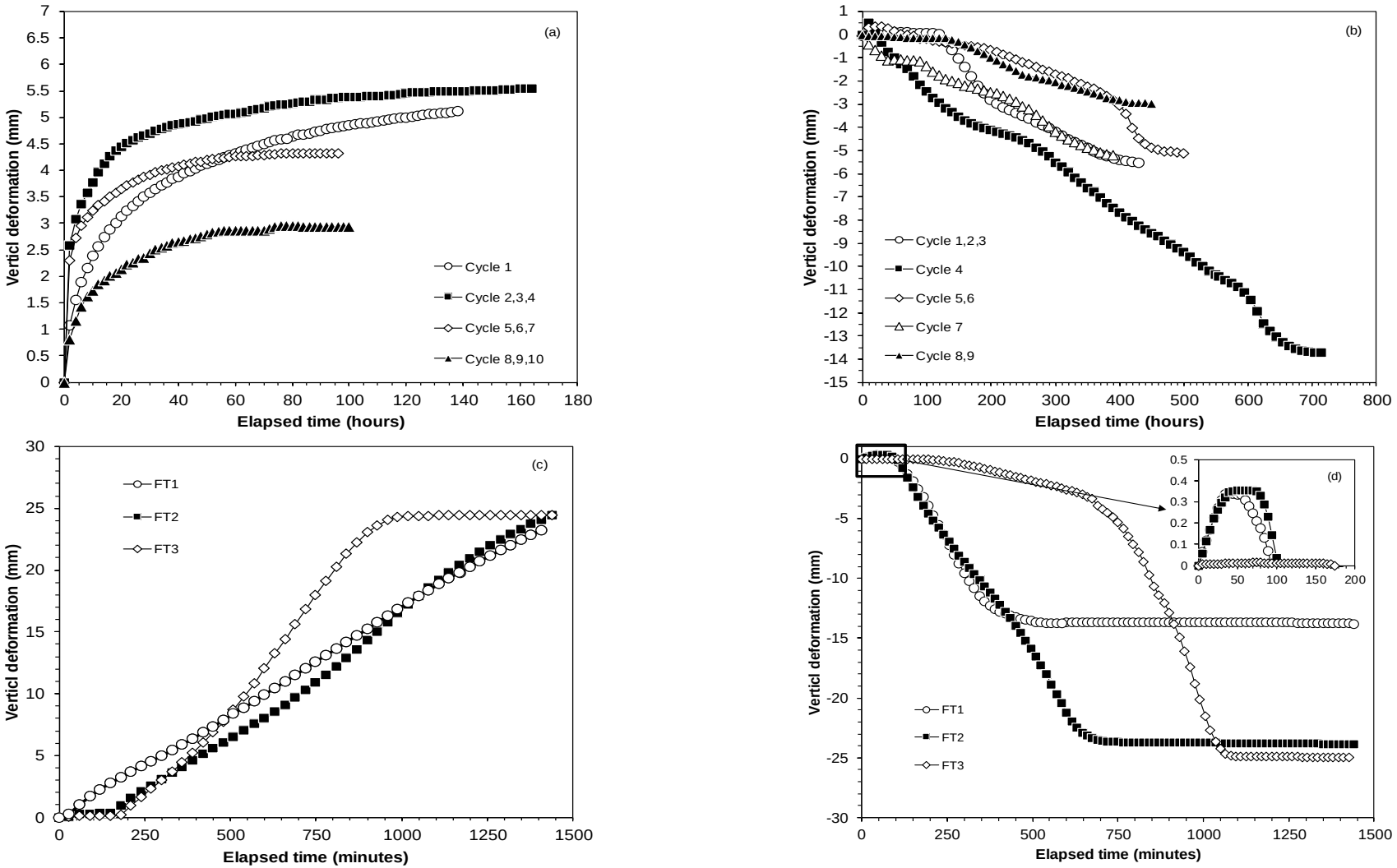

Fig. (6.3): Elapsed time versus vertical deformation in various cycles during (a) wetting, (b) drying, (c) freezing and (d) thawing of Speswhite kaolin specimen

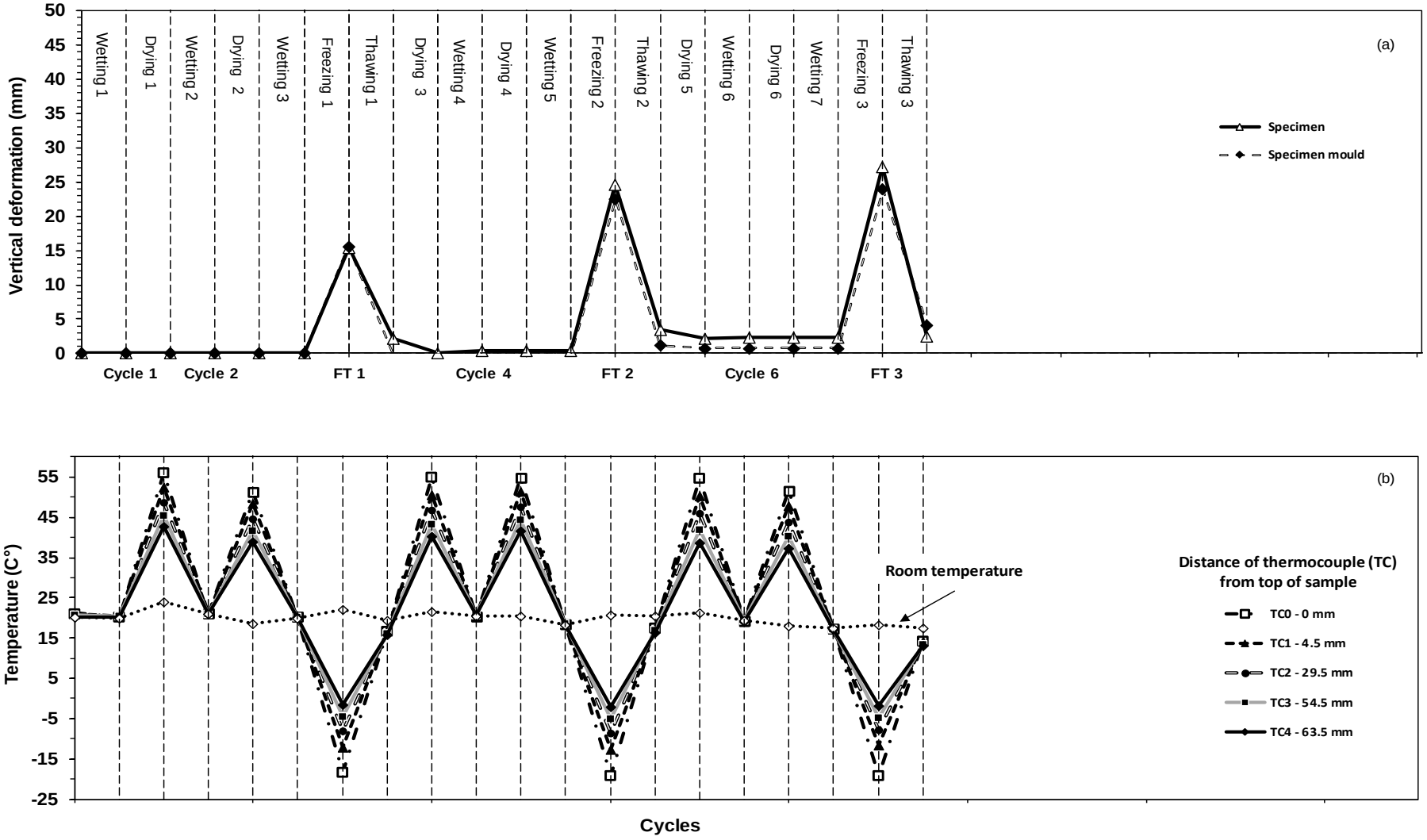

Fig. (6.4): (a) Vertical deformation and (b) temperature changes of Pegwell Bay soil specimen with increasing WD and intermittent FT cycles

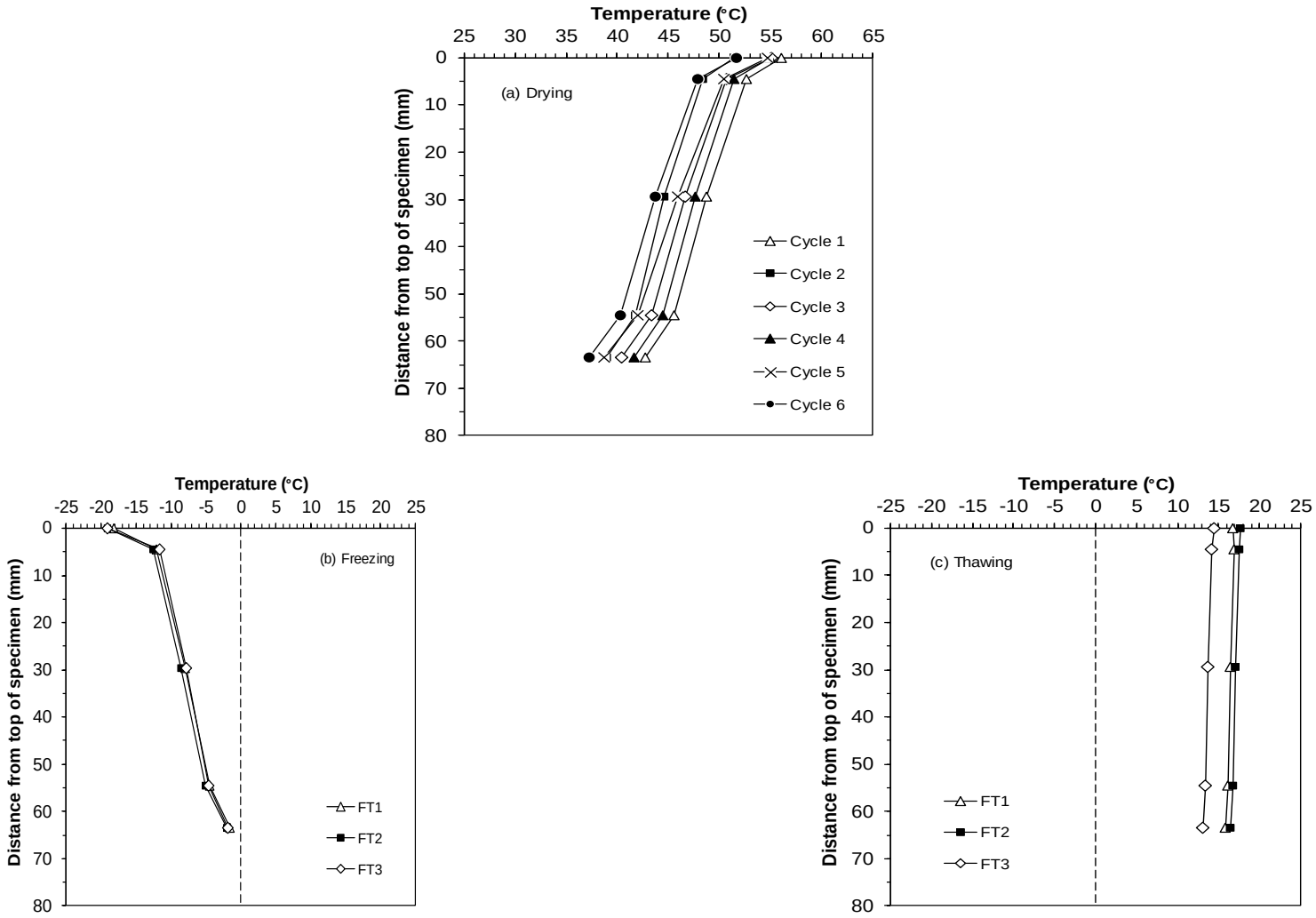

Fig. (6.5): Temperature profiles at the end of (a) drying, (b) freezing and (c) thawing stages with increasing WD and intermittent FT cycles for Pegwell Bay soil

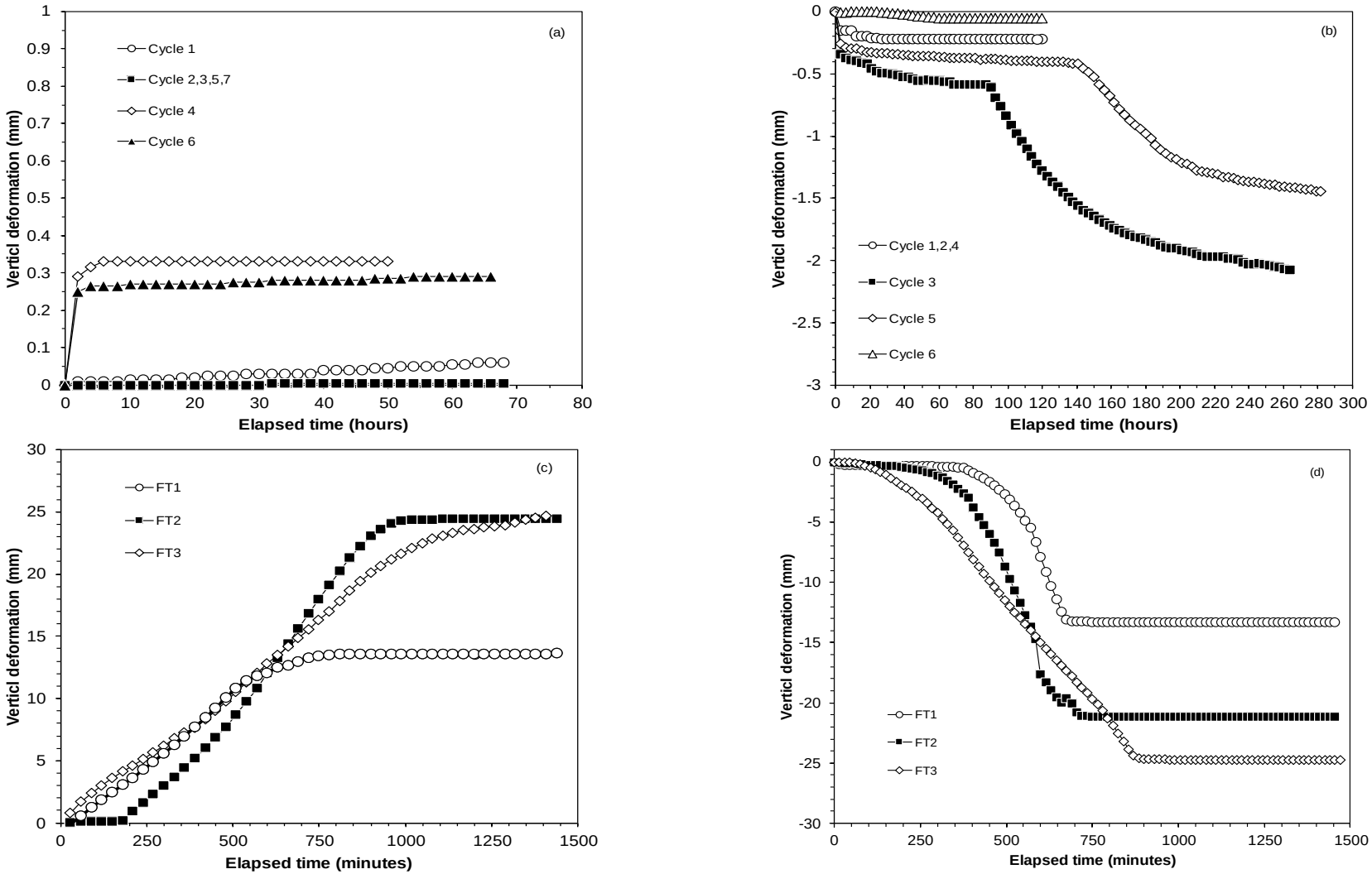

Fig. (6.6): Elapsed time versus vertical deformation in various cycles during (a) wetting, (b) drying, (c) freezing and (d) thawing of Pegwell Bay soil

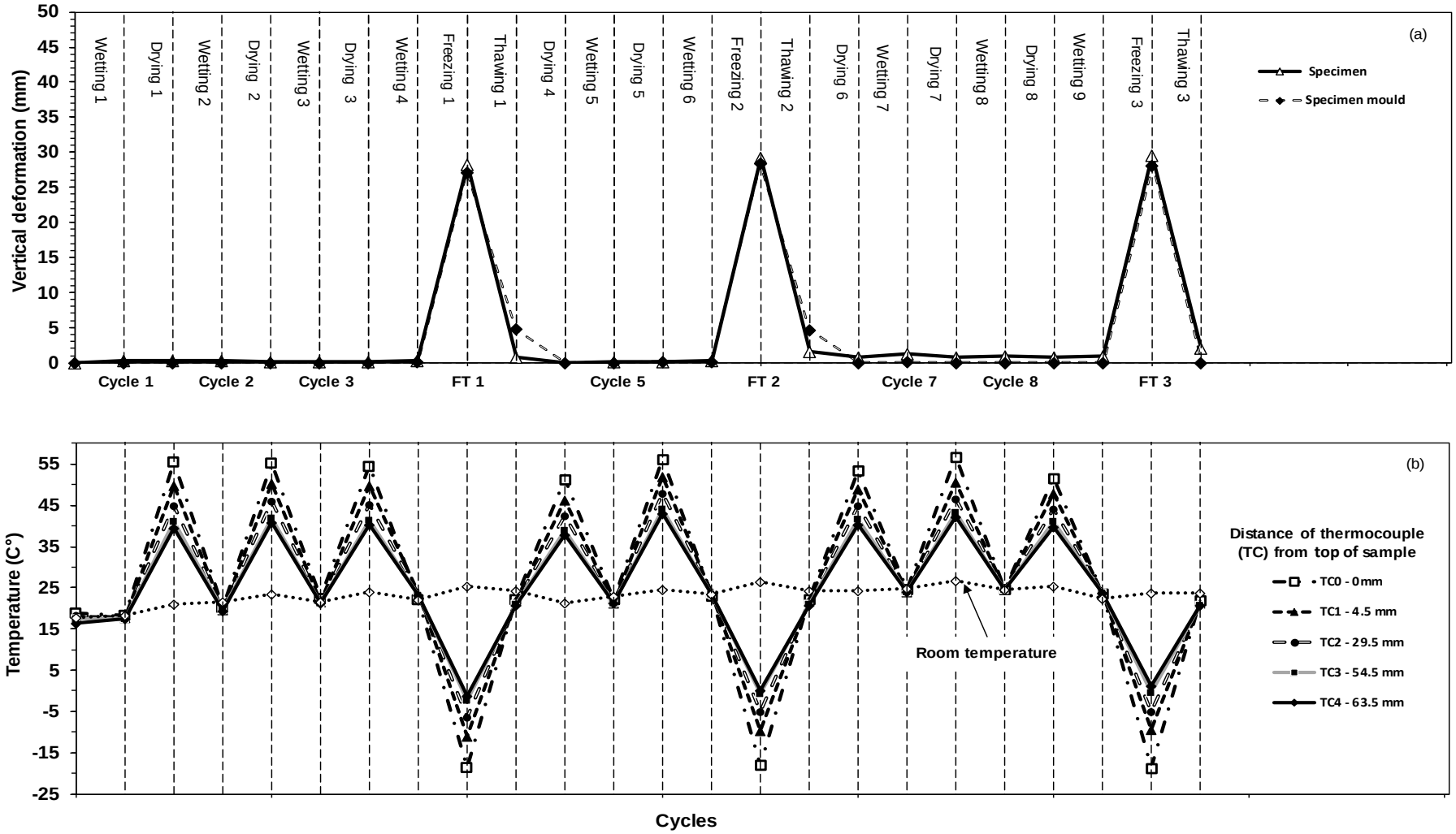

Fig. (6.7): (a) Vertical deformation and (b) temperature changes of cement kiln dust specimen with increasing WD and intermittent FT cycles

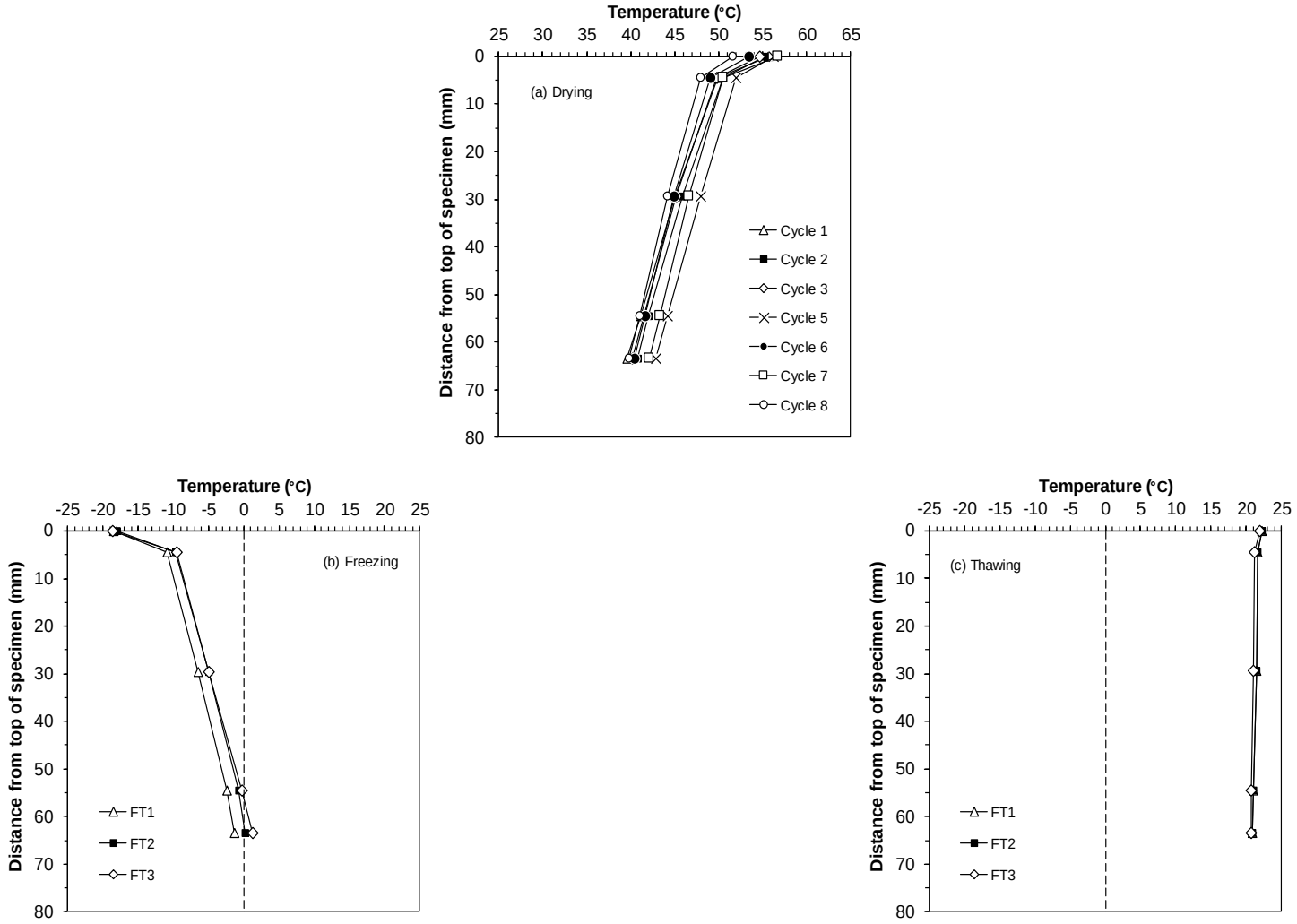

Fig. (6.8): Temperature profiles at the end of (a) drying, (b) freezing and (c) thawing stages with increasing WD and intermittent FT cycles for cement kiln dust

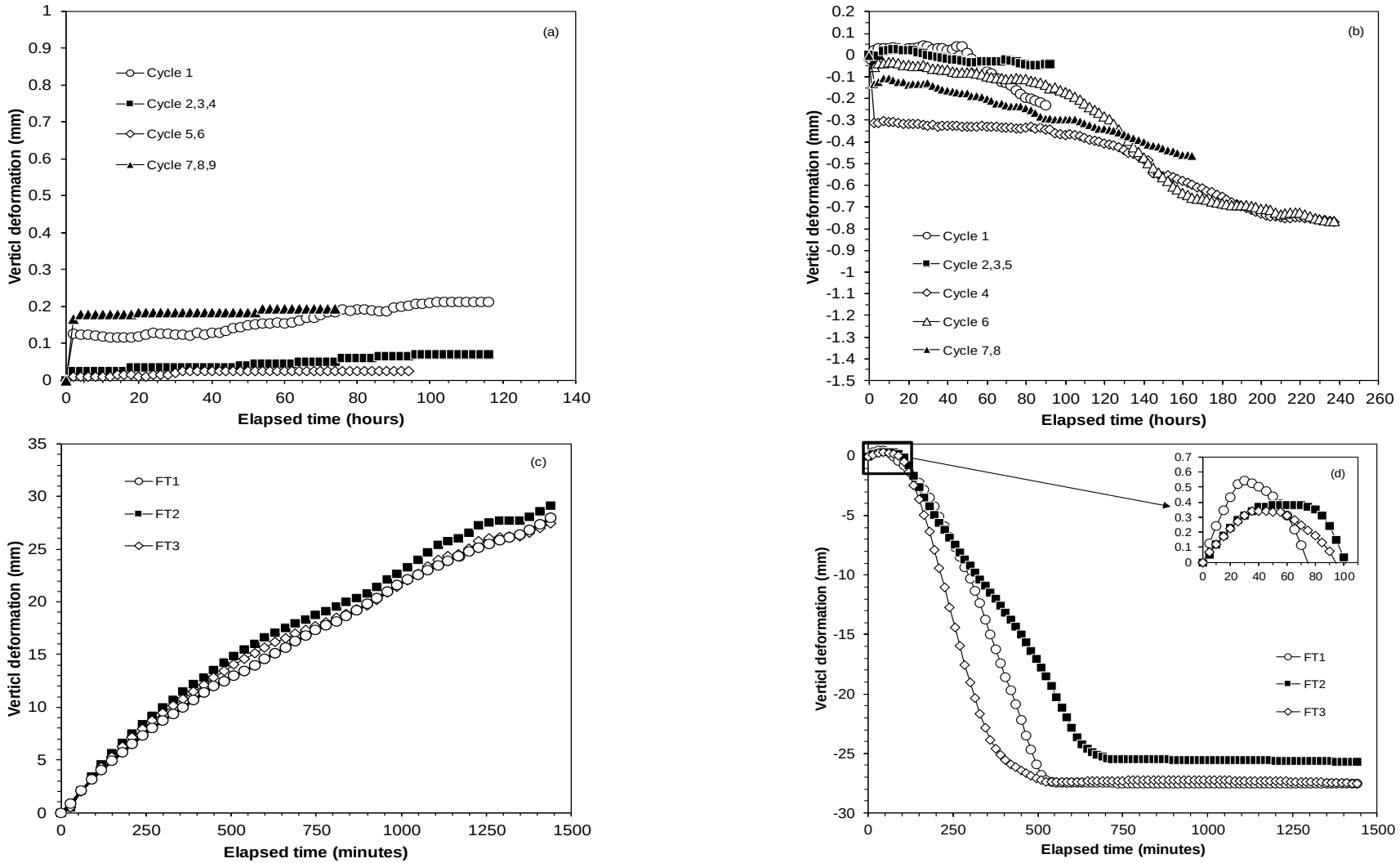

Fig. (6.9): Elapsed time versus vertical deformation in various cycles during (a) wetting, (b) drying, (c) freezing and (d) thawing of cement kiln dust

Table 6.1: Vertical deformation and vertical strain of compacted Speswhite kaolin with increasing wet-dry and intermittent freeze-thaw cycles

Cycle	Wetting		Drying		Freezing		Thawing	
	Vertical deformation (mm)	Vertical strain (%)	Vertical deformation (mm)	Vertical strain (%)	Vertical deformation (mm)	Vertical strain (%)	Vertical deformation (mm)	Vertical strain (%)
1	+5.1	+7.9	-5.0	-7.7	--	--	--	--
2	+5.5	8.5	-5.6	-8.7	--	--	--	--
3	+5.5	+8.5	-5.6	-8.6	--	--	--	--
4	+5.4	+8.3	--	--	--	--	--	--
FT1	--	--	--	--	+23.5	+36.1	-13.8	-21.2
4	--	--	-13.7	-21.1	--	--	--	--
5	+4.3	+6.6	-5.1	-7.8	--	--	--	--
6	+4.3	+6.5	-4.9	-7.5	--	--	--	--
7	+4.4	+6.8	--	--	--	--	--	--
FT2	--	--	--	--	+24.5	+37.6	-23.9	-36.7
7	--	--	-5.3	-8.2	--	--	--	--
8	+3.1	+4.8	-3.0	-4.6	--	--	--	--
9	+3.0	+4.6	-2.9	-4.5	--	--	--	--
10	+2.9	+4.5	--	--	--	--	--	--
FT3	--	--	--	--	+24.4	+37.6	-24.5	-37.6

Table 6.2: Vertical deformation and vertical strain of compacted Pegwell Bay soil with increasing wet-dry and intermittent freeze-thaw cycles

Cycle	Wetting		Drying		Freezing		Thawing	
	Vertical deformation (mm)	Vertical strain (%)	Vertical deformation (mm)	Vertical strain (%)	Vertical deformation (mm)	Vertical strain (%)	Vertical deformation (mm)	Vertical strain (%)
1	+0.0	+0.0	-0.0	-0.0	--	--	--	--
2	+0.0	+0.0	-0.0	-0.0	--	--	--	--
3	+0.0	+0.0	--	--	--	--	--	--
FT1	--	--	--	--	+15.4	+23.7	-13.3	-15.7
3	--	--	-2.1	-3.2	--	--	--	--
4	+0.3	+0.5	-0.1	-0.2	--	--	--	--
5	+0.0	+0.0	--	--	--	--	--	--
FT2	--	--	--	--	+24.3	+37.4	-21.1	-32.5
5	--	--	-1.4	-2.2	--	--	--	--
6	+0.3	+0.4	-0.1	-0.1	--	--	--	--
7	+0.0	+0.0	--	--	--	--	--	--
FT3	--	--	--	--	+24.9	+38.3	-24.7	-38.0

Table 6.3: Vertical deformation and vertical strain of compacted cement kiln dust with increasing wet-dry and intermittent freeze-thaw cycles

Cycle	Wetting		Drying		Freezing		Thawing	
	Vertical deformation (mm)	Vertical strain (%)	Vertical deformation (mm)	Vertical strain (%)	Vertical deformation (mm)	Vertical strain (%)	Vertical deformation (mm)	Vertical strain (%)
1	+0.2	+0.3	-0.0	-0.0	--	--	--	--
2	0	0	-0.0	-0.0	--	--	--	--
3	+0.0	+0.0	-0.0	-0.0	--	--	--	--
4	+0.1	+0.1	--	--	--	--	--	--
FT1	--	--	--	--	+28.0	+43.1	-27.5	-42.3
4	--	--	-0.7	-1.1	--	--	--	--
5	+0.2	+0.3	-0.0	-0.0	--	--	--	--
6	+0.1	+0.1	--	--	--	--	--	--
FT2	--	--	--	--	+29.1	+44.7	-27.8	-42.7
6	--	--	-0.8	-1.2	--	--	--	--
7	+0.4	+0.7	-0.5	-0.7	--	--	--	--
8	+0.2	+0.3	-0.2	-0.3	--	--	--	--
9	+0.2	+0.3	--	--	--	--	--	--
FT3	--	--	--	--	+28.7	+44.1	-27.5	-42.3

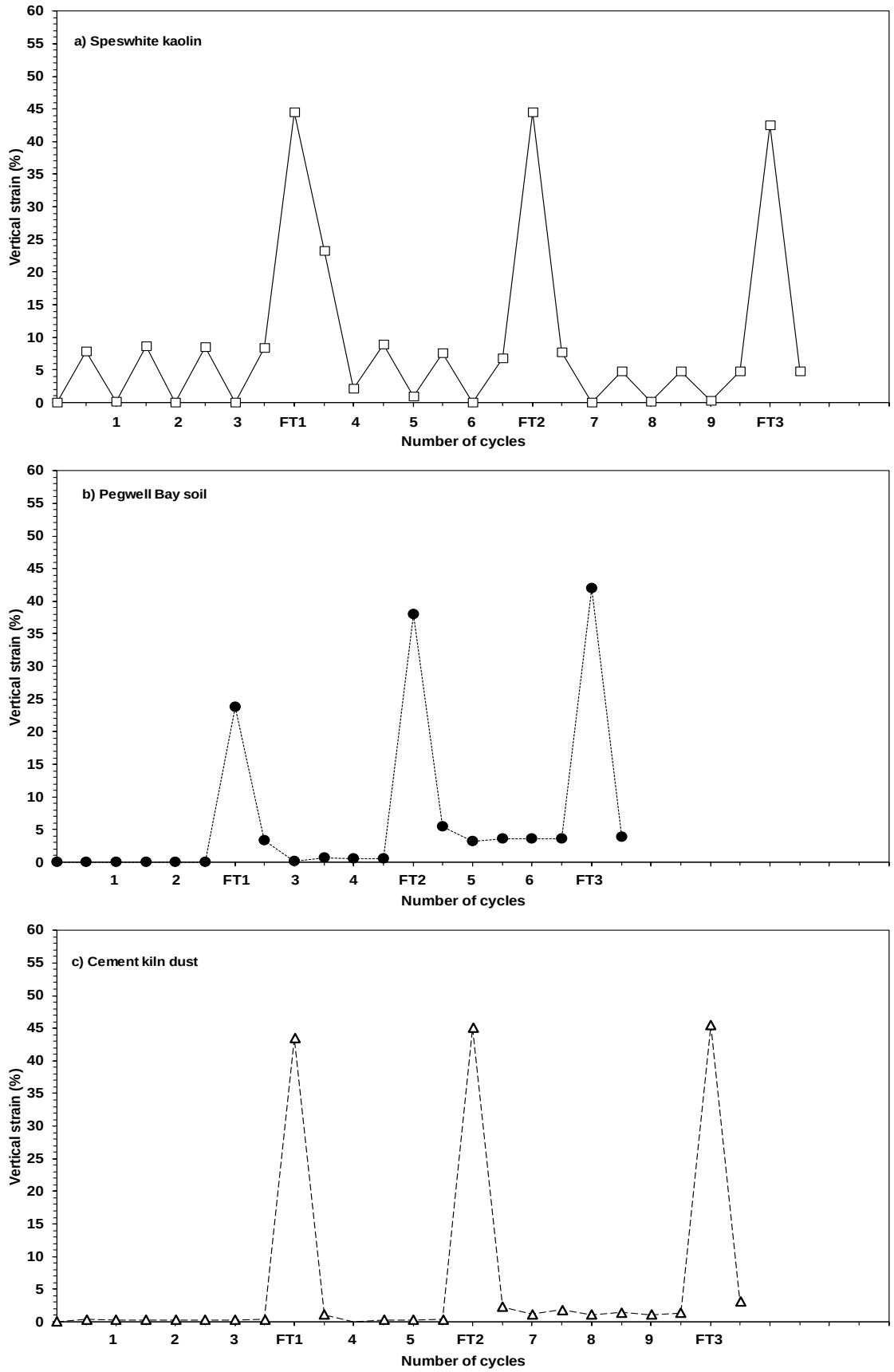

Fig. (6.10): Vertical strain of (a) Speswhite kaolin, (b) Pegwell Bay soil and (c) cement kiln dust with increasing number of wet-dry and intermittent freeze-thaw cycles

6.3.4 Segregation potential

The elapsed time versus frost heave of the specimens of Speswhite kaolin, Pegwell Bay soil and cement kiln dust are shown in Figures 6.3c, 6.6c and 6.9c respectively. In all cases and for any cycle, a thermal steady state was reached after an elapsed time of 400 min. Tables 6.4, 6.5 and 6.6 present the parameters that were derived from the frost heave results and the segregation potentials (SP_t) of Speswhite kaolin, Pegwell Bay soil and cement kiln dust respectively.

The frost heave rate (*dh/dt*) were calculated based on the frost heave (*dh*) and the elapsed time (*dt*) after the steady state. The values of velocity of arriving pore water (v_φ) were calculated based on the heave rates and using Equation 2.6. The temperatures T1 and T2 corresponding an elapsed time of 600 minutes were considered for calculating the temperature gradients (ΔT_f) in the frozen fringe when the materials had reached a steady state condition. The values of T1 and T2 were obtained from the TC1 and TC4 data. The thickness of the specimens between the position of TC1 and TC4 in all cases was 59 mm. The segregation potential (SP_t) for the materials were calculated based on Equation 2.7 (Konrad and Morgenstern 1980, 1981, 1982)

Table 6.4: Heave rate (*dh/dt*), velocity of water flow (v_φ), thermal gradient (ΔT_f) and segregation potential (SP_t) of the compacted Speswhite kaolin

FT cycle	*dh* (mm)	*dt* (min)	*dh/dt* (mm/hr)	v_φ = (*dh/dt*)/1.09 (mm/hr)	T1[1] (°C)	T2[1] (°C)	t (mm)	ΔT_f = [(T1-T2)/t] (°C/mm)	SP_t = (v_φ/ ΔT_f) (mm^2/°C.hr)
1	5.22		1.04	0.96	-9.2	+4.2		0.23	4.20
2	5.34	300	1.07	0.98	-11.6	+1.9	59.0	0.23	4.29
3	11.14		2.23	2.04	-12.8	0		0.22	9.37

Table 6.5: Heave rate (*dh/dt*), thermal gradient (ΔT_f) and the Segregation potential (SP_t) of compacted Pegwell Bay soil specimen

FT cycle	*dh* (mm)	*dt* (min)	*dh/dt* (mm/hr)	v_φ = (*dh/dt*)/1.09 (mm/hr)	T1[1] (°C)	T2[1] (°C)	t (mm)	ΔT_f = [(T1-T2)/t] (°C/mm)	SP_t = (v_φ/ ΔT_f) (mm^2/°C.hr)
1	4.17		0.83	0.76	-12.2	+2.8		0.25	3.00
2	11.14	300	2.23	2.04	-12.2	+2.4	59.0	0.25	8.22
3	5.04		1.01	0.92	-13.3	+1.4		0.25	3.70

Table 6.6: Heave rate (*dh/dt*), thermal gradient (ΔT_f) and the segregation potential (SP_t) of compacted cement kiln dust specimen

FT cycle	*dh* (mm)	*dt* (min)	*dh/dt* (mm/hr)	v_φ = (*dh/dt*)/1.09 (mm/hr)	T1[1] (°C)	T2[1] (°C)	t (mm)	ΔT_f = [(T1-T2)/t] (°C/mm)	SP_t = (v_φ/ ΔT_f) (mm^2/°C.hr)
1	5.37		1.07	0.98	-9.2	+4.5		0.23	4.25
2	5.18	300	1.04	0.95	-11.5	+2.2	59.0	0.23	4.10
3	4.89		0.98	0.90	-12.7	+0.6		0.23	3.95

It can be seen in Tables 6.4 to 6.6 that in general, the frost heave rate (*dh/dt*), the velocity of water flow (v_φ) and the segregation potential for the materials studied increased with increasing number of FT cycles. An increase in the segregation potential and the associated parameters are primarily due to the impact of WD cycles. As compared to the specimens that were subjected to one cycle of freeze-thaw (Table 5.4), the segregation potentials of specimens subjected to WD cycles were found be higher.

6.3.5 Water content

The WD tests with intermittent FT cycles were terminated after implementing three FT cycles. The tests were terminated at the end of the last thawing stages in the last FT cycle for all specimens. The specimens were cut into three slices, and the water contents of the slices were measured by the oven-drying method. The water contents of the specimens are shown in Figure 6.11. For the sake of comparisons, the initial compaction water contents of the specimens are shown in Figure 6.11.

It can be seen in Figure 6.11 that the variations of the water content along the depth of the specimens were not very significant and remained between 3 to 5% from top to bottom of the specimens. As compared to the initial water contents, the water contents of the specimens of Spewhite kaolin and Pegwell Bay soil were found to be higher, whereas the water content of the specimen of cement kiln dust remained nearly unchanged in the top parts but decreased towards the bottom part of the specimen. As compared to the specimens subjected to one cycle of freeze-thaw (Figure 5.14), the water contents of the specimens that were subjected to WD and FT cycles were found to be similar for the specimen of Speswhite kaolin, higher for Pegwell Bay soil and lower for the specimen of cement kiln dust.

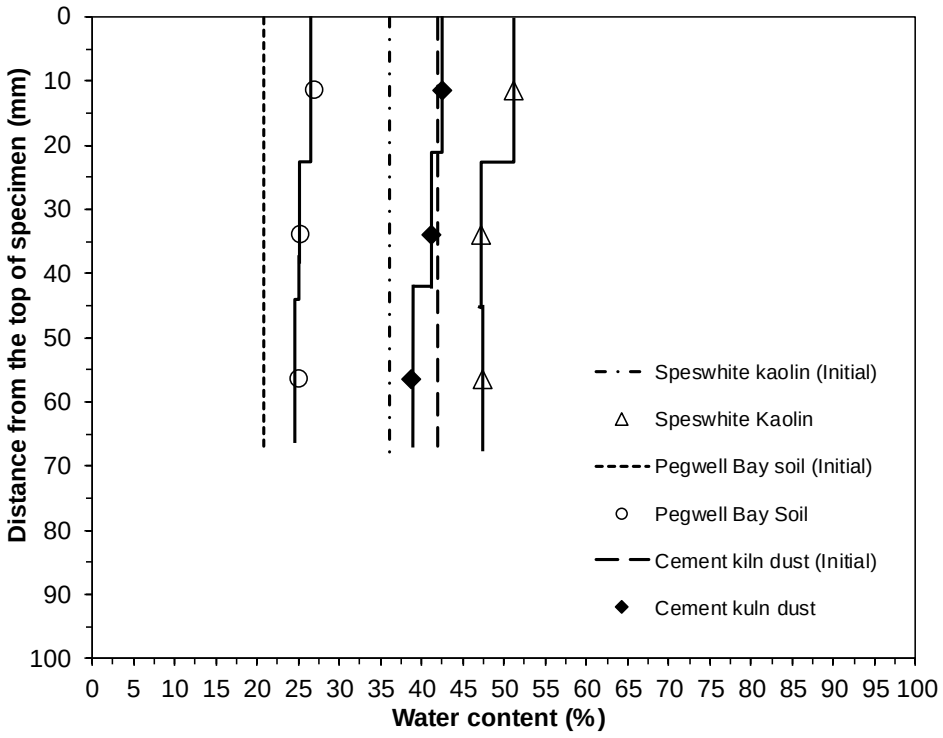

Fig. (6.11): Water content profiles of the materials at the end of the tests

6.4 Concluding remarks

This chapter presented the results of cyclic wet-dry tests on compacted specimens of Speswhite kaolin, Pegwell Bay soil and cement kiln dust. Intermittent freeze-thaw cycles were considered to study the effect of such actions on the volume change behaviour of the materials. The vertical deformations of the specimens with increasing number of cycles were measured. The temperature at various salient depths was monitored during the tests. The water content of the specimens at the end of the tests was measured. The following points emerged from the test results.

1. Wet-dry cycles caused a decrease in the vertical strains associated with wetting and drying processes for Speswhite kaolin, whereas it did not cause any appreciable volume change of Pegwell Bay soil and cement kiln dust in which cases the measured vertical strains were less than about 0.5%.
2. The deformation of the materials attained an equilibrium after several wet-dry cycles at which the magnitudes of strains during wetting and drying processes were found to be similar. The tests results agree well with the findings reported in the literature (Ring 1966; Basma et al. 1996; Tripathy and Subba Rao 2009)
3. Intermittent freeze-thaw cycles destabilised the equilibrium strain that was achieved by the materials during the previous wet-dry cycles; however, a new equilibrium in terms of vertical strain was attained by the material with an increasing number of wet-dry cycles, but with a reduced equilibrium strain.
4. Wet-dry cycles caused an increase in the frost heave and thaw settlement for all the materials studied indicating that the hydraulic conductivity increased due to exposure of the specimens to increasing number of wet-dry cycles.

5. The cyclic wet-dry and freeze-thaw processes affected the segregation potential of the materials. The segregation potential was found to increase for the specimens that were subjected previously to wet-dry cycles as compared to the specimens that underwent one freeze-thaw cycle.
6. The water contents at the end of tests were found to be similar to the initial water content in case of the specimen of cement kiln dust, whereas higher water contents were noted for Speswhite kaolin and Pegwell Bay soil specimens. Differences in the water contents were also noted for specimens that were subjected to one cycle of freeze-thaw and that were subjected to wet-dry and intermittent freeze-thaw cycles.

CHAPTER 7

Cyclic wet-freeze-thaw-dry tests on compacted specimens

7.1 Introduction

Compacted geomaterials may undergo numerous cycles of wetting, drying, freezing and thawing processes during their use in many civil engineering applications (roadways, railway formations, foundations etc.). The freezing, thawing, drying and wetting processes are driven by the climatic conditions. In temperate regions of the world, the geomaterials are often subjected to drying and wetting processes, whereas in the cold regions freezing and thawing processes are more common. In certain parts of the world, it may be expected that all of these processes are of significant interest.

Considerable field and laboratory research works have been aimed at understanding the effects of cyclic wetting-drying on the volume change behaviour of various soils (Dasog et al. 1988; Day 1994; Al-Homoud et al. 1995; Basma et al. 1996; Rao et al. 2001; Tripathy et al. 2002; Subba Rao and Tripathy 2003; Alonso et al. 2005; Rao and Revanasiddappa 2006; Tripathy and Subba Rao 2009; Toll et al. 2016a, b; Rosenbalm and Zapata 2017) Similarly, several studies have focused on the cyclic freeze-thaw behaviour of soils (Chamberlain and Gow 1979; Chamberlain 1981a, b; Konrad 1989a; Konrad 1989d; Viklander 1998a, b; Wang et al. 2007; Qi et al. 2008; Hui and Ping 2009; Aldaood et al. 2014; Wang et al. 2016). Additionally, various studies have explored the effects of freezing-thawing beside wetting-drying on various properties of soils (Sillanpää and Webber 1961; Pardini et al. 1996; Gullà et al. 2006; Ahmed and Ugai 2011; Özbek 2014; Diagne et al. 2015). Studies of the behaviour of geomaterials by subjecting the

materials to alternate wet-dry cycles or freeze-thaw cycles have enhanced the understanding of the volume change, shear strength and permeability. The changes in the volume of materials cause changes in the shear strength and permeability that in turn, influence the stability of structures founded on them.

The objectives of this chapter were; (*i*) to study the one-dimensional volume change behaviour of the compacted Speswhite kaolin, Pegwell Bay soil and cement kiln dust with increasing number of wet-freeze-thaw-dry (WFTD) cycles, (*ii*) to explore the effects of WFTD cycles on the segregation potential of the materials and (*iii*) to study the effects of WFTD cycles on the water content of the materials.

This chapter is presented in several sections. The experimental program (Test series IV; section 3.8) is recalled in section 7.2. Under test results and discussion (section 7.3), the experimental results and the analyses of the results of the cyclic WFTD tests on compacted specimens are presented. Section 7.3 presents the volume change the materials upon saturation, frost heave, settlement during thawing and deformation during the drying process with an increasing number of WFTD cycles. The temperature profiles with increasing number of WFTD are presented for freezing, thawing and drying processes. The volume-mass properties of the materials are also presented. The concluding remarks are presented in section 7.4.

7.2 Experimental program

The experimental program and the experimental methods for testing the compacted specimens by subjecting them to cycles of wetting, freezing, thawing and drying are presented in detail in chapter 3 (Test series IV; section 3.8). Compacted specimens were prepared within the specimen mould (Figure 3.22) by statically compacting the chosen materials to the targeted dry densities at predetermined water contents. For each material, one compaction condition (dry density and water content) was chosen. Compaction of the specimens was carried out using a static compaction machine (Figure 3.22). Table 3.4 shows the initial compaction conditions of the specimens tested. The diameter and height of the specimens were 103.5 and 65 mm respectively.

The sequence of the climatic processes at any specific location is quite complex. The sequence usually involves an overlapping of various meteorological seasons. The sequence of the climatic processes adopted in this study was based on the climatic conditions applicable to the northern hemisphere which usually encounters four distinct seasons, such as winter (December, January and February), spring (March, April, May), summer (June, July August) and autumn (September, October and November). The duration of the seasons can have a significant impact on various geomaterials. The experimental program adopted in this study does not replicate the length of the seasons and are only laboratory-scale testing of materials with assumed temperature and hydraulic boundary conditions for predetermined periods of testing.

The sequence of the climatic processes adopted was wetting (W), freezing (F), thawing (T) and drying (D). One complete cycle was comprised of subjecting a specimen to all the processes (wetting, freezing, thawing and drying). The specimen was further subjected to several such cycles. The cyclic WFTD tests were carried out at an applied

vertical pressure of 2.0 kPa using the test set up shown in Figures 3.12 and 3.13. The details of the test set up are presented in section 3.7.1. The vertical deformation of the specimens during wetting, freezing, thawing and drying processes were measured at the top of the cooling/ heating chamber. Additionally, the vertical displacements of the specimen mould were measured during all stages of the tests. The temperature at the predetermined levels along the depth of the specimens were monitored during the tests.

The wetting of the specimens were carried out at the room temperature until the deformation of the specimens was found to be stabilised. The supplied water to the specimens was at ambient laboratory temperature of 21 ± 2 °C. During the wetting process, the water table was kept at the top the specimens, whereas during freezing and thawing stages the water table was kept at the bottom of the specimens. No water was supplied to the specimens during the drying process. During the freezing process, the temperature at the top of the specimens was lowered to -19.5 ± 0.5 °C and maintained for 24 hours, whereas the thawing process occurred at the ambient laboratory temperature. The temperature at the top of the specimen was maintained at 52 ± 1.5 °C during the drying process (section 3.7.1.2). The drying stage was terminated when the vertical deformation of the specimen attained a constant value. After termination of the drying stage and before starting the next wetting stage, a duration of 24 hours was allowed for the temperature in the specimen to attain the room temperature. The vertical deformation at that stage was recorded prior to the commencement of the next wetting stage.

7.3 Test results and discussion

The results of the cyclic wet-freeze-thaw-dry (WFTD) tests on compacted specimens of Speswhite kaolin, Pegwell Bay soil and cement kiln dust are shown in Figures 7.1 to 7.9. Figures 7.1, 7.4 and 7.7 show the vertical deformation of the specimens as affected by the temperature and hydraulic boundary conditions with an increasing number of WFTD cycles. Figures 7.2, 7.5 and 7.8 show the temperature profiles in the specimens at the end of each stage and with increasing number of WFTD cycles. Figures 7.3, 7.6 and 7.9 show the elapsed time versus vertical deformation of the specimens for various wetting, freezing, thawing and drying stages. The displacements of the specimen mould for each stage are shown in Figures 7.1a, 7.4a and 7.6a. Figures 7.1b, 7.4b and 7.6b show the equilibrium temperatures for each stage of the tests. The ambient laboratory temperatures during the tests are also shown in Figures 7.1b, 7.4b and 7.6b.

Tables 7.1, 7.2 and 7.3 show the magnitudes of vertical deformation and vertical strain of the materials studied corresponding to the termination of wetting, freezing, thawing and drying stages with an increasing number of WFTD cycles for Speswhite kaolin, Pegwell Bay soil and cement kiln dust respectively. The vertical strain of the specimens was calculated based on the change in the height of the specimen in any stage and the initial height of the compacted specimen (65 mm) and expressed as a percentage. This allowed interpreting the magnitude and location of movement bands of the specimens with an increasing number of WFTD cycles.

A complete cycle is comprised of wetting, freezing, thawing and drying stages. The type of a movement band (uprising, descending) with increasing number of cycles depends upon the positions of the highest and the lowest deformations or strains with reference to the zero deformation or zero strain. The magnitude of a movement band is

the difference in the magnitudes of the highest and lowest deformations or strains in that cycle. Figure 7.10 shows the vertical strain of the specimens with increasing number of WFTD cycles.

The response of the specimens to temperature and hydraulic boundary conditions was reflected on the changes in the height of the specimens in each stage of the tests. The positions of the thermocouples with respect to the top of the specimen changed during the tests. Therefore, for the sake of consistency in the presentation of the test results, the initial positions of the thermocouples (Section 3.7.1.1) were considered.

7.3.1 Temperature profiles

It can be seen in Figures 7.1, 7.4 and 7.7 that the temperature at the top of the specimens was lowered down to -19 °C during the freezing stages, whereas the temperature during the drying stages was increased to +52 °C (see Figure 3.21; Test series IV). The temperature at the end of thawing and during the wetting stages was the ambient laboratory temperature. The ambient laboratory temperature was higher when the Pegwell Bay soil specimen was tested. The rise and fall of the temperature during the appropriate cycles were consistent indicating that the test set up and the accessories (the Vortex Tube assemblies) functioned efficiently during the tests.

At the end of freezing stages, the temperature along the depth of the specimens was found to be different as indicated by the readings of the thermocouples (TC1 to TC4). For the specimen of Speswhite kaolin the temperature measured by TC1 was about -10 °C, whereas the temperature measured by TC4 was about +0.5 °C. For the specimen of Pegwell Bay soil, the temperature measured by TC1 was about -10 °C, whereas the temperature measured by TC4 was about 0 °C. Similarly, for the specimen of cement kiln dust, the temperature measured by TC1 was about -6 °C, whereas that measured by TC4

was about 0 °C. The temperature at the end of drying stages were also found to different along the depth of the specimens. For the specimen of Speswhite kaolin, the temperature measured by TC1 was about +48 °C, whereas that measured by TC4 was about +41 °C. For the specimen of Pegwell Bay soil, the temperature measured by TC1 was about +51 °C, whereas that measured by TC4 was about 44 °C. Similarly, for the specimen of cement kiln dust, the temperature measured by TC1 was about +46 °C, whereas that measured by TC4 was about 38 °C. The differences in the temperatures along the depth of the specimens are attributed to the thermal conductivity of the materials.

The temperature profiles shown in Figures 7.2, 7.4 and 7.6 show that there were no significant differences in the profiles for each stage and with increasing number of cycles, except in the thawing stages in which case, the temperature was affected due to a fluctuation of the ambient laboratory temperature. Based on the temperature profiles, it can be stated that the differences in the volume change behaviour of the materials on account of the cyclic wet-freeze-thaw-dry processes are the responses of the materials to the thermal and hydraulic boundary conditions adopted in this investigation.

7.3.2 Vertical deformation and vertical strain

The upward movement of the specimen mould during the freezing stages and the downward movement of it during the thawing stages (see Figures 7.1, 7.4 and 7.7) were anticipated as shown in the test results presented in chapters 3, 4, 5 and 6. These movements did not leave any residual strain which indicated that there was not any loss of materials during the tests.

The shapes of the elapsed time versus vertical deformation plots for the specimens during wetting, freezing, thawing and drying were found to be dissimilar (Figures 7.3, 7.6 and 7.9). The mechanisms of swelling in geomaterials are associated with the hydration

and osmotic effects, whereas the mechanisms of volume decrease upon drying are associated with an increase in matric suction. The shapes of wetting and drying plots can also be considered to be affected by the temperature during the tests since both occur at different temperatures. For any cycle, the magnitudes of deformation of the materials due to the wetting process were found to be lesser than the magnitudes of deformation due to the drying process (Tables 7.1 to 7.3). Similarly, the frost heave is associated with the density effects of fluids (water and ice) and the formation of ice lenses, whereas the thaw settlement is associated with the dissipation of pore water pressure, both are impacted by the permeability of the materials. For any cycle, the magnitudes of frost heave of the materials were found to be greater than the magnitudes of thaw settlement (Table 7.1 to 7.3).

During the commencements of thawing stages, additional heave was noted for all the materials studied. The additional heave is associated with a decrease in effective stress resulting from the increase in pore-water pressure (Eigenbrod et al. 1996; Eigenbrod 1996). The time required to attain an equilibrium in terms of vertical deformation in thawing stages decreased with an increase in the number of cycles.

Since the overburden pressure in the WFTD cycles test is only 2 kPa, a vertical displacement occurred during drying stages and disappeared when the specimen reached to the room temperature, as shown in Figure 7.3d. The thermal expansion during the cycles varied from 0.3 mm to 0.9 mm, that might be attributed to the temperature lost during the transition stage (last 24 hour of drying) and the change in dry density of specimen during WFTD cycles.

7.3.3 Movement band

From the test results presented in Figures 7.1 to 7.9 and Tables 7.1 to 7.3 for the three materials considered in this study some specific features can be noted. As compared to the vertical strains observed in the first wetting cycles, the vertical strain generally decreased for Speswhite kaolin, whereas it increased and decreased for the specimens of Pegwell Bay soil and cement kiln dust. The vertical strain of all the materials firstly increased and then decreased with an increasing number of freezing cycles, whereas it increased for the thawing cycles and decreased for the drying cycles. This resulted in an accumulation of vertical strain in the specimens which in turn, caused a shifting of the movement band in an upward direction as shown in Figures 7.1, 7.4, 7.7 and 7.10.

Tripathy et al. (2002) and Tripathy and Subba Rao (2009) have shown that the movement type accompanied by a shifting of the movement band in an upward direction with an increasing number of swell-shrink cycles (uprising movement) is associated with smaller applied pressures and partial shrinkage of soil specimens, whereas there may be a complete downward shift of the movement band (descending movement) in case of higher applied pressures and full shrinkage conditions. The movement type in the case of geomaterials due to alternate freezing and thawing depends upon the initial density. Viklander (1998a) stated that a net increase in the void ratio of compacted soils occurs upon freeze-thaw processes due to changes in the particle rearrangements. The uprising movement is shown by all the materials in this study (Figure 7.10) is attributed to the small magnitude of applied pressure during the tests and the combination of freeze-thaw and dry-wet processes.

Studies in the past have shown that soils subjected to wet-dry or freeze-thaw cycles attain an equilibrium condition after about four cycles (Ring 1966; Basma et al. 1996;

Tripathy and Subba Rao 2009; Konrad 1989b; Viklander and Eigenbrod 2000). The magnitudes of vertical strains during wetting and drying or freezing and thawing become similar once the equilibrium condition is attained for a given pattern of wet-dry or freeze-thaw cycles. The vertical strain in each stage (i.e. wetting, freezing, thawing and drying) stabilised after about three WFTD cycles for the all the materials studied (Figure 7.10). The movement band encompassing strains corresponding to wetting, freezing, thawing and drying was nearly repeatable after three cycles. The equilibrium band movement (i.e. the difference in the magnitudes of strain corresponding to the frost heave and that at the end of a drying cycle) for Speswhite kaolin, Pegwell Bay soil and cement kiln dust were found to be about 28.9, 37.7 and 41.4% respectively.

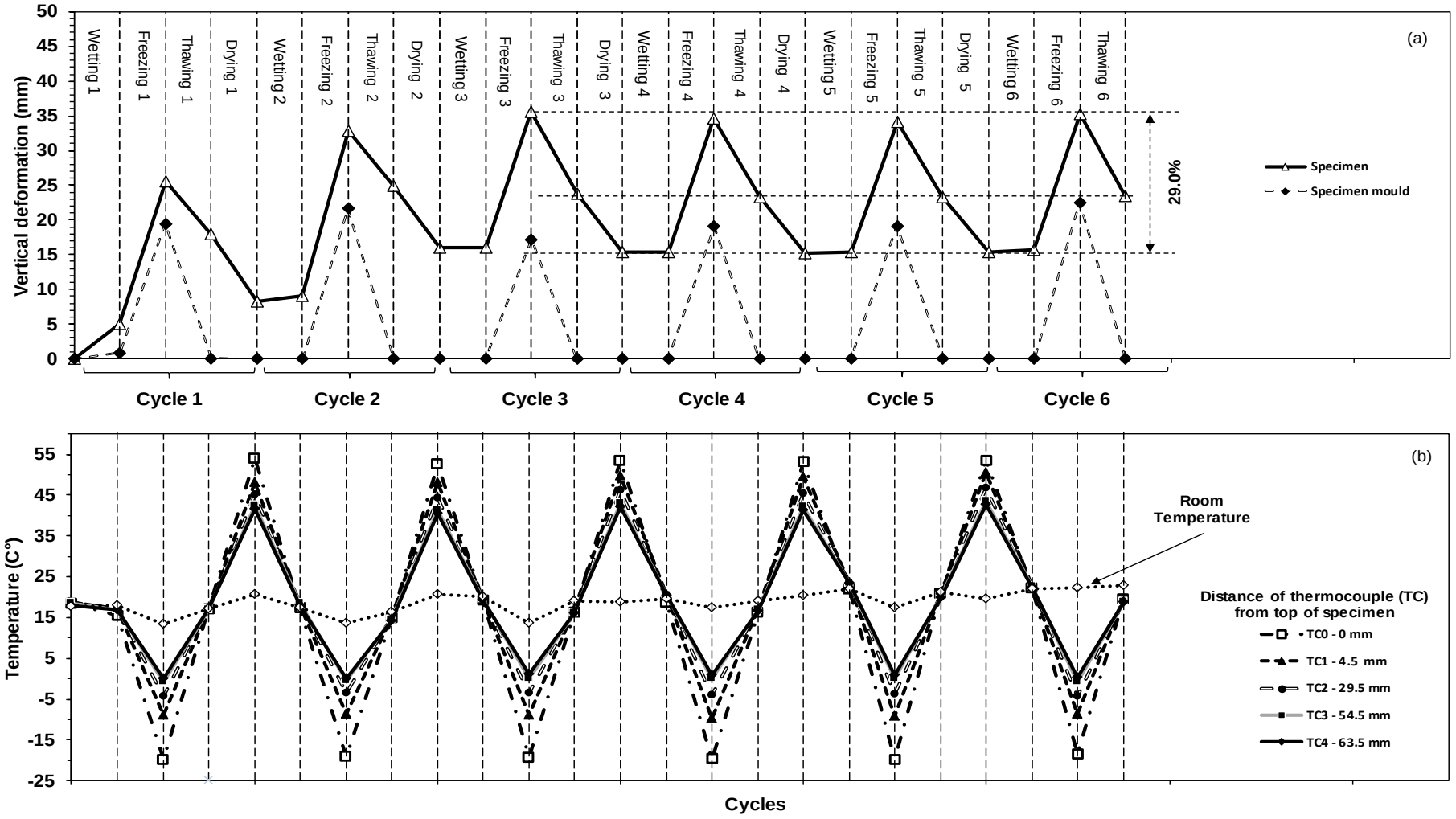

Fig. (7. 1): (a) Vertical deformation and (b) temperature change of Speswhite kaolin specimen with increasing of WFTD cycles

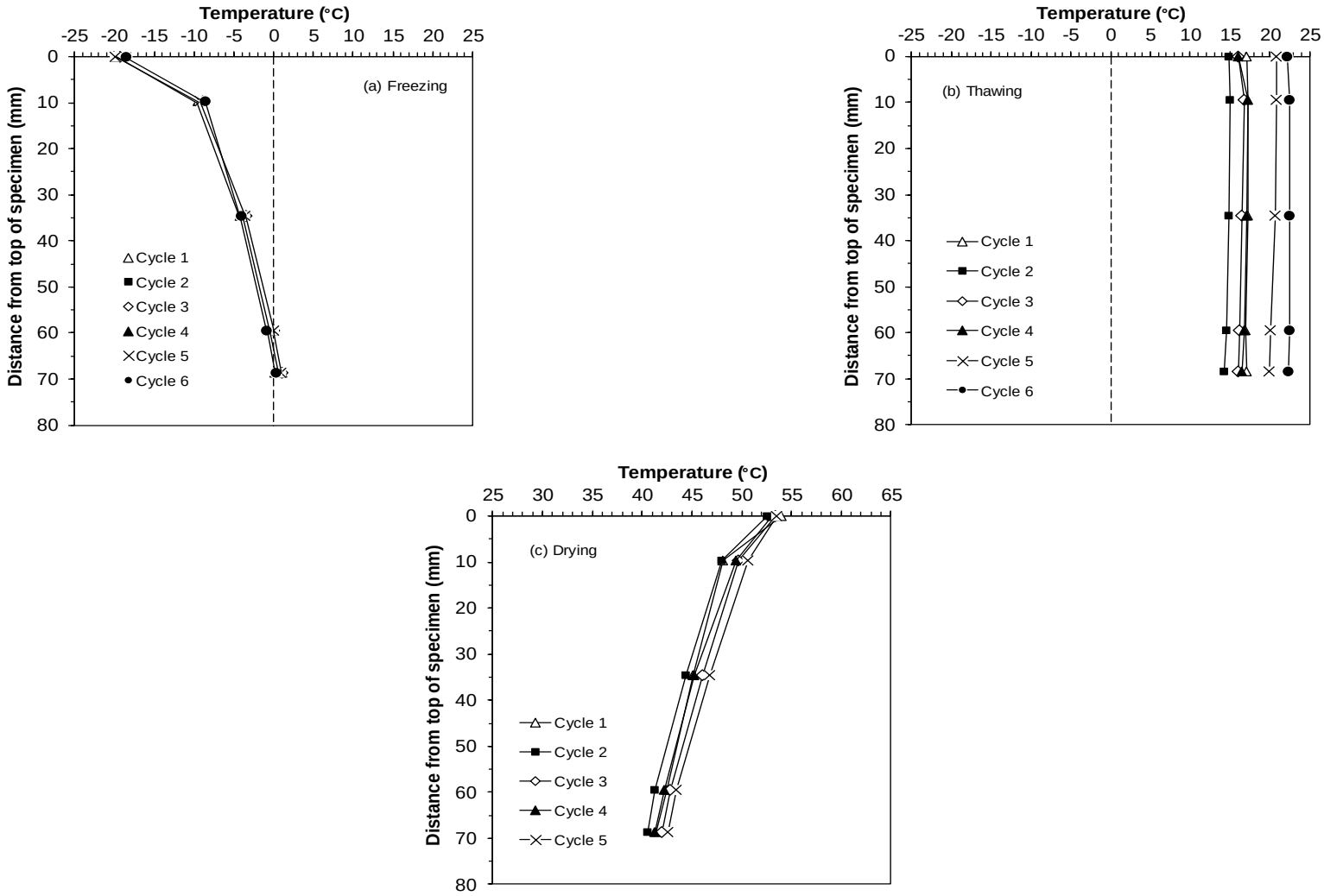

Fig. (7.2): Temperature profiles at the end of (a) freezing, (b) thawing and (c) drying stages with increasing number of WFTD cycles for Speswhite kaolin

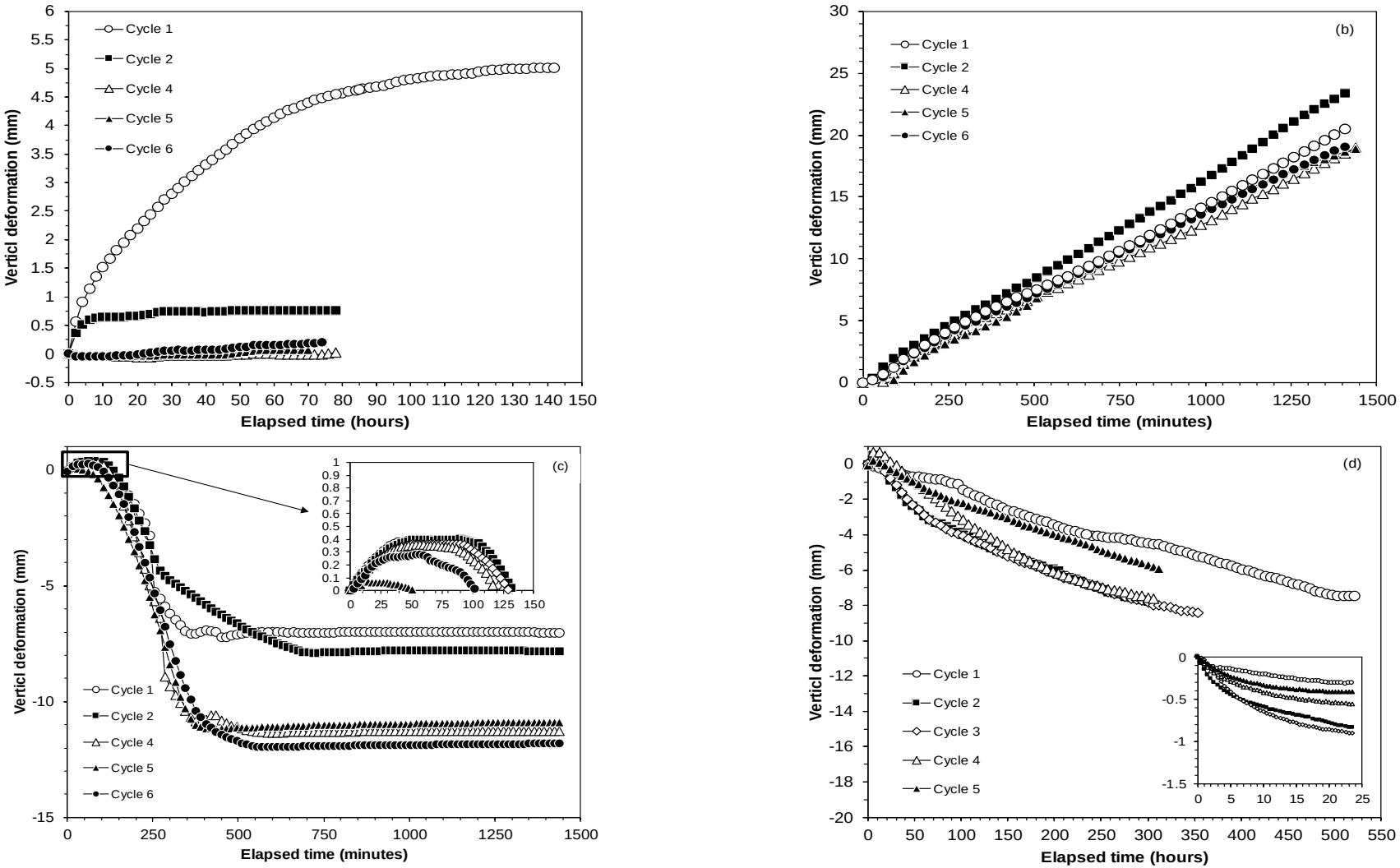

Fig. (7.3): Elapsed time versus vertical deformation for various cycles during (a) wetting, (b) freezing, (c) thawing and (d) drying of Speswhite kaolin specimen

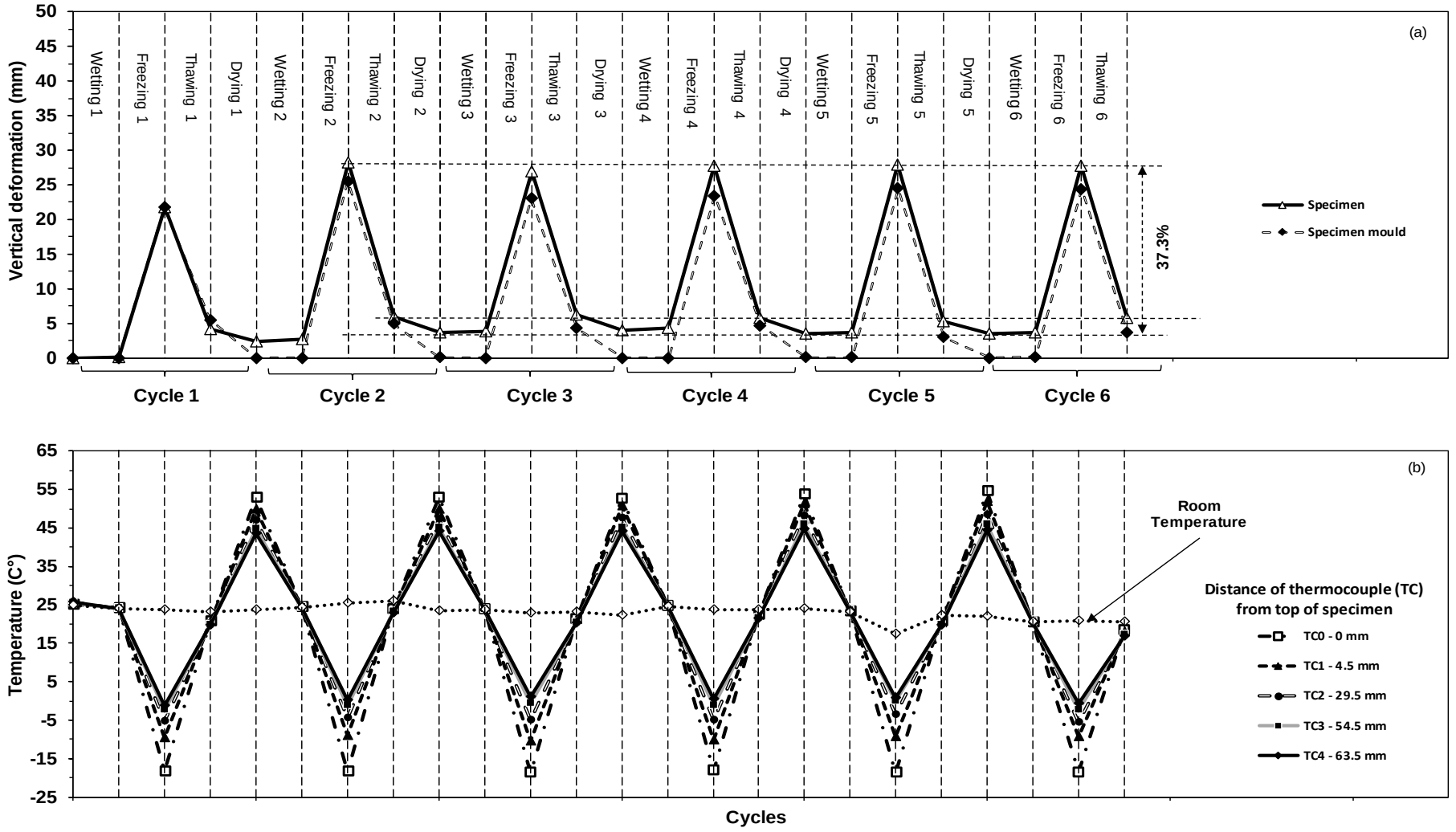

Fig. (7.4): (a) Vertical deformation and (b) temperature change of Pegwell Bay soil specimen with increasing of WFTD cycles

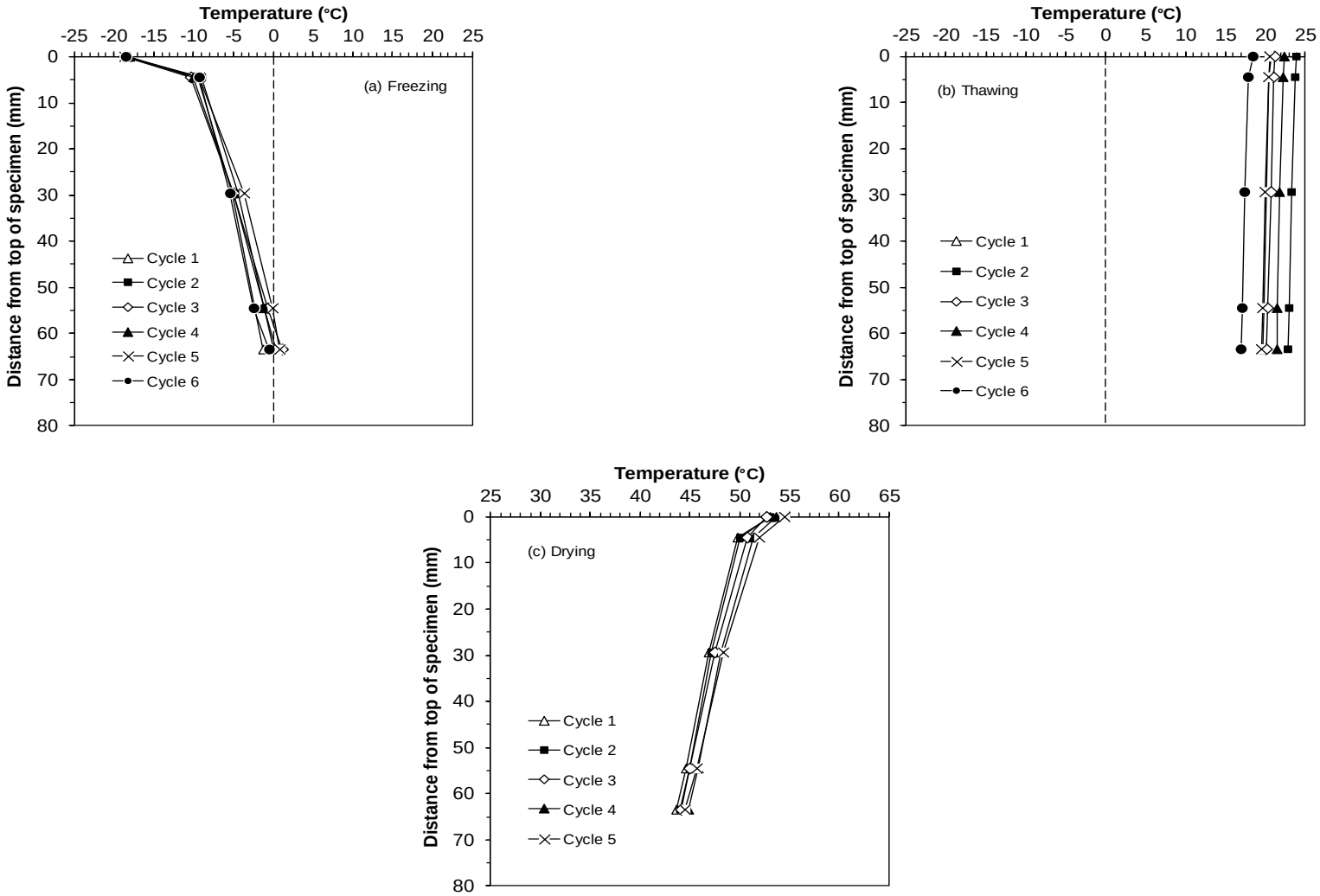

Fig. (7. 5): Temperature profiles at the end of (a) freezing, (b) thawing and (c) drying stages with increasing number of WFTD cycles for Pegwell Bay soil

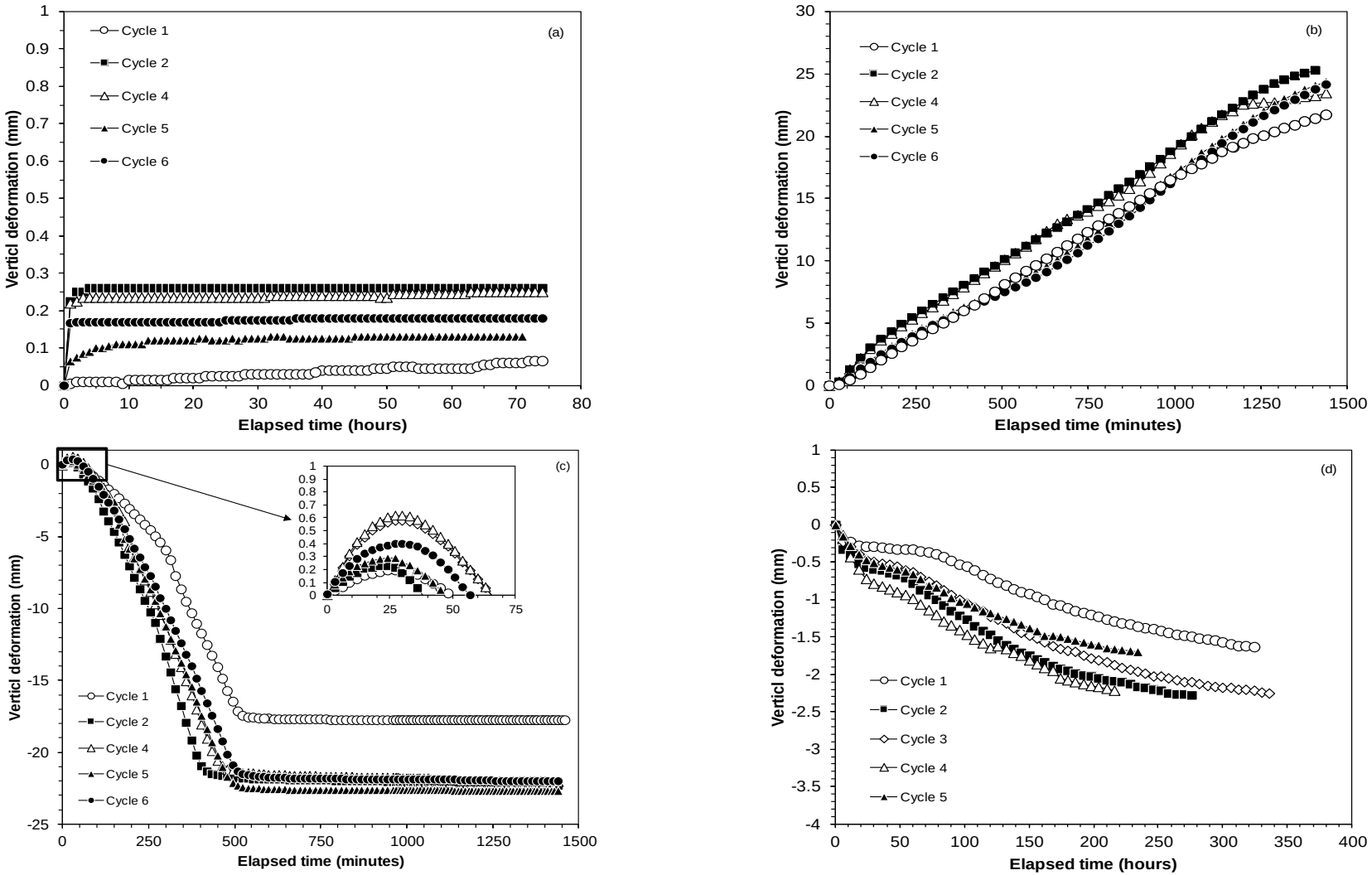

Fig. (7.6): Elapsed time versus vertical deformation for various cycles during (a) wetting, (b) freezing, (c) thawing and (d) drying of Pegwell Bay soil

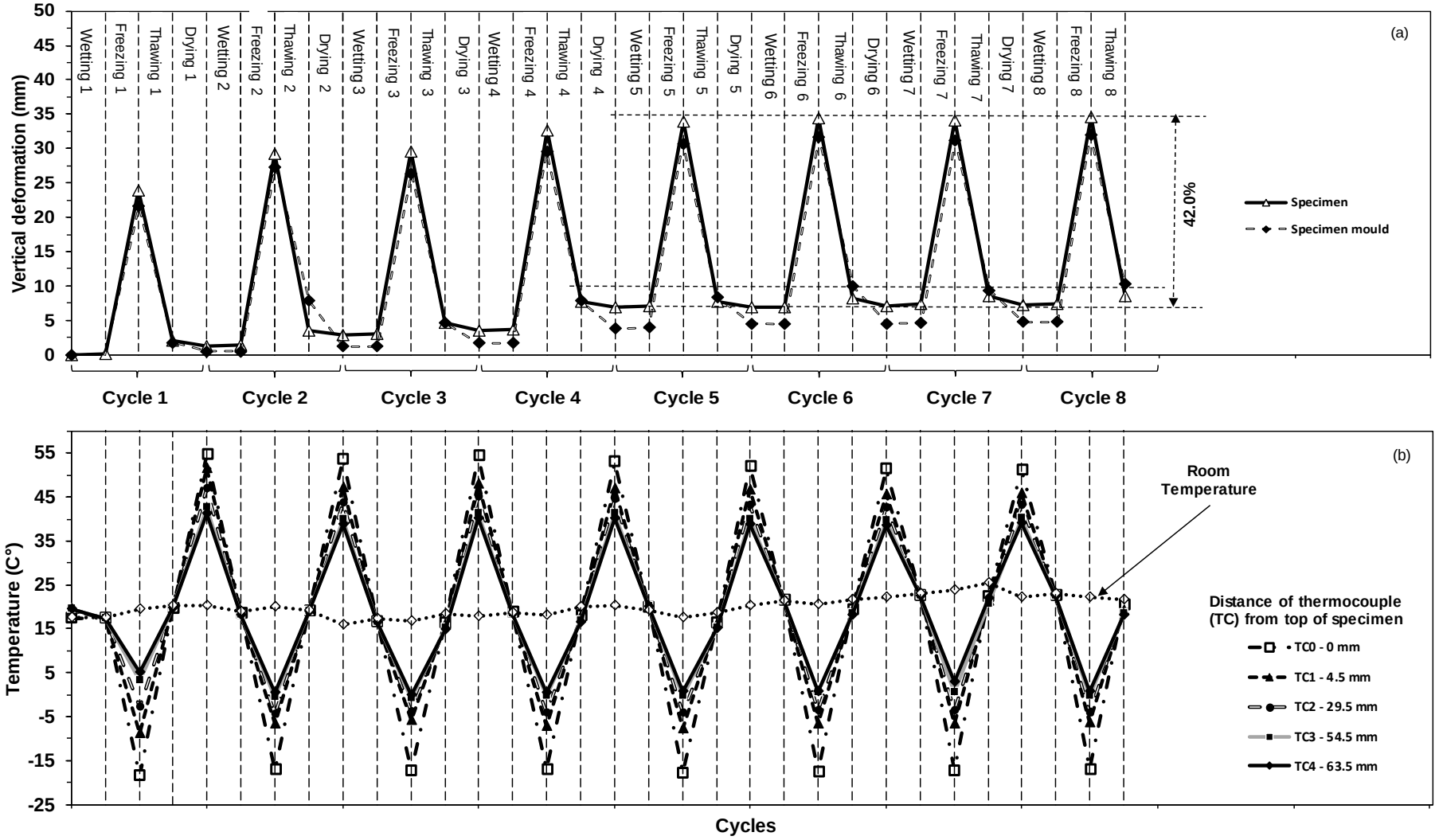

Fig. (7.7): (a) Vertical deformation and (b) temperature change of cement kiln dust specimen with increasing of WFTD cycles

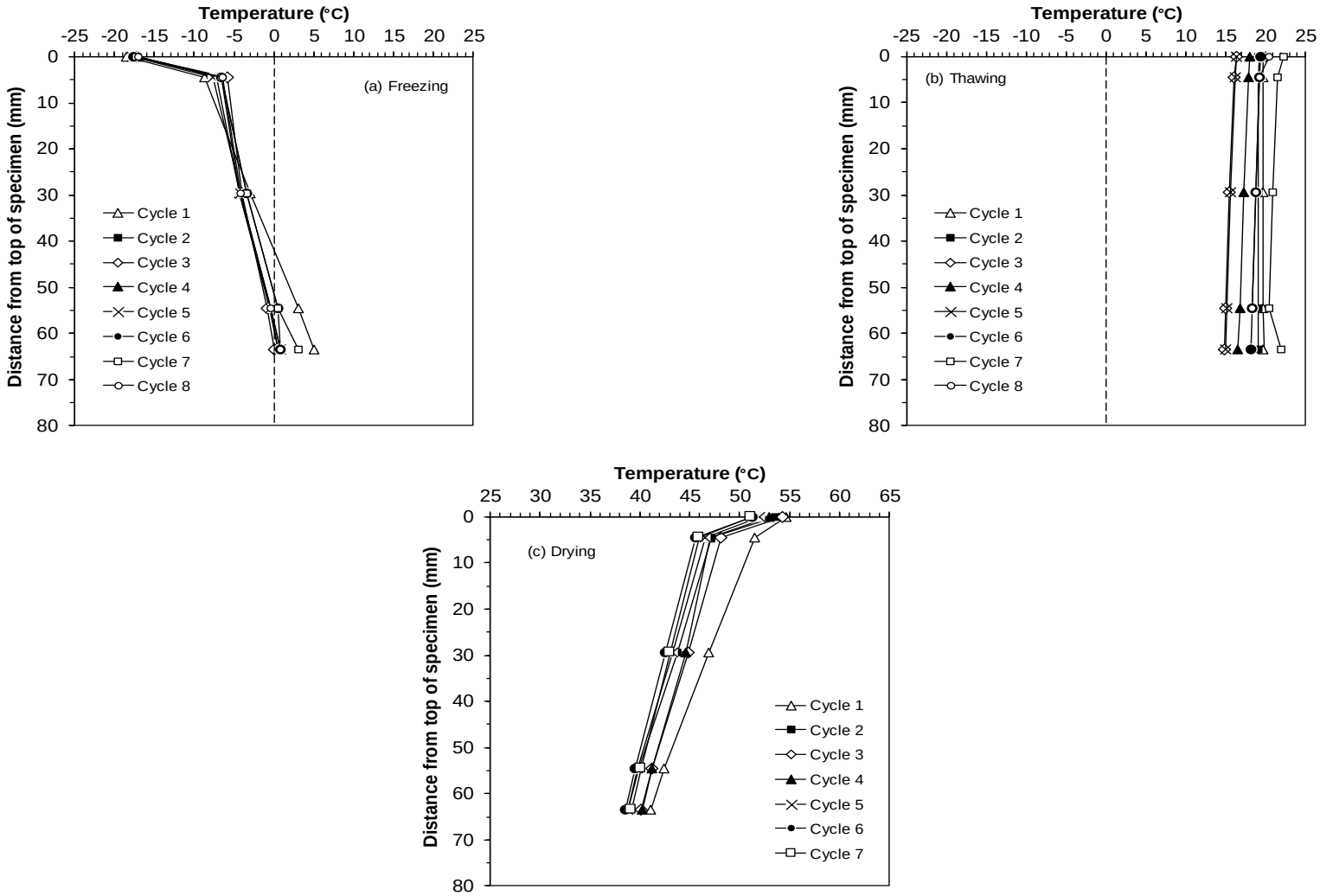

Fig. (7.8): Temperature profiles at the end of (a) freezing, (b) thawing and (c) drying stages with increasing number of WFTD cycles for cement kiln dust

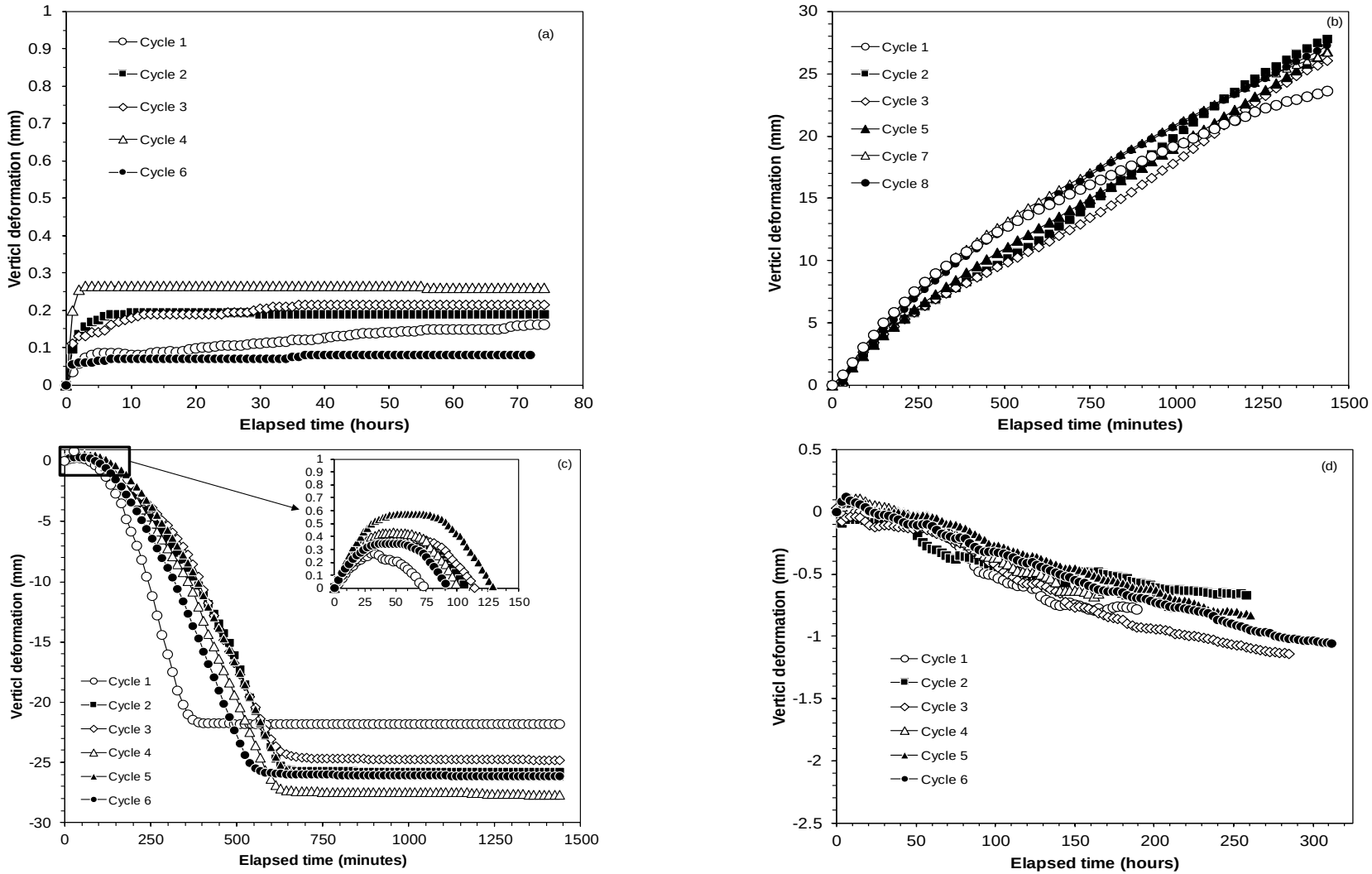

Fig. (7.9): Elapsed time versus vertical deformation for various cycles during (a) wetting, (b) freezing, (c) thawing and (d) drying of cement kiln dust

Table 7.1: Vertical deformation and vertical strain of compacted Speswhite kaolin with increasing WFTD cycles

Cycle	Wetting		Freezing		Thawing		Drying	
	Vertical deformation (mm)	Vertical strain (%)	Vertical deformation (mm)	Vertical strain (%)	Vertical deformation (mm)	Vertical strain (%)	Vertical deformation (mm)	Vertical strain (%)
1	+5.0	+7.7	+20.5	+31.5	-7.5	-11.5	-9.8	-15.1
2	+0.8	+1.2	+23.8	+36.6	-7.8	-12.0	-9.0	-13.8
3	+0.0	+0.0	+19.7	+30.3	-11.8	-18.2	-8.5	-13.1
4	+0.0	+0.0	+19.3	+29.7	-11.3	-17.4	-8.1	-12.5
5	+0.0	+0.0	+18.9	+29.1	-10.9	-16.8	-7.9	-12.2
6	+0.3	+0.5	+19.6	+30.2	-11.8	-18.2	--	--

Table 7.2: Vertical deformation and vertical strain of compacted Pegwell Bay soil with increasing WFTD cycles

Cycle	Wetting		Freezing		Thawing		Drying	
	Vertical deformation (mm)	Vertical strain (%)	Vertical deformation (mm)	Vertical strain (%)	Vertical deformation (mm)	Vertical strain (%)	Vertical deformation (mm)	Vertical strain (%)
1	+0.1	+0.2	+21.7	+33.4	-17.7	-27.2	-1.6	-2.5
2	+0.2	+0.3	+25.5	+39.2	-22.3	-34.3	-2.3	-3.5
3	+0.2	+0.3	+23.1	+35.5	-20.6	-31.7	-2.3	-3.5
4	+0.2	+0.3	+23.5	+36.2	-22.0	-33.8	-2.2	-3.4
5	+0.1	+0.2	+24.4	+37.5	-22.7	-34.9	-1.8	-2.8
6	+0.1	+0.2	+24.1	+37.1	-22.0	-33.8	--	--

Table 7.3: Vertical deformation and vertical strain of compacted cement kiln dust with increasing WFTD cycles

Cycle	Wetting		Freezing		Thawing		Drying	
	Vertical deformation (mm)	Vertical strain (%)	Vertical deformation (mm)	Vertical strain (%)	Vertical deformation (mm)	Vertical strain (%)	Vertical deformation (mm)	Vertical strain (%)
1	+0.2	+0.3	+23.7	+36.5	-21.8	-33.5	-0.8	-1.2
2	+0.2	+0.3	+27.9	+42.9	-25.8	-39.7	-0.7	-1.1
3	+0.2	+0.3	+26.5	+40.8	-24.9	-38.3	-1.1	-1.7
4	+0.2	+0.3	+28.9	+44.5	-24.9	-38.3	-0.8	-1.2
5	+0.1	+0.2	+26.8	+41.2	-26.6	-40.9	-0.8	-1.2
6	+0.1	+0.2	+27.3	+42.0	-26.1	-40.2	-1.1	-1.7
7	+0.3	+0.5	+26.7	+41.1	-25.7	-39.5	-1.2	-1.8
8	+0.1	+0.2	+27.3	+42.0	-26.0	-40.0	--	--

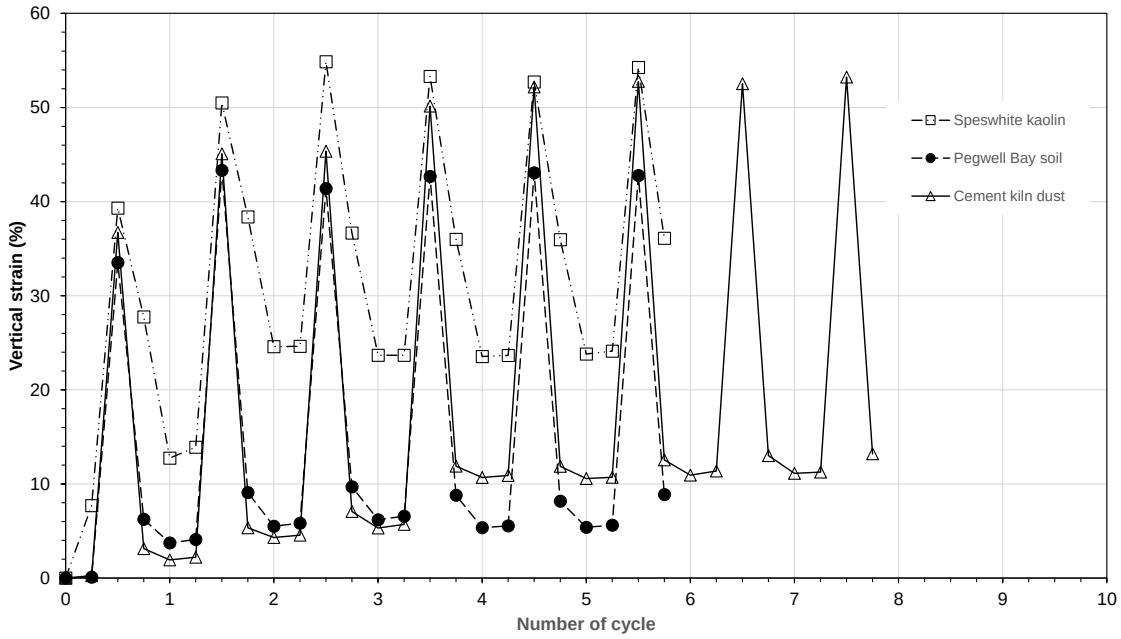

Fig. (7.10). Vertical strain of the materials with increasing number of WFTD cycles

At equilibrium, the vertical strains corresponding to wetting, freezing, thawing and drying stages were found to be dissimilar (Tables 7.1 to 7.3). The sum of vertical strains during wetting and freezing processes were found to be nearly equal to the sum of vertical strains occurred during thawing and drying processes.

7.3.4 Segregation potential

The elapsed time versus frost heave of the specimens of Speswhite kaolin, Pegwell Bay soil and cement kiln dust are shown in Figures 7.3b, 7.6b and 7.9b respectively. In all cases and for any cycle, a thermal steady state was reached after an elapsed time of 400 min. Tables 7.4, 7.5 and 7.6 present the parameters that were derived from the frost heave results and the segregation potentials (SP_t) of Speswhite kaolin, Pegwell Bay soil and cement kiln dust respectively.

The frost heave rate (*dh/dt*) were calculated based on the frost heave (*dh*) and the elapsed time (*dt*) after the steady state. The values of velocity of arriving pore water (v_φ) were calculated based on the heave rates and using Equation 2.6. The temperatures T1 and T2 corresponding an elapsed time of 600 minutes were considered for calculating the temperature gradients (ΔT_f) in the frozen fringe when the materials had reached a steady state condition. The values of T1 and T2 were obtained from the TC1 and TC4 data. The thickness of the specimens between the position of TC1 and TC4 in all cases was 59 mm. The segregation potential (SP_t) for the materials were calculated based on Equation 2.7 (Konrad and Morgenstern 1980, 1981, 1982)

Table 7.4: Heave rate (*dh/dt*), velocity of water flow (v_φ), thermal gradient (ΔT_f) and segregation potential (SP_t) of the compacted Speswhite kaolin during the freezing stages of WFTD cycles

WFTD Cycle	*dh* (mm)	*dt* (min)	*dh/dt* (mm/hr)	v_φ = (*dh/dt*)/1.09 (mm/hr)	T1[1] (°C)	T2[1] (°C)	t (mm)	ΔT_f = [(T1-T2)/t] (°C/mm)	SP_t = (v_φ/ ΔT_f) (mm^2/°C.hr)
1	3.76	300	0.75	0.69	-7.2	+4.3	59.0	0.22	3.17
2	4.71		0.94	0.86	-8.1	+4.2		0.21	4.14
3	4.59		0.92	0.84	-7.8	+4.4		0.21	4.08
4	4.56		0.91	0.84	-7.7	+5.6		0.23	3.71
5	4.63		0.93	0.85	-7.1	+6.5		0.23	3.69
6	4.53		0.91	0.83	-9.1	+4.4		0.23	3.64

Table 7.5: Total Frost heave, Heave rate (*dh/dt*), thermal gradient (ΔT_f) and the Segregation potential (SP_t) of compacted Pegwell Bay soil during the freezing stages of WFTD cycles

WFTD Cycle	*dh* (mm)	*dt* (min)	*dh/dt* (mm/hr)	v_φ = (*dh/dt*)/1.09 (mm/hr)	T1[1] (°C)	T2[1] (°C)	t (mm)	ΔT_f = [(T1-T2)/t] (°C/mm)	SP_t = (v_φ/ ΔT_f) (mm^2/°C.hr)
1	5.31	300	1.06	0.97	-11.2	+2.4	59.0	0.23	4.22
2	5.08		1.02	0.93	-9.7	+4.3		0.24	3.92
3	5.04		1.01	0.92	-8.9	+5.3		0.24	3.85
4	4.96		0.99	0.91	-9.6	+4.6		0.24	3.79
5	4.69		0.94	0.86	-8.4	+5.2		0.23	3.75
6	4.46		0.89	0.82	-8.4	+4.6		0.22	3.72

Table 7.6: Total Frost heave, Heave rate (*dh/dt*), thermal gradient (ΔT_f) and the Segregation potential (SP_t) of Cement kiln dust during the freezing stages of WFTD cycles

WFTD Cycle	*dh* (mm)	*dt* (min)	*dh/dt* (mm/hr)	v_φ = (*dh/dt*)/1.09 (mm/hr)	T1[1] (°C)	T2[1] (°C)	t (mm)	ΔT_f = [(T1-T2)/t] (°C/mm)	SP_t = (v_φ/ ΔT_f) (mm^2/°C.hr)
1	4.32		0.86	0.79	-7.1	+7.7		0.25	3.16
2	5.35		1.07	0.98	-8.2	+5.5		0.23	4.22
3	4.36		0.87	0.80	-6.8	+5.6		0.21	3.80
4	5.55		1.11	1.02	-6.8	+6.5		0.23	4.51
5	4.90	300	0.98	0.90	-6.5	+6.6	59.0	0.22	4.06
6	5.27		1.05	0.97	-5.7	+7.8		0.23	4.22
7	4.99		1.00	0.91	-5.7	+7.0		0.22	4.25
8	5.33		1.07	0.98	-5.2	+8.1		0.23	4.33

It can be seen in Tables 7.4 to 7.6 that the frost heave rate (*dh*/*dt*) and the velocity of water flow (v_φ) of Speswhite kaolin were generally smaller than that of the other two materials. In general, the segregation potential increased and then decreased as it occurred for the frost heave. The values of (*dh*/*dt*), v_φ, ΔT_f and SP_t were found to be similar for Pegwell Bay soil and cement kiln dust.

7.3.5 Water content

The cyclic WFTD tests were terminated after the equilibrium was attained in terms of the movement band in which case the combined strains during wetting and freezing processes were equal to the combined strains due to thawing and drying processes. The tests were terminated at the end of thawing stages in cycle 6 for the specimens of

Speswhite kaolin and Pegwell Bay soil and at the end of cycle 8 for the specimen of cement kiln dust. The specimens were cut into three slices, and the water contents of the slices were measured by the oven-drying method. Figure 7.11 shows the water contents of the specimens. For the sake of comparisons, the initial compaction water contents of the specimens are shown in Figure 7.11.

It can be seen in Figure 7.11 that the variations of the water content along the depth of the specimens were not very significant. As compared to due to the initial water contents, the water contents of the specimens of Spewhite kaolin and Pegwell Bay soil were found to be greater, whereas the water content of the specimens of cement kiln dust remained nearly unchanged. The water contents of the specimens were found to be lesser than that occurred for the specimens subjected to one cycle of freeze-thaw (chapter 5).

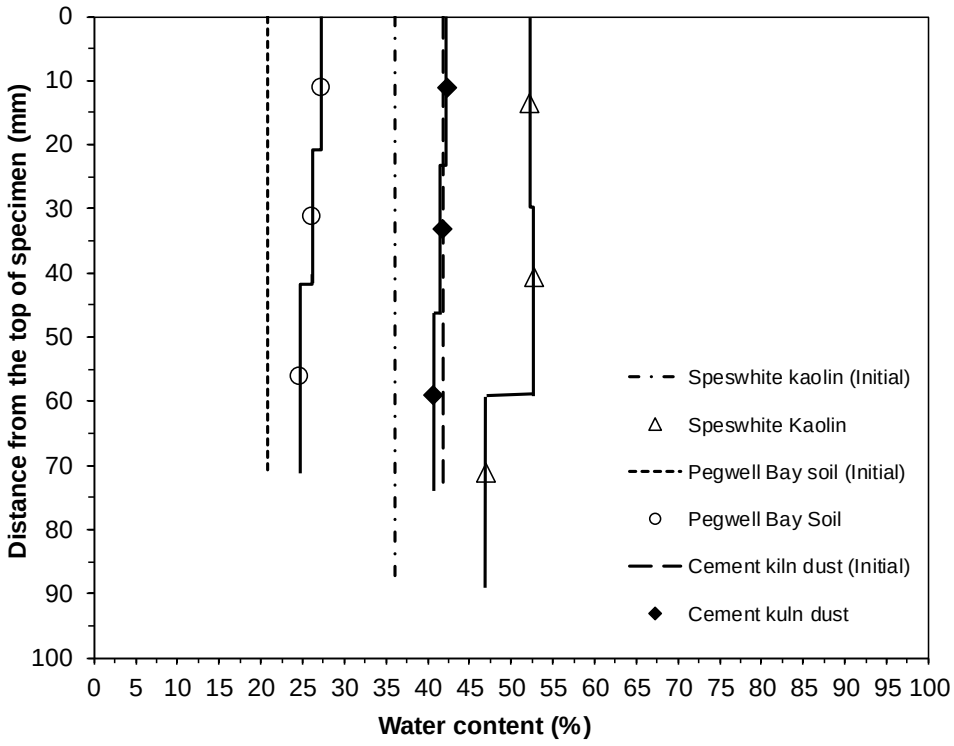

Fig. (7.11): Water content profiles at the end of the cyclic WFTD tests

7.4 Concluding remarks

This chapter presented the cyclic wet-freeze-thaw-dry test results of compacted specimens of Speswhite kaolin, Pegwell Bay soil and cement kiln dust. The vertical deformations of the specimens with increasing number of WFTD cycles were measured. The temperature at various salient depths was monitored during the tests. The water content of the specimens at the end of the tests was measured. The following points emerged from the test results.

1. The shapes of elapsed time versus vertical deformation of the materials during wetting, freezing, thawing and drying were found to be dissimilar. The differences in the shapes of the time versus vertical deformation plots for various climatic processes are attributed to the differences in the mechanisms governing swelling, freezing, thawing and drying processes.
2. For any given cycle, the magnitudes of deformation of the materials due to the wetting process were found to be lesser than the magnitudes of deformation due to the drying process. Similarly, the magnitudes of frost heave of the materials were found to be greater than the magnitudes of thaw settlement. This resulted in an accumulation of vertical strain in the specimens which in turn, caused a shifting of the movement band of the specimens in an upward direction. The specimens exhibited an uprising movement with an increasing WFTD cycles.
3. The vertical strain in each stage (i.e. wetting, freezing, thawing and drying) were found to be dissimilar but stabilized after about three WFTD cycles for the materials studied. The movement band encompassing strains corresponding to wetting, freezing, thawing and drying was found to be nearly repeatable after three cycles. The sum of vertical strains during wetting and freezing processes were

found to be nearly equal to the sum of vertical strains occurred during thawing and drying processes. The equilibrium band movement (i.e. the difference in the magnitudes of strain corresponding to the frost heave and that at the end of a drying cycle) for Speswhite kaolin, Pegwell Bay soil and cement kiln dust were found to be about 28.9, 37.7 and 41.4% respectively.

4. The cyclic WFTD processes affected the segregation potential of the materials. The segregation potential of Speswhite kaolin was found to be smaller than Pegwell Bay soil and cement kiln dust. In general, the segregation potential increased and then decreased as it occurred for the frost heave with an increasing number of WFTD cycles.
5. The impact of an increase in the WFTD cycles was found to decrease the water content of the materials.

CHAPTER 8

Conclusions

Soils and various geomaterials (mixtures of soil and various industrial wastes and admixtures) are being used in many civil engineering applications (roadways, railway formations, foundations etc.). These materials may undergo numerous cycles of wetting, drying, freezing and thawing processes during their use. The freezing, thawing, drying and wetting processes are driven by the climatic conditions. The aim of this thesis was to study the one-dimensional volume change behaviour of geomaterials when subjected to various climatic processes.

Three different materials were used in the investigation (Speswhite kaolin, Pegwell Bay soil, and a cement kiln dust). The physical and chemical properties of the materials were determined following the standard laboratory procedures prior to carrying out the main tests. The materials used contained a significant amount of fine fractions. The percentages of silt- and clay-size fractions in the materials were greater than 90%. The properties of the materials were found to be different in terms of the plasticity properties, compaction and compressibility characteristics.

The laboratory tests were carried out using a specialised column cell test set up that enabled carrying out freezing, thawing, drying and wetting tests at a nominal pressure of 2 kPa. Vortex Tube assemblies in conjunction with compressed air supply were used to implement freezing and drying front at the top of cylindrical specimens (105 mm dia and

65 mm high) of the chosen materials. Using the Vortex Tubes and with appropriate accessories (generators), the temperature at the top of the specimens was lowered down to about – 19 °C during the freezing process, whereas the temperature was raised to about + 52 °C during the drying process. The temperature during thawing and wetting processes occurred at the ambient laboratory temperature. The water level was at the base of the specimens during freezing and thawing process, whereas it was maintained at the top of the specimens during the wetting process. No water was supplied to the specimens in the drying tests. The vertical deformation of the specimens and the temperature at selected depths were monitored during the tests.

Four series of tests were carried out on the selected materials. In test series I, initially saturated slurried specimens were subjected to freezing and thawing processes (Chapter 4). Similarly, compacted specimens of the materials were subjected to freezing and thawing processes in Test series II (Chapter 5). In Test series III (Chapter 6), compacted specimens were first subjected to wet-dry cycles until an equilibrium was reached in terms of the vertical strain and then, the specimens were subjected to a freeze-thaw cycle. The wet-dry cycles and the intermittent freeze-thaw cycles were then repeated. In Test series IV (Chapter 7), compacted specimens were subjected to an increasing number of wet-freeze-thaw-dry cycles.

The vertical strains of specimens corresponding to wetting, freezing, thawing and drying processes were calculated based on the vertical deformation measurements. Based on the frost heave during the freezing process and the temperature profiles, the segregation potential was calculated. The water contents of the specimens at selected stages of the tests were determined. The test results allowed comparing the vertical strains of the materials for given conditions of testing. Additionally, for any given material the

changes in the strain with an increasing number of wet-dry cycles, freeze-thaw cycles and wet-freeze-thaw-dry cycles were studied.

Based on the findings reported in this thesis, the following conclusions were drawn.

Test set up

1. The test setup used in this investigation facilitated implementing the wetting, freezing, thawing and drying processes and carrying out the required tests on the chosen materials. Specimens were not required to be dismantled for implementing any of the processes. Therefore, there was a smooth transition between the various processes adopted. A major limitation of the test up is that the current design does not allow testing materials at higher applied stresses.

Properties of the materials used

2. The values of liquid limit, plastic limit and shrinkage limit of the cement kiln dust used were found to be lower than that of Spewhite kaolin, whereas the maximum dry density and optimum water content values from compaction tests of these two materials were found to be similar. As per the USCS, Speswhite kaolin, Pegwell Bay soil and cement kiln dust were classified as CH, CL and ML respectively. Based on the compressibility test results of the materials at an applied pressure of 2 kPa, the coefficient of permeability of Pegwell Bay soil and cement kiln dust was found to be similar (10^{-8} m/s), whereas that of Speswhite kaolin was an order of magnitude lower (10^{-9} m/s).
3. The compressibility behaviour of the materials at smaller applied pressures remained in the order according to the liquid limit values of the materials. The pressure-void ratio plot of Speswhite remained higher followed by cement kiln dust and Pegwell Bay soil. However, at an applied vertical pressure greater than

about 80 kPa, the cement kiln dust exhibited a lesser volumetric deformation than Speswhite kaolin. A lesser volumetric response of cement kiln dust as compared to Speswhite kaolin is attributed to the effect of the cement phase reaction which formed bonding between the particles of cement kiln dust thereby offering a greater resistance to compression.

Wetting under seating pressure

4. Under an applied nominal vertical pressure of 2 kPa, the swelling strain of compacted specimen of Speswhite kaolin was about 7.5%, whereas very minor swelling strains were exhibited by the specimens of Pegwell Bay soil (0.15%) and cement kiln dust (0.30%). A higher swelling strain exhibited by Speswhite kaolin is on account of a greater specific surface of the clay and the physico-chemical interaction between the clay particles and the pore fluid.

Cyclic wet-dry effects on volume change

5. An increase in wet-dry cycles caused a decrease in the swelling and shrinkage stains (as compared to that occurred in the first wetting and drying cycles) of compacted Speswhite kaolin. An equilibrium in terms of the vertical strain was attained after about three wet-dry cycles at which, the magnitudes of swelling and shrinkage strain were found to be similar. The tests results agree well with the findings reported in the literature. The effects of wet-dry cycles did not alter the volume change behaviour of Pegwell Bay soil and cement kiln dust; in both cases, the swelling and shrinkage strains remained less than 0.5% with an increasing number of wet-dry cycles.

6. For the materials subjected several wet-dry cycles, an intermittent freeze-thaw cycle destabilised the equilibrium strain that was achieved by the materials during the previous wet-dry cycles; however, a new equilibrium in terms of vertical strain was attained by the materials with an increasing number of wet-dry cycles, but with a reduced equilibrium strain.

Frost heave and thaw settlement

7. The materials studied exhibited frost heave of different magnitudes in response to a freezing front at the top surface and a hydraulic front at the opposite end. For a freezing process of 24 hours, initially saturated slurried specimen of Speswhite kaolin exhibited a greater frost heave than the compacted specimen of the same material, whereas the frost heave values of compacted specimens of Pegwell Bay soil and cement kiln dust were found to be distinctly greater than that exhibited by the initially saturated slurried specimens of the same materials. The higher frost susceptibility of compacted materials as compared to initially saturated slurried materials was well supported by the higher values of the calculated segregation potential and increased the water content of the materials. The water content increase was found to mainly towards the hydraulic front which enabled the formation of ice lenses within the materials.
8. For initially saturated slurried materials, the magnitude of thaw settlement of Speswhite kaolin was the greatest among the three materials, whereas, for compacted saturated materials, the magnitude of thaw settlement of Speswhite kaolin was the least among the three materials. The differences in thaw settlements are primarily due to the differences in the permeability of the materials.

9. The materials used with a history of several wet-dry cycles and upon subjected to freeze-thaw cycles exhibited a greater frost heave, a higher segregation potential and a greater magnitude of thaw settlement as compared to the same materials but without a history of wet-dry cycles. The results clearly showed that wet-dry cycles tend to increase the permeability of geomaterials which aid increasing their frost susceptibility.

Cyclic wet-freeze-thaw-dry effects

10. For the materials subjected to wet-freeze-thaw-dry cycles, in any cycle, the vertical deformation that occurred due to the wetting process was found to be far smaller than the frost heave. The frost heave was greater than the thaw settlement, whereas the magnitude of thaw settlement was found to be far greater than that of the deformation that occurred due to the drying of the materials. With an increasing number of wet-freeze-thaw-dry cycles, the vertical deformation due to both wetting and drying decreased, the frost heave increased and then decreased, whereas the thaw settlement increased. The combined influence of the deformation patterns in each of the processes resulted in an accumulation of the vertical strain and the materials exhibited an uprising movement with an increasing number of wet-freeze-thaw-dry cycles. Such an uprising movement pattern has been reported in the literature for soils that underwent several wet-dry cycles.

11. The vertical strain due to wetting, freezing, thawing and drying processes were found to be dissimilar but stabilised after three wet-freeze-thaw-dry cycles. The movement band encompassing strains corresponding to wetting, freezing, thawing and drying was found to be nearly repeatable after three cycles. At equilibrium, the sum of vertical strains during wetting and freezing processes were found to be nearly equal to the sum of vertical strains that occurred during thawing and drying processes. The segregation potential of the materials was affected by wet-freeze-thaw-dry cycles.

References

Ahmed, A. and Ugai, K. 2011. Environmental effects on durability of soil stabilized with recycled gypsum. *Cold regions science and technology* 66(2), pp. 84–92.

Aho, S. and Saarenketo, T. 2006. Design and repair of roads suffering from spring thaw weakening. *The ROADEX III Project, Northern Periphery*.

Al-Homoud, A.S., Basma, A.A., Husein Malkawi, A.I. and Al Bashabsheh, M.A. 1995. Cyclic Swelling Behavior of Clays. *Journal of Geotechnical Engineering* 121(7), pp. 562–565.

Albrecht, B.A. and Benson, C.H. 2001. Effect of desiccation on compacted natural clays. *Journal of Geotechnical and Geoenvironmental Engineering* 127(1), pp. 67–75.

Albusoda, B.S. and Salem, L.A. 2012. Stabilization of dune sand by using cement kiln dust (CKD). *Journal of Earth Sciences and Geotechnical Engineering* 2(1), pp. 131–143.

Aldaood, A., Bouasker, M. and Al-Mukhtar, M. 2014. Impact of freeze–thaw cycles on mechanical behaviour of lime stabilized gypseous soils. *Cold Regions Science and Technology* 99, pp. 38–45.

Allam, M.M. and Sridharan, A. 1981. Effect of wetting and drying on shear strength. *Journal of the Geotechnical Engineering Division, American Society of Civil Engineers* 107(4), pp. 421–438.

Alonso, E.E., Romero, E., Hoffmann, C. and García-Escudero, E. 2005. Expansive bentonite-sand mixtures in cyclic controlled-suction drying and wetting. *Engineering Geology* 81(3), pp. 213–226.

Alonso, E.E., Lloret, A., Gens, A. and Yang, D.Q. 1995. Experimental behaviour of highly expansive double-structure clay. In: *PROCEEDINGS OF THE FIRST INTERNATIONAL CONFERENCE ON UNSATURATED SOILS/UNSAT'95/PARIS/FRANCE/6-8 SEPTEMBER 1995. VOLUME 1*.

Andersland, O. B., and Ladanyi, B. 1994. *An introduction to frozen ground engineering*. Springer Science & Business Media.

Andersland, O.B. and Ladanyi, B. 2004. *Frozen ground engineering*. John Wiley & Sons.

ASTM 2010. D4943 Standard Test Method for Shrinkage Factors of Soils by the Wax Method.

ASTM 2013. D5918 Standard Test Methods for Frost Heave and Thaw Weakening Susceptibility of Soils.

ASTM 2015. D560/D560M Standard Test Methods for Freezing and Thawing Compacted Soil-Cement Mixtures.

Baghdadi, Z.A., Fatani, M.N. and Sabban, N.A. 1995. Soil modification by cement kiln dust. *Journal of Materials in Civil Engineering* 7(4), pp. 218–222.

Ballantyne, C.K. and Harris, C. 1994. *The Periglaciation of Great Britain*. CUP Archive.

Barden, L. 1965. Consolidation of compacted and unsaturated clays. *Geotechnique* 15(3), pp. 267–286.

Basma, A.A., Al-Homoud, A.S., Husein Malkawi, A.I. and Al-Bashabsheh, M. a. 1996. Swelling-shrinkage behavior of natural expansive clays. *Applied Clay Science* 11(2–4), pp. 211–227.

Batenipour, H., Alfaro, M., Graham, J. and Kalynuk, K. 2012. Segregation Potential from a Highway Embankment on Thawed Permafrost. *Cold Regions Engineering 2012* (August), pp. 114–123.

Baumgartl, T. and Köck, B. 2004. Modeling Volume Change and Mechanical Properties with Hydraulic Models. *Soil Science Society of America Journal* 68(1), p. 57.

Benson, C.H. and Othman, M.A. 1993. Hydraulic conductivity of compacted clay frozen and thawed in situ. *Journal of Geotechnical Engineering* 119(2), pp. 276–294.

Black, P.B. and Tice, A.R. 1989. Comparison of soil freezing curve and soil water curve data for Windsor sandy loam. *Water Resources Research* 25(10), pp. 2205–2210.

Boardman, B.T. and Daniel, D.E. 1996. Hydraulic Conductivity of Desiccated Geosynthetic Clay Liners. *Journal of Geotechnical Engineering* 122(3), pp. 204–208.

Bowders, J.J. and McClelland, S. 1994. The effects of freeze/thaw cycles on the permeability of three compacted soils. *Hydraulic conductivity and waste contaminant transport in soil*, pp. 461–481.

Boyd, J.L. and Sivakumar, V. 2011. Experimental observations of the stress regime in unsaturated compacted clay when laterally confined. *Géotechnique* 61(4), pp. 345–363.

BS 1377-2 1990. Methods of test for soils for civil engineering purposes: Part 2: Classification tests. *British Standards Institution.*

BS 1377-4 1990. Soils for civil engineering purposes. Part 4: Compaction-related tests. *British Standards Institution.*

BS 1377-5 1990. Soils for civil engineering purposes. Part 5: Compressibility, permeability and durability tests. *British Standards Institution.*

BS 812-124 2009. Testing aggregates Part 124: Method for determination of frost heave. *British Standards Institution*.

Buchwald, A. and Schulz, M. 2005. Alkali-activated binders by use of industrial by-products. *Cement and concrete research* 35(5), pp. 968–973.

Budhu, M. 2008. *Soil mechanics and foundation*. John Wiley & Sons.

Burton, G.J., Pineda, J. a., Sheng, D. and Airey, D. 2015. Microstructural changes of an undisturbed, reconstituted and compacted high plasticity clay subjected to wetting and drying. *Engineering Geology* 193, pp. 363–373.

Cao, J., Phillips, R., Popescu, R., Audibert, J.M.E. and Testbeds, C. 2002. Penetration Resistance of Suction Caissons in Clay. In: *Proceedings of The Twelfth (2002) International Offshore and Polar Engineering Conference*. pp. 26–31.

Carrascal, E. and Sala Lizarraga, J.M. 2013. Mass, energy, entropy and exergy rate balance in a ranque-hilsh vortex tube. *Journal of Technology and Science Education* 3(3), pp. 122–131.

Carslaw, H.S. and Jaeger, J.C. 1959. *Heat in solids*. Clarendon Press, Oxford.

Casagrande, A. and Fadum, R.E. 1940. Notes on Soil Testing for Engineering Purposes. Harvard Univ. *Grad. School of Engineering Publ, 268*, p.74

Cerato, A.B., Miller, G.A. and Hajjat, J.A. 2009. Influence of Clod-Size and Structure on Wetting-Induced Volume Change of Compacted Soil. *Journal of Geotechnical & Geoenvironmental Engineering* 135(11), pp. 1620–1628.

Chamberlain, E.J. 1981a. *Frost Susceptibility of Soil, Review of Index Tests* (No. CRREL-81-2). COLD REGIONS RESEARCH AND ENGINEERING LAB HANOVER NH.

Chamberlain, E.J. 1981b. Overconsolidation effects of ground freezing. *Engineering geology* 18(1–4), pp. 97–110.

Chamberlain, E.J. and Gow, A.J. 1979. Effect of freezing and thawing on the permeability and structure of soils. *Engineering geology* 13(1–4), pp. 73–92.

Chamberlain, E.J., Iskandar, I. and Hunsicker, S.E. 1990. Effect of freeze-thaw cycles on the permeability and macrostructure of soils. *Cold Region Research and Engineering Laboratory* 90(1), pp. 145–155.

Chen, F.H. 2012. *Foundations on expansive soils*. Elsevier.

Cheng, G. and Chamberlain, E.J. 1988. Observations of moisture migration in frozen soils during thawing. In: *Fifth International Conference on Permafrost*. pp. 308–312.

Chung, H., Sills, G. and Kamon, M. 2016. Electrokinetically Enhanced Settlement and Remediation of. *Journal of ASTM International* 3(6), pp. 274–286.

Craig H. Benson and Othman, M. a. 1993. Hydraulic conductivity of compacted clay frozen and thawed in situ. *J. Geotech. Engrg.* 119(2), pp. 276–294.

Crescimanno, G. and Provenzano, G. 1999. Soil shrinkage characteristic curve in clay soils: Measurement and prediction. *Soil Science Society of America Journal* 63(1), pp. 25–32.

Cui, Z.-D., He, P.-P. and Yang, W.-H. 2014. Mechanical properties of a silty clay subjected to freezing–thawing. *Cold Regions Science and Technology* 98, pp. 26–34.

Daou, L., Périssol, C., Luglia, M., Calvert, V. and Criquet, S. 2016. Effects of drying–rewetting or freezing–thawing cycles on enzymatic activities of different Mediterranean soils. *Soil Biology and Biochemistry* 93, pp. 142–149.

Darbari, Z., Jaradat, K.A. and Abdelaziz, S.L. 2017. Heating–freezing effects on the pore size distribution of a kaolinite clay. *Environmental Earth Sciences* 76(20), p. 713.

Dasog, G.S., Acton, D.F., Mermut, A.R. and JONG, E.D.E. 1988. Shrink-swell potential and cracking in clay soils of Saskatchewan. *Canadian Journal of Soil Science* 68(2), pp. 251–260.

Day, R.W. 1994. Swell-Shrink Behavior of Compacted Clay. *Journal of Geotechnical Engineering* 120(3), pp. 618–623.

Derbyshire, E. and Mellors, T.W. 1988. Geological and geotechnical characteristics of some loess and loessic soils from China and Britain: A comparison. *Engineering Geology* 25(2–4), pp. 135–175.

Diagne, M., Tinjum, J.M. and Nokkaew, K. 2015. The effects of recycled clay brick content on the engineering properties, weathering durability, and resilient modulus of recycled concrete aggregate. *Transportation Geotechnics* 3, pp. 15–23.

Dif, A.E. and Bluemel, W.F. 1991. Expansive Soils under Cyclic Drying and Wetting. *Geotechnical Testing Journal, GTJODJ* 14(1), pp. 96–102.

Doehne, E. and Stulik, D.C. 1990. Application of the environmental scanning electron microscope to conservation science. *Scanning Microscopy* 4(2), pp. 275–286.

Eigenbrod, K.D. 1996. Effects of cyclic freezing and thawing on volume changes and permeabilities of soft fine-gained soils. *Canadian Geotechnical Journal* 33(4), pp. 529–537.

Eigenbrod, K.D., Knutsson, S. and Sheng, D. 1996. Pore-water pressures in freezing and thawing fine-grained soils. *Journal of cold regions engineering* 10(2), pp. 77–92.

Fleureau, J.-M., Verbrugge, J.-C., Huergo, P.J., Correia, A.G. and Kheirbek-Saoud, S. 2002. Aspects of the behaviour of compacted clayey soils on drying and wetting paths. *Canadian Geotechnical Journal* 39(6), pp. 1341–1357.

Fookes, P.G. and Best, R. 1969. Consolidation characteristics of some late Pleistocene periglacial metastable soils of East Kent. *Quarterly Journal of Engineering Geology and Hydrogeology* 2(2), pp. 103–128.

Fouli, Y., Cade-Menun, B.J. and Cutforth, H.W. 2013. Freeze–thaw cycles and soil water content effects on infiltration rate of three Saskatchewan soils. *Canadian Journal of Soil Science* 93(4), pp. 485–496.

Fredlund, D.G. and Hasan, J.U. 1979. One-dimensional consolidation theory: unsaturated soils. *Canadian Geotechnical Journal* 16(3), pp. 521–531.

Fredlund, D.G. and Rahardjo, H. 1993. *Soil Mechanics for Unsaturated Soils*. Hoboken, NJ, USA: John Wiley & Sons, Inc.

Fredlund, D.G., Xing, A. and Huang, S. 1994. Predicting the permeability function for unsaturated soils using the soil-water characteristic curve. *Canadian Geotechnical Journal* 31(4), pp. 533–546.

Gallage, C.P.. and Uchimura, T. 2006. Effects of wetting and drying on the unsaturated shear strength of a silty sand under low suction. *Unsaturated soils 2006*, pp. 1247–1258.

Gallipoli, D. 2012. A hysteretic soil-water retention model accounting for cyclic variations of suction and void ratio. *Géotechnique* 62(7), pp. 605–616.

Gallipoli, D., Gens, A., Sharma, R. and Vaunat, J. 2003a. An elasto-plastic model for unsaturated soil incorporating the effects of suction and degree of saturation on mechanical behaviour. *Géotechnique.* 53(1), pp. 123–136.

Gallipoli, D., Wheeler, S.J. and Karstunen, M. 2003b. Modelling the variation of degree of saturation in a deformable unsaturated soil. *Géotechnique.* 53(1), pp. 105–112.

Gan, J.K.-M. and Fredlund, D.G. 1996. Shear strength characteristics of two saprolitic soils. *Canadian Geotechnical Journal* 33(4), pp. 595–609.

Gilpin, R.R. 1980. A model for the prediction of ice lensing and frost heave in soils. *Water Resources Research* 16(5), pp. 918–930.

Glendinning, M.C. 2007. Modelling the Freezing and Thawing Behaviour of Saturated Soils. PhD Thesis, Cardiff University.

Goh, S.G., Rahardjo, H., Leong, E.C. and Asce, M. 2014. Shear Strength of Unsaturated Soils under Multiple Drying-Wetting Cycles. *Journal of Geotechnical and Geoenvironmental Engineering* 140(2), p. 6013001.

Google Inc. 2017. No Title [Online] Available at: https://www.google.co.uk/maps/@51.2034126,0.4105192,9.75z [Accessed: 3 October 2017].

Graham, J. and Au, V.C.S. 1985. Effects of freeze–thaw and softening on a natural clay at low stresses. *Canadian Geotechnical Journal* 22(1), pp. 69–78.

Grim, R.E. 1953. *Clay Mineralogy*. Mcgraw-Hill Book Company, Inc; New York; Toronto; London.

Guan, G.S., Rahardjo, H. and Choon, L.E. 2010. Shear Strength Equations for Unsaturated Soil under Drying and Wetting. *Journal of Geotechnical and Geoenvironmental Engineering* 136(4), pp. 594–606.

Gullà, G., Mandaglio, M.C. and Moraci, N. 2006. Effect of weathering on the compressibility and shear strength of a natural clay. *Canadian Geotechnical Journal* 43(6), pp. 618–625.

Haines, W.B. 1923. The volume-changes associated with variations of water content in soil. *The Journal of Agricultural Science* 13(3), p. 296.

Harlan, R.L. 1973. Analysis of coupled heat-fluid transport in partially frozen soil. *Water Resources Research* 9(5), pp. 1314–1323.

Harris, J.S. 1995. *Ground freezing in practice*. Thomas Telford.

Hendry, M.T., Onwude, L.U. and Sego, D.C. 2016. A laboratory investigation of the frost heave susceptibility of fine-grained soil generated from the abrasion of a diorite aggregate. *Cold Regions Science and Technology* 123, pp. 91–98.

Henry, K.S. 2000. *A review of the thermodynamics of frost heave*. ENGINEER RESEARCH AND DEVELOPMENT CENTER HANOVER NH COLD REGIONS RESEARCH AND ENGINEERING LAB.

Herring, S.C., Hoerling, M.P., Kossin, J.P., Peterson, T.C. and Stott, P.A. 2015. Explaining extreme events of 2014 from a climate perspective. *Bulletin of the American Meteorological Society* 96(12), pp. S1–S172.

Ho, L., Fatahi, B. and Khabbaz, H. 2014. Analytical solution for one-dimensional consolidation of unsaturated soils using eigenfunction expansion method. *International Journal for Numerical and Analytical Methods in Geomechanics* 38(10), pp. 1058–1077.

Holtz, R.D. and Kovacs, W.D. 1981. *An introduction to geotechnical engineering*. (No. Monograph)

Huang, S. 1998. Development and verification of a coefficient of permeability function for a deformable unsaturated soil. *Canadian Geotechnical Journal* 35, pp. 411–425.

Hui, B. and Ping, H. 2009. Frost heave and dry density changes during cyclic freeze-thaw of a silty clay. *Permafrost and periglacial Processes* 20(1), pp. 65–70.

Jackson, K.A., Uhlmann, D.R. and Chalmers, B. 1966. Frost heave in soils. *Journal of Applied Physics* 37(2), pp. 848–852.

Jamshidi, R.J. and Lake, C.B. 2014. Hydraulic and strength properties of unexposed and freeze–thaw exposed cement-stabilized soils. *Canadian Geotechnical Journal* 52(3), pp. 283–294.

Janoo, V.C. and Berg, R.L. 1996. *PCC Airfield Pavement Response During Thaw-Weakening Periods. A Field Study*. COLD REGIONS RESEARCH AND ENGINEERING LAB HANOVER NH.

Jones, D.E. and Holtz, W.G. 1973. Expansive Soils-the hidden disaster. *Civil Engineering-ASCE* 43(8), pp. 49–51.

Kim, W.-H. and Daniel, D.E. 1992. Effects of freezing on hydraulic conductivity of compacted clay. *Journal of Geotechnical Engineering* 118(7), pp. 1083–1097.

Kim, Y.S., Seong, J.H. and Kim, S.S. 2013. The strength change characteristics of weathering soil due to repeat freezing- thawing and drying-wetting. *Proceedings of the 18th International Conference on Soil Mechanics and Geotechnical Engineering, Paris 2013*, pp. 365–368.

Kodikara, J., Barbour, S.L. and Fredlund, D.G. 1999. Changes in clay structure and behaviour due to wetting and drying. *Proceedings of the 8th Australian-New Zealand conference on geomechanics, Hobart*, pp. 179–186.

Kong, L.-W., Zeng, Z.-X., Bai, W. and Wang, M. 2017. Engineering geological properties of weathered swelling mudstones and their effects on the landslides occurrence in the Yanji section of the Jilin-Hunchun high-speed railway. *Bulletin of Engineering Geology and the Environment*, pp. 1–13.

Konrad, J.-M. 1984. Soil freezing characteristics versus heat extraction rate. *Proceedings of the American Society of Mechanical Engineers Annual Winter Meeting* (DBR Paper No. 1257).

Konrad, J.-M. 1987. Procedure for determining the segregation potential of freezing soils. *GEOTECHNICAL TESTING JOURNAL*, pp. 51–58.

Konrad, J.-M. 1989a. Effect of freeze–thaw cycles on the freezing characteristics of a clayey silt at various overconsolidation ratios. *Canadian Geotechnical Journal* 26(2), pp. 217–226.

Konrad, J.-M. 1989b. Influence of cooling rate on the temperature of ice lens formation in clayey silts. *Cold regions science and technology* 16(1), pp. 25–36.

Konrad, J.-M. 1989c. Influence of overconsolidation on the freezing characteristics of a clayey silt. *Canadian Geotechnical Journal* 26(1), pp. 9–21.

Konrad, J.-M. 1989d. Physical processes during freeze-thaw cycles in clayey silts. *Cold Regions Science and Technology* 16(3), pp. 291–303.

Konrad, J.-M. 1999. Frost susceptibility related to soil index properties. *Canadian Geotechnical Journal* 36(3), pp. 403–417.

Konrad, J.-M. 2005. Estimation of the segregation potential of fine-grained soils using the frost heave response of two reference soils. *Canadian Geotechnical Journal* 42(1), pp. 38–50.

Konrad, J.-M. 2008. Freezing-induced water migration in compacted base-course materials. *Canadian Geotechnical Journal* 45(7), pp. 895–909.

Konrad, J.-M. 2010. Hydraulic conductivity changes of a low-plasticity till subjected to freeze–thaw cycles. *Géotechnique* 60(9), pp. 679–690.

Konrad, J.-M. and Lemieux, N. 2005. Influence of fines on frost heave characteristics of a well-graded base-course material. *Canadian geotechnical journal* 42(2), pp. 515–527.

Konrad, J.-M. and Morgenstern, N.R. 1980. A mechanistic theory of ice lens formation in fine-grained soils. *Canadian Geotechnical Journal* 17(4), pp. 473–486.

Konrad, J.-M. and Morgenstern, N.R. 1981. The segregation potential of a freezing soil. *Canadian Geotechnical Journal* 18(4), pp. 482–491.

Konrad, J.-M. and Morgenstern, N.R. 1982a. Effects of applied pressure on freezing soils. *Canadian Geotechnical Journal* 19(4), pp. 494–505.

Konrad, J.-M. and Morgenstern, N.R. 1982b. Prediction of frost heave in the laboratory during transient freezing. *Canadian Geotechnical Journal* 19(3), pp. 250–259.

Konrad, J.-M. and Morgenstern, N.R. 1984. Frost heave prediction of chilled pipelines buried in unfrozen soils. *Canadian Geotechnical Journal* 21(1), pp. 100–115.

Konrad, J.-M. and Samson, M. 2000a. Hydraulic conductivity of kaolinite-silt mixtures subjected to closed-system freezing and thaw consolidation. *Canadian Geotechnical Journal* 37(4), pp. 857–869.

Konrad, J.-M. and Samson, M. 2000b. Influence of freezing temperature on hydraulic conductivity of silty clay. *Journal of geotechnical and geoenvironmental engineering* 126(2), pp. 180–187.

Konrad, J.-M. and Seto, J.T.C. 1994. Frost heave characteristics of undisturbed sensitive Champlain Sea clay. *Canadian Geotechnical Journal* 31(2), pp. 285–298.

Konrad, J.M. 1987. The influence of heat extraction rate in freezing soils. *Cold Regions Science and Technology* 14(2), pp. 129–137.

Konrad, J.M. 1988. Influence of freezing mode on frost heave characteristics. *Cold Regions Science and Technology* 15(2), pp. 161–175.

Koopmans, R.W.R. and Miller, R.D. 1966. Soil freezing and soil water characteristic curves. *Soil Science Society of America Journal* 30(6), pp. 680–685.

Kraus, J.F., Benson, C.H., Erickson, A.E. and Chamberlain, E.J. 1997. Freeze-thaw cycling and hydraulic conductivity of bentonitic barriers. *Journal of Geotechnical and Geoenvironmental Engineering* 123(3), pp. 229–238.

Kwiatkowski, K., Stipanovic Oslakovic, I., Hartmann, A. and Ter Maat, H. 2014. Potential impact of climate change on porous asphalt with a focus on winter damage. *Materials and Infrastructures 2*, pp. 159–176.

Lambe, T.W. and Whitman, R. V 1969. Soil mechanics, series in soil engineering. *Jhon Wiley & Sons*.

Lawton, E.C., Fragaszy, R.J. and Hetherington, M.D. 1992. Review of wetting-induced collapse in compacted soil. *Journal of geotechnical engineering* 118(9), pp. 1376–1394.

Legout, C., Leguédois, S. and Le Bissonnais, Y. 2005. Aggregate breakdown dynamics under rainfall compared with aggregate stability measurements. *European Journal of Soil Science* 56(2), pp. 225–237.

Li, A., Niu, F., Zheng, H., Akagawa, S., Lin, Z. and Luo, J. 2017. Experimental measurement and numerical simulation of frost heave in saturated coarse-grained soil Anyuan. *Cold Regions Science and Technology* 137, pp. 68–74.

Lin, L.-C. and Benson, C.H. 2000. Effect of wet-dry cycling on swelling and hydraulic conductivity of GCLs. *Journal of Geotechnical and Geoenvironmental Engineering* 126(1), pp. 40–49.

Liu, J., Chang, D. and Yu, Q. 2016. Influence of freeze-thaw cycles on mechanical properties of a silty sand. *Engineering Geology* 210, pp. 23–32.

Liu, Q., Yasufuku, N., Omine, K. and Hazarika, H. 2012. Automatic soil water retention test system with volume change measurement for sandy and silty soils. *Soils and Foundations* 52(2), pp. 368–380.

Liu, W., Yang, Q., Tang, X. and Yang, G. 2016. Effect of Drying and Wetting on the Shear Strength of a Low-Plasticity Clay With Different Initial Dry Densities. *Journal of Testing and Evaluation* 44(4), p. 20140096.

Liu, Z., Zhang, B., Zhang, B. and Tao, J. 2013. A New Method for Soil Water Characteristic Curve Measurement Based on Similarities Between Soil Freezing and Drying. *Geotechnical Testing Journal* 35(1), pp. 1–9.

Ma, T., Wei, C., Xia, X., Zhou, J. and Chen, P. 2017. Soil Freezing and Soil Water Retention Characteristics: Connection and Solute Effects. *Journal of Performance of Constructed Facilities* 31(1), p. D4015001.

Makusa, G.P., Bradshaw, S.L., Berns, E., Benson, C.H. and Knutsson, S. 2014. Freeze–thaw cycling concurrent with cation exchange and the hydraulic conductivity of geosynthetic clay liners. *Canadian Geotechnical Journal* 51(6), pp. 591–598.

Malusis, M.A., Yeom, S. and Evans, J.C. 2011. Hydraulic conductivity of model soil–bentonite backfills subjected to wet–dry cycling. *Canadian Geotechnical Journal* 48(8), pp. 1198–1211.

Matsuoka, N. 2001. Solifluction rates, processes and landforms: A global review. *Earth-Science Reviews* 55(1–2), pp. 107–134.

McCarthy, D.F. 1977. *Essentials of soil mechanics and foundations*. Reston Publishing Company.

McRoberts, E.C. and Morgenstern, N.R. 1974. The stability of thawing slopes. *Canadian Geotechnical Journal* 11(4), pp. 447–469.

Meehl, G.A., Karl, T., Easterling, D.R., Changnon, S., Pielke, R., Changnon, D., Evans, J., Groisman, P.Y., Knutson, T.R., Kunkel, K.E., Mearns, L.O., Parmesan, C., Pulwarty, R., Root, T., Sylves, R.T., Whetton, P. and Zwiers, F. 2000. An Introduction to Trends in Extreme Weather and Climate Events: Observations, Socioeconomic Impacts, Terrestrial Ecological Impacts, and Model Projections *. *Bulletin of the American Meteorological Society* 81(3), pp. 413–416.

Miller, G.A. and Azad, S. 2000. Influence of soil type on stabilization with cement kiln dust. *Construction and Building Materials* 14(2), pp. 89–97.

Miller, R.D. 1972. Freezing and heaving of saturated and unsaturated soils. *Highway Research Record* (393).

Miller, R.D. 1978. Frost heaving in non-colloidal soils. In: *Proceeding 3rd International Conference Permafrost*. National Research Council of Canada, pp. 707–713.

Mitchell, J.K. and Soga, K. 2005. *Fundamentals of Soil Behavior*.

Moon, D.H., Wazne, M., Yoon, I.-H. and Grubb, D.G. 2008. Assessment of cement kiln dust (CKD) for stabilization/solidification (S/S) of arsenic contaminated soils. *Journal of Hazardous Materials* 159(2–3), pp. 512–518.

Morgenstern, N.R. and Smith, L.B. 1973. Thaw-consolidation tests on remoulded clays. *Canadian Geotechnical Journal* 10(1), pp. 25–40.

Morgenstern, N.R. t and Nixon, J.F. 1971. One-dimensional consolidation of thawing soils. *Canadian Geotechnical Journal* 8(4), pp. 558–565.

Mu, S. and Ladanyi, B. 1987. Modelling of coupled heat, moisture and stress field in freezing soil. *Cold Regions Science and Technology* 14(3), pp. 237–246.

Murton, J.B. 2014. Periglacial and Glacial Engineering Geology Working Party Kent Field Trip 16 – 18 th May 2014. (May), pp. 1–43.

Murton, J.B., Bateman, M.D., Baker, C.A., Knox, R. and Whiteman, C.A. 2003. The Devensian periglacial record on Thanet, Kent, UK. *Permafrost and Periglacial Processes* 14(3), pp. 217–246.

N. A Tsytovich 1960. *Bases and Foundations of Frozen Soil*. National Academy of Sciences, National Research Council.

Nasr, A.M.A. 2015. Geotechnical Characteristics of Stabilized Sabkha Soils from the Egyptian–Libyan Coast. *Geotechnical and Geological Engineering* 33(4), pp. 893–911.

Nishimura, S., Gens, A., Olivella, S. and Jardine, R.J. 2009. THM-coupled finite element analysis of frozen soil: formulation and application. *Géotechnique* 59(3), pp. 159–171.

Nixon, J.F. 1973. Thaw–Consolidation of Some Layered Systems. *Canadian Geotechnical Journal* 10(4), pp. 617–631.

Nixon, J.F. 1982. Field frost heave predictions using the segregation potential concept. *Canadian Geotechnical Journal* 19(4), pp. 526–529.

Nixon, J.F. 1991. Discrete ice lens theory for frost heave in soils. *Canadian Geotechnical Journal* 28(6), pp. 843–859.

Nixon, J.F. 1992. Discrete ice lens theory for frost heave beneath pipelines. *Canadian Geotechnical Journal* 29(3), pp. 487–497.

Nixon, J.F. and McRoberts, E.C. 1973. A study of some factors affecting the thawing of frozen soils. *Canadian Geotechnical Journal* 10(3), pp. 439–452.

Nixon, J.F. and Morgenstern, N.R. 1973. The residual stress in thawing soils. *Canadian Geotechnical Journal* 10(4), pp. 571–580.

Nixon, J.F. and Morgenstern, N.R. 1974. Thaw-consolidation tests on undisturbed fine-grained permafrost. *Canadian Geotechnical Journal* 11(1), pp. 202–214.

Nowamooz, H., Jahangir, E. and Masrouri, F. 2013. Volume change behaviour of a swelling soil compacted at different initial states. *Engineering Geology* 153, pp. 25–34.

Nowamooz, H. and Masrouri, F. 2010a. Influence of suction cycles on the soil fabric of compacted swelling soil. *Comptes Rendus Geoscience* 342(12), pp. 901–910.

Nowamooz, H. and Masrouri, F. 2010b. Relationships between soil fabric and suction cycles in compacted swelling soils. *Engineering Geology* 114(3–4), pp. 444–455.

O'Neal, M.R., Nearing, M.A., Vining, R.C., Southworth, J. and Pfeifer, R.A. 2005. Climate change impacts on soil erosion in Midwest United States with changes in crop management. *Catena* 61(2–3), pp. 165–184.

O'Neill, K. and Miller, R.D. 1985. Exploration of a Rigid Ice Model of Frost Heave. *Water Resources Research* 21(3), pp. 281–296.

Osipov, V.I., Bik, N.N. and Rumjantseva, N.A. 1987. Cyclic swelling of clays. *Applied Clay Science* 2(4), pp. 363–374.

Othman, M.A., Benson, C.H., Chamberlain, E.J. and Zimmie, T.F. 1994. Laboratory testing to evaluate changes in hydraulic conductivity of compacted clays caused by freeze-thaw: state-of-the-art. In: *Hydraulic conductivity and waste contaminant transport in soil*. ASTM International, pp. 227–254.

Özbek, A. 2014. Investigation of the effects of wetting–drying and freezing–thawing cycles on some physical and mechanical properties of selected ignimbrites. *Bulletin of Engineering Geology and the Environment* 73(2), pp. 595–609.

Padilla, F. and Villeneuve, J.-P. 1992. Modeling and experimental studies of frost heave including solute effects. *Cold Regions Science and Technology* 20(2), pp. 183–194.

Pardini, G., Guidi, G.V., Pini, R., Regüés, D. and Gallart, F. 1996. Structure and porosity of smectitic mudrocks as affected by experimental wetting—drying cycles and freezing—thawing cycles. *Catena* 27(3), pp. 149–165.

Penner, E. 1986. Aspects of ice lens growth in soils. *Cold regions science and technology* 13(1), pp. 91–100.

Pires, L.F., Bacchi, O.O.S. and Reichardt, K. 2007. Assessment of soil structure repair due to wetting and drying cycles through 2D tomographic image analysis. *Soil and Tillage Research* 94(2), pp. 537–545.

Pires, L.F., Cooper, M., Cássaro, F.A.M., Reichardt, K., Bacchi, O.O.S. and Dias, N.M.P. 2008. Micromorphological analysis to characterize structure modifications of soil samples submitted to wetting and drying cycles. *Catena* 72(2), pp. 297–304.

Plastic pipe instute (PPI) 2001. Thermal Expansion and Contraction in Plastics Piping Systems PPI TR-21 / 2001. . Available at: http://www.plasticpipe.org.

Priemé, A. and Christensen, S. 2001. Natural perturbations, drying–wetting and freezing–thawing cycles, and the emission of nitrous oxide, carbon dioxide and methane from farmed organic soils. *Soil Biology and Biochemistry* 33(15), pp. 2083–2091.

Qi, J., Ma, W. and Song, C. 2008. Influence of freeze-thaw on engineering properties of a silty soil. *Cold Regions Science and Technology* 53(3), pp. 397–404.

Qi, J., Yao, X., Yu, F. and Liu, Y. 2012. Study on thaw consolidation of permafrost under roadway embankment. *Cold Regions Science and Technology* 81, pp. 48–54.

Qin, A., Chen, G., Tan, Y. and Sun, D. 2008. Analytical solution to one-dimensional consolidation in unsaturated soils. *Applied Mathematics and Mechanics* 29(10), pp. 1329–1340.

Qin, A., Sun, D. and Tan, Y. 2010. Analytical solution to one-dimensional consolidation in unsaturated soils under loading varying exponentially with time. *Computers and Geotechnics* 37(1), pp. 233–238.

Rajaram, G. and Erbach, D.C. 1999. Effect of wetting and drying on soil physical properties. *Journal of Terramechanics* 36(1), pp. 39–49.

Ranganatham, B.V. and Satyanarayana, B. 1965. A Rational Method Of Predicting Swelling Potential For Compacted Expansive Clays. *Proceeding of the 6th ICSMFE*, pp. 92–96.

Rao, A.S. et al. 2004. Prediction of swelling characteristics of remoulded and compacted expansive soils using free swell index. *Quarterly Journal of Engineering Geology and Hydrogeology* 37(3), pp. 217–226.

Rao, S.M., Reddy, B.V.V. and Muttharam, M. 2001. The impact of cyclic wetting and drying on the swelling behaviour of stabilized expansive soils. *Engineering Geology* 60(1–4), pp. 223–233.

Rao, S.M. and Revanasiddappa, K. 2006. Influence of cyclic wetting drying on collapse behaviour of compacted residual soil. *Geotechnical and Geological Engineering* 24(3), pp. 725–734.

Rempel, A. W. 2007. Formation of ice lenses and frost heave. *Journal of Geophysical Research: Earth Surface* 112(2), pp. 1–17.

Ren, J. and Vanapalli, S.K. 2017. Prediction of the Resilient Modulus of Frozen Unbound Road Materials Using the Soil-Freezing Characteristic Curve. *Canadian Geotechnical Journal* 0, pp. 1–32.

Le Riche, H.H. 1973. The distribution of minor elements among the components of a soil developed in loess. *Geoderma* 9(1), pp. 43–57.

Ring, G.W. 1966. Shrink-swell potential of soils. *Highway Research Record* (119).

Romero, E. and Simms, P.H. 2008. Microstructure investigation in unsaturated soils: a review with special attention to contribution of mercury intrusion porosimetry and environmental scanning electron microscopy. In: *Laboratory and Field Testing of Unsaturated Soils*. Springer, pp. 93–115.

Rosenbalm, D. and Zapata, C.E. 2017. Effect of Wetting and Drying Cycles on the Behavior of Compacted Expansive Soils. *Journal of Materials in Civil Engineering* 29(1), p. 4016191.

Sariosseiri, F. and Muhunthan, B. 2008. Geotechnical properties of Palouse loess modified with cement kiln dust and Portland cement. In: *GeoCongress 2008: Characterization, Monitoring, and Modeling of GeoSystems*. pp. 92–99.

Seed, H.B. et al. 1962. Prediction of swelling potential for compacted clays. *Transactions of the American Society of Civil Engineers* 128(1), pp. 1443–1477.

Seguel, O. and Horn, R. 2006. Structure properties and pore dynamics in aggregate beds due to wetting-drying cycles. *Journal of Plant Nutrition and Soil Science* 169(2), pp. 221–232.

Sheng, D., Axelsson, K. and Knutsson, S. 1995. Frost heave due to ice lens formation in freezing soils 1. Theory and verification. *Nordic hydrology* 26(June 2017), pp. 125–146.

Siddique, R. 2006. Utilization of cement kiln dust (CKD) in cement mortar and concrete-an overview. *Resources, Conservation and Recycling* 48(4), pp. 315–338.

Sillanpää, M. and Webber, L.R. 1961. The effect of freezing-thawing and wetting-drying cycles on soil aggregation. *Canadian Journal of Soil Science* 41(2), pp. 182–187.

Simonsen, E. and Isacsson, U. 1999. Thaw weakening of pavement structures in cold regions. *Cold regions science and technology* 29Simonsen(2), pp. 135–151.

Simonsen, E. and Isacsson, U. 2001. Soil behavior during freezing and thawing using variable and constant confining pressure triaxial tests. *Canadian Geotechnical Journal* 38(4), pp. 863–875.

Singh, R.M. 2007. Experimental and numerical investigation of heat and mass movement in unsaturated clays. PhD Thesis, Cardiff University. Cardiff University.

Sivakumar, R., Sivakumar, V., Blatz, J. and Vimalan, J. 2006. Twin-cell stress path apparatus for testing unsaturated soils. *Geotechnical Testing Journal* 29(2), pp. 175–179.

Sivakumar, V., Sivakumar, R., Murray, E.J., MacKinnon, P. and Boyd, J. 2010. Mechanical behaviour of unsaturated kaolin (with isotropic and anisotropic stress history). Part 1: wetting and compression behaviour. *Géotechnique* 60(8), pp. 581–594.

Sivakumar, V., Sivakumar, R., Thom, R., Murray, E.J. and Mackinnon, P. 2007. Pore size distribution of unsaturated compacted kaolin: the initial states and final states following saturation. *Géotechnique* 57(5), pp. 469–474.

Sivakumar, V., Tan, W.C., Murray, E.J. and McKinley, J.D. 2006. Wetting, drying and compression characteristics of compacted clay. *Géotechnique* 56(1), pp. 57–62.

Sivakumar, V., Zaini, J., Gallipoli, D. and Solan, B. 2015. Wetting of compacted clays under laterally restrained conditions: initial state, overburden pressure and mineralogy. *Géotechnique* 65(2), pp. 111–125.

Smith, J.S. 2004. Scaled geotechnical centrifuge modelling of gelifluction. PhD thesis, Cardiff University.

Solanki, P., Zaman, M.M. and Khalife, R. 2013. Effect of freeze-thaw cycles on performance of stabilized subgrade. In: *Proceedings for Geo-Congress-Sound Geotechnical Research to Practice: Honoring Robert D. Holtz II, Geotechnical Special Publication*. pp. 566–580.

Spaans, E.J.A. and Baker, J.M. 1996. The soil freezing characteristic: Its measurement and similarity to the soil moisture characteristic. *Soil Science Society of America Journal* 60(1), p. 13.

Stirk, G.B. 1954. Some aspects of soil shrinkage and the effect of cracking upon water entry into the soil. *Australian Journal of Agricultural Research* 5(2), pp. 279–296.

Subba Rao, K.S. and Tripathy, S. 2003. Effect of aging on swelling and swell-shrink behaviour of a compacted expansive soil. *Geotechnical Testing Journal* 26(1), pp. 36–46.

Svec, O.J. 1989. A new concept of frost-heave characteristics of soils. *Cold regions science and technology* 16(3), pp. 271–279.

Taber, S. 1929. Frost Heaving. *Journal of Geology* 37 (5)(December), pp. 428–461.

Taber, S. 1930. The mechanics of frost heaving. *The Journal of Geology*, pp. 303–317.

Tadza, M. 2011. Soil-water characteristic curves and shrinkage behaviour of highly plastic clays: an experimental investigation. PhD Thesis, Cardiff University. Cardiff University.

Tang, L., Cong, S., Geng, L., Ling, X. and Gan, F. 2018. The effect of freeze-thaw cycling on the mechanical properties of expansive soils. *Cold Regions Science and Technology* 145(November 2017), pp. 197–207.

Terzaghi, K. 1944. *Theoretical soil mechanics*. Chapman And Hali, Limited John Wiler And Sons, Inc; New York.

Terzaghi, K., Peck, R.B. and Mesri, G. 1996. *Soil mechanics in engineering practice*. John Wiley & Sons.

Thom, R., Sivakumar, R., Sivakumar, V., Murray, E.J. and Mackinnon, P. 2007. Pore size distribution of unsaturated compacted kaolin: the initial states and final states following saturation. *Géotechnique* 57(5), pp. 469–474.

Thomas, H.R., Cleall, P., Li, Y.-C., Harris, C. and Kern-Luetschg, M. 2009. Modelling of cryogenic processes in permafrost and seasonally frozen soils. *Géotechnique* 59(3), pp. 173–184.

Todres, H.A., Mishulovich, A. and Ahmed, J. 1992. *Cement kiln dust management: Permeability* (No. RD103T).

Toll, D.G. and Ali Rahman, Z. 2017. Critical state shear strength of an unsaturated artificially cemented sand. *Géotechnique* 67(3), pp. 208–215.

Toll, D.G., Asquith, J.D., Hughes, P.N. and Osinski, P. 2016a. Soil Water Retention Behaviour of a Sandy Clay Fill Material. *Procedia Engineering* 143(Ictg), pp. 308–314.

Toll, D.G., Hughes, P.N. and Asquith, J.D. 2016b. Soil water retention behaviour for an instrumented embankment. *3Rd European Conference on Unsaturated Soils - E-Unsat 2016* 9, pp. 0–3.

Toll, D.G., Mendes, J., Hughes, P.N., Glendinning, S. and Gallipoli, D. 2012. Climate change and the role of unsaturated soil mechanics. *5th Asia-Pacific Conference on Unsaturated Soils 2012* 1(1), pp. 137–145.

Toll, D.G., Mendes, J., Karthikeyan, M., Gallipoli, D., Augarde, C.E., Phoon, K.K. and Lin, K.Q. 2008. Effects of climate change on slopes for transportation infrastructure. In: *1st ISSMGE International Conference on Transportation Geotechnics*. pp. 507–513.

Tripathy, S. and Subba Rao, K.S. 2009. Cyclic swell-shrink behaviour of a compacted expansive soil. *Geotechnical and Geological Engineering* 27(1), pp. 89–103.

Tripathy, S., Subba Rao, K.S. and Fredlund, D.G. 2002. Water content - void ratio swell-shrink paths of compacted expansive soils. *Canadian Geotechnical Journal* 959, pp. 938–959.

Tripathy, S., Tadza, Y.M. and Thomas, H.R. 2014. Soil-water characteristic curves of clays. *Canadian geotechnical journal* 51(8), pp. 869–883.

Utomo, W.H. and Dexter, A.R. 1982. Changes in soil aggregate water stability induced by wetting and drying cycles in non-saturated soil. *Journal of Soil Science* 33(4), pp. 623–637.

Vanapalli, S.K., Fredlund, D.G., Pufahl, D.E. and Clifton, A.W. 1996. Model for the prediction of shear strength with respect to soil suction. *Canadian Geotechnical Journal* 33(3), pp. 379–392.

Venkatarama-Reddy, B. V and Jagadish, K.S. 1993. The static compaction of soils. *Geotechnique* 43(2), pp. 337–341.

Viklander, P. 1998a. Laboratory study of stone heave in till exposed to freezing and thawing. *Cold Regions Science and Technology* 27(2), pp. 141–152.

Viklander, P. 1998b. Permeability and volume changes in till due to cyclic freeze/thaw. *Canadian Geotechnical Journal* 35(3), pp. 471–477.

Viklander, P. and Eigenbrod, D. 2000. Stone movements and permeability changes in till caused by freezing and thawing. *Cold Regions Science and Technology* 31(2), pp. 151–162.

Viklander, P. and Knutsson, S. 1997. Permeability changes in a fine-grained till du to cycles of freezing and thawing. In: *International Symposium on Ground Freezing and Frost Action in Soils: 15/04/1997-17/04/1997*. Balkema Publishers, AA/Taylor & Francis The Netherlands, pp. 193–202.

Wang, D.Y., Ma, W., Niu, Y.H., Chang, X.X. and Wen, Z. 2007. Effects of cyclic freezing and thawing on mechanical properties of Qinghai-Tibet clay. *Cold Regions Science and Technology* 48(1), pp. 34–43.

Wang, J., Gao, X. and Jiao, S. 2009. The application of vortex tube in deep mine cooling. In: *2009 International Conference on Energy and Environment Technology, ICEET 2009*. IEEE, pp. 395–398.

Wang, S., Lv, Q., Baaj, H., Li, X. and Zhao, Y. 2016. Volume change behaviour and microstructure of stabilized loess under cyclic freeze–thaw conditions. *Canadian Journal of Civil Engineering* 43(999), pp. 865–874.

Wang, T., Liu, Y., Yan, H. and Xu, L. 2015. An experimental study on the mechanical properties of silty soils under repeated freeze–thaw cycles. *Cold Regions Science and Technology* 112, pp. 51–65.

Weir, A.H., Catt, J.A. and Madgett, P.A. 1971. Postglacial soil formation in the loess of Pegwell Bay, Kent (England). *Geoderma* 5(2), pp. 131–149.

WMO (World Meteorological Organization) 2001. WMO statement on the status of the global climate in 2001. [Online] Available at: http://www.wmo.ch/wordPress/Press 670.html.

Yong, R.N., Boonsinsuk, P. and Murphy, D. 1982. Short-term cyclic freeze-thaw effect on strength properties of a sensitive clay. In: *Proc. 3rd Int. Symp. Ground Freezing, Hanover, NH*. pp. 97–104.

Zhang, Z.X. and Kushwaha, R.L. 1998. Modeling soil freeze-thaw and ice effect on canal bank. *Canadian Geotechnical Journal* 35(4), pp. 655–665.

Zheng, H., Asce, S.M. and Kanie, S. 2015. Combined Thermal-Hydraulic-Mechanical Frost Heave Model Based on Takashi ' s Equation. *Journal of Cold Regions Engineering* 4014019(19), pp. 1–19.

Zheng, Y., Ma, W., Mu, Y. and Bing, H. 2015. Analysis of Soil Structures and the Mechanisms under the Action of Freezing and Thawing Cycles. *16th International Conference on Cold Regions Engineering*, pp. 25–33.

Zhou, B., Gu, L., Ding, Y., Shao, L., Wu, Z., Yang, X., Li, C., Li, Z., Wang, X. and Cao, Y. 2011. The great 2008 Chinese ice storm: its socioeconomic–ecological impact and sustainability lessons learned. *Bulletin of the American Meteorological Society* 92(1), pp. 47–60.

Zhou, Y. and Zhou, G. 2012. Intermittent freezing mode to reduce frost heave in freezing soils—experiments and mechanism analysis. *Canadian Geotechnical Journal* 49(6), pp. 686–693.

Zimmie, T.F. and La Plante, C. 1990. Effect of freeze/thaw cycles on the permeability of a fine-grained soil. In: *Hazardous and Industrial Wastes- Proceedings of the Mid-Atlantic Industrial Waste Conference*. pp. 580–593.